Bunch shape monitors with RF scanning of low energy secondary electrons

A.V.Feschenko

**Institute For Nuclear Research (INR),
Moscow 117312, Russia**

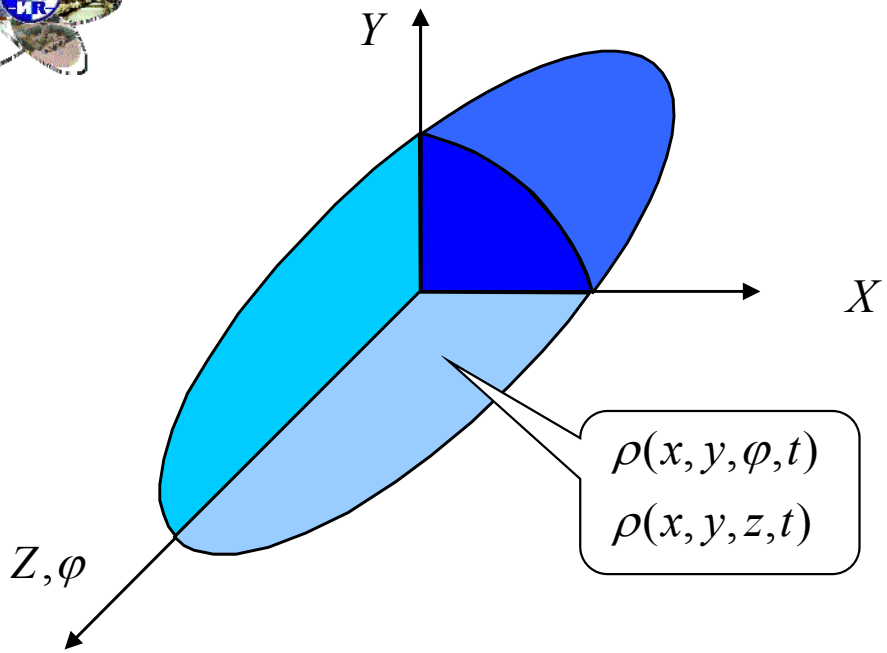

For complete beam description a behavior of a 6-dimensional distribution function in time is required

$$j(x,x',y,y',\varphi,W,t)$$

Beam Current Transformer:

$$J(t)=\int j(x,x',y,y',\varphi,W,t)dxdx'dydy'd\varphi dW$$

Wire scanner:

$$J(x,t)=\int j(x',y,y',\varphi,W,t)dx'dydy'd\varphi dW$$

Horizontal emittance detector:

$$J(x,x',t)=\int j(y,y',\varphi,W,t)dydy'd\varphi dW$$

……etc…….

Process of acceleration can be described as a behavior of particles in Energy-Phase plane *(W,φ)*

that is why

the beam distribution functions versus *W and (or) φ*

are extremely important and interesting.

However, they are the most difficult to measure.

Energy Spectrum:

$$J(W,t) = \int j(x,x',y,y',\varphi,W,t)dxdx'dydy'd\varphi$$

Phase Spectrum (Bunch Shape):

$$J(\varphi,t) = \int j(x,x',y,y',W,t)dxdx'dydy'dW$$

Longitudinal phase space distribution:

$$J(\varphi,W,t) = \int j(x,x',y,y',W,t)dxdx'dydy'$$

The main requirement for Bunch Shape Measurements is Phase Resolution

For typical Bunch Phase Durations ~10° phase resolution must be about 1°

For f=400 MHz phase resolution of 1° is equivalent to time resolution of 7 ps.

The equivalent bandwidth: ΔF =72 GHz.

Basic Limitation of Band Width of detectors using transfer of information about longitudinal distribution through beam electromagnetic field.

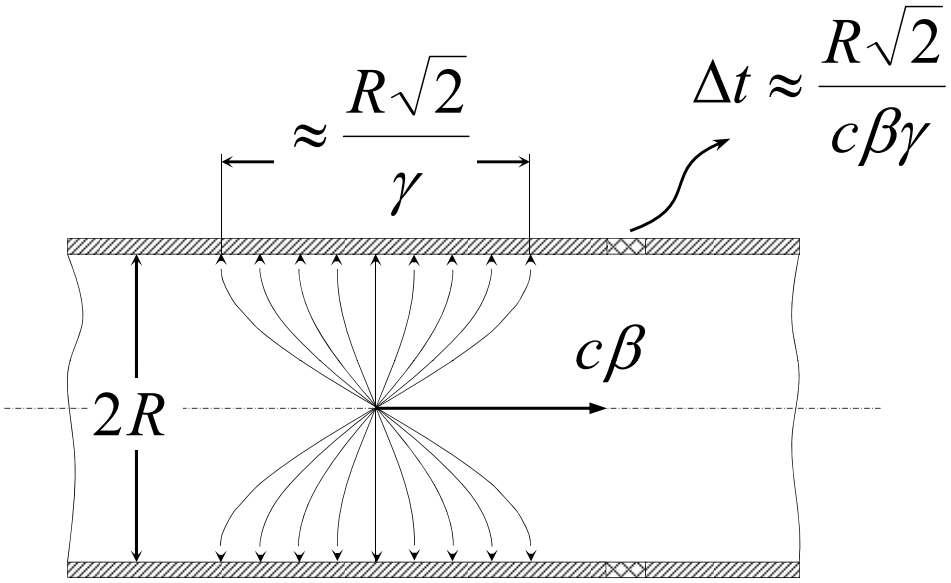

Configuration of electric field of point charge moving in a metal pipe.

For W=100 MeV and *R*=2 cm

***ΔF*=2.5 GHz.**

The way out is localization of space region where the information transfer occurs.

There are different possibilities to shrink the area of information transfer:

1. Cherenkov radiation;
2. Detached electrons in case of H- (including photo-detachment);
3. δ-electrons;
4. Transition radiation;
5. X-rays;
6. Low energy secondary electrons;
7. etc.

The main characteristics of Low Energy Secondary Electrons influencing BSM parameters

- Energy distribution
- Angular distribution
- Time dispersion (delay of emission)

These characteristics depend neither on type nor on energy of primary particles

Time dispersion is principal reason of limitation of BSM phase resolution.

Theoretical value of time dispersion for metals is 10^{-14}s ÷ 10^{-15}s.

Experiment gives the upper limit of time dispersion. Depending on the accuracy the upper limit was found to be from (4±2)ps to several hundred ps.

(Witkover R.L. A Non-destructive Bunch Length Monitor For a Proton Linear Accelerator // Nucl. Instr. And Meth. – 1976, V. 137, No. 2, - pp. 203-211)

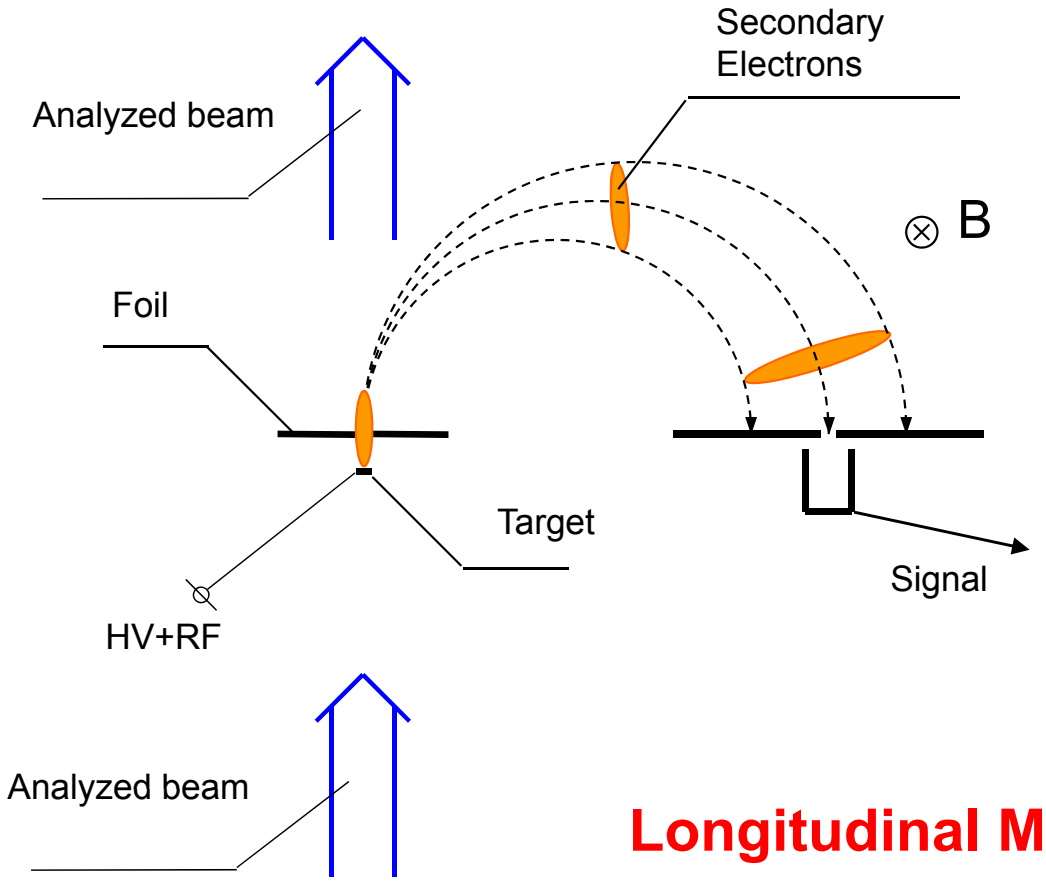

Longitudinal Modulation

I.A.Prudnikov et all. A Device to Measure Bunch Phase Length of an Accelerated Beam. USSR invention license. H05h7/00, No.174281, 1963 (in Russian).

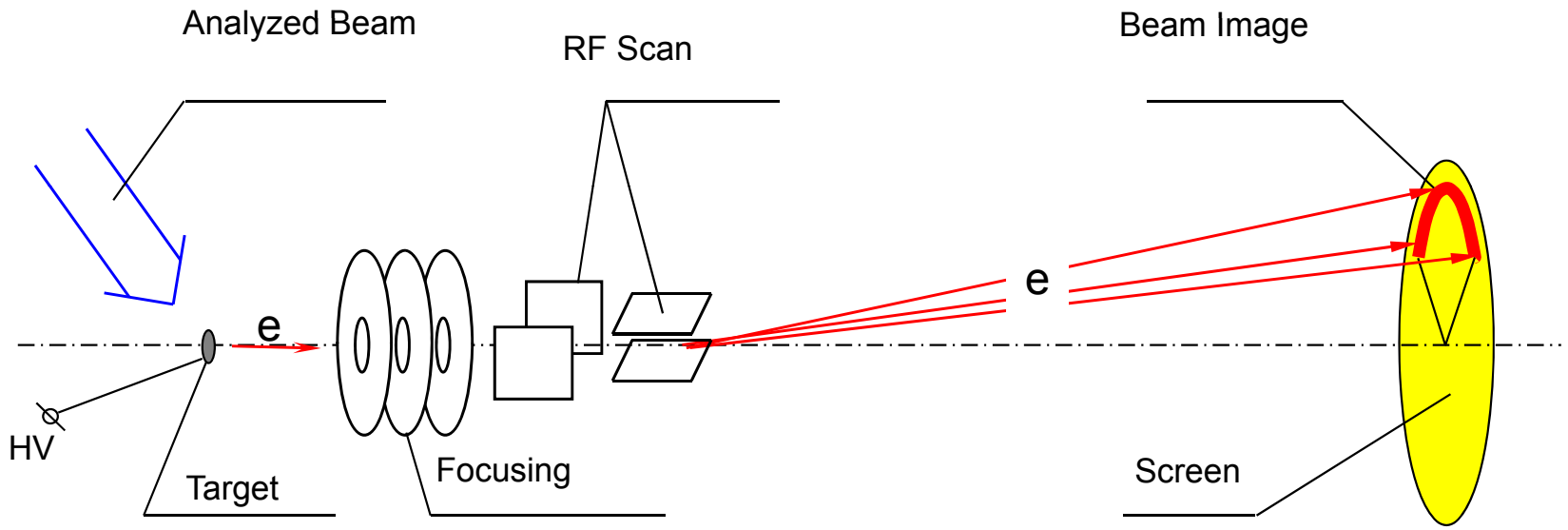

Transverse Circular Modulation

Configuration of INR Bunch Shape Monitor

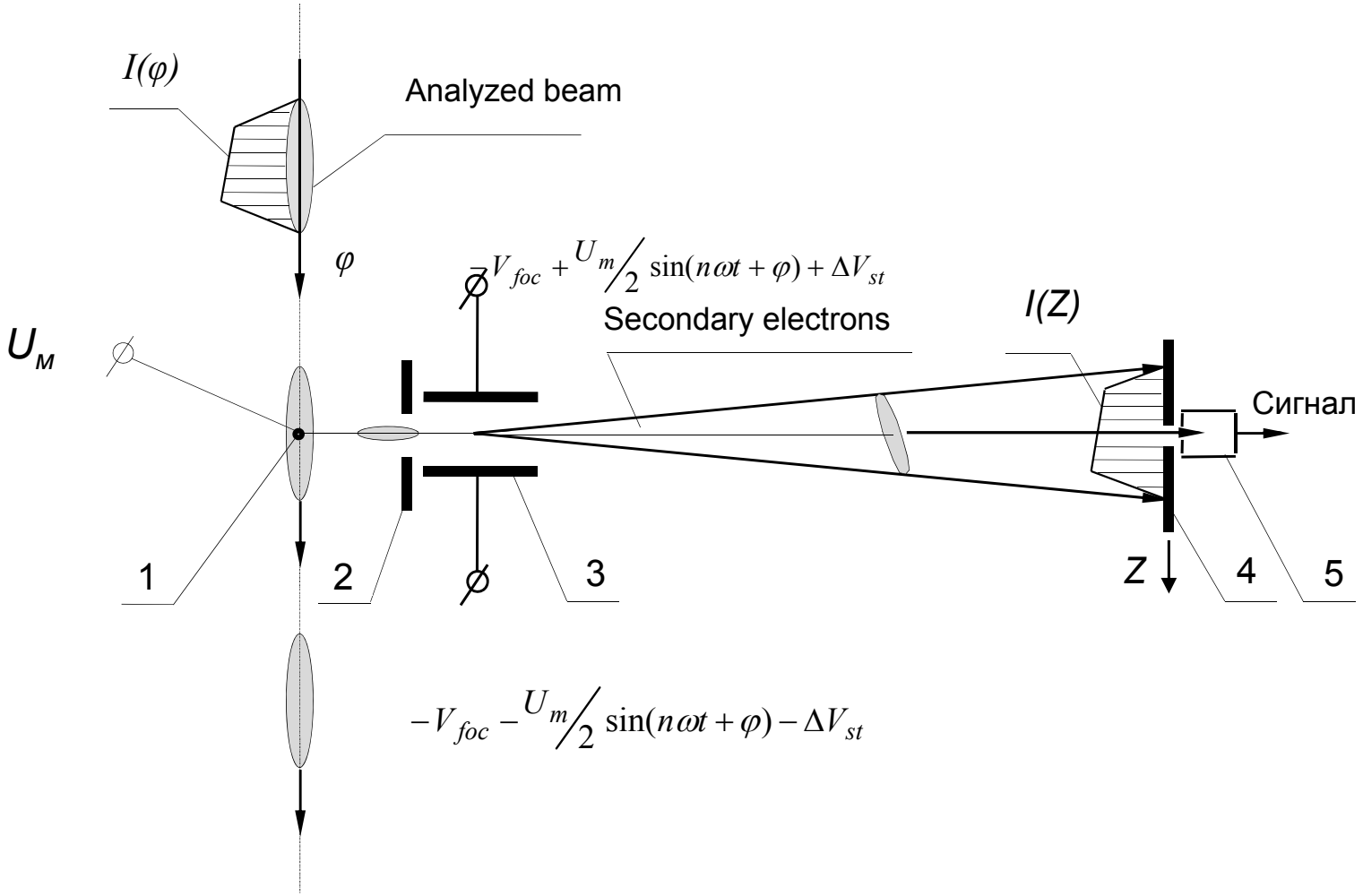

1 - target, 2 - input collimator, 3 - rf deflector combined with electrostatic lens, 4 - output collimator, 5 – collector of electrons

Example of electron trajectories

Trajectories for optimum focusing and rf deflection off

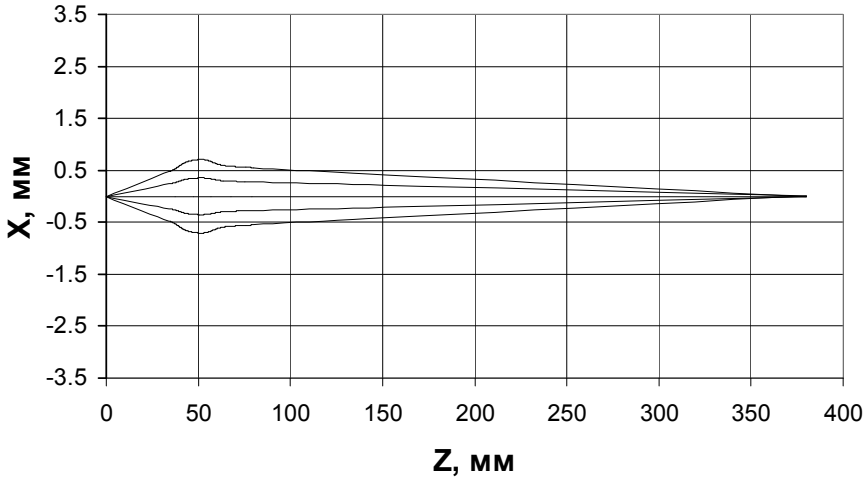

Trajectories electrons efor two groups of electrons entering rf deflector at different phases (phase difference equals 5° at f=1300 MHz)

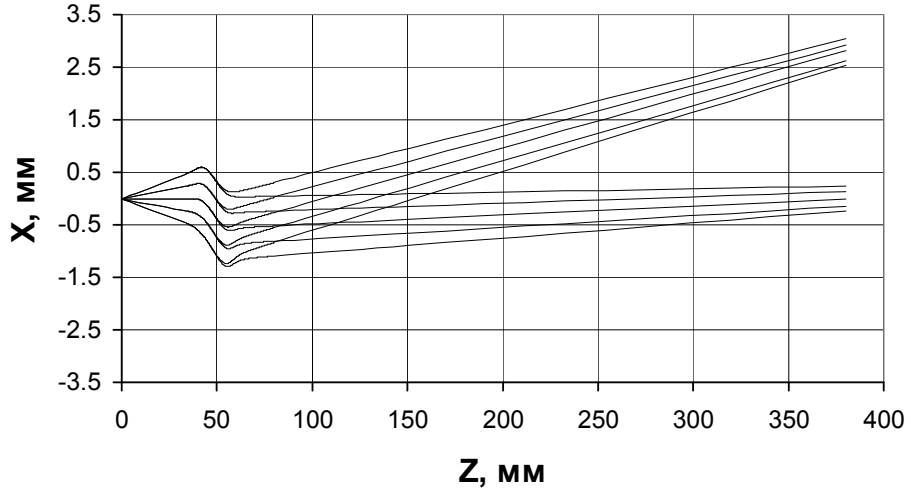

Evaluation of phase resolution

Displacement of electrons at output collimator

$$Z_L = Z_{\max} \sin\varphi$$

Phase resolution $$\Delta\varphi = \frac{\Delta Z_L}{Z_{\max}}$$

where ΔZ_L - full width at a half maximum of electron beam size for a δ-function bunch, Z_{max} – amplitude of electron displacement at output collimator.

In practice we use: $$\Delta\varphi = \frac{\sqrt{(2\sigma)^2 + (\Delta Z_0)^2}}{Z_{\max}}$$

where ΔZ_0 – focused beam size observed experimentally for rf deflection off, σ – rms size of the focused electron beam for a δ-function bunch

Dependence of Phase Resolution on Amplitude of Deflecting Voltage for different Input Collimators

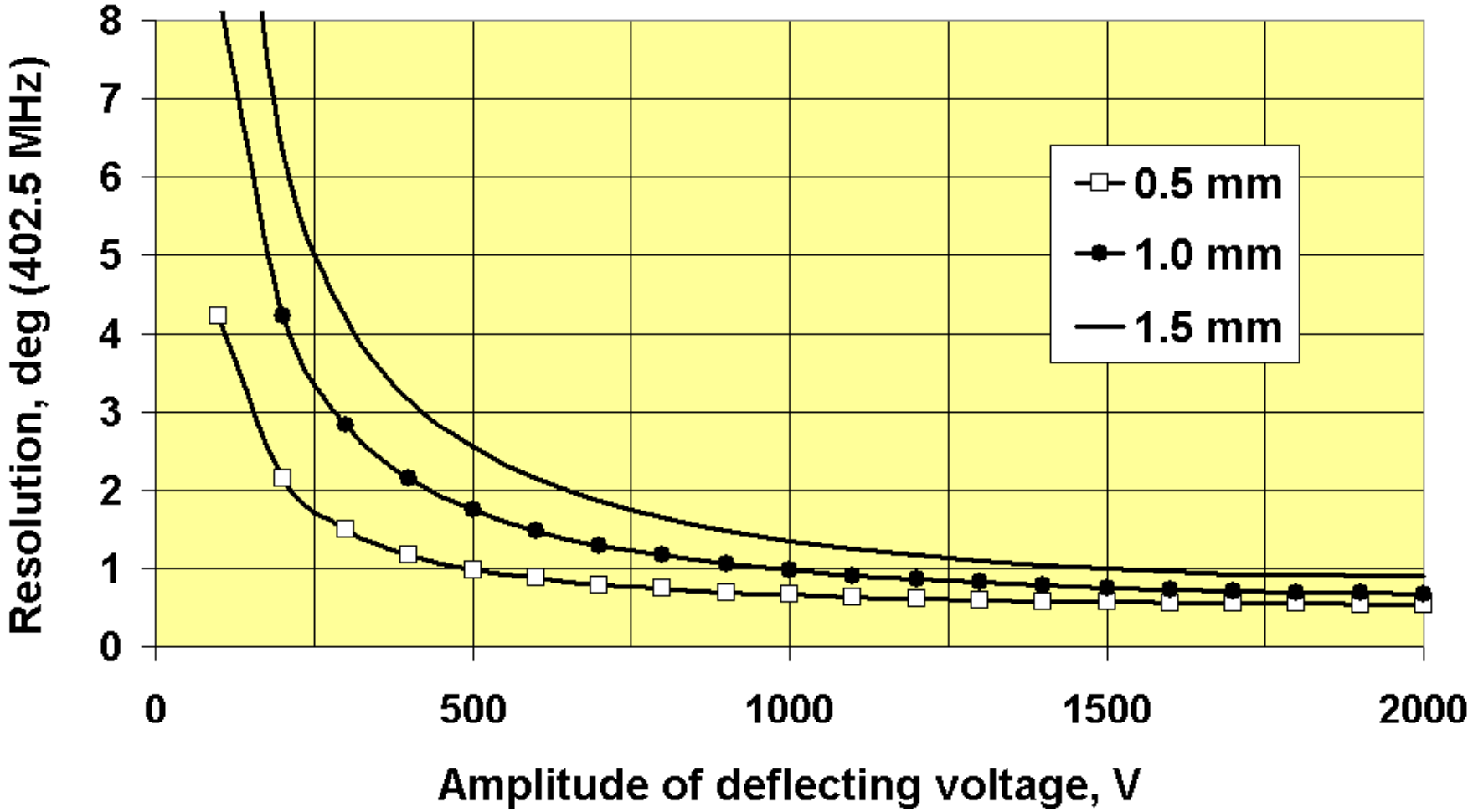

Influence of analyzed beam space charge

Two main effects:

- **Increasing of the focused beam size. This effect results in aggravation of phase resolution.**
- **Changing of the average position of the focused electron beam at the output collimator. This effect is the reason of the error of phase reading.**

Model 1 implies that the boundary conditions are kept constant while the bunch passes the detector chamber. The fields are found by multiple solving of a Poisson equation in the beam frame for fixed bunch positions as the bunch passes the chamber. Electrostatic fields found in the beam frame produce both electric and magnetic components in the lab frame. The field effecting secondary electrons is represented as a superposition of electromagnetic field of the bunch and an unperturbed electrostatic field due to target HV potential (-10 kV). We suppose that the target potential is kept invariable and hence the model is valid if the time of flight of the bunch through the wire $\Delta\Phi/(360f)$ is essentially smaller than the time of signal propagation from the target center to the holders $L/(2c)$. Here $\Delta\Phi$ is the bunch duration (deg), f- bunch repetition frequency, L - target length and c - velocity of light. In our case L =45 mm and the model is supposed to be valid for $\Delta\Phi$ essentially larger than 10°.

Model 2 is used if $\Delta\Phi/(360f)$ is smaller than $L/(2c)$. Electrostatic fields of the bunch in the beam frame are found by Poison equation multiple solving for boundary conditions with the target absence. The field effecting secondary electrons is found similarly to the first model as a superposition of electromagnetic field of the bunch and an unperturbed electrostatic field due to HV potential applied to the target.

Influence of analyzed beam space charge

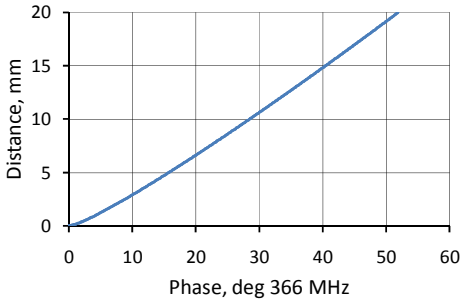

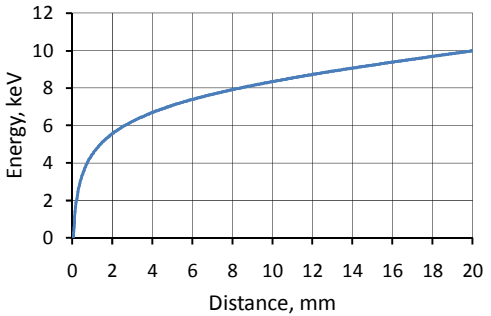

Distance passed by electron versus time and electron energy versus distance

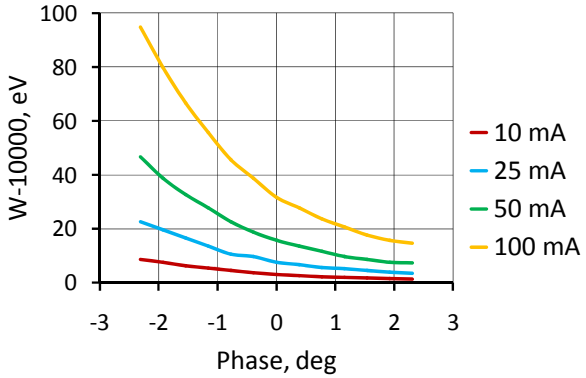

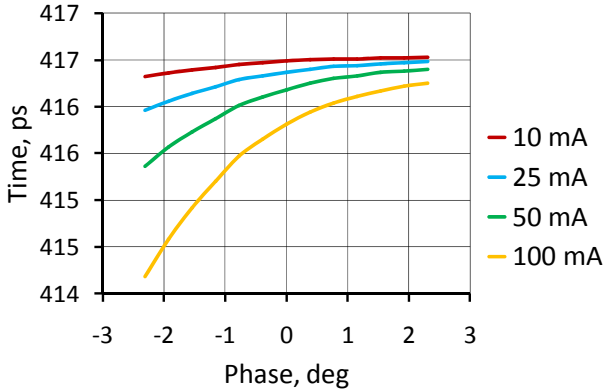

Energy deviation and time of flight of electron from target to input collimator W=200 MeV, H-minus, σy=1.2 mm, σz=1.2 mm, σφ=1.1°, Zo=0 mm, f=366 MHz (Model #2)

Influence of analyzed beam space charge

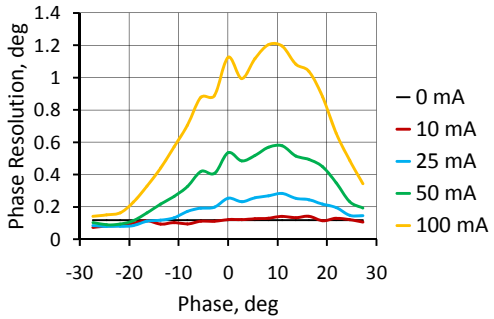

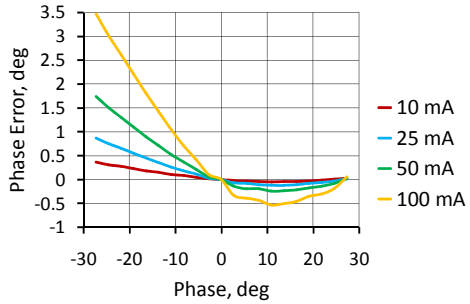

Resolution and phase reading error for W=3 MeV H-minus, σy=2.6 mm, σz=2.6 mm, σφ=13º, Zo=0 mm, f=366 MHz (Model #1)

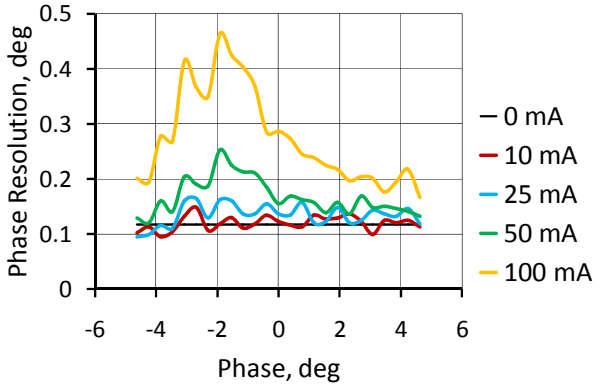

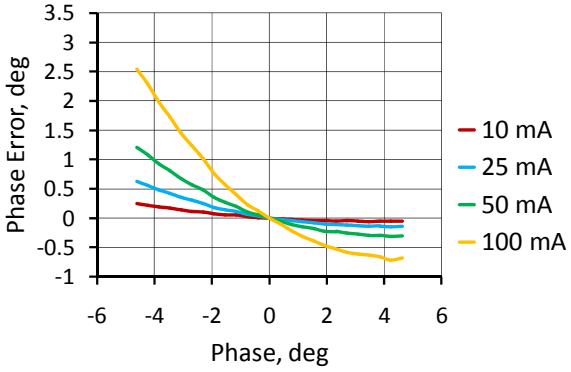

Resolution and phase reading error for W=200 MeV, H-minus, σy=1.2 mm, σz=1.2 mm, σφ=2.1º, Zo=0 mm, f=366 MHz (Model #2)

Influence of currents induced in the target by an analyzed beam

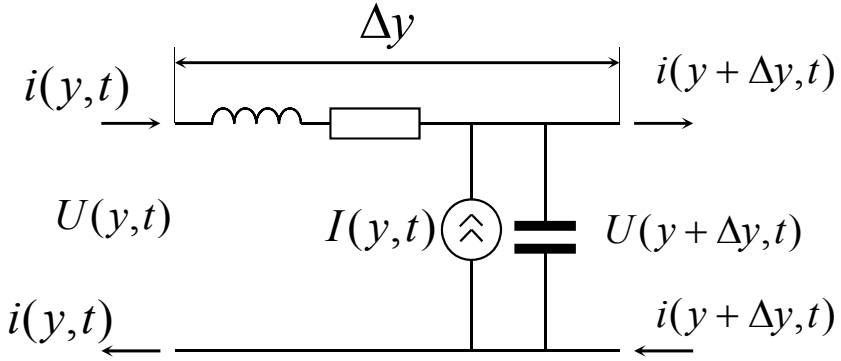

$$\frac{\partial U(y,t)}{\partial y} = L\frac{\partial i(y,t)}{\partial t} + Ri(y,t)$$

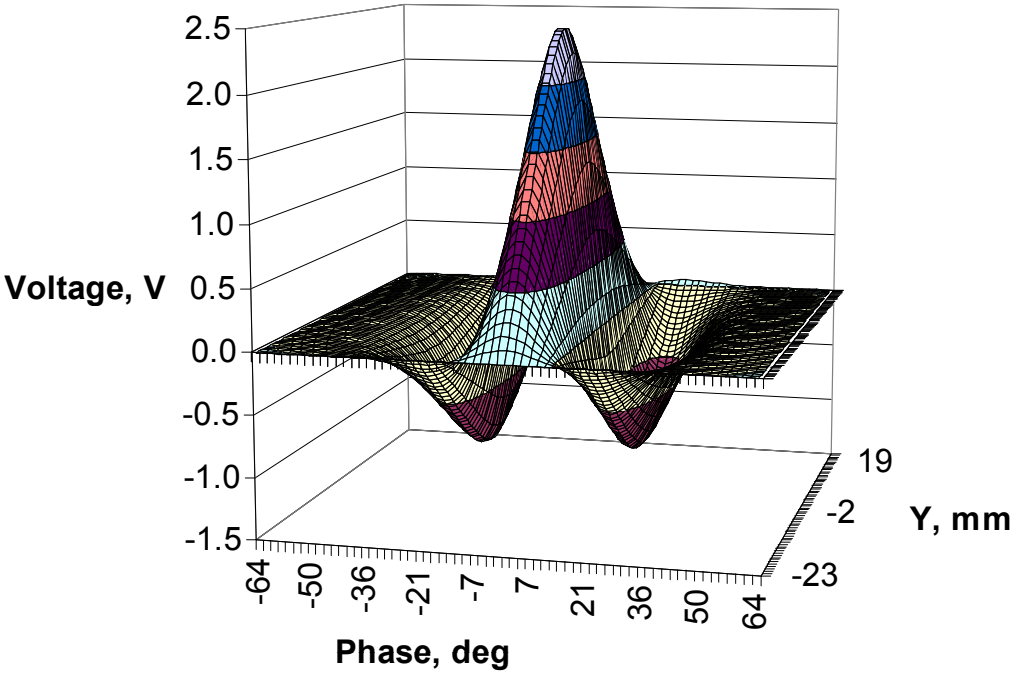

Result of calculation of target voltage variation for 150 mA CERN Linac-2 beam

Influence of secondary emission current

$$\frac{\partial^2 U}{\partial y^2} - LC\frac{\partial^2 U}{\partial t^2} - RC\frac{\partial U}{\partial t} = RI + L\frac{\partial I}{\partial t}$$

Transmission line current generator due to secondary emission

$$I(y,t) = \frac{I_0 T}{2\pi\sigma_y\sigma_t} e^{-\frac{\left(t-\frac{T}{2}\right)^2}{2\sigma_t} - \frac{(y-y_0)^2}{2\sigma_y}}$$

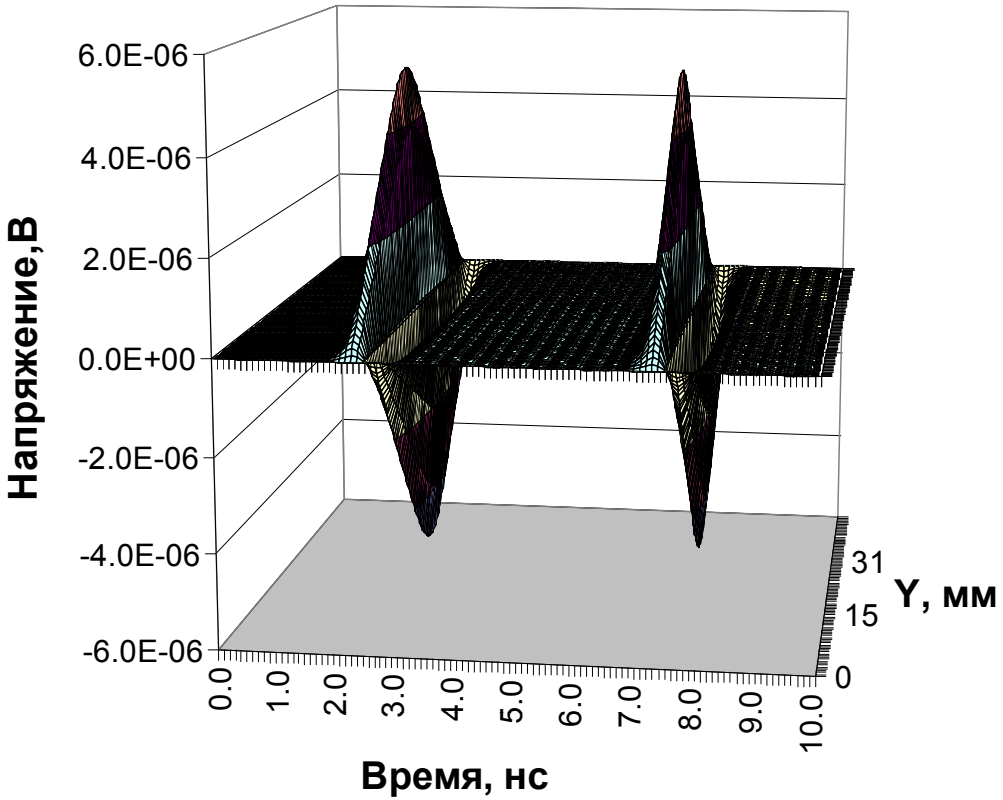

Result of calculation of target voltage variation for 150 mA CERN Linac-2 beam

Results of experimental test of space charge influence in INR linac at 20 MeV beam

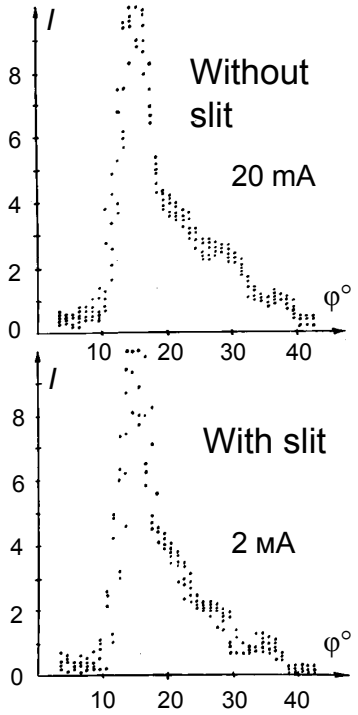

PECULIARITIES OF BUNCH SHAPE MEASUREMENTS OF H-MINUS BEAMS

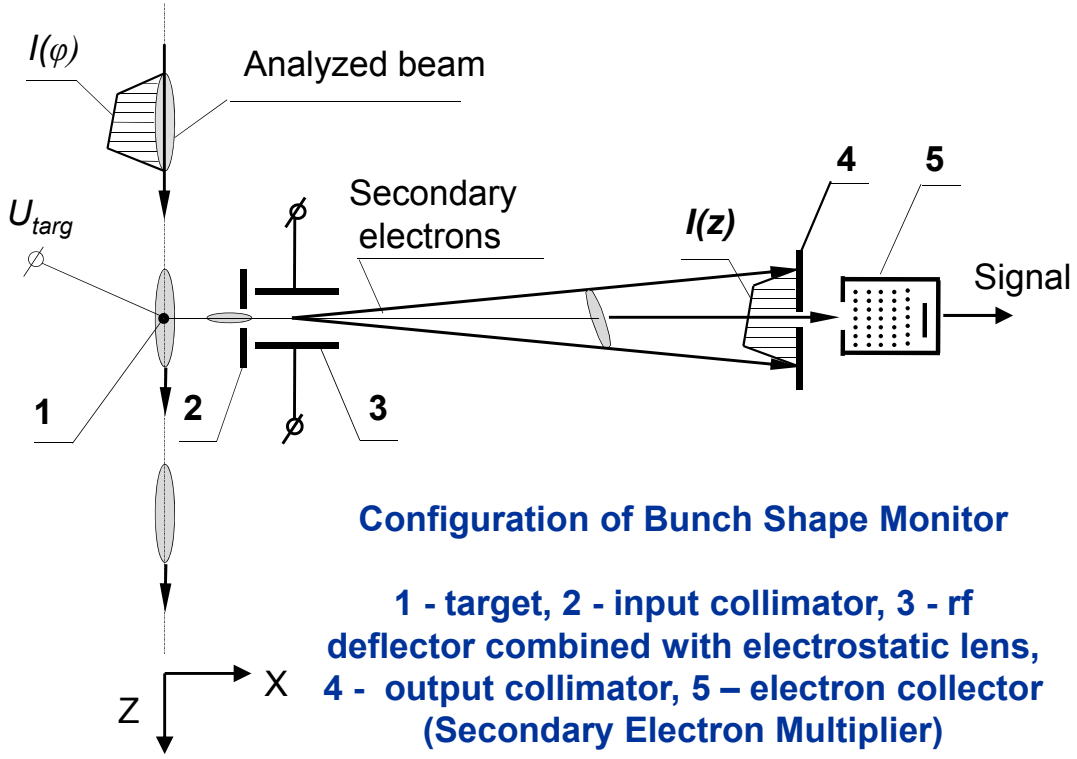

Configuration of Bunch Shape Monitor

1 - target, 2 - input collimator, 3 - rf deflector combined with electrostatic lens, 4 - output collimator, 5 – electron collector (Secondary Electron Multiplier)

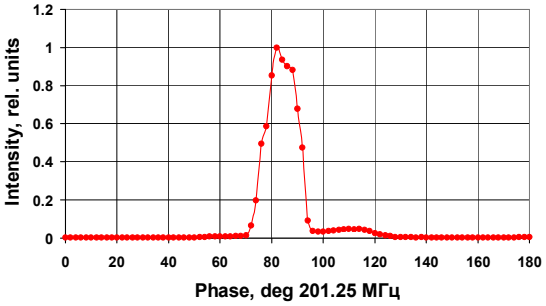

Bunch shape measurement of 10 MeV H^- beam (DESY Linac-3)

A. Mirzoyan et al. Voprosy Atomnoi Nauki i Tekhniki. V. 4,5 (31,32), Kharkov, 1997, p. 92,

(in Russian)

For tungsten $\frac{1}{n\sigma} << \frac{R}{\rho}$

where *σ* – total electron loss cross section

***n*- number of atoms per 1 cm^3**

***R* - CSDA range, g/cm^2**

***ρ* - density**

Simulation of interaction of electrons with a target (Geant4)

Relation of electron and ion energies $W_e = W_i \, m_e / m_i$

W_i, MeV	W_e, keV
10	5.44
100	54.4
1000	544

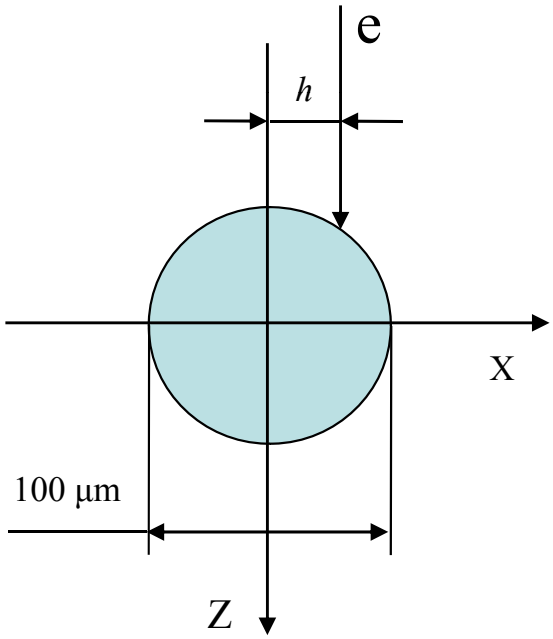

h= 0μm, 1μm, 2μm….. 49μm

N=100000 for each *h*

For negative *h* - symmetry

Results of simulation

(Red lines – electrons, green lines – photons)

h=0 μm

h=30 μm

h=49 μm

W=54.4 keV

(100 MeV)

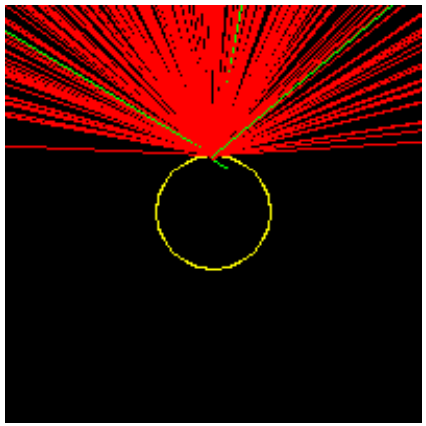

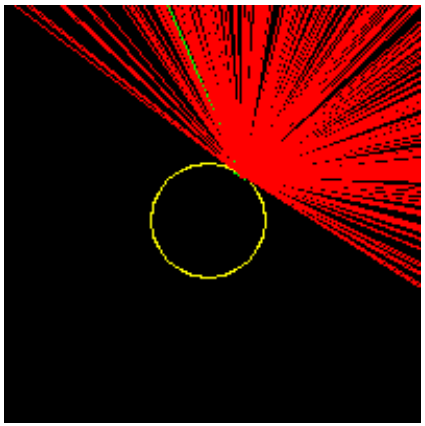

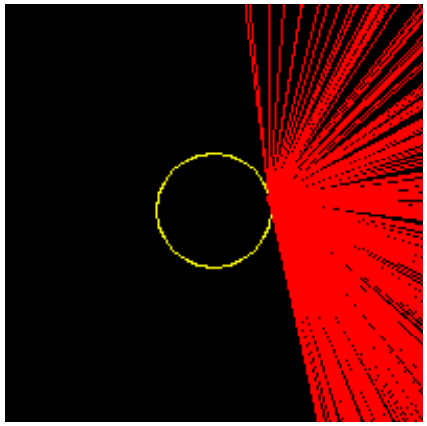

W=163.2 keV

(300 MeV)

W=326.4 keV

(600 MeV)

W=544 keV

(1000 MeV)

h=0 μm

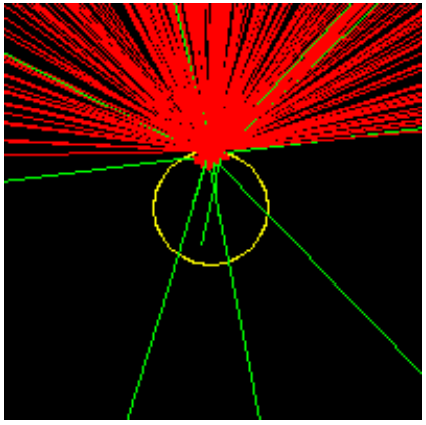

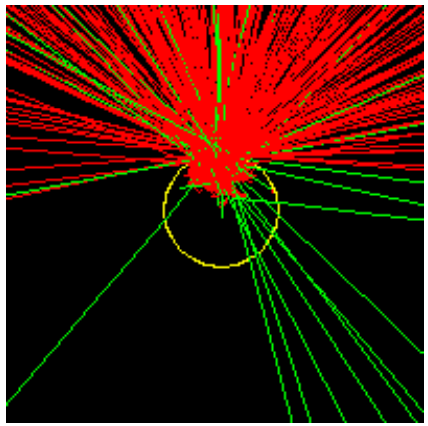

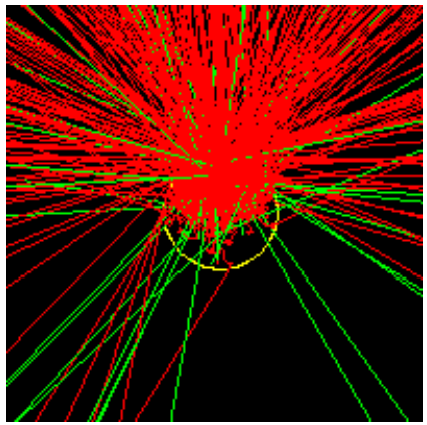

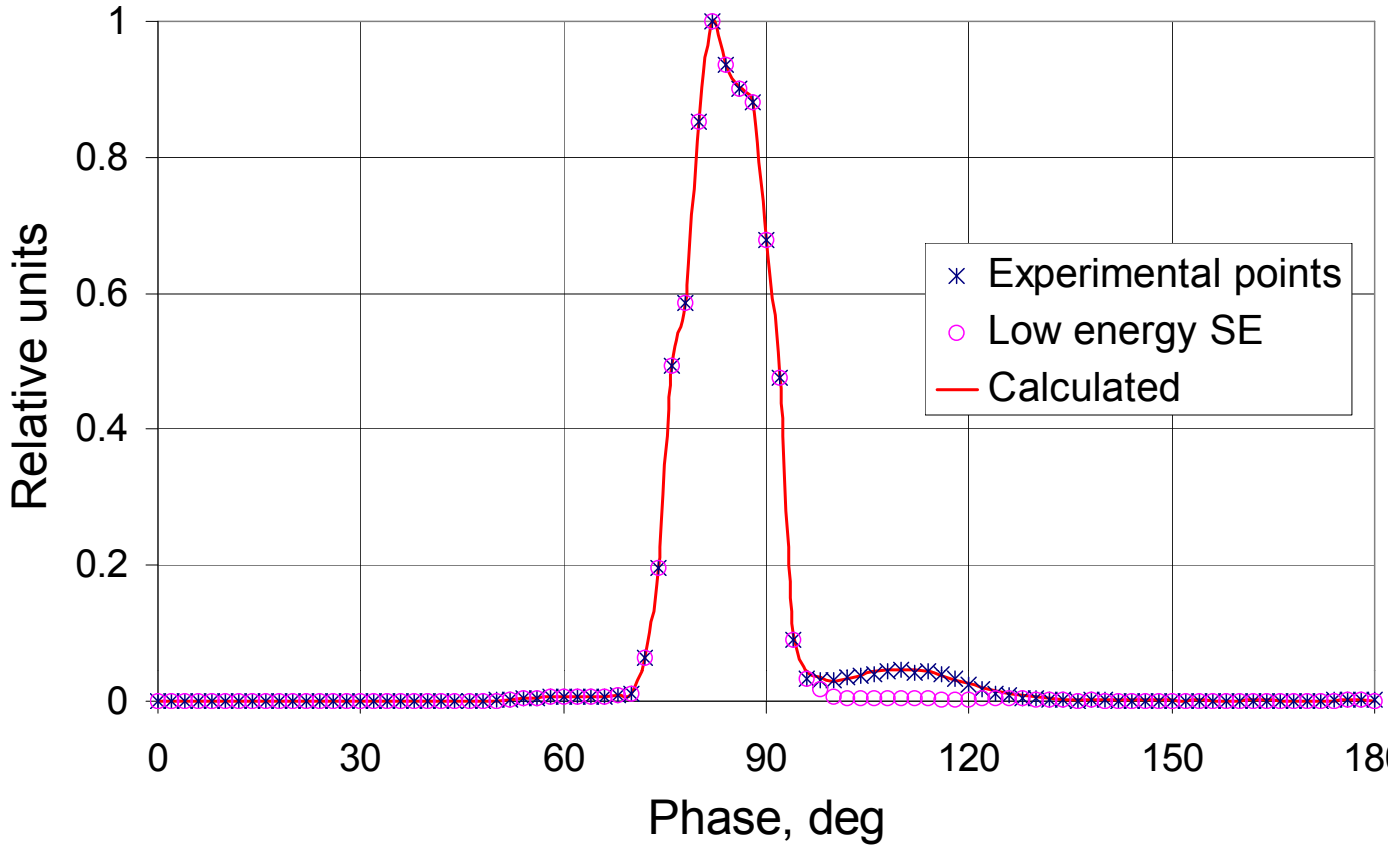

Experimental and calculated longitudinal distributions of 10 MeV beam

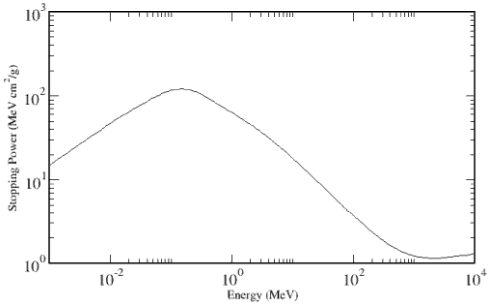

Electronic stopping power in tungsten vs proton energy

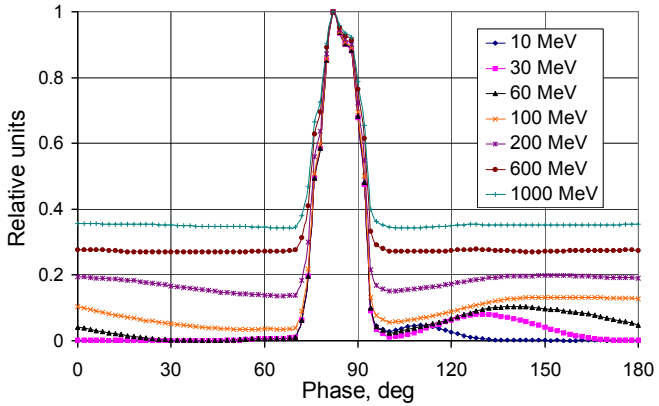

Prediction of experimental longitudinal distributions behavior at different energies

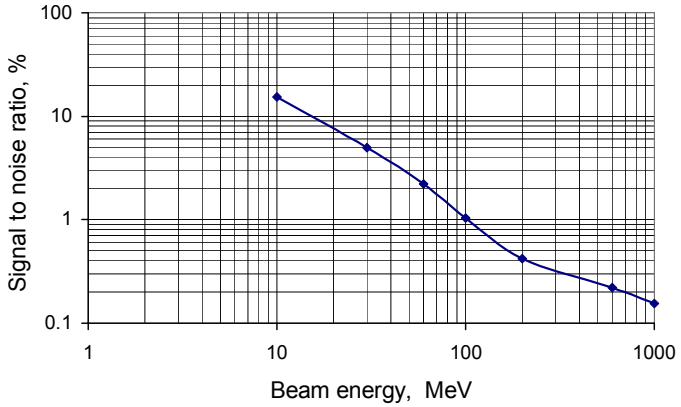

Prediction of integrated signal to noise ratio behavior

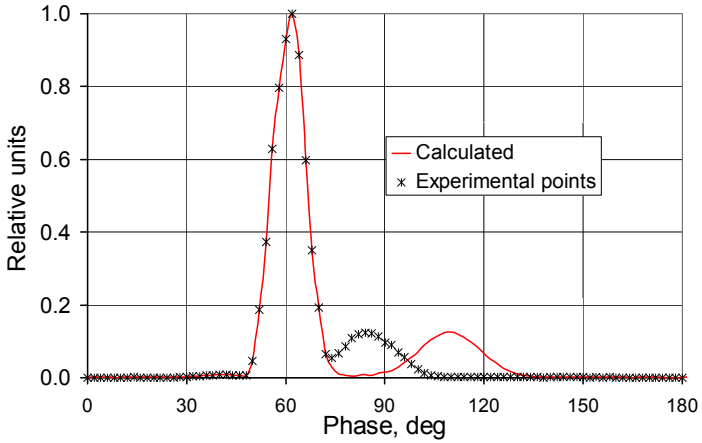

Experimental and calculated longitudinal distributions of 30 MeV beam (Integrated signal to noise ratio = 4.4)

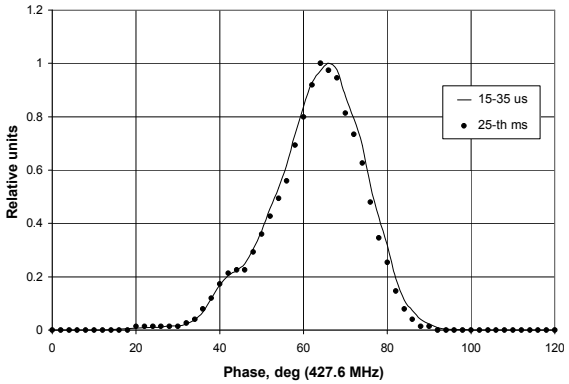

Experimental longitudinal distribution of 2.5 MeV beam (SSC, 1993)

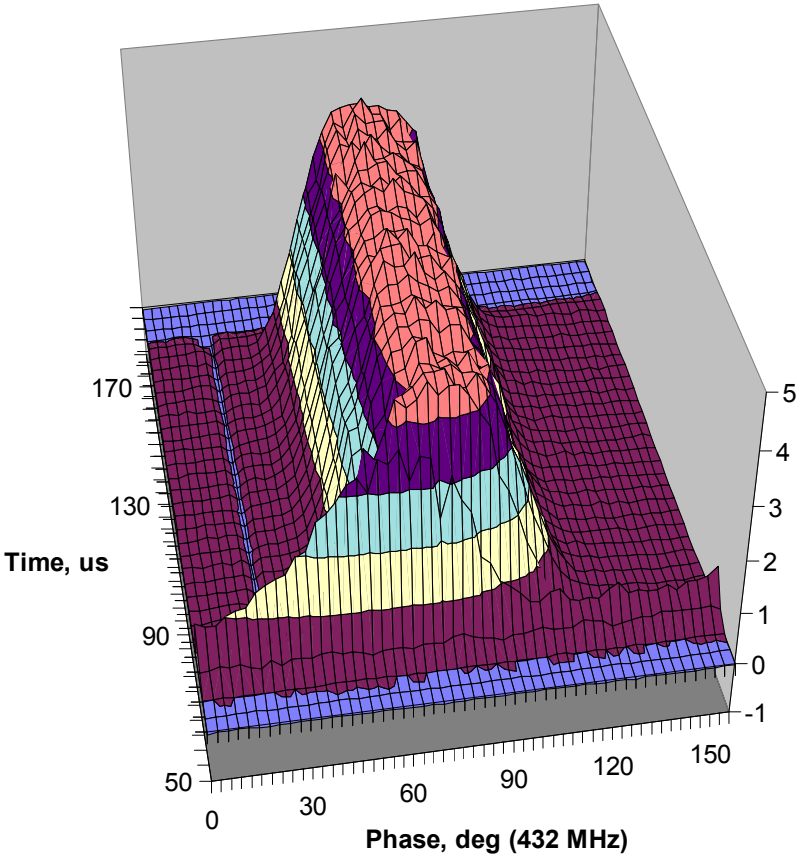

Experimental longitudinal distribution of 3.0 MeV beam (KEK, 1996)

BSM with electron energy separation

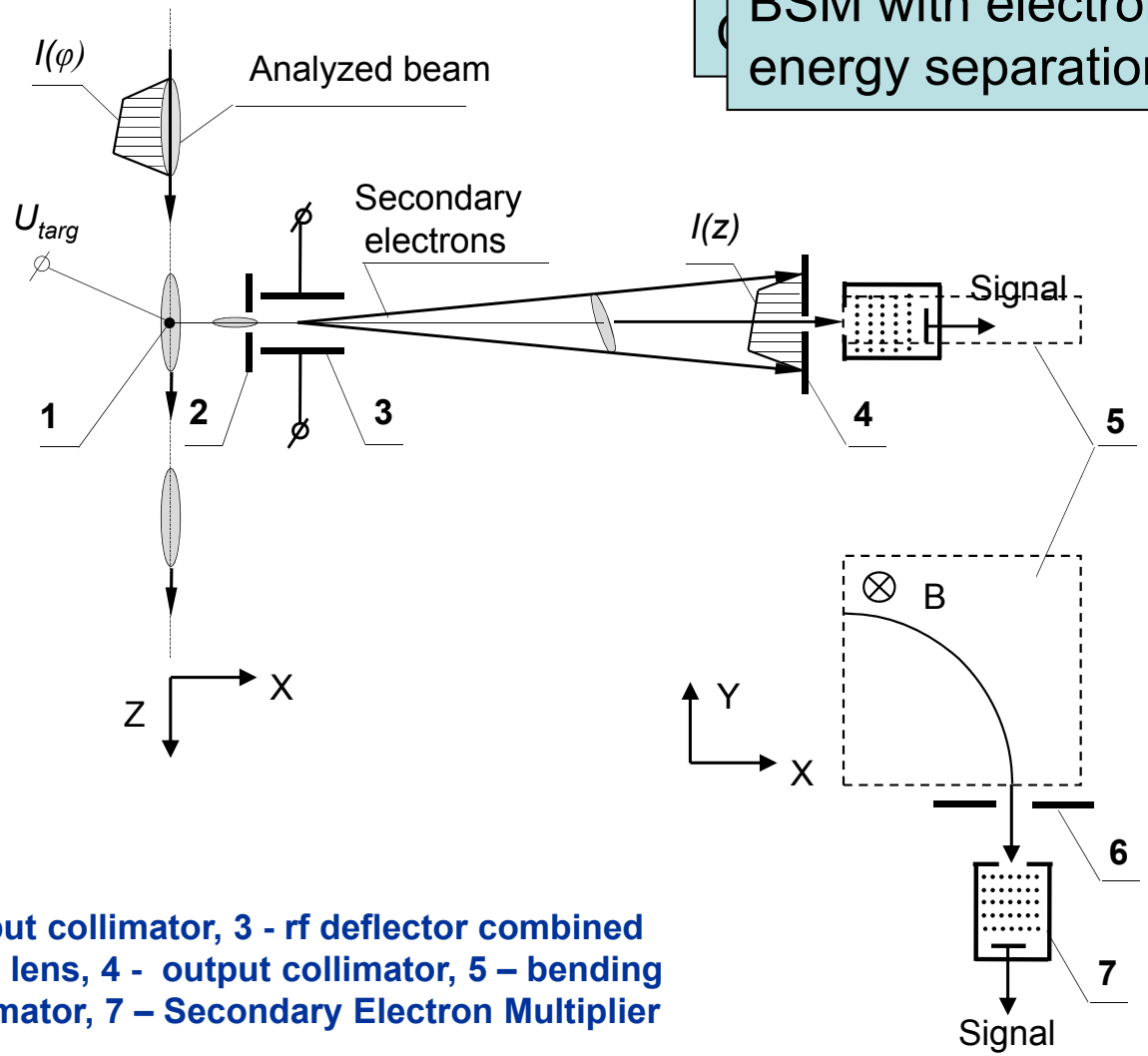

1 - target, 2 - input collimator, 3 - rf deflector combined with electrostatic lens, 4 - output collimator, 5 – bending magnet, 6 – collimator, 7 – Secondary Electron Multiplier

Search for detached electrons influence

Measurements of longitudinal distribution for different set points of separating magnet

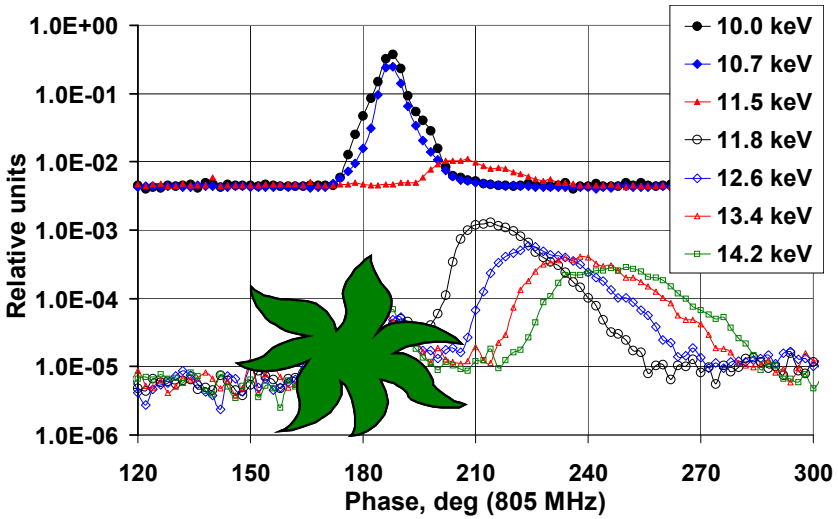

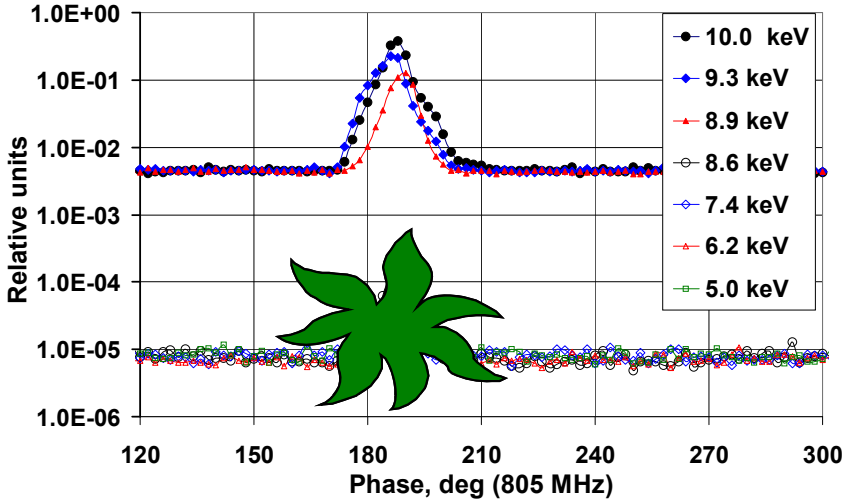

The first INR Bunch Shape Monitor

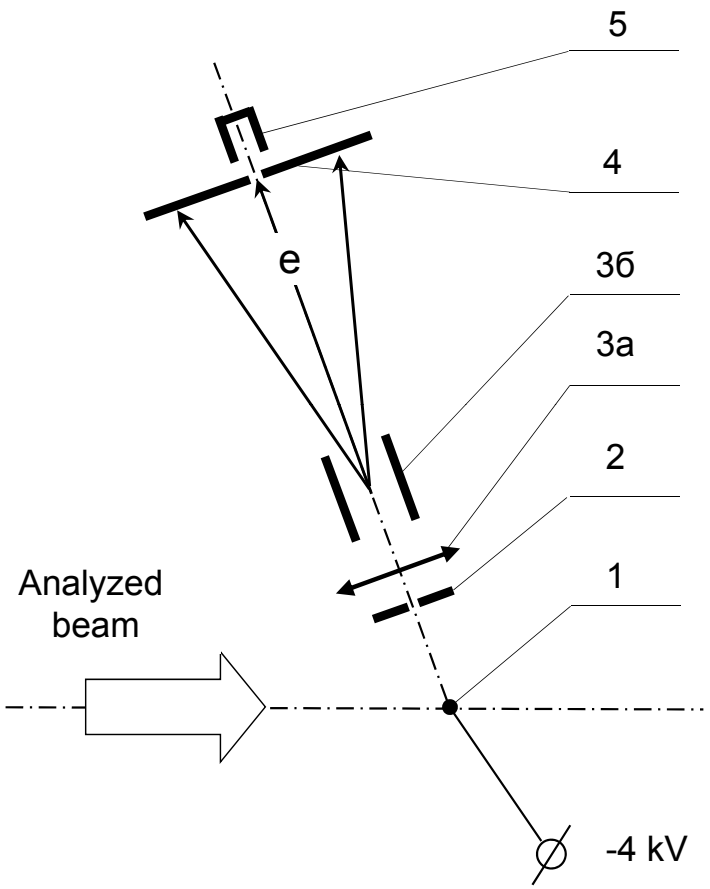

(1 – target, 2 – input collimator, 3a – electrostatic lens, 3б – rf deflector, 4 – output collimator, 5 – collector of electrons)

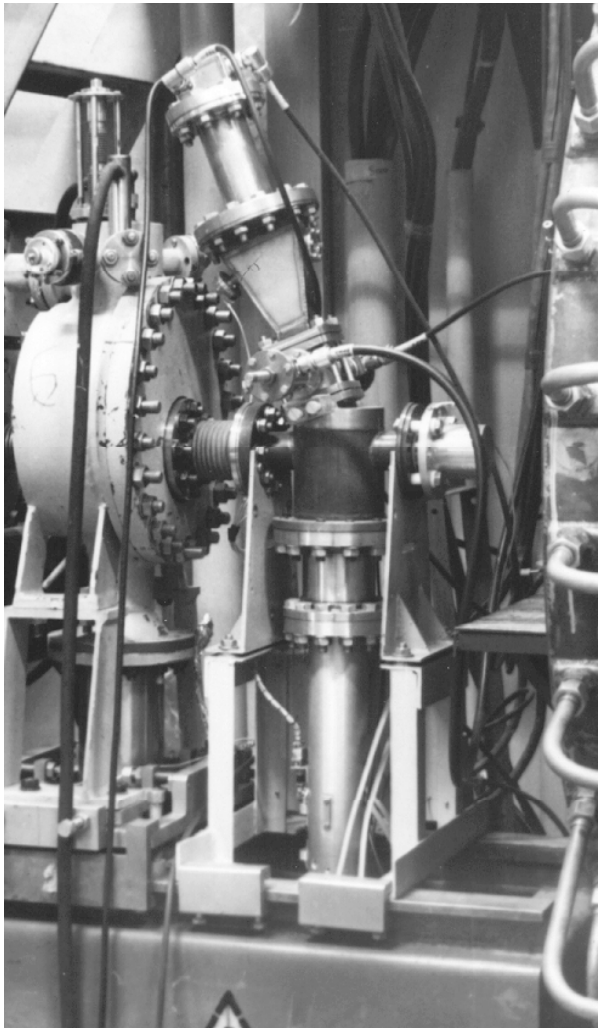

Detector Modifications

1. Bunch Shape Monitor (BSM)
2. Bunch Length and Velocity Detector (BLVD)
3. Detector of Thee-Dimensional Distribution of Particles in Bunches (3D-BSM)

BSMs for DESY Linac-3 and CERN Linac-2

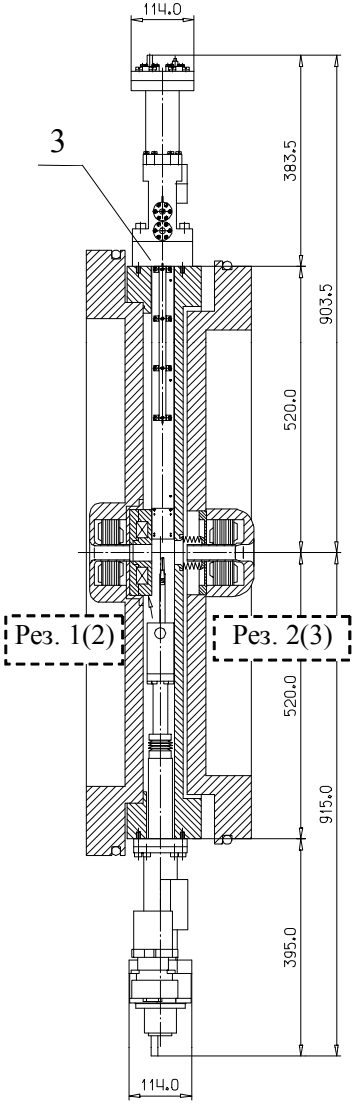

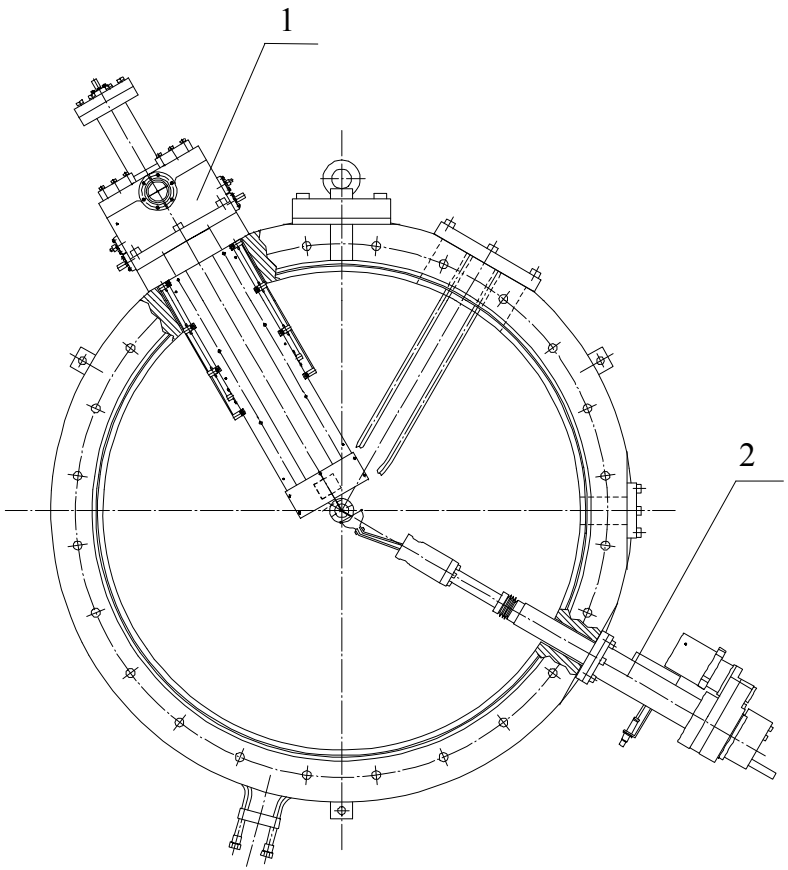

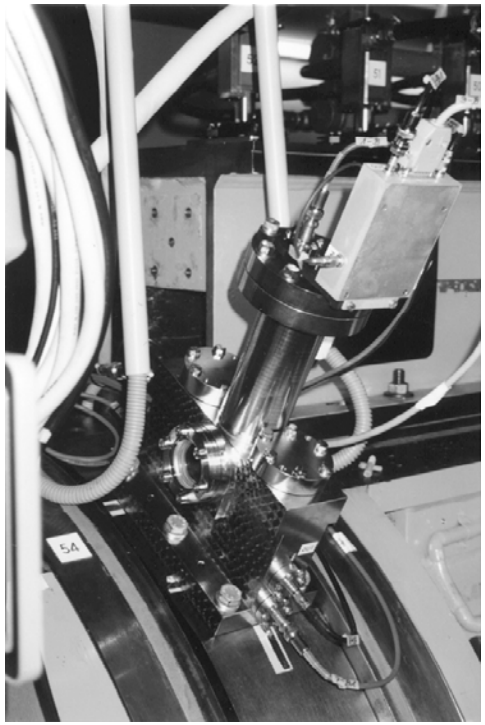

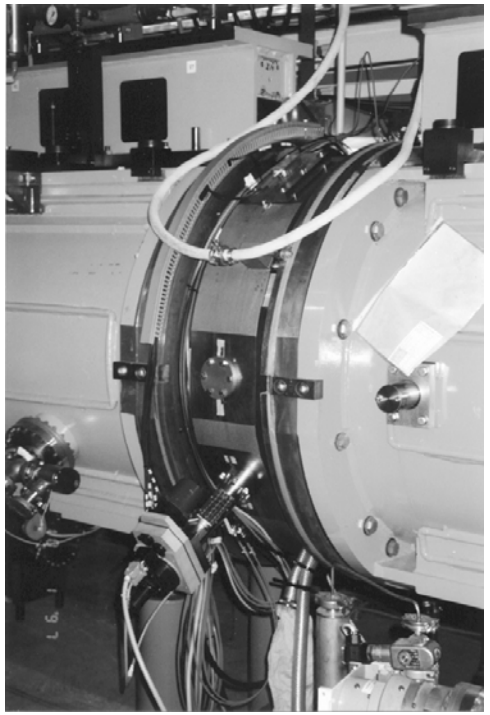

General View of SNS test BSM

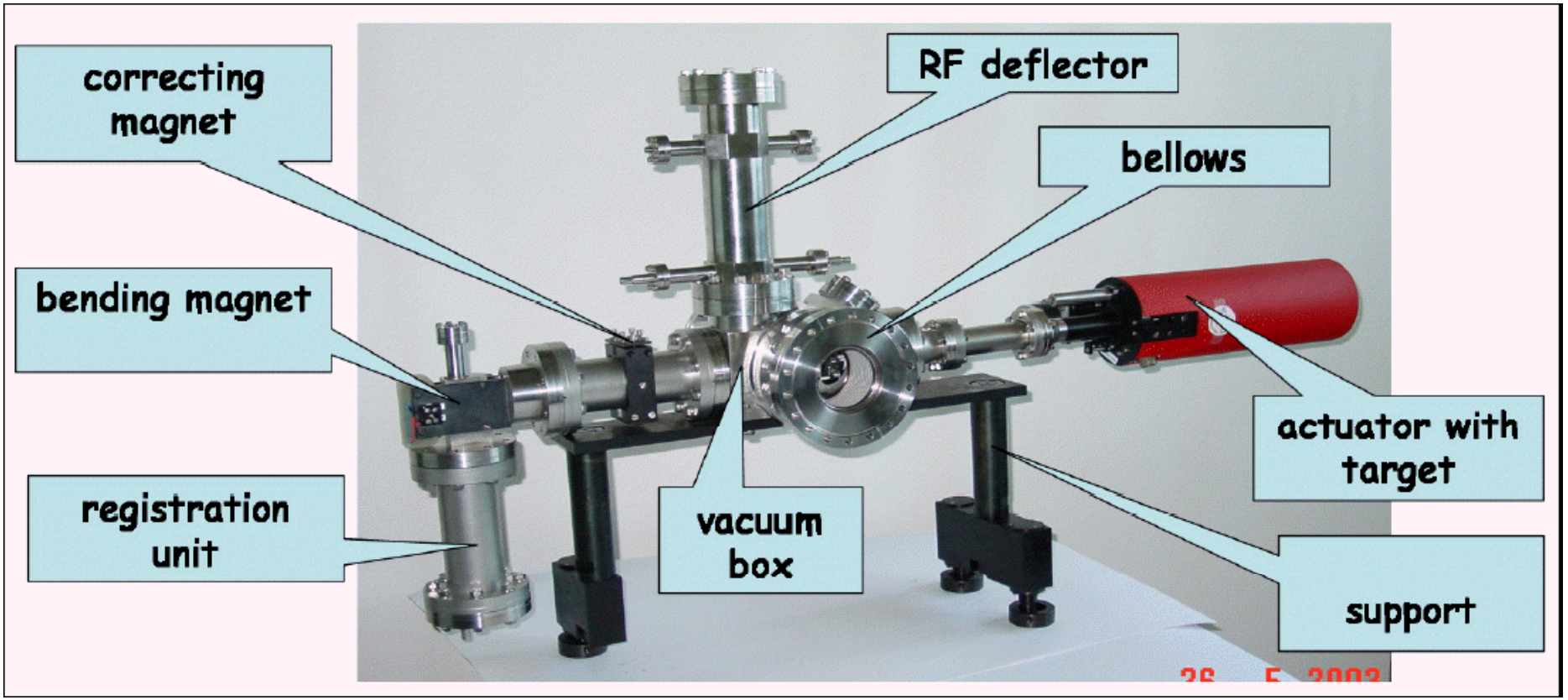

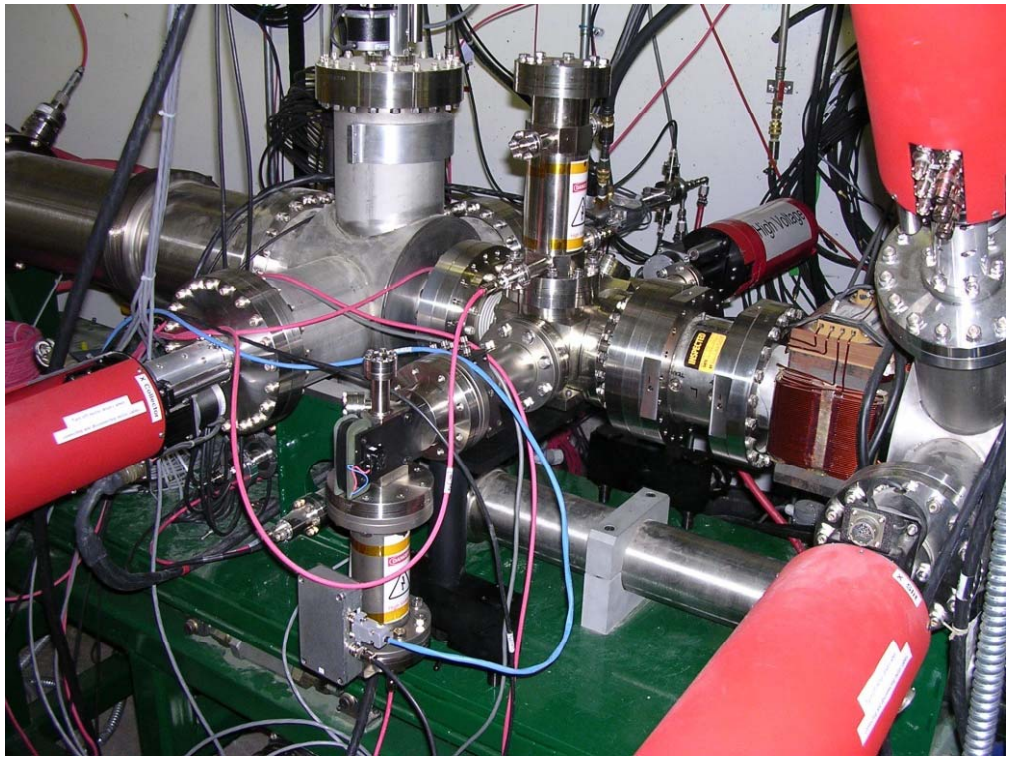

BSM installed in D-plate (August 2003)

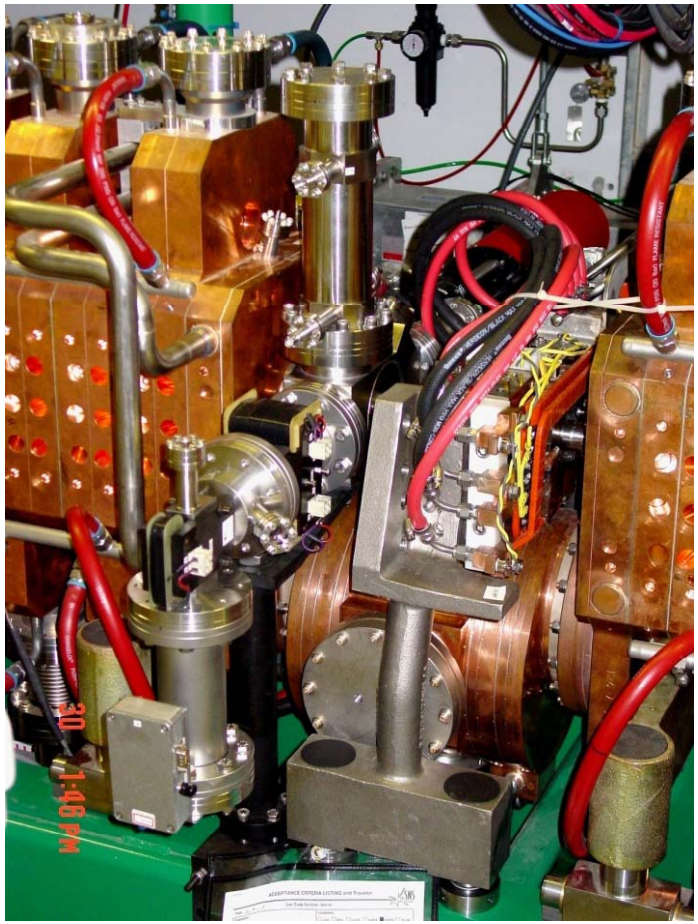

BSM installed in intersegments 7, 9 and 11 of CCL Module #1 (July 2004)

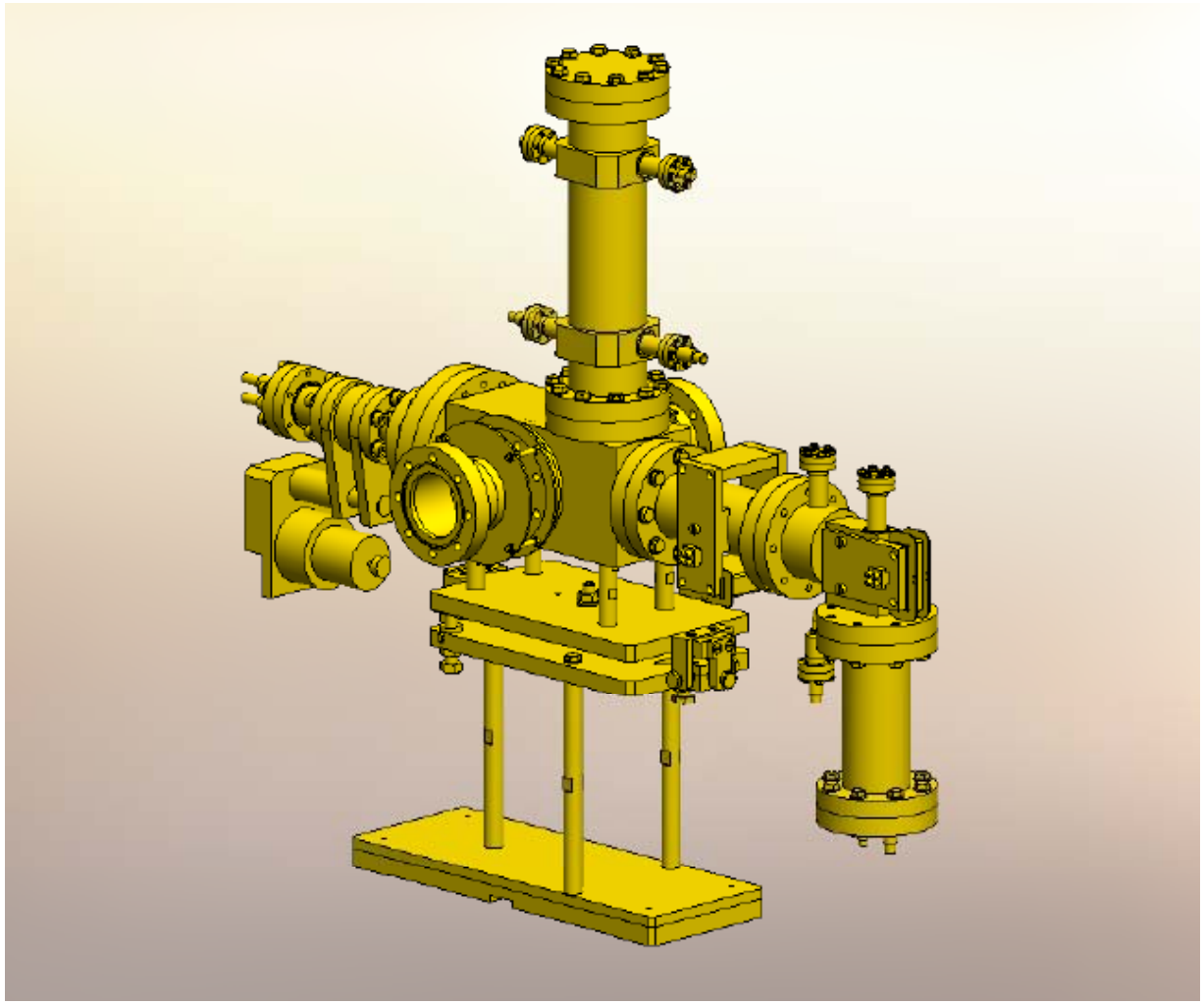

BSM for new CERN Linac-4

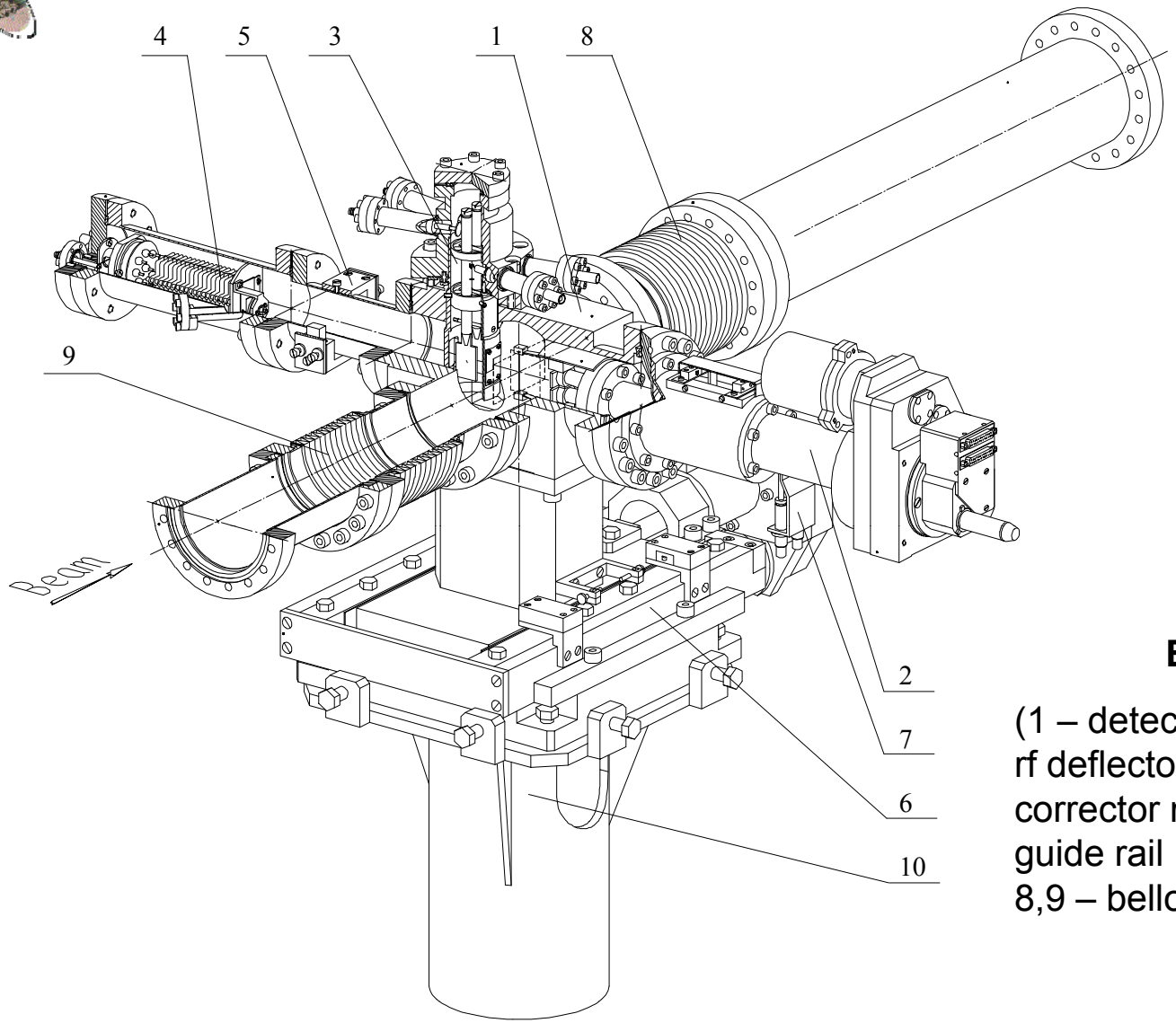

BLVD for DESY Linac-3

(1 – detector body, 2 – target actuator, 3 – rf deflector, 4 – registration unit, 5 – corrector magnet, 6 – longitudinal motion guide rail , 7 – longitudinal motion actuator, 8,9 – bellows, 10 – support)

Three Dimensional Bunch Shape Monitor (3D-BSM)

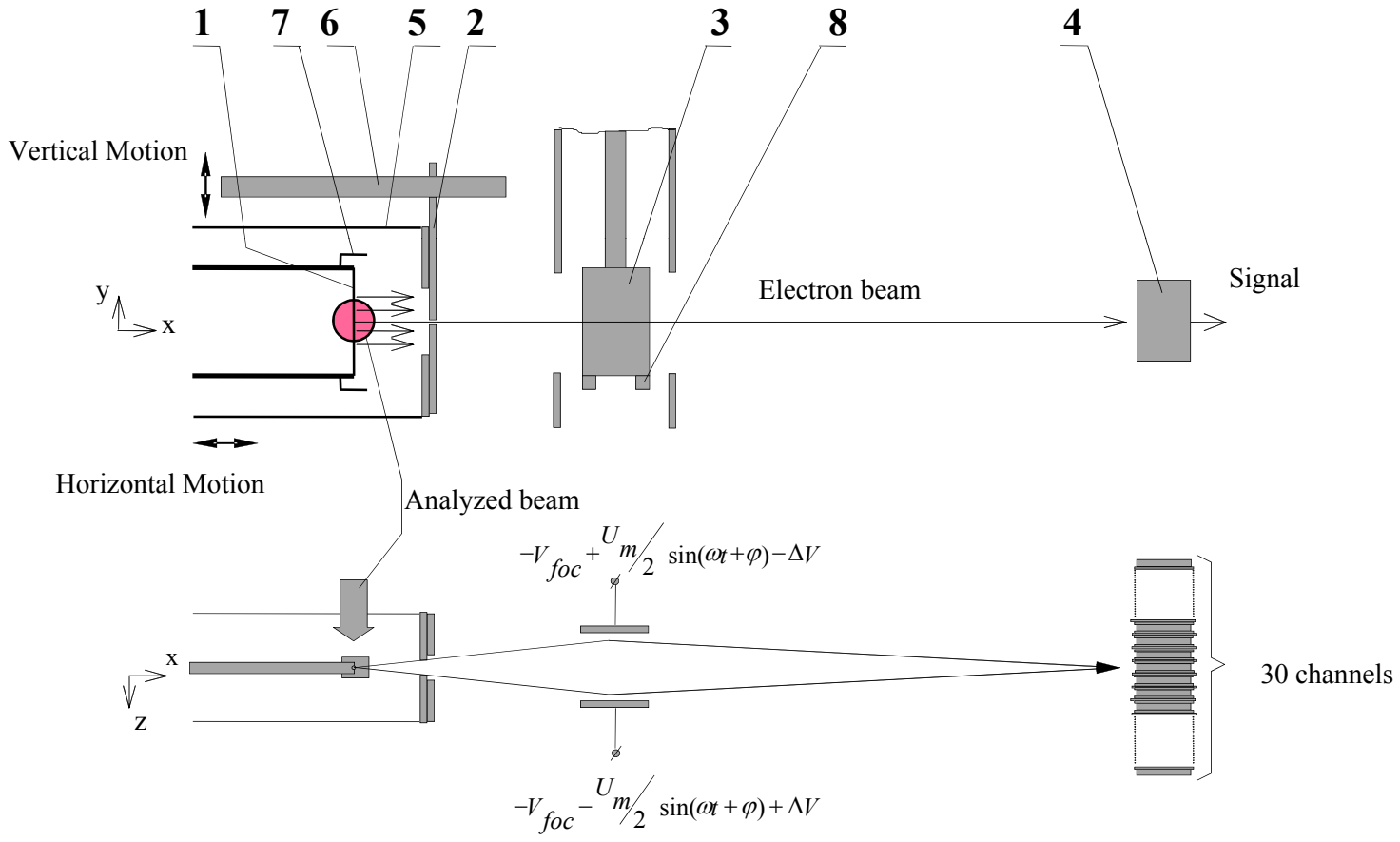

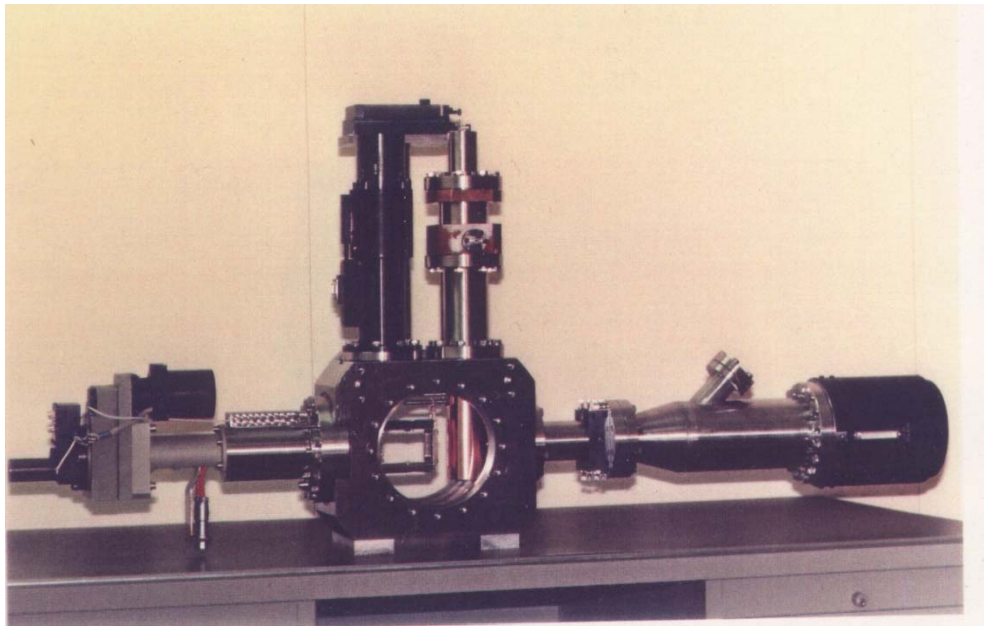

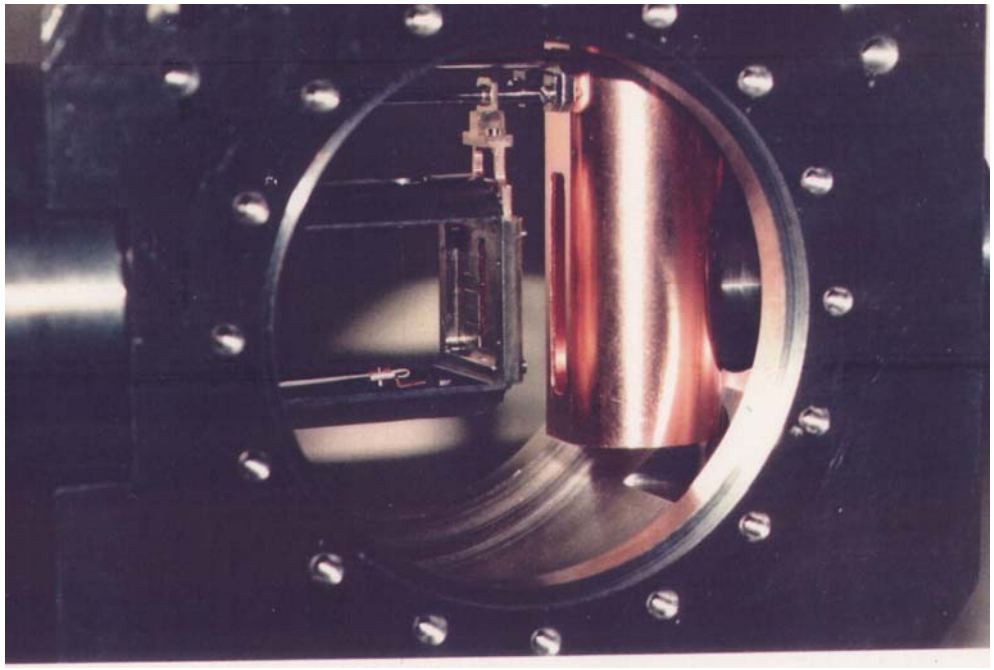

3D-BSM view

Examples of rf deflectors for BSMs.

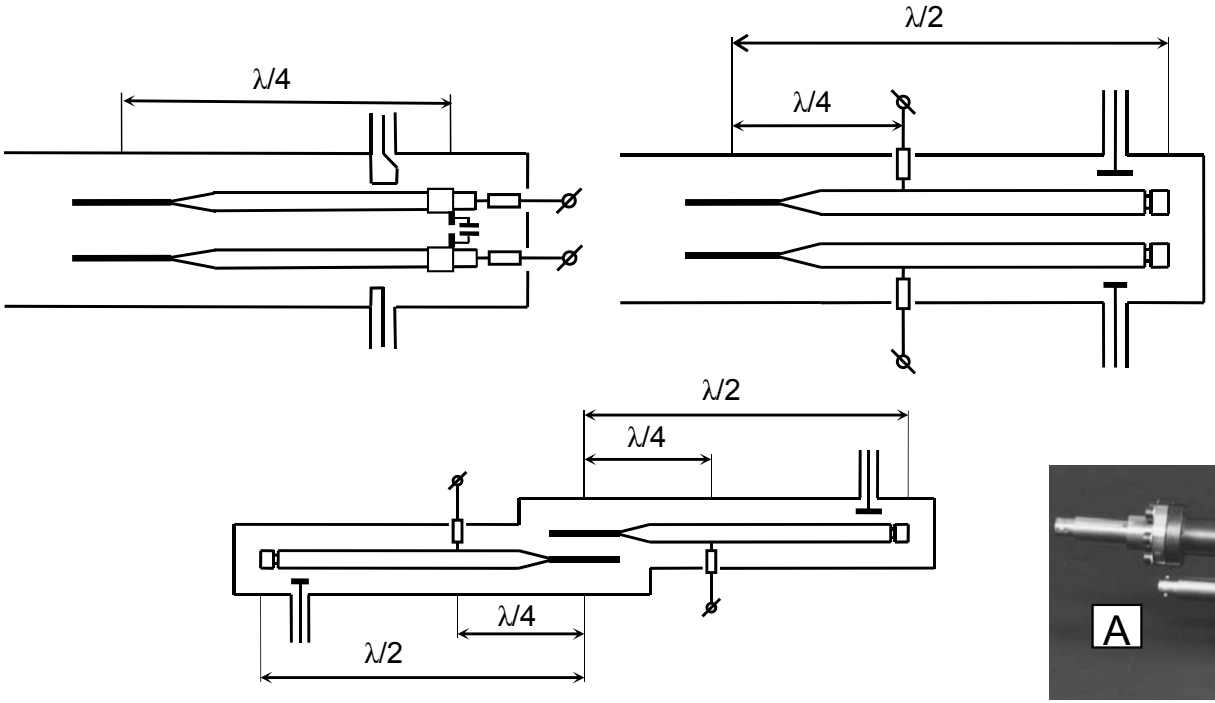

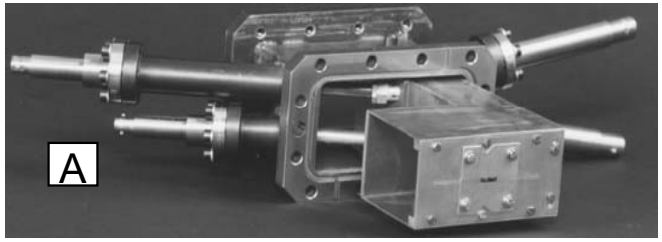

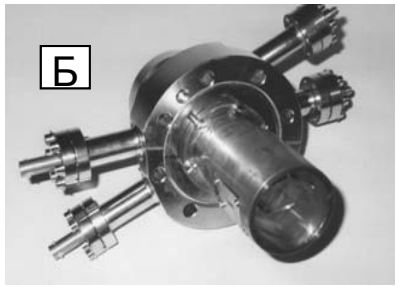

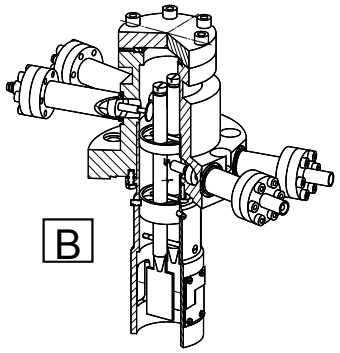

Some Experimental Results

Setting of accelerating field amplitude in DTL Tank 1 of INR Linac (20 MeV). Simulations.

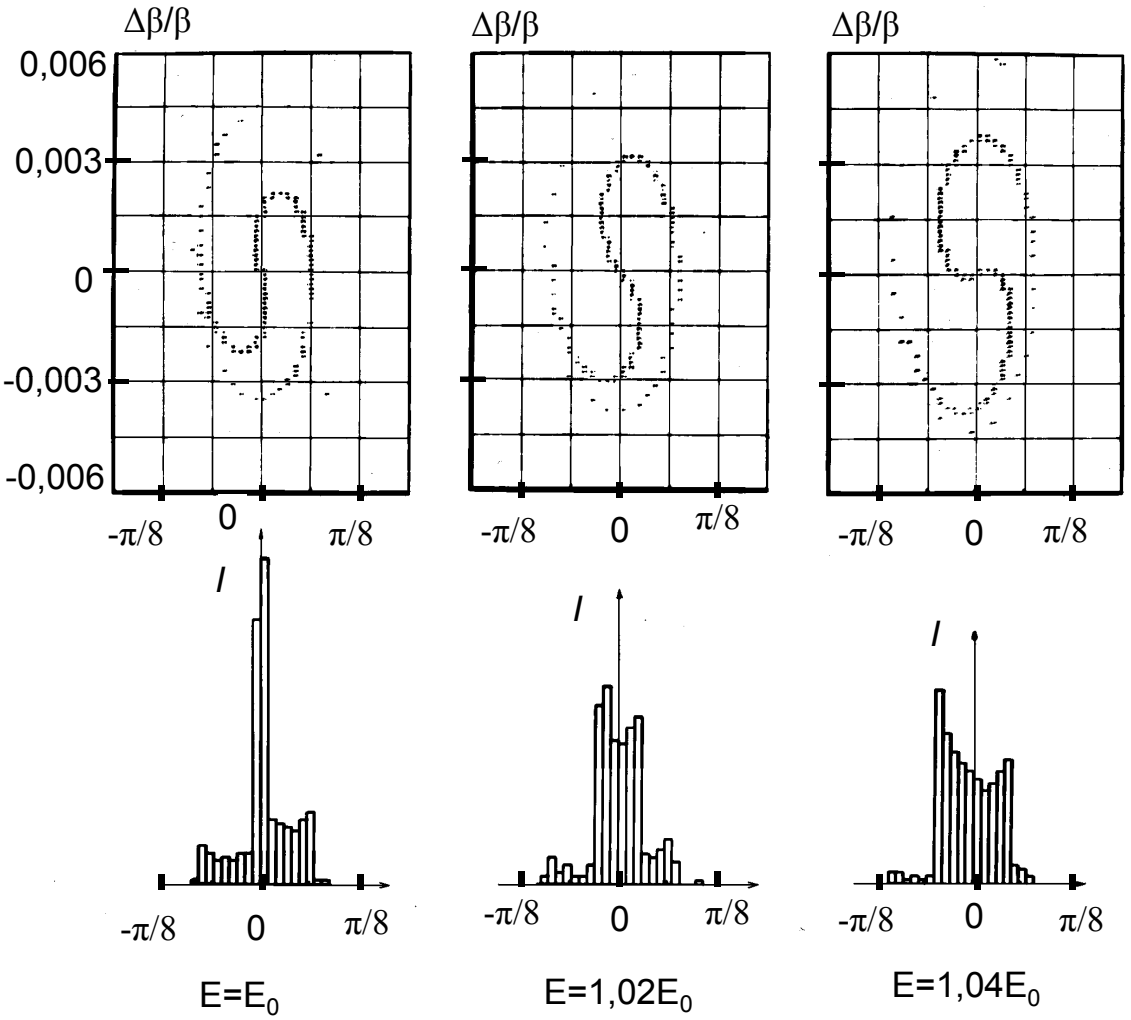

Beam portraits in longitudinal phase space at the exit of Tank 1 for different amplitudes

Setting of accelerating field amplitude in DTL Tank 1 of INR Linac (20 MeV). Experimental results.

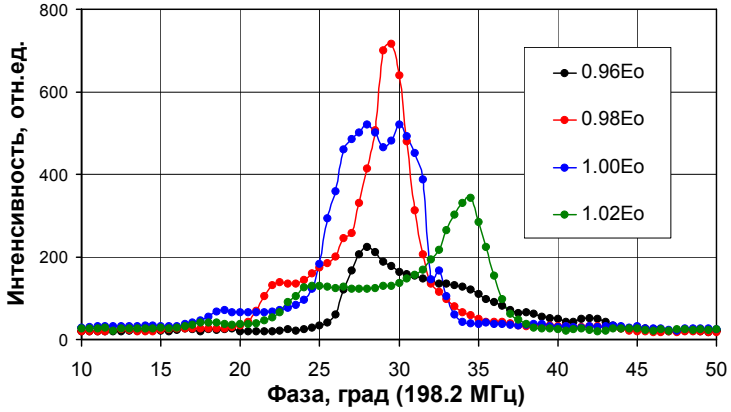

Bunch shapes for different amplitudes.

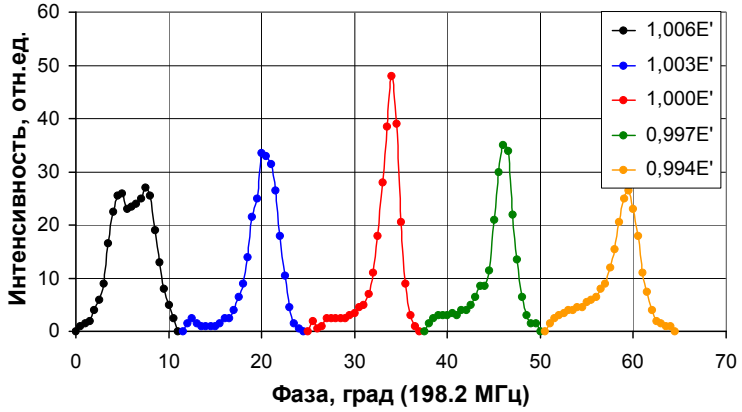

Bunch shapes in the vicinity of extremum of functions $I_m(E)$ и $\Phi(E)$.

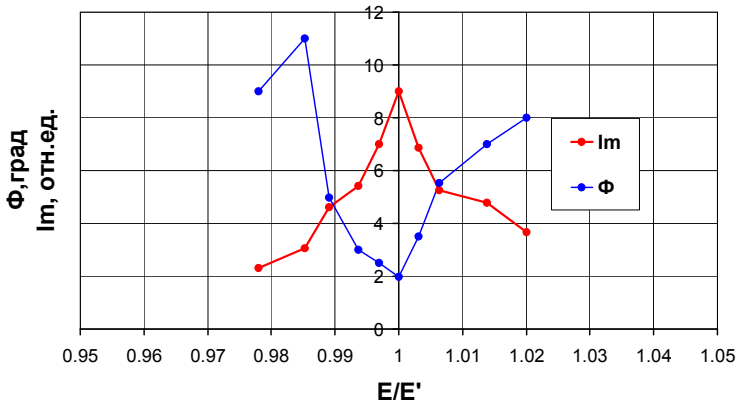

Functions $I_m(E)$ and $\Phi(E)$ in the vicinity of extremum for nominal injection energy

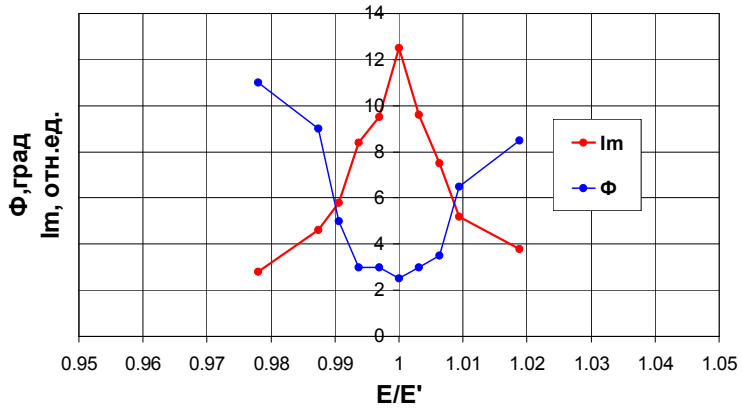

Functions $I_m(E)$ and $\Phi(E)$ in the vicinity of extremum for injection energy less than nominal value by 1%.

Longitudinal emittance at the exit of low energy part of INR linac(100 MeV). Longitudinal matching.

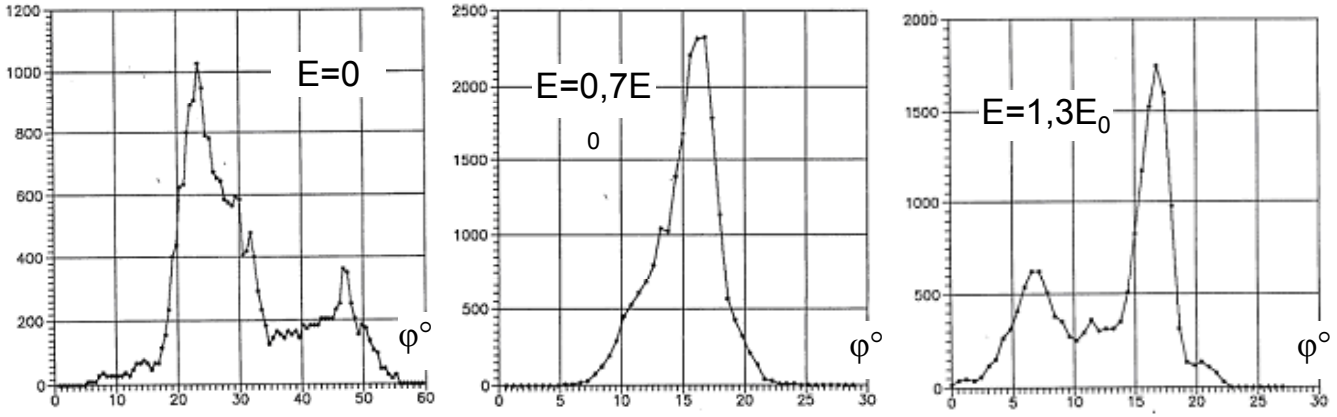

Bunch shapes for different amplitudes in the last DTL tank 5

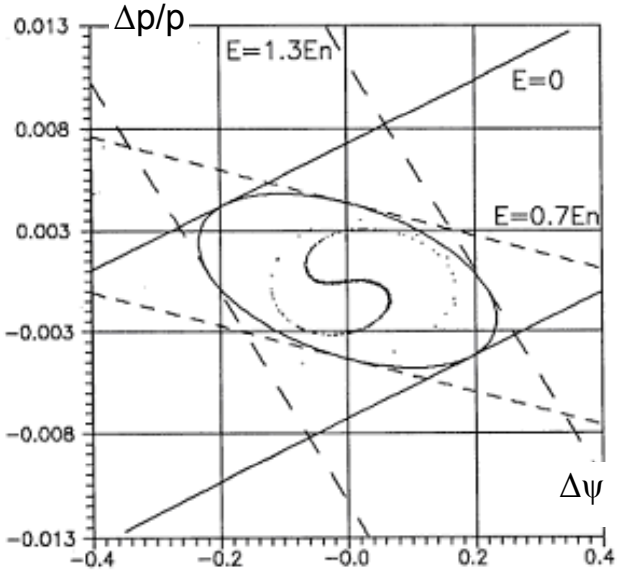

Longitudinal emittance at the exit of DTL Tank 4 .

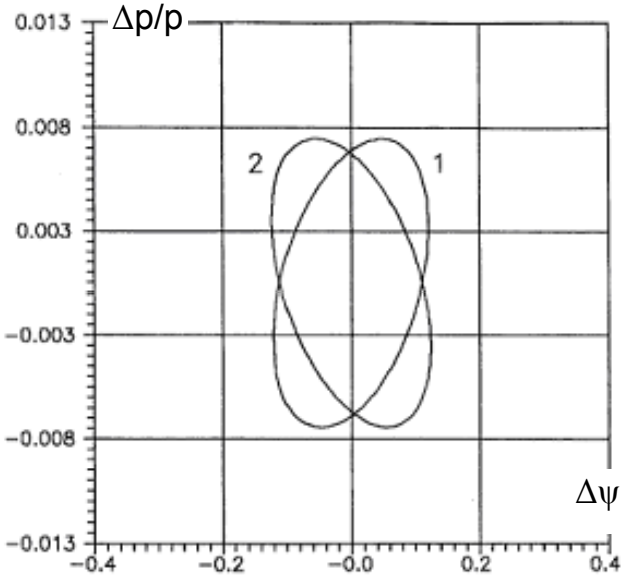

Longitudinal emittance at the exit of DTL Tank 5 (1) and entrance of high energy part (2).

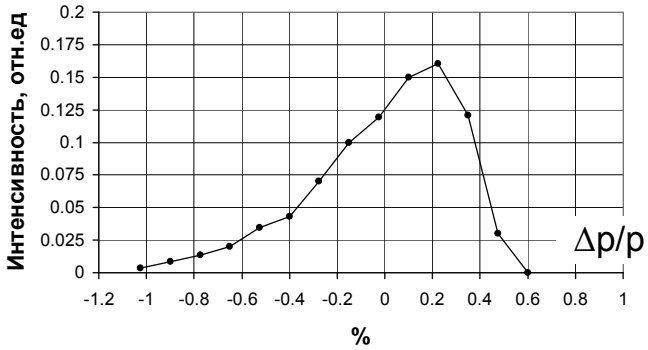

Energy spectrum at the exit of low energy part of INR linac

Longitudinal emittance at the intermediate extraction region (160 MeV) of INR linac

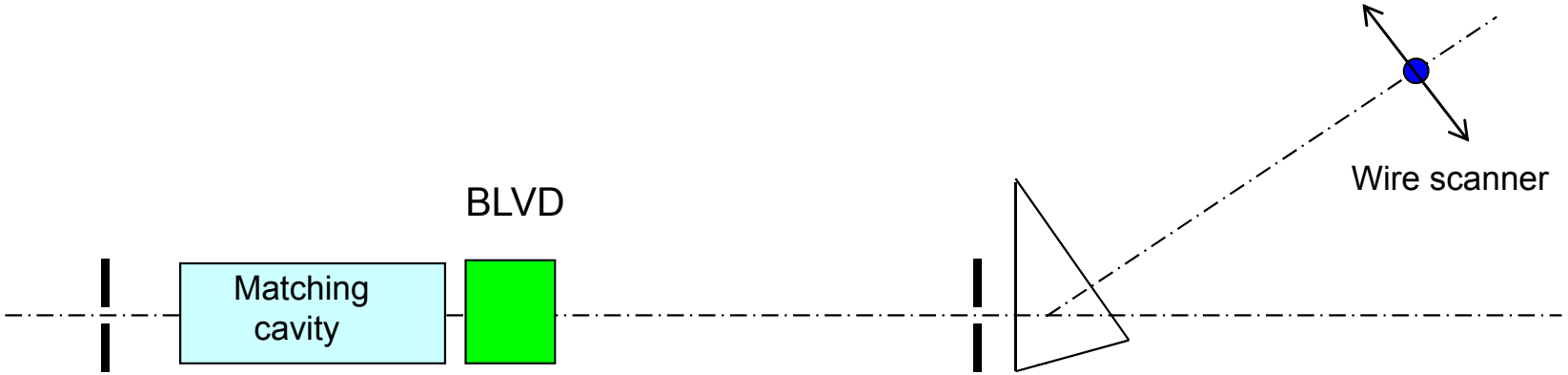

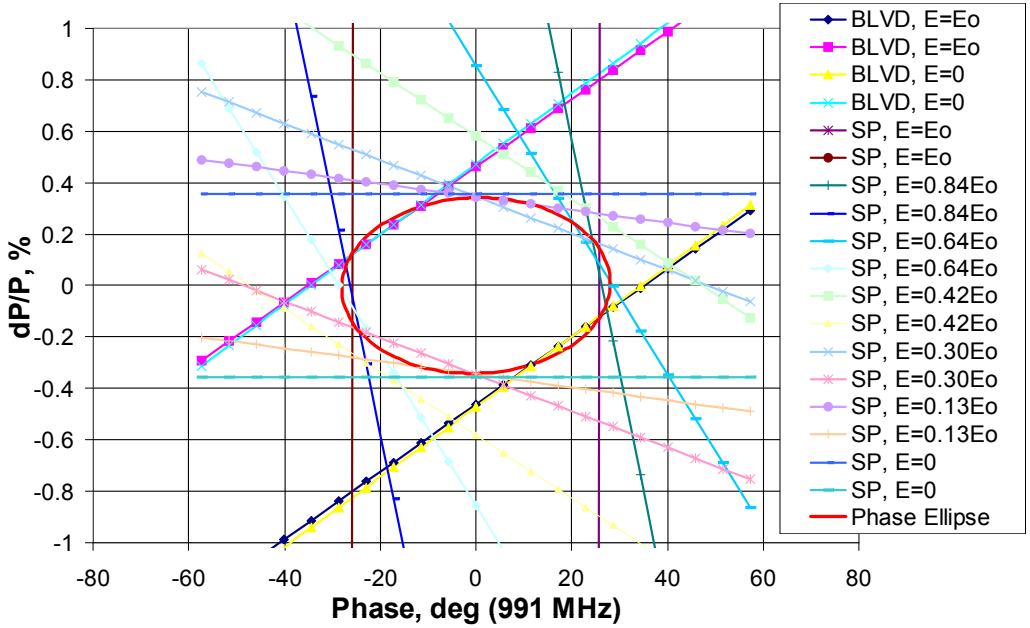

RMS emittance evaluation.

Some results of 3D-measurements at CERN Linac-2

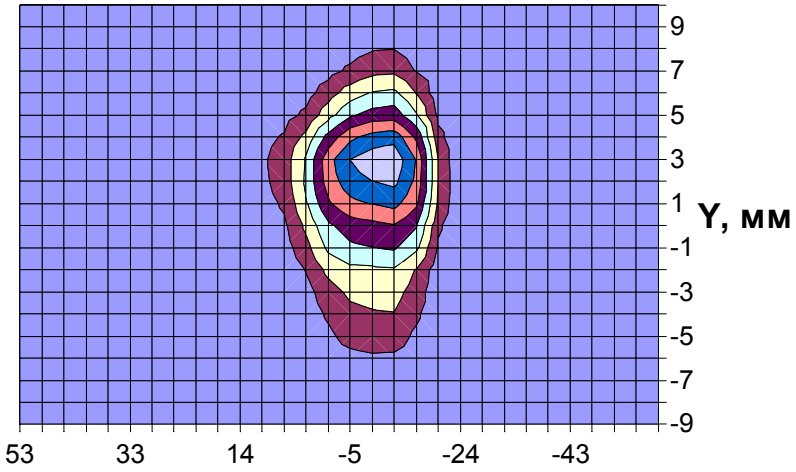

Integral projection of bunch on longitudinal vertical plane (phase-Y).

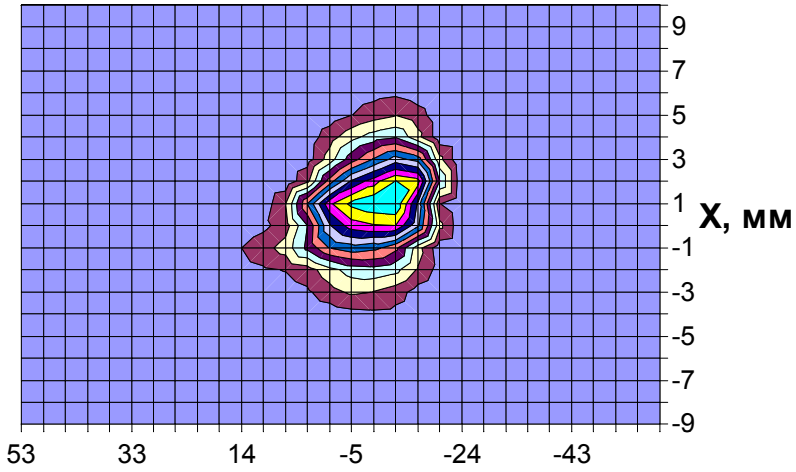

Integral projection of bunch on longitudinal horizontal plane (phase-X).

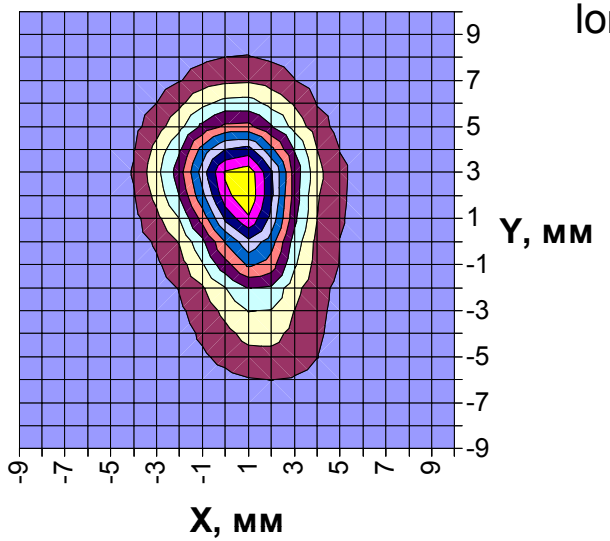

Integral beam cross section

Behavior of 3-D distribution projection on longitudinal vertical and horizontal planes within the beam pulse

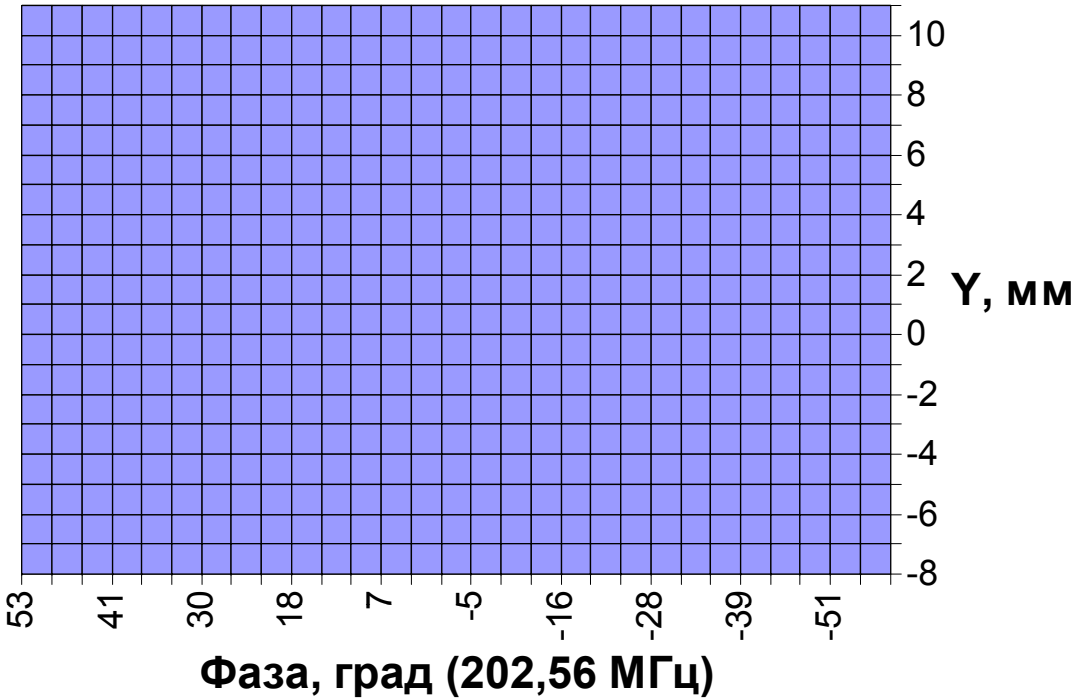

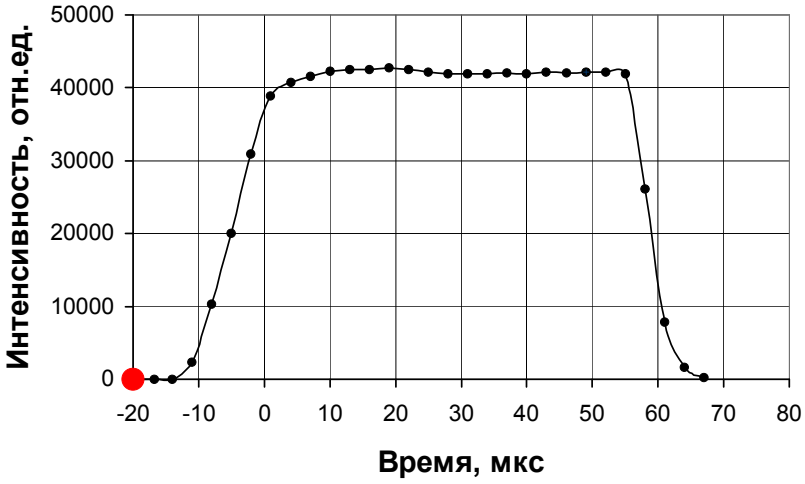

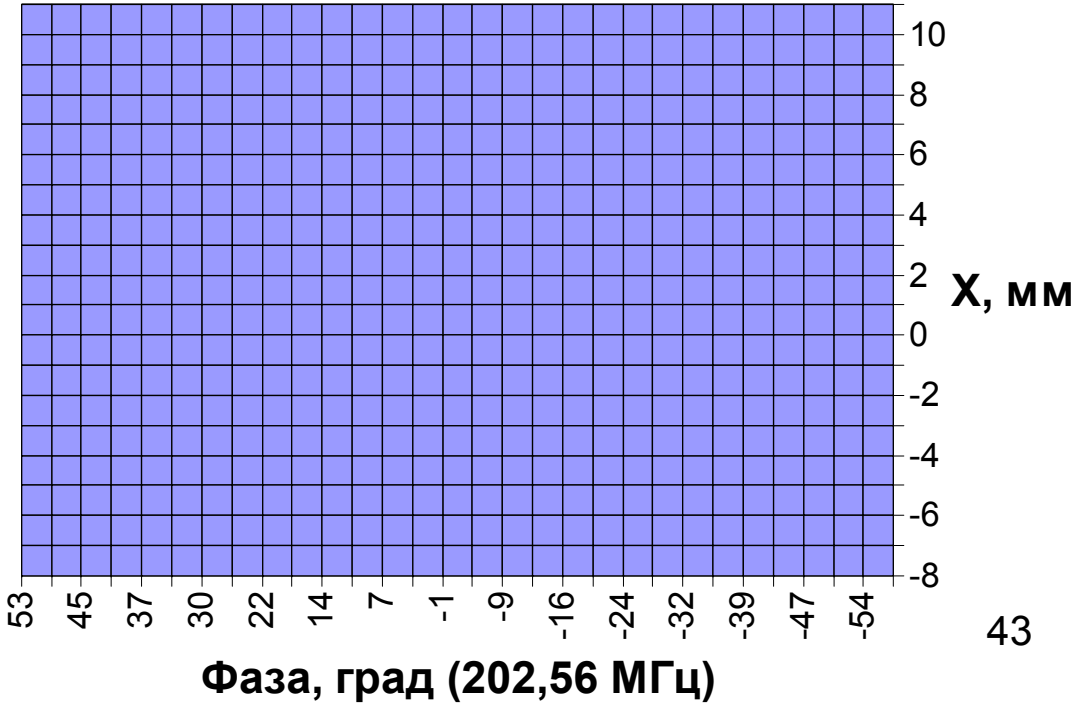

Behavior of 3-D distribution projection on longitudinal vertical and horizontal planes within the beam pulse

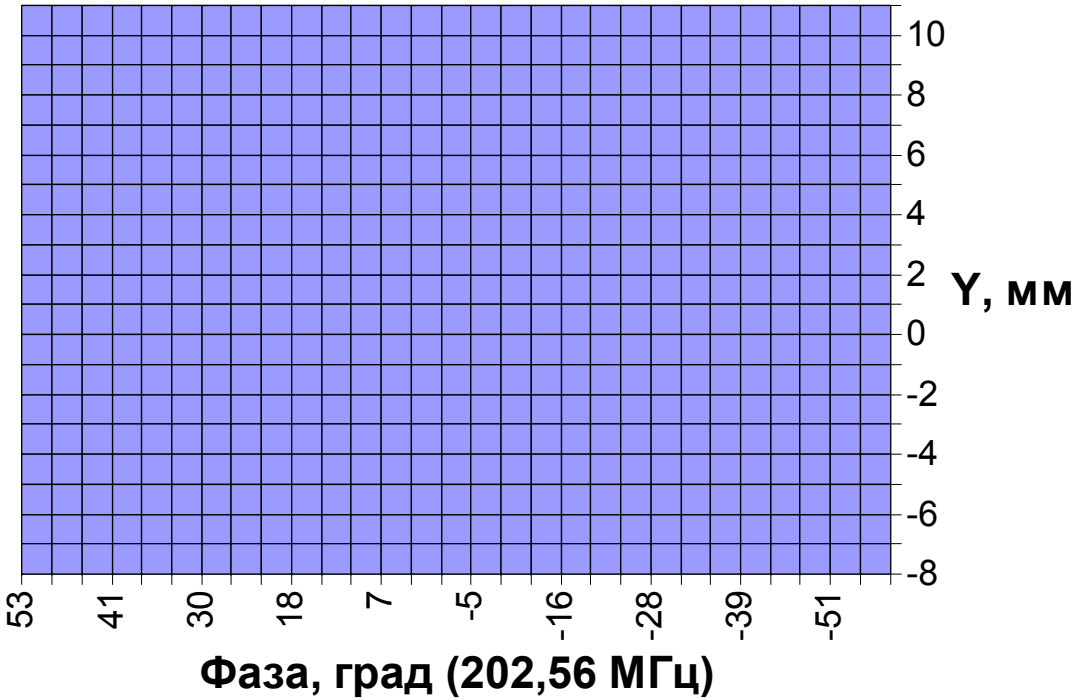

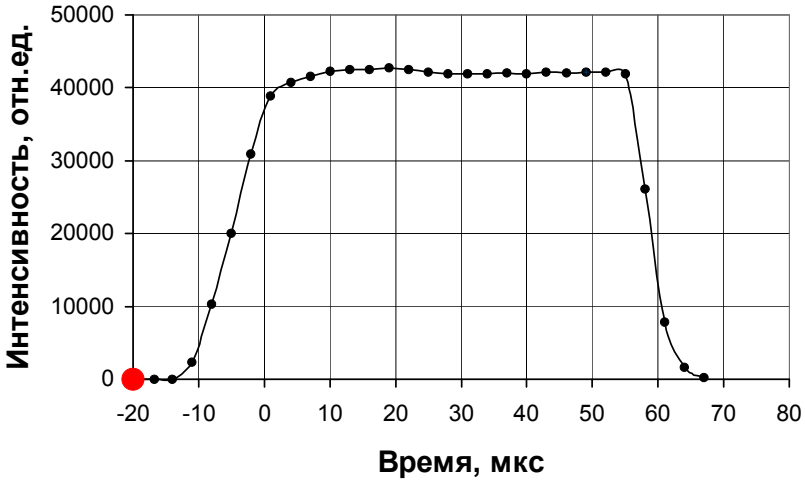

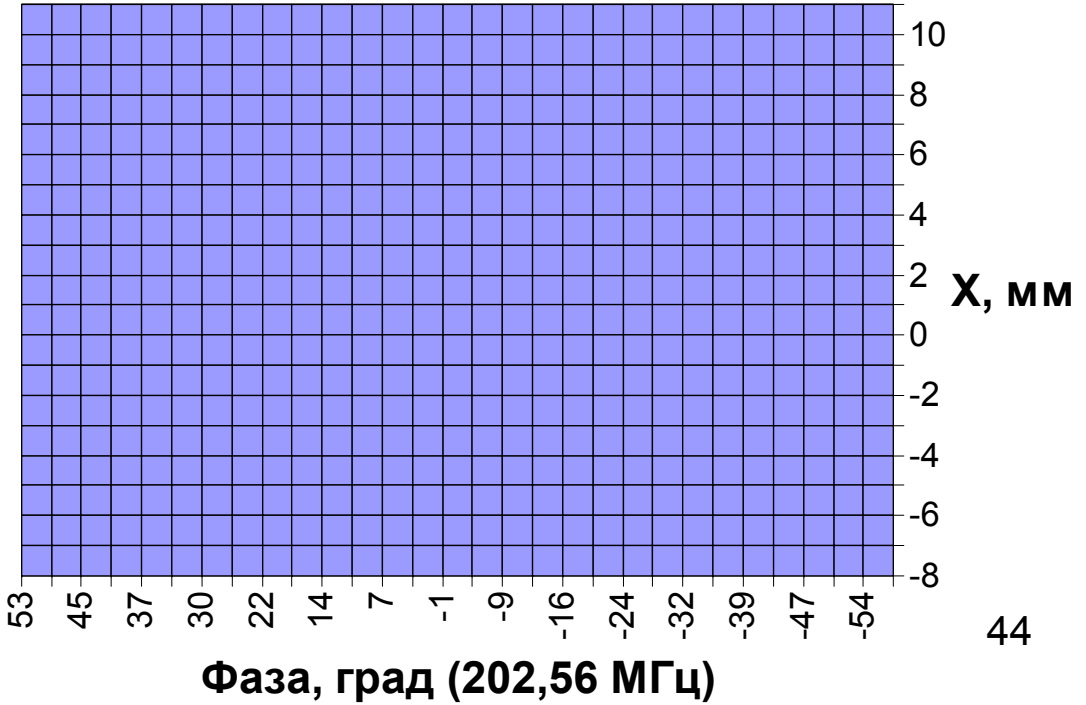

Behavior of 3-D distribution projection on longitudinal vertical and horizontal planes within the beam pulse

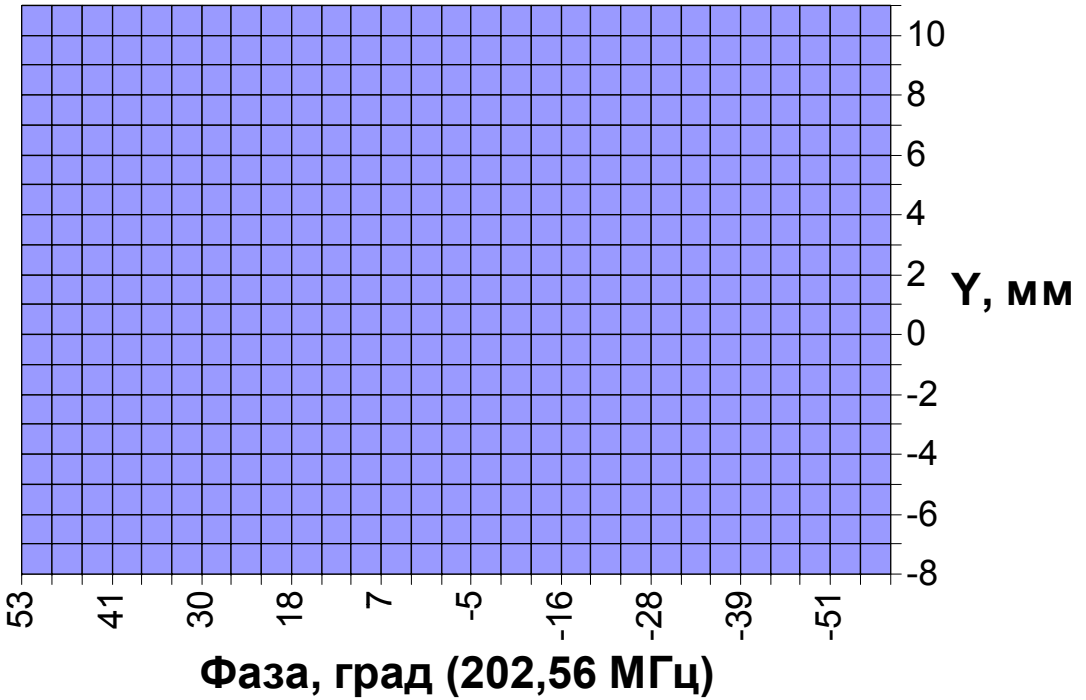

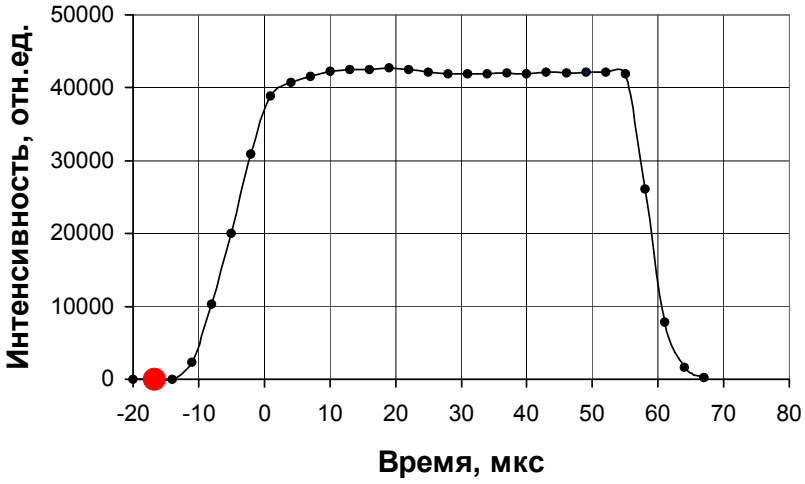

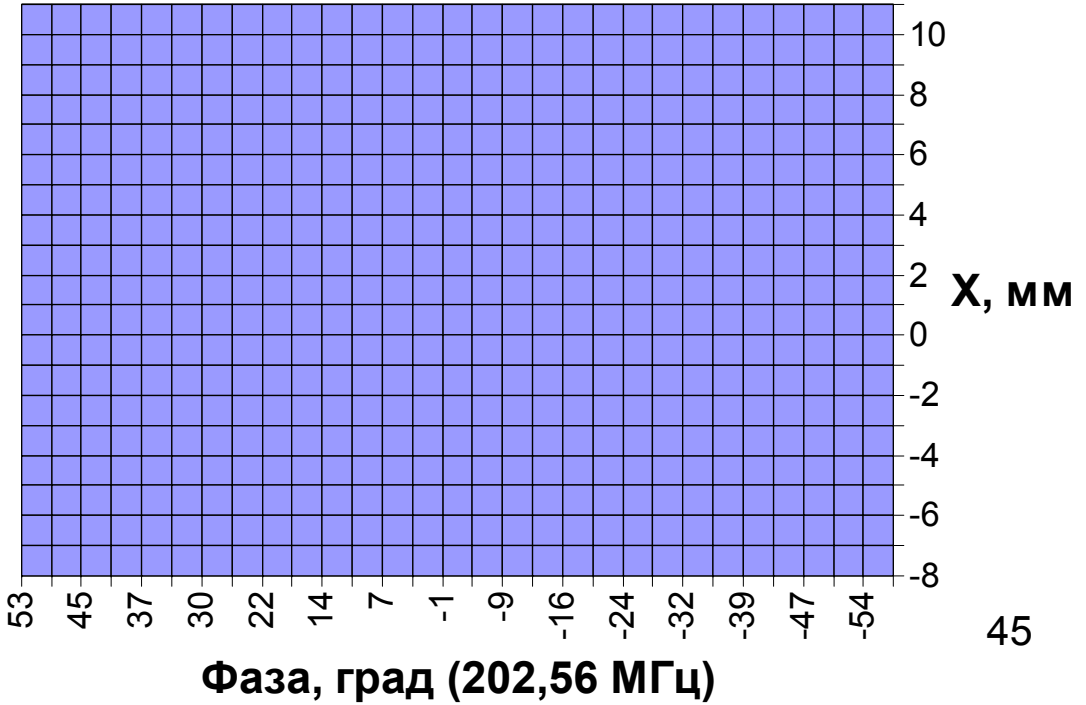

Behavior of 3-D distribution projection on longitudinal vertical and horizontal planes within the beam pulse

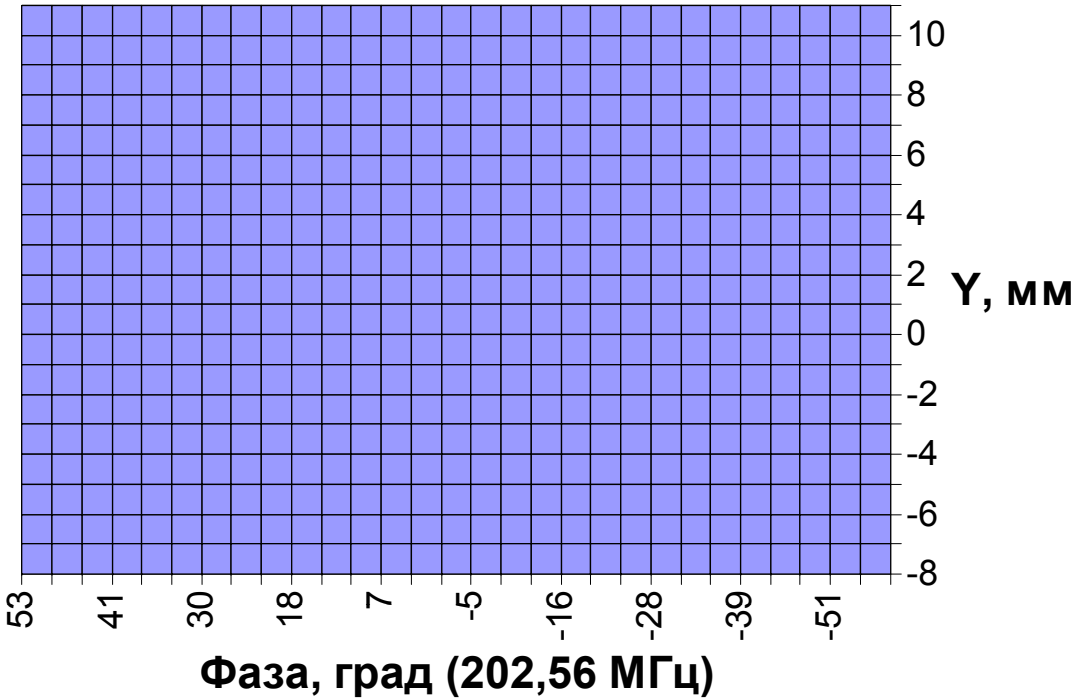

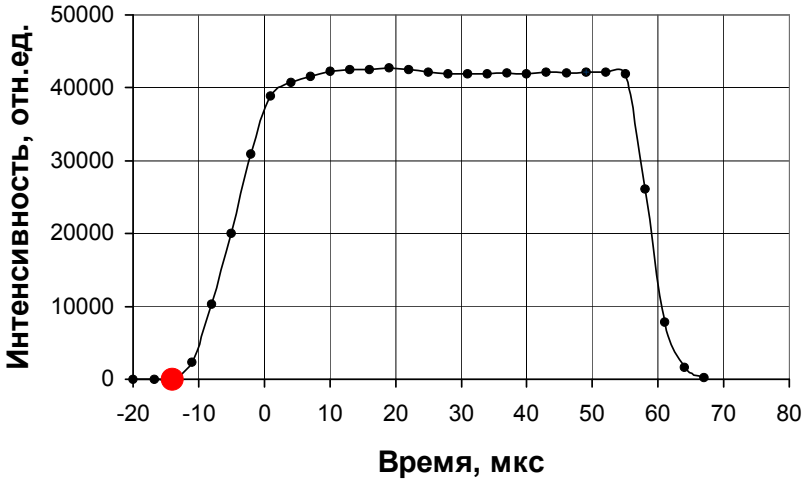

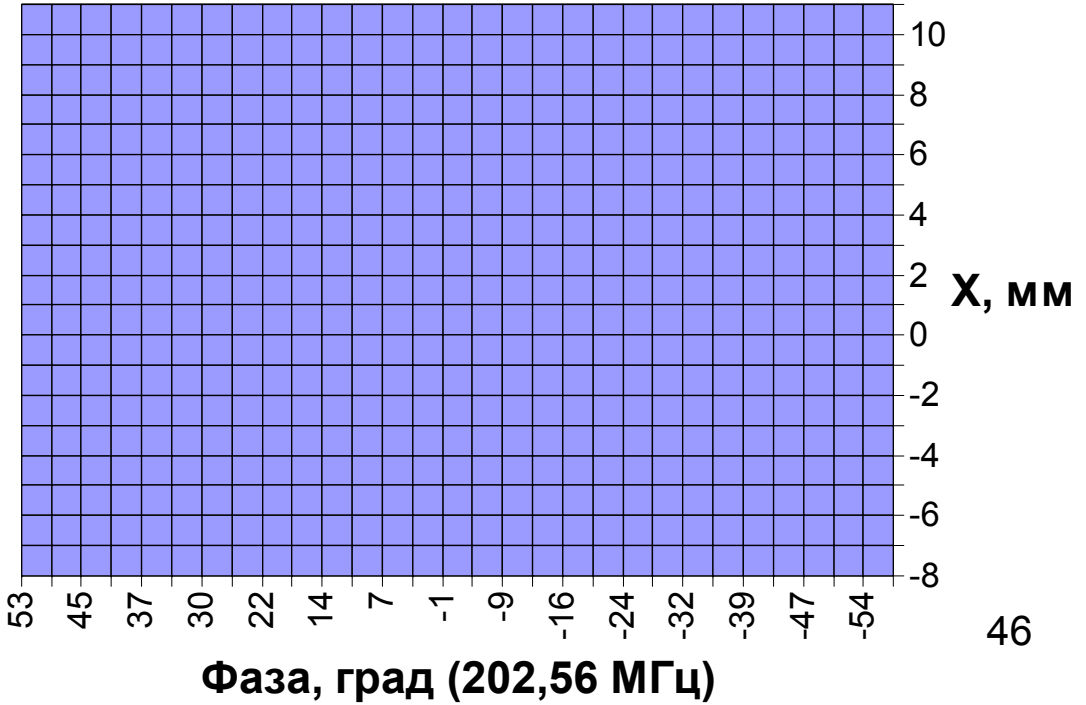

Behavior of 3-D distribution projection on longitudinal vertical and horizontal planes within the beam pulse

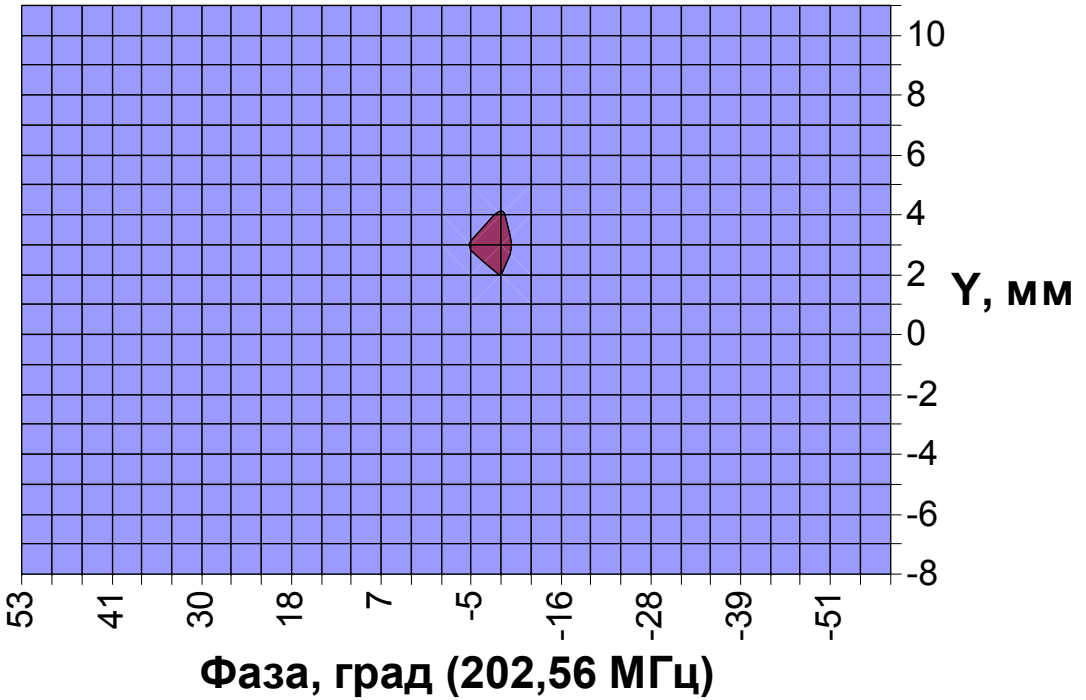

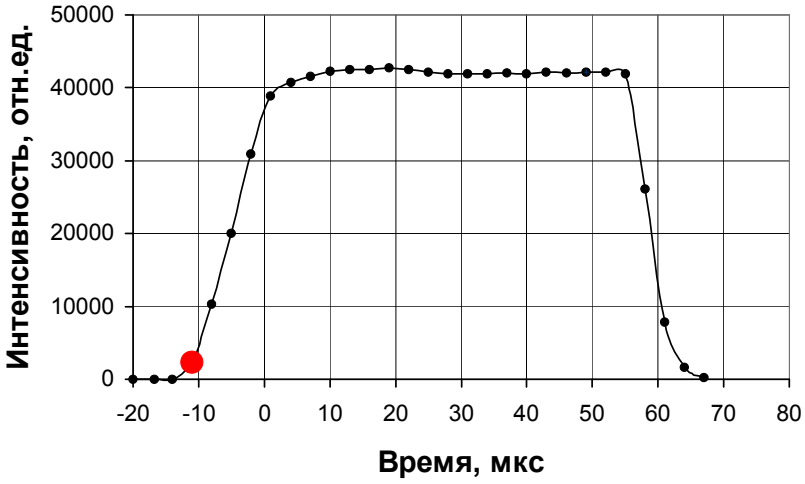

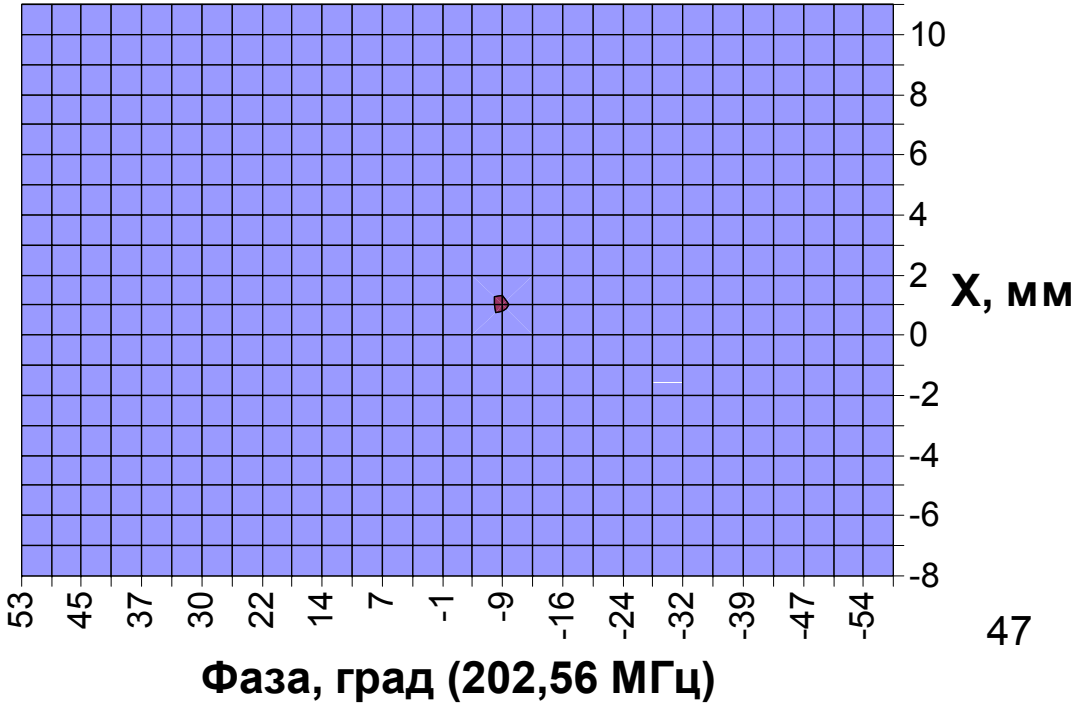

Behavior of 3-D distribution projection on longitudinal vertical and horizontal planes within the beam pulse

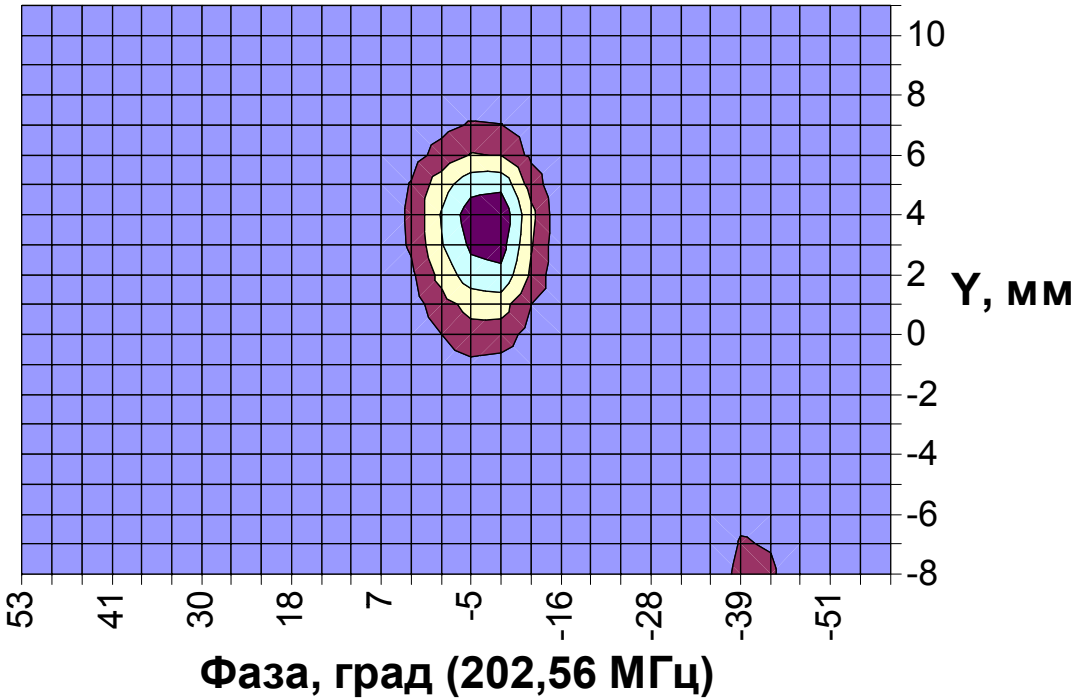

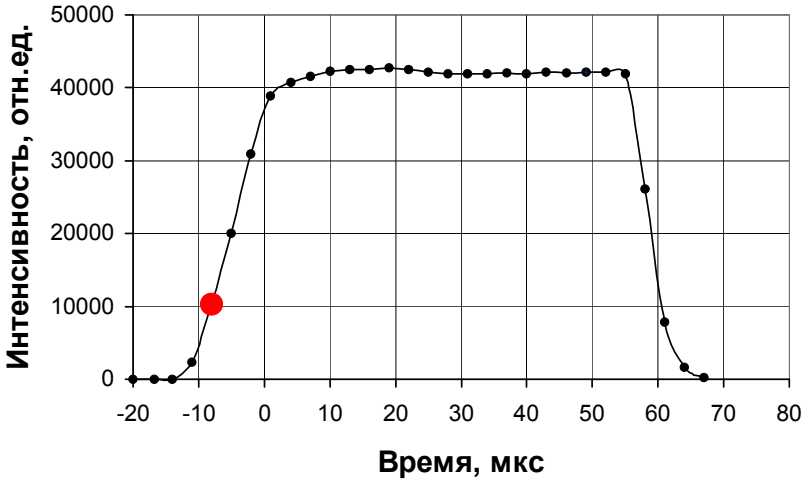

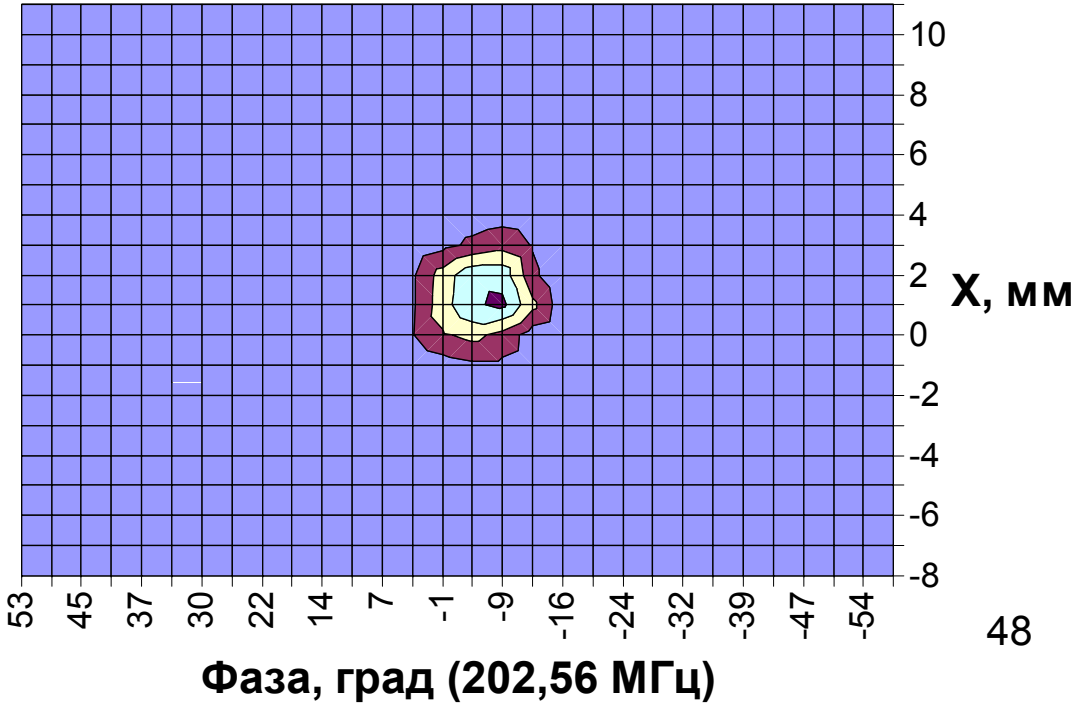

Behavior of 3-D distribution projection on longitudinal vertical and horizontal planes within the beam pulse

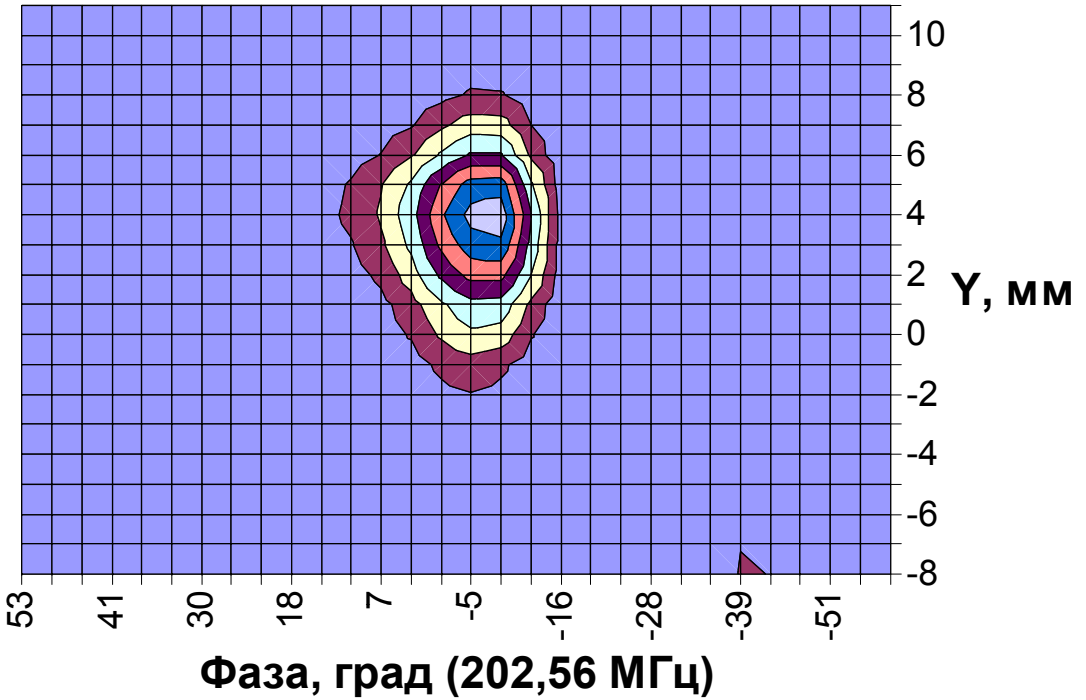

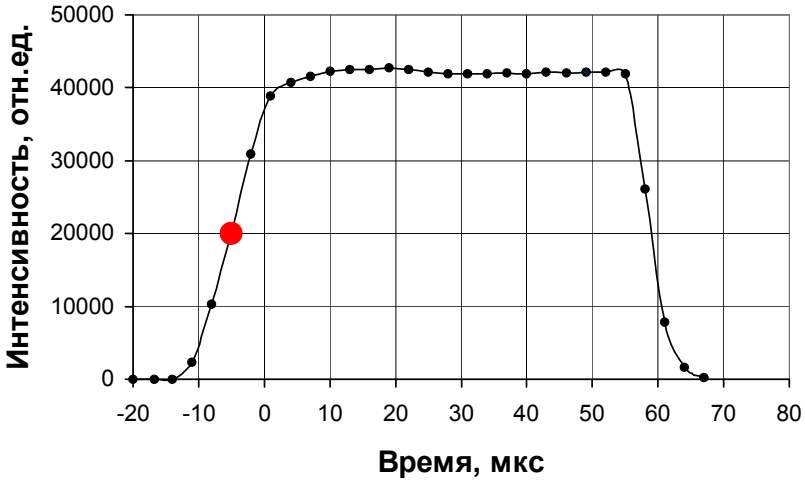

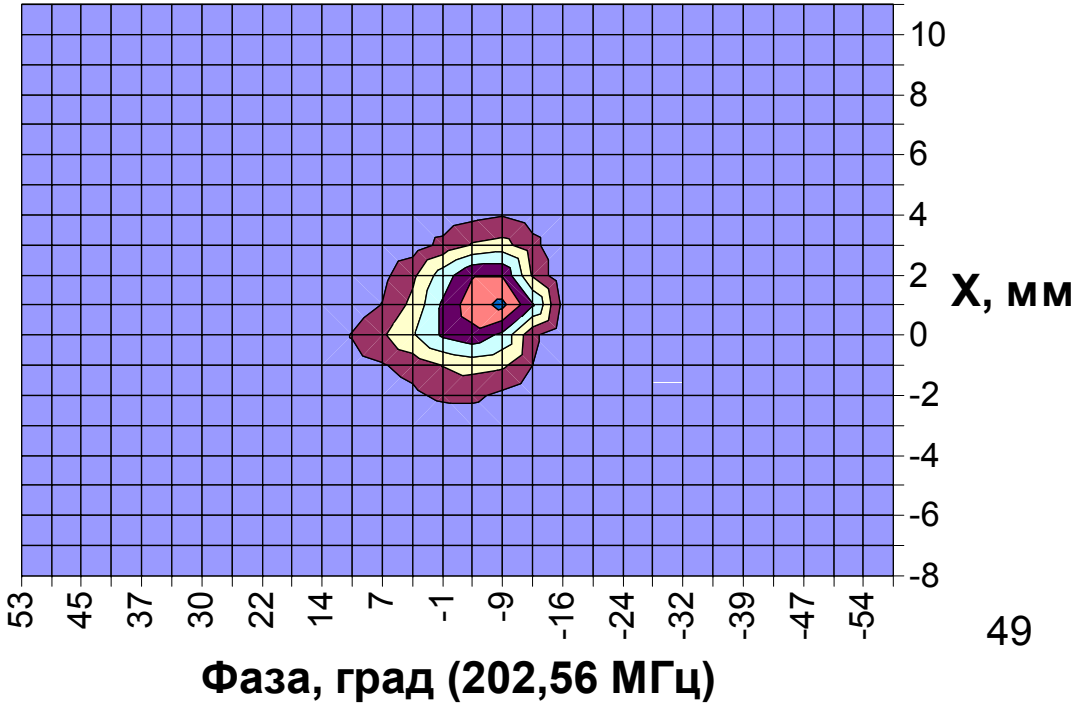

Behavior of 3-D distribution projection on longitudinal vertical and horizontal planes within the beam pulse

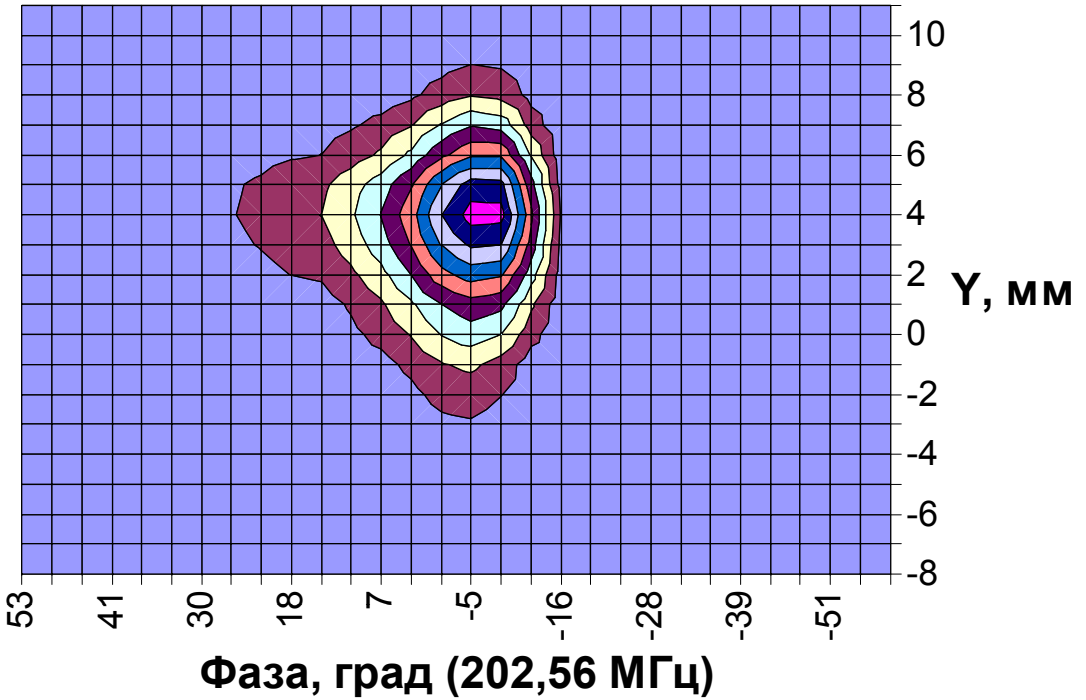

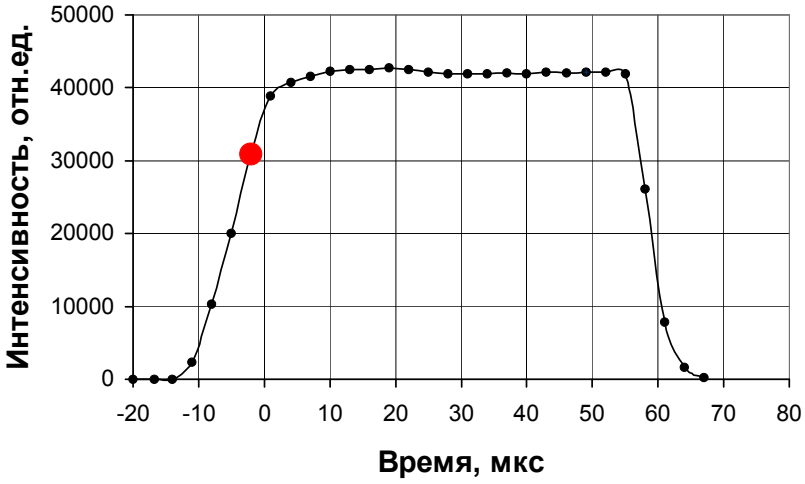

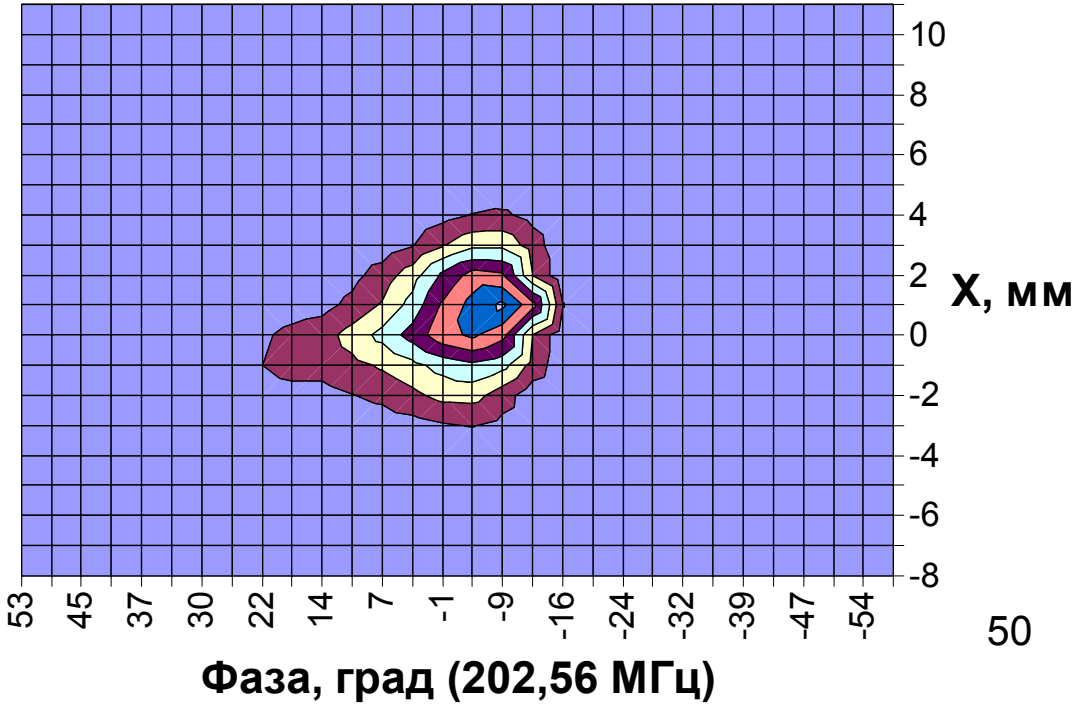

Behavior of 3-D distribution projection on longitudinal vertical and horizontal planes within the beam pulse

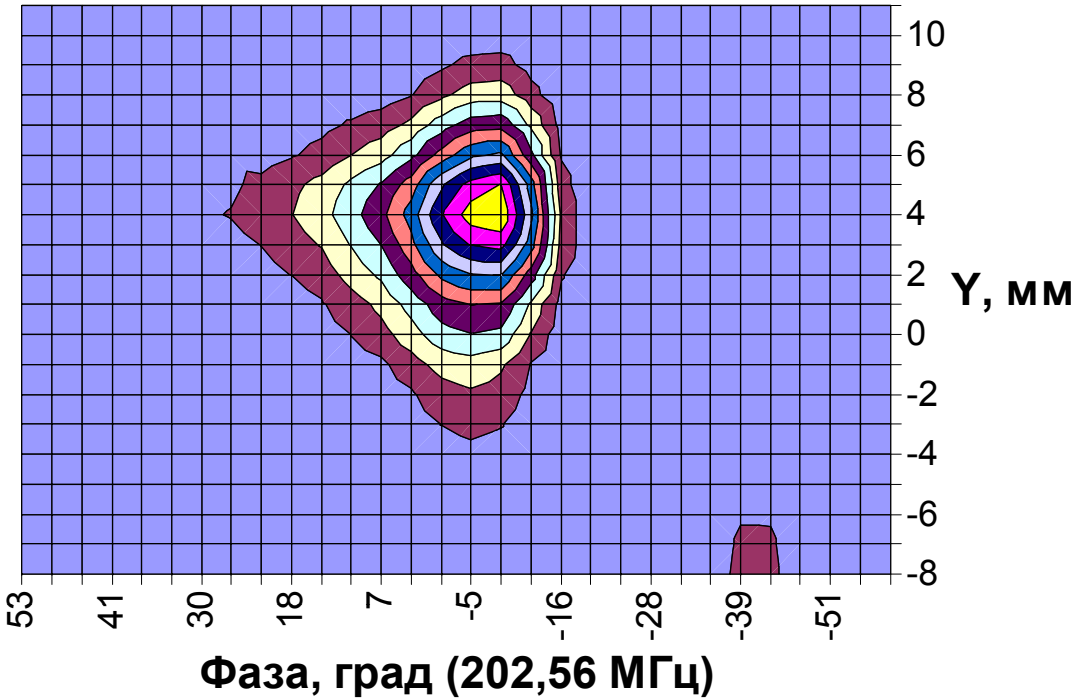

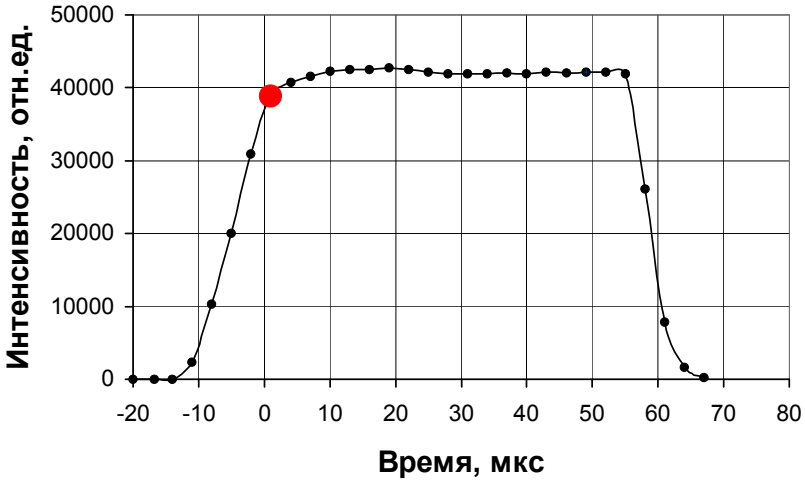

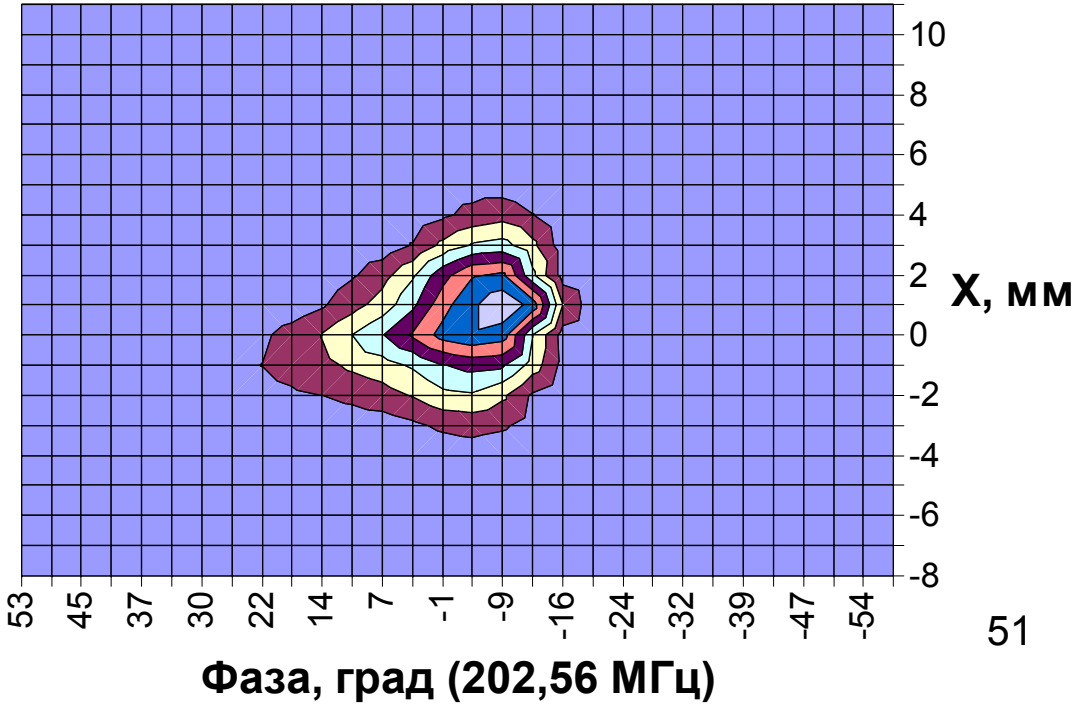

Behavior of 3-D distribution projection on longitudinal vertical and horizontal planes within the beam pulse

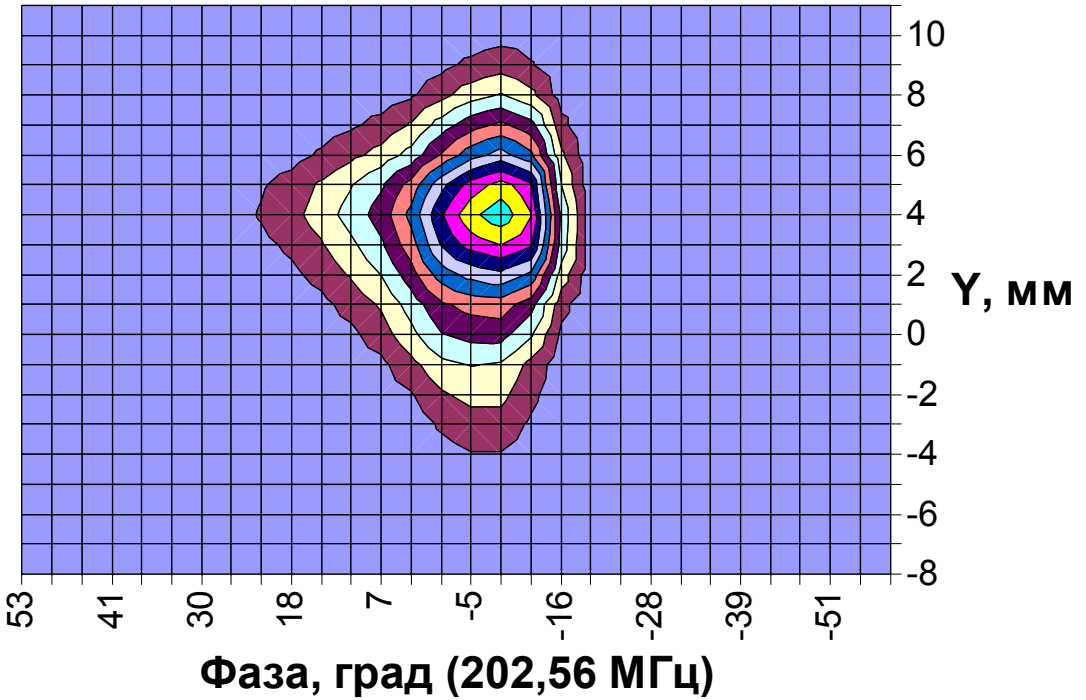

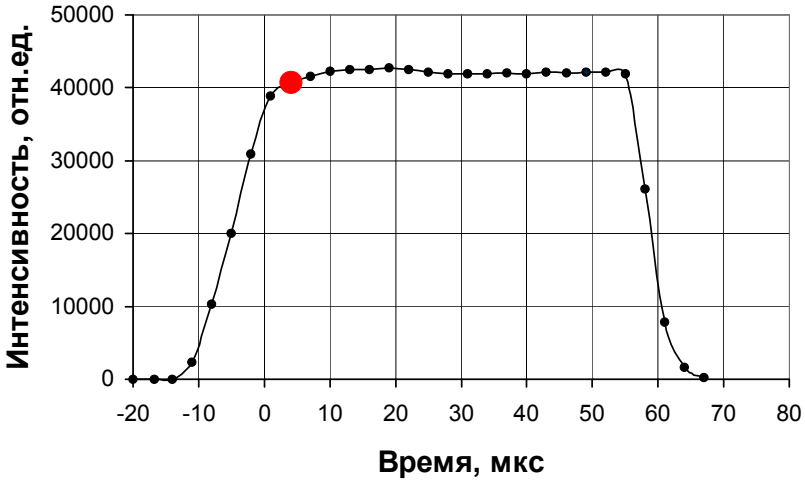

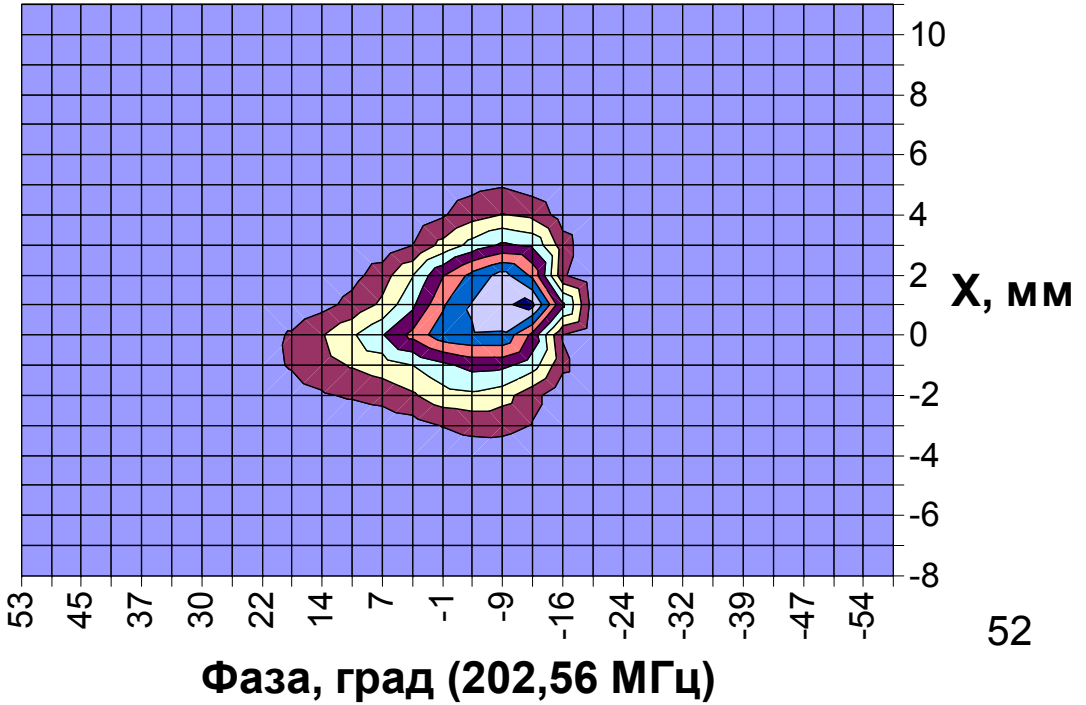

Behavior of 3-D distribution projection on longitudinal vertical and horizontal planes within the beam pulse

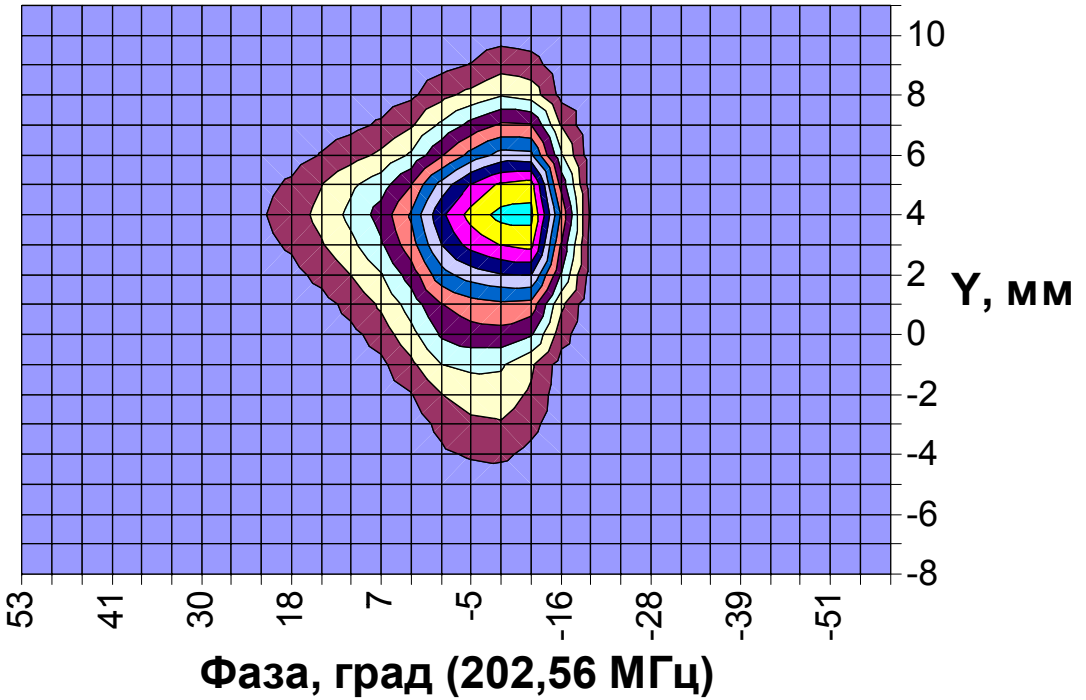

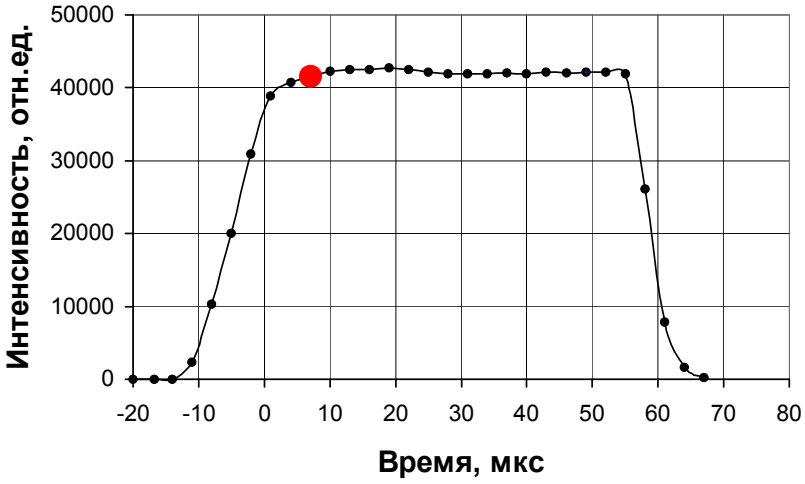

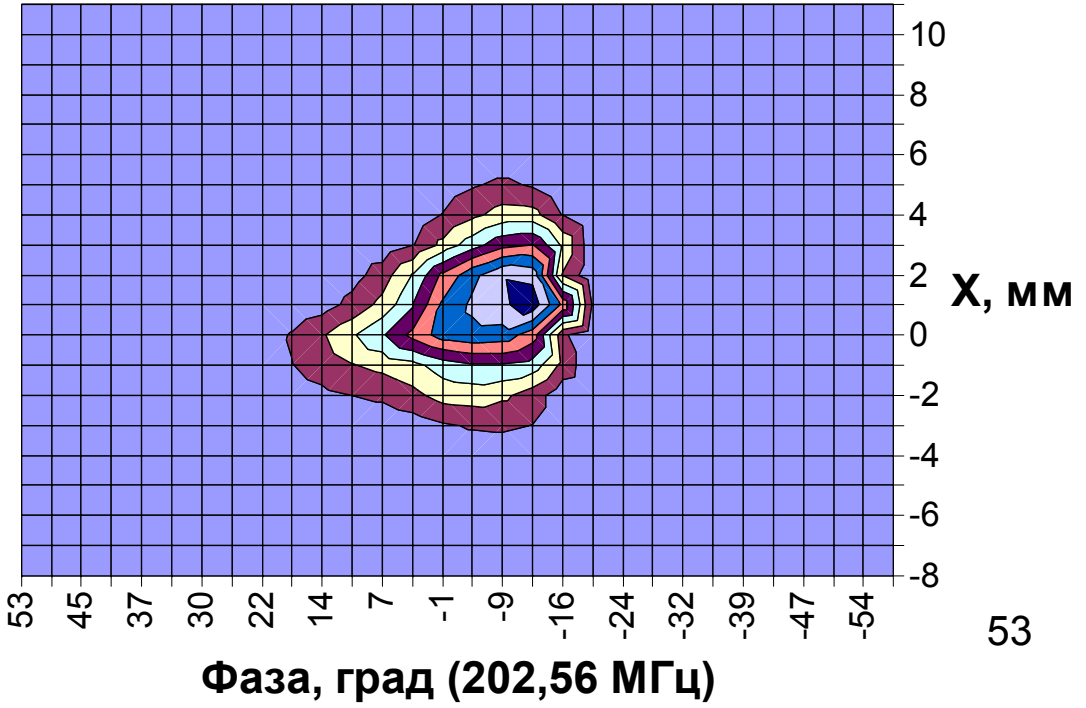

Behavior of 3-D distribution projection on longitudinal vertical and horizontal planes within the beam pulse

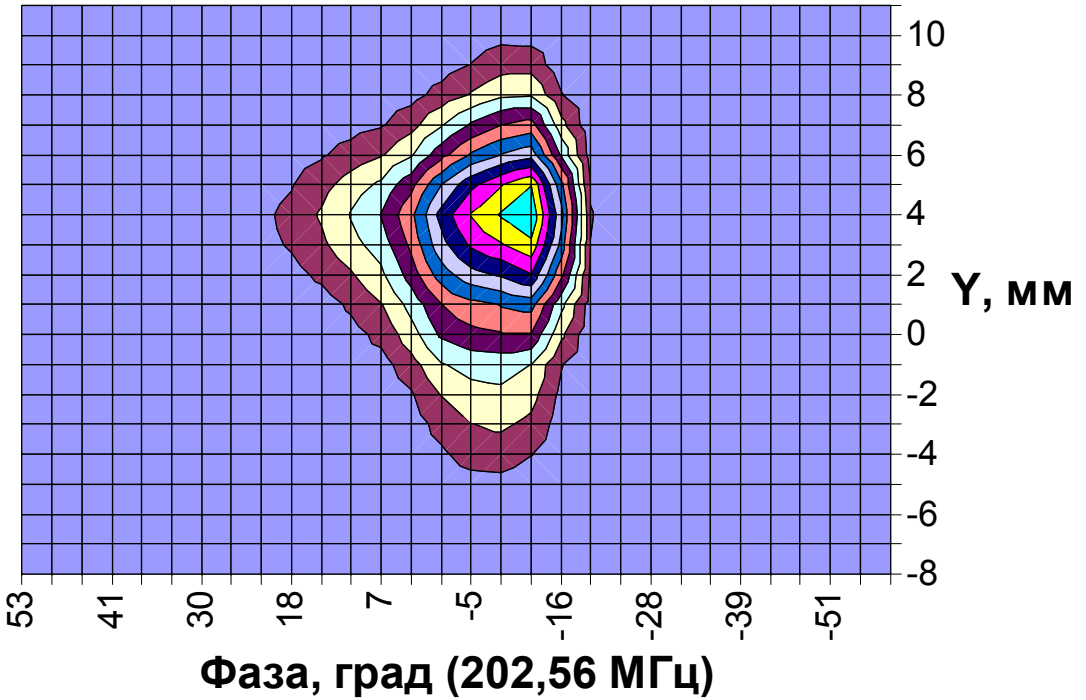

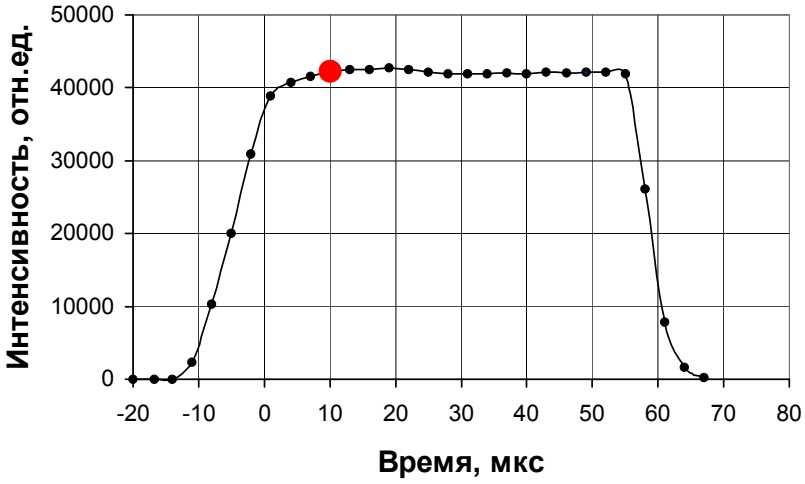

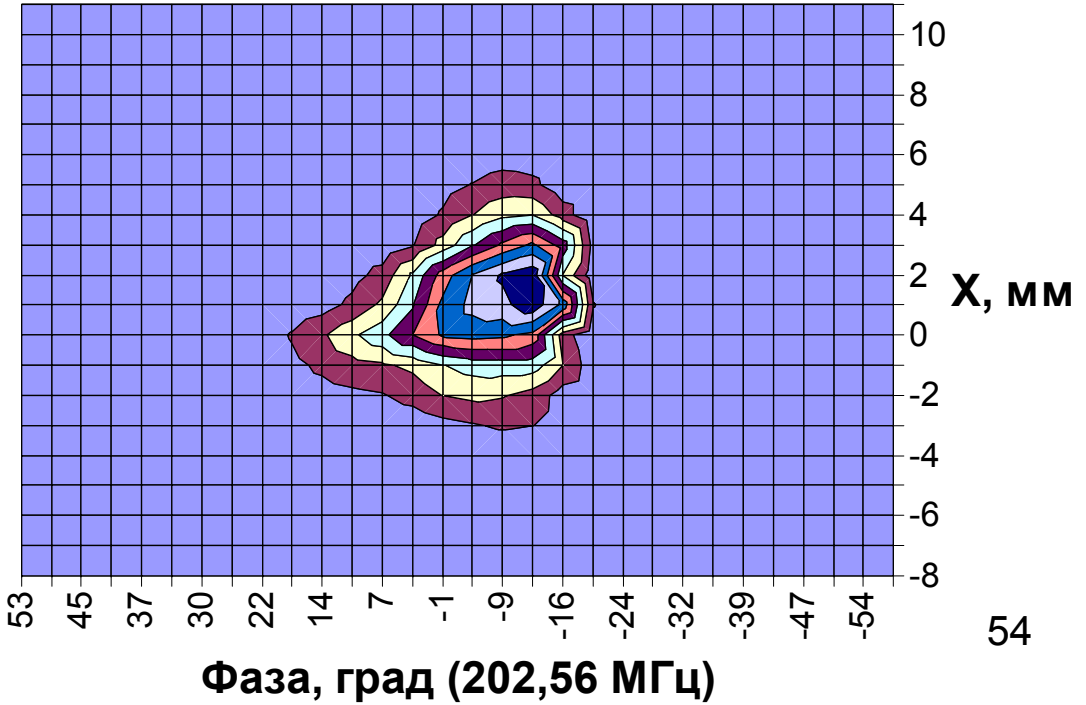

Behavior of 3-D distribution projection on longitudinal vertical and horizontal planes within the beam pulse

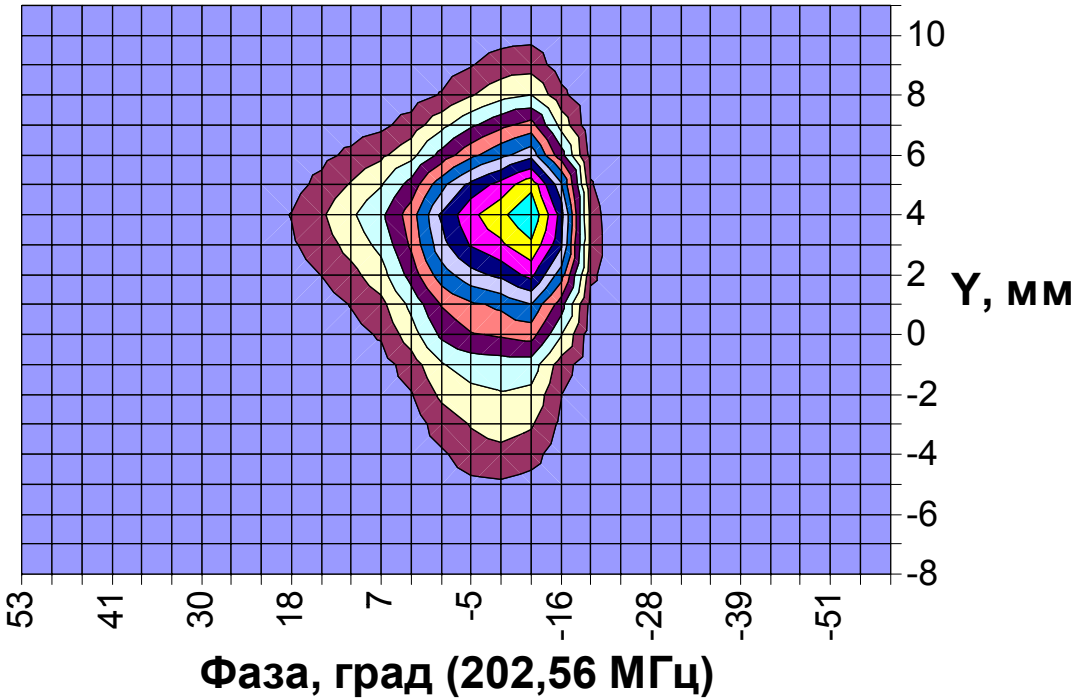

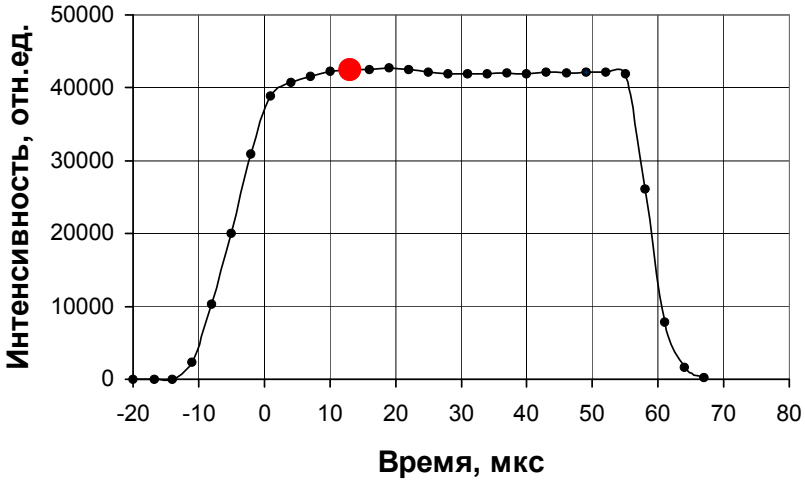

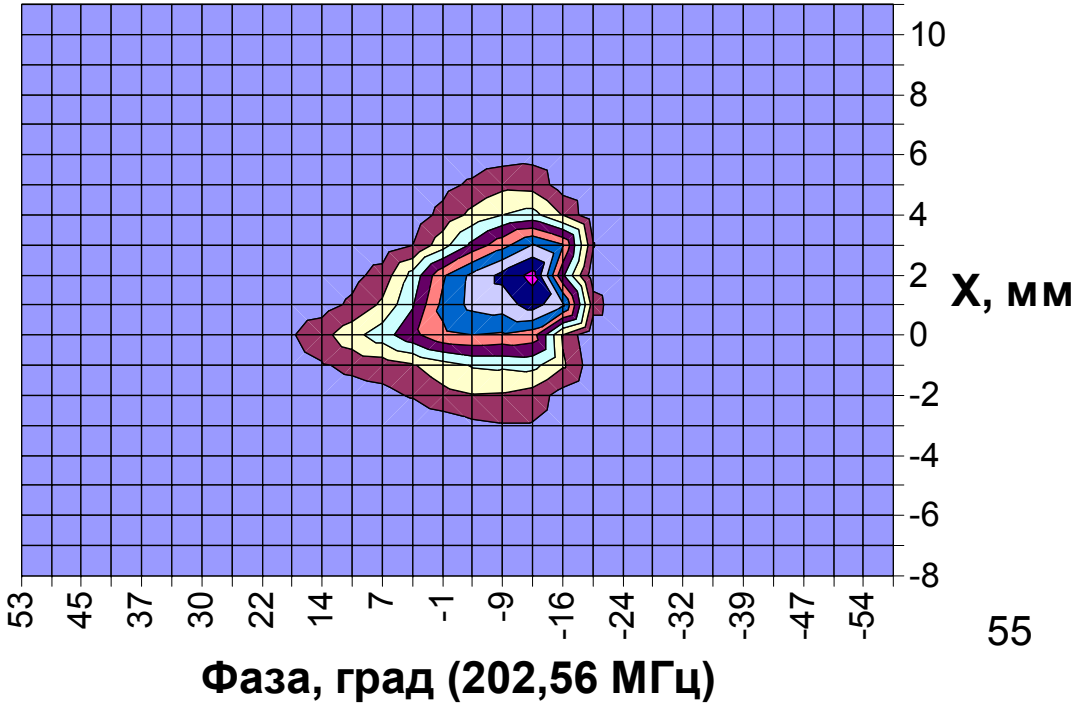

Behavior of 3-D distribution projection on longitudinal vertical and horizontal planes within the beam pulse

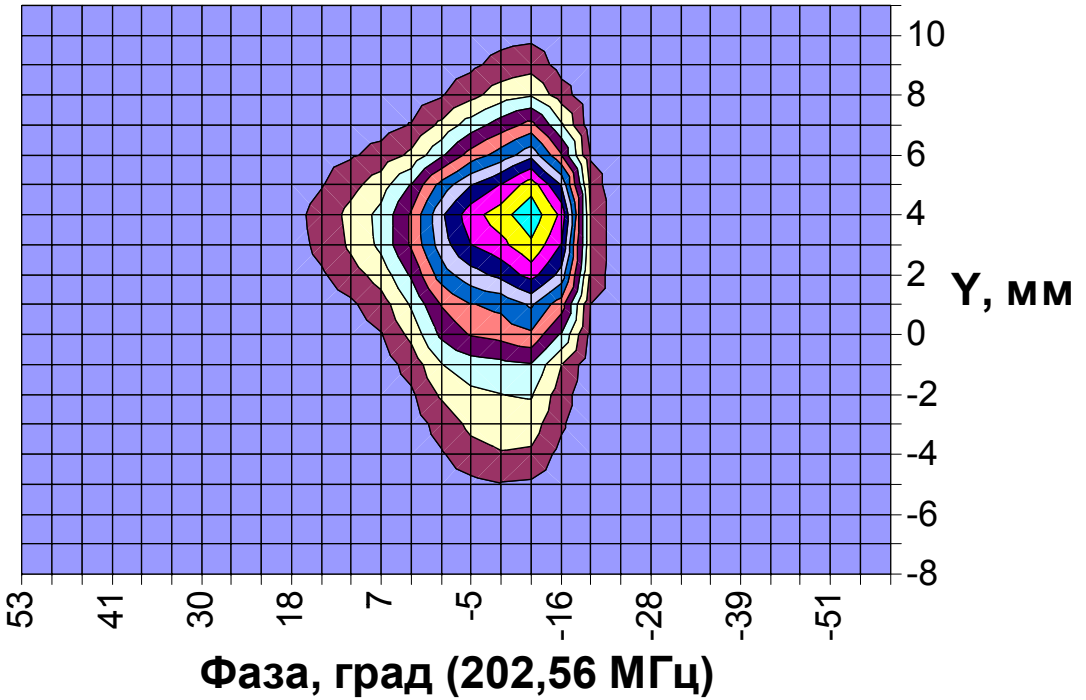

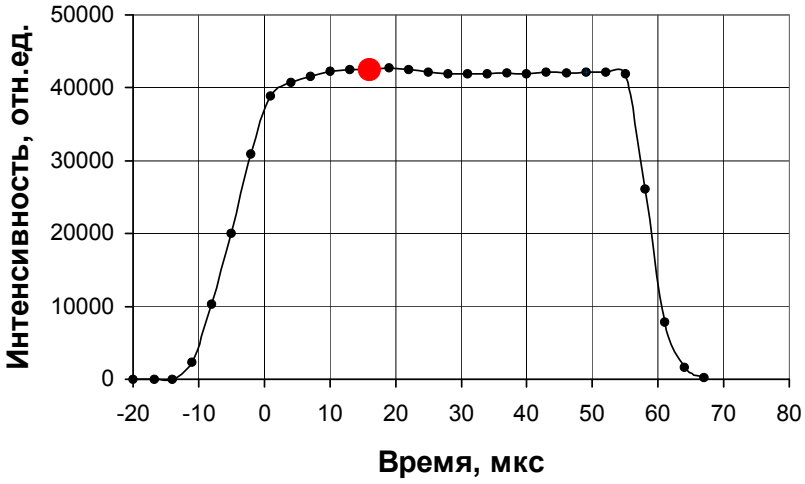

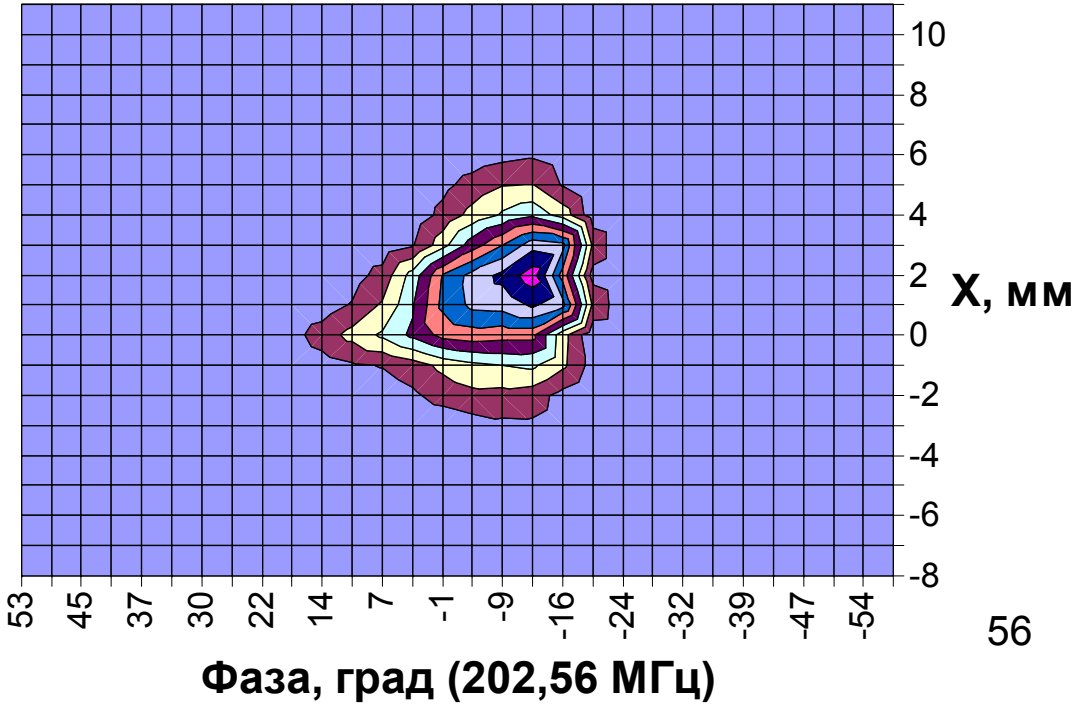

Behavior of 3-D distribution projection on longitudinal vertical and horizontal planes within the beam pulse

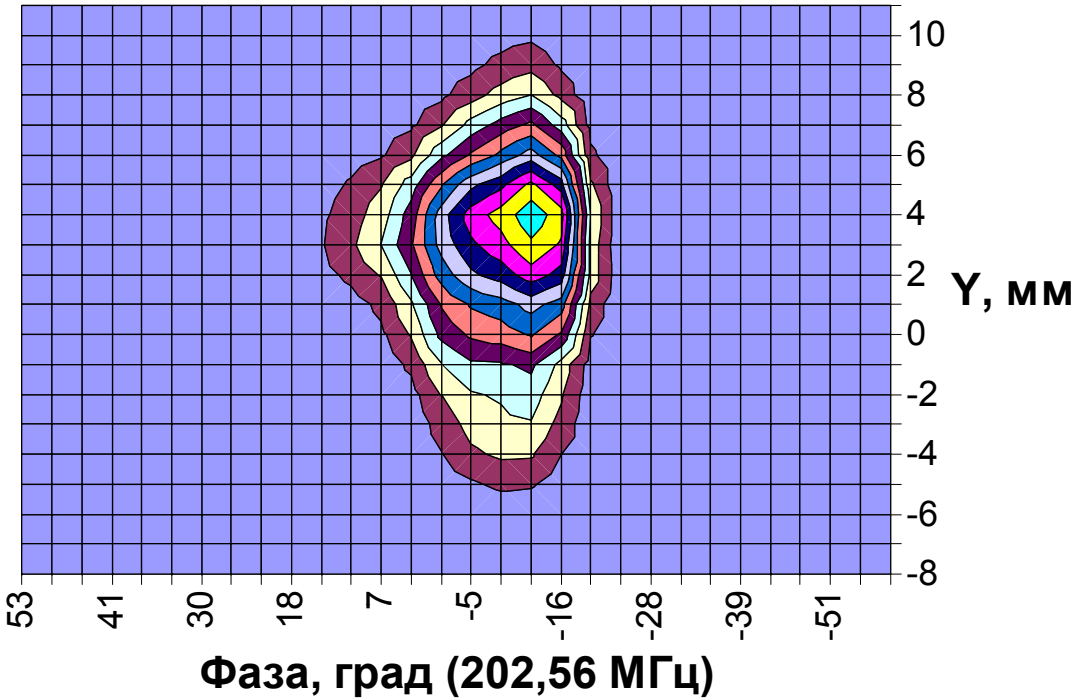

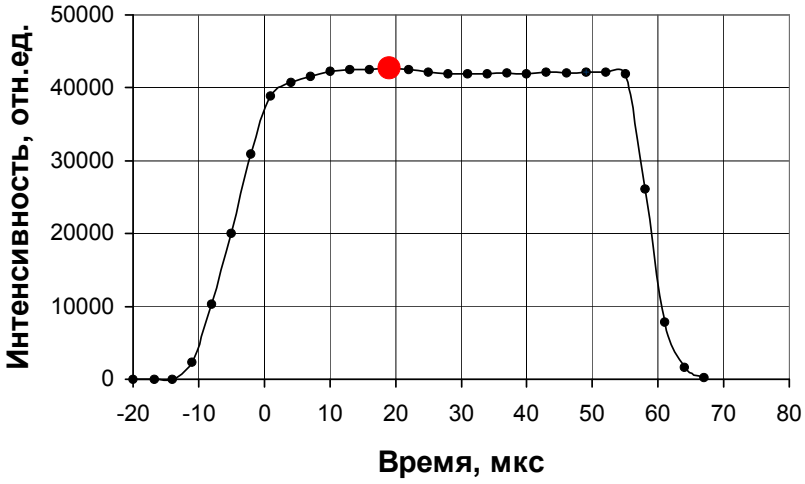

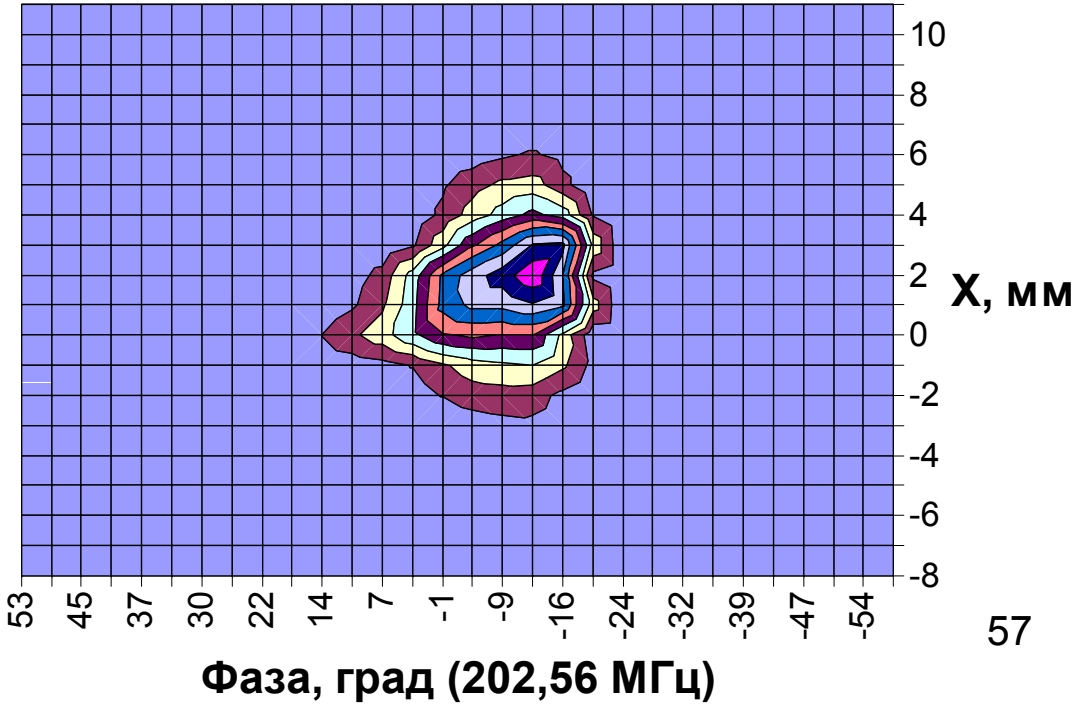

Behavior of 3-D distribution projection on longitudinal vertical and horizontal planes within the beam pulse

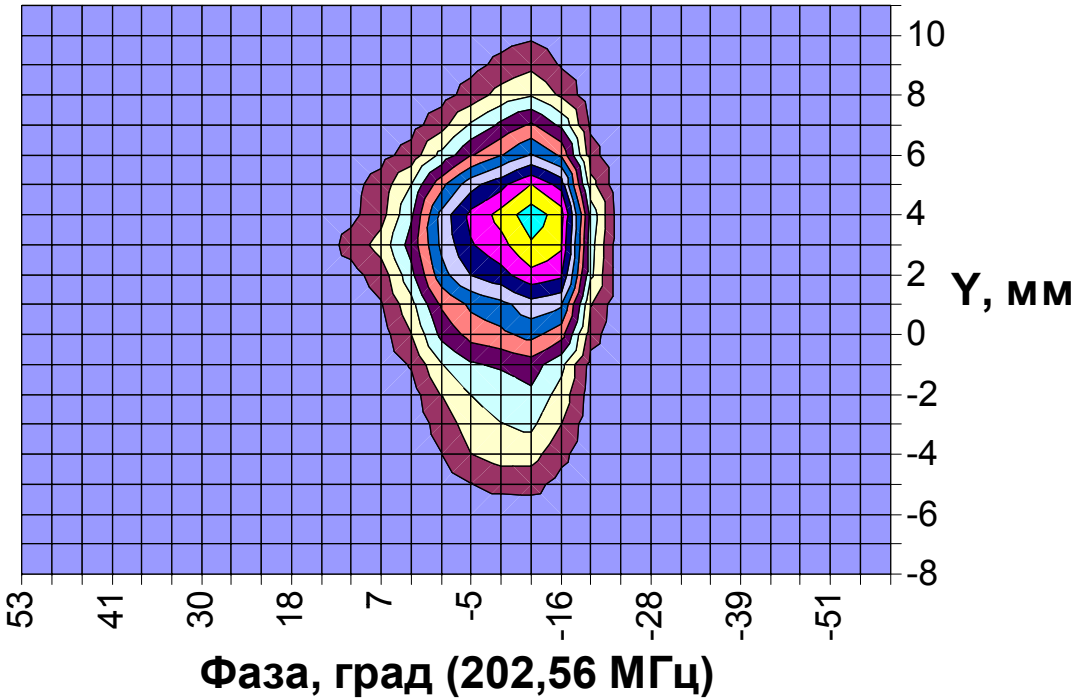

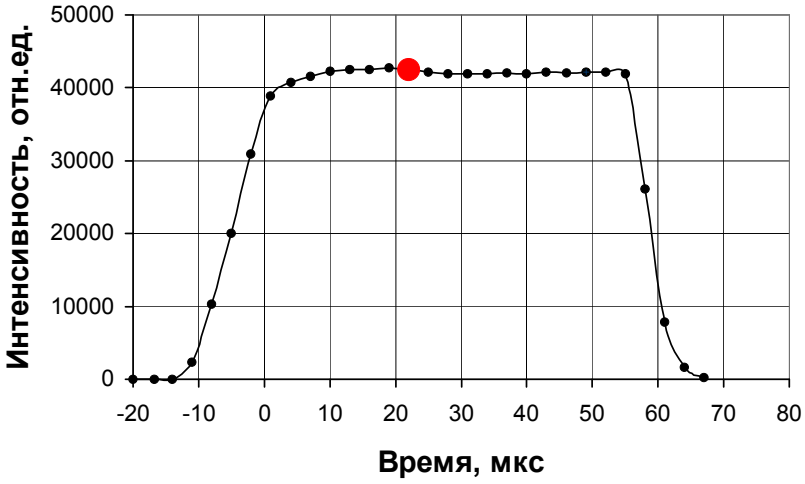

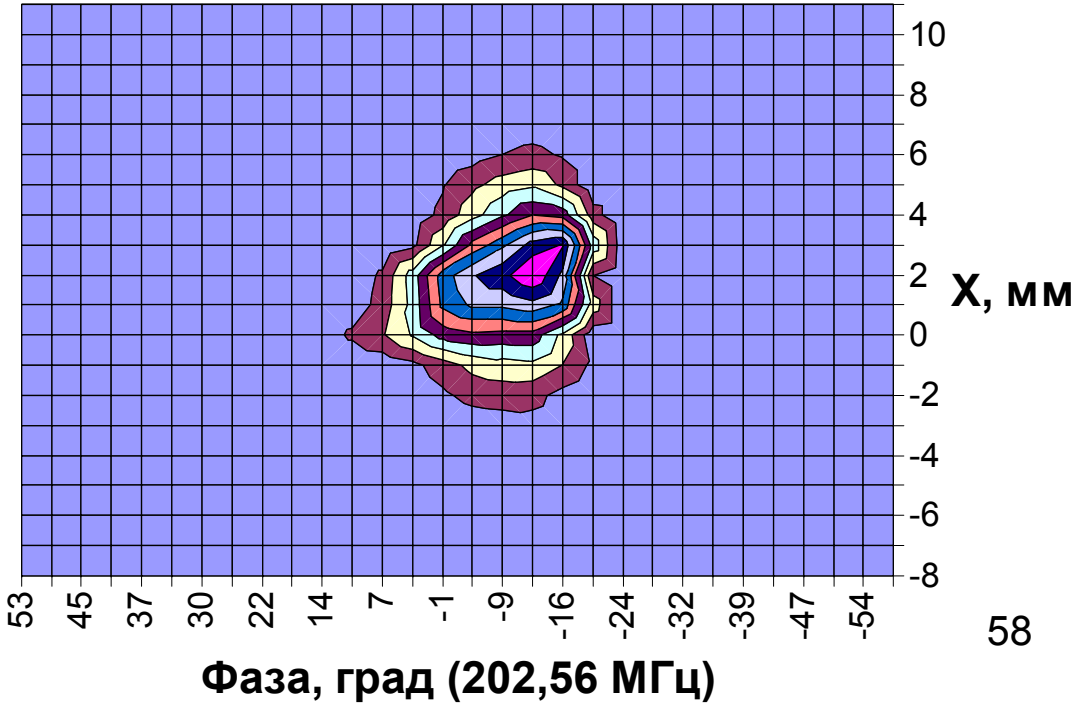

Behavior of 3-D distribution projection on longitudinal vertical and horizontal planes within the beam pulse

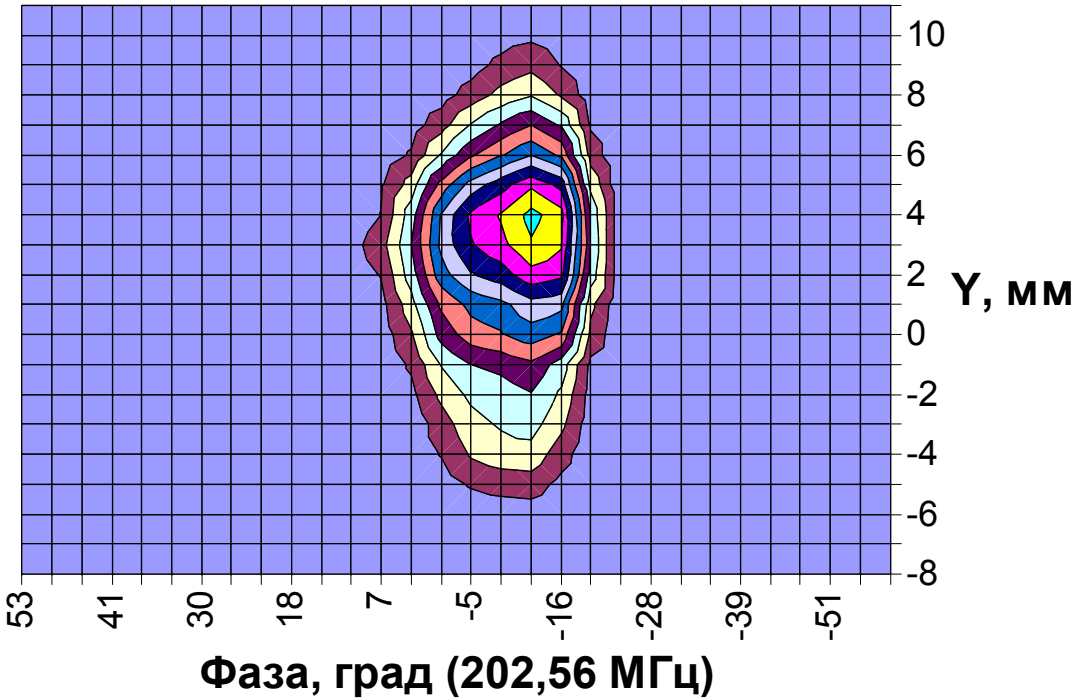

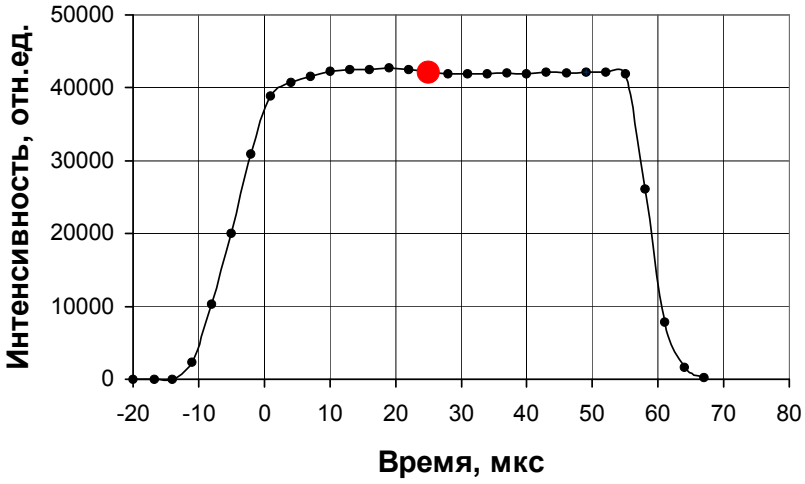

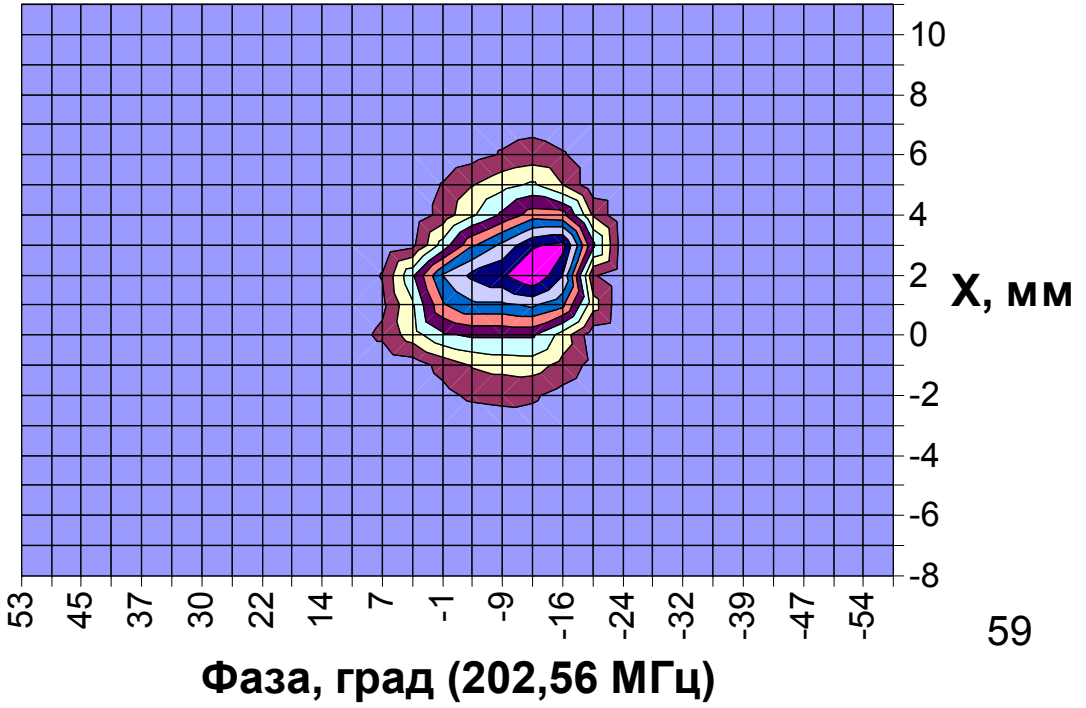

Behavior of 3-D distribution projection on longitudinal vertical and horizontal planes within the beam pulse

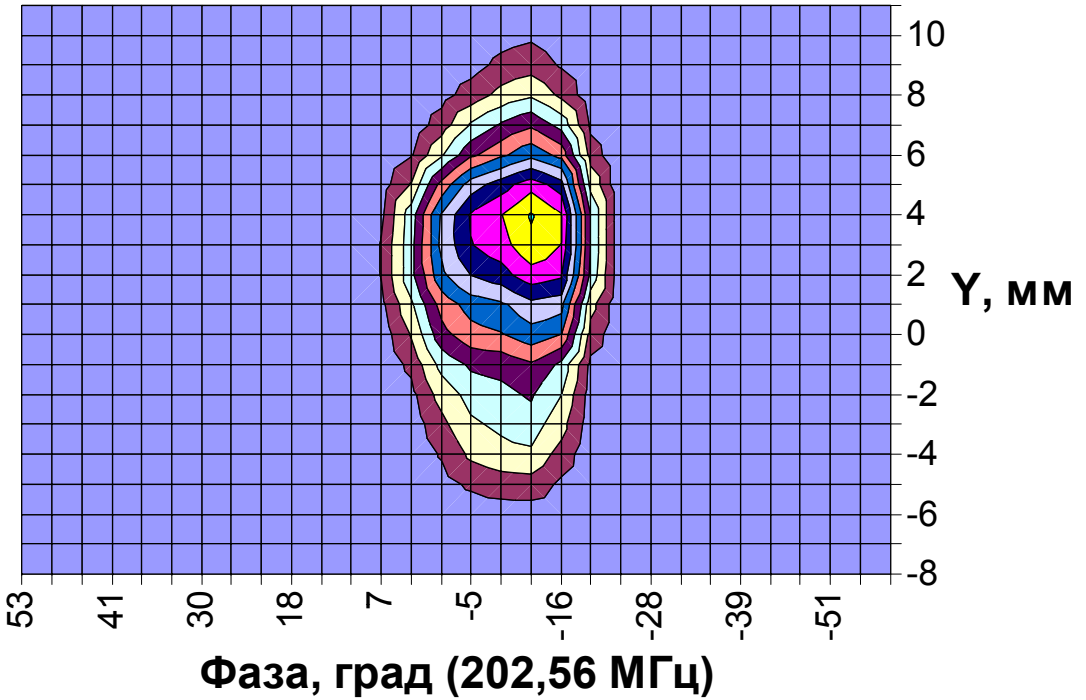

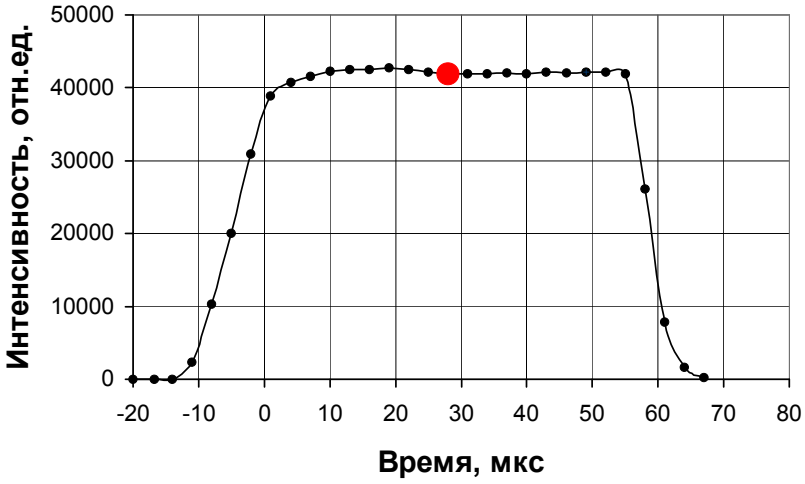

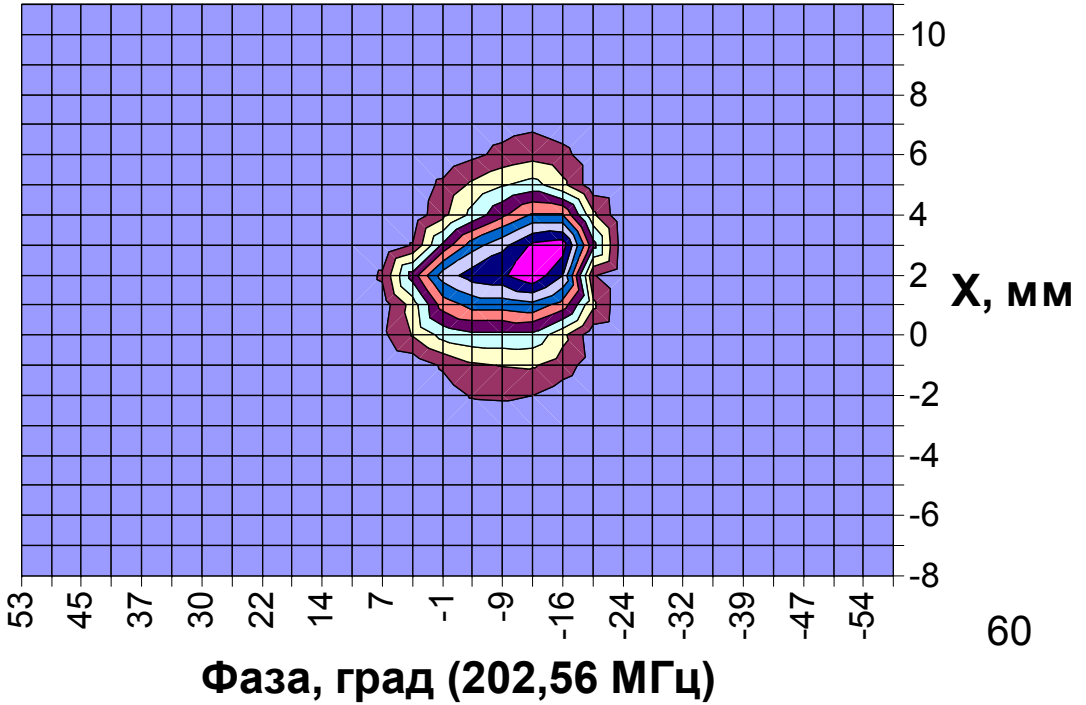

Behavior of 3-D distribution projection on longitudinal vertical and horizontal planes within the beam pulse

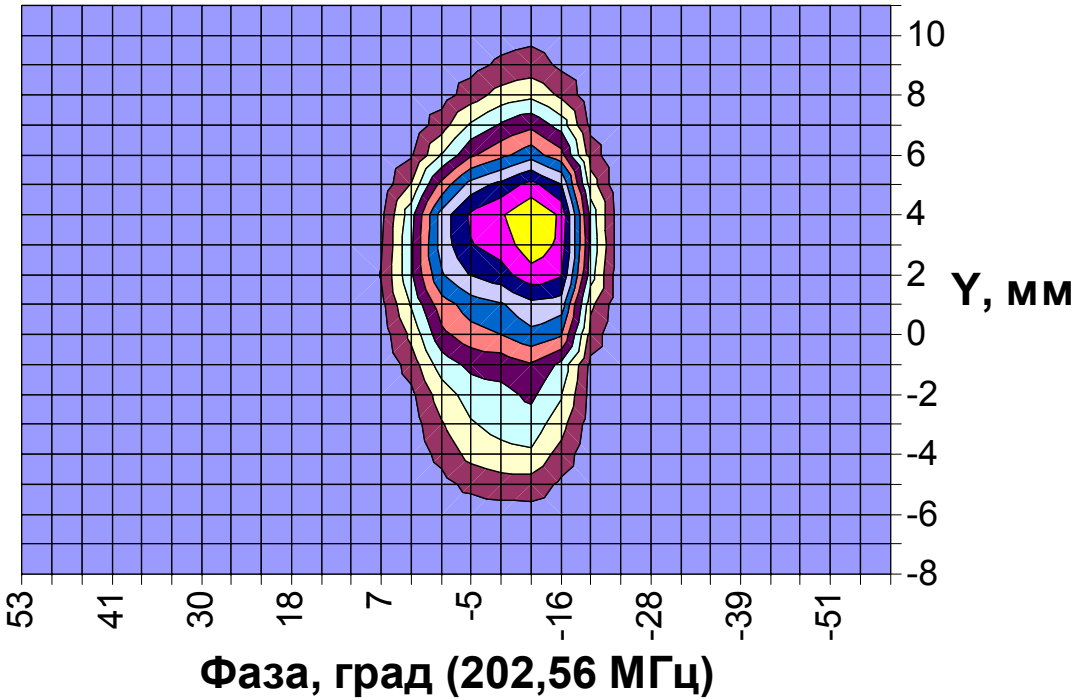

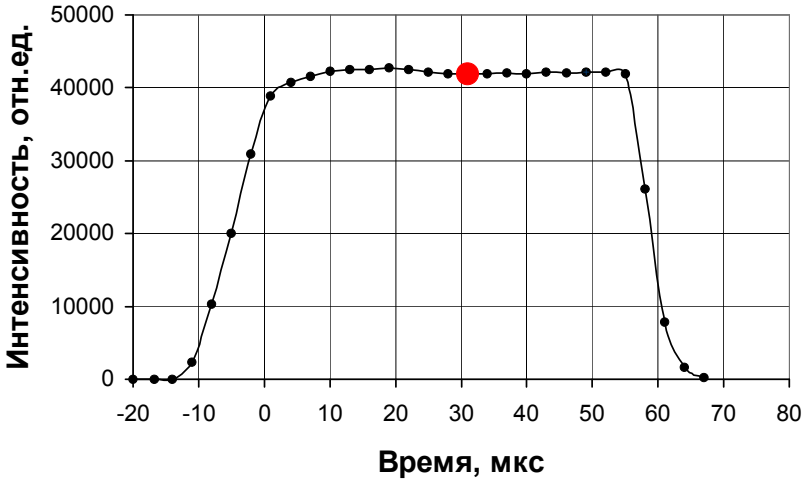

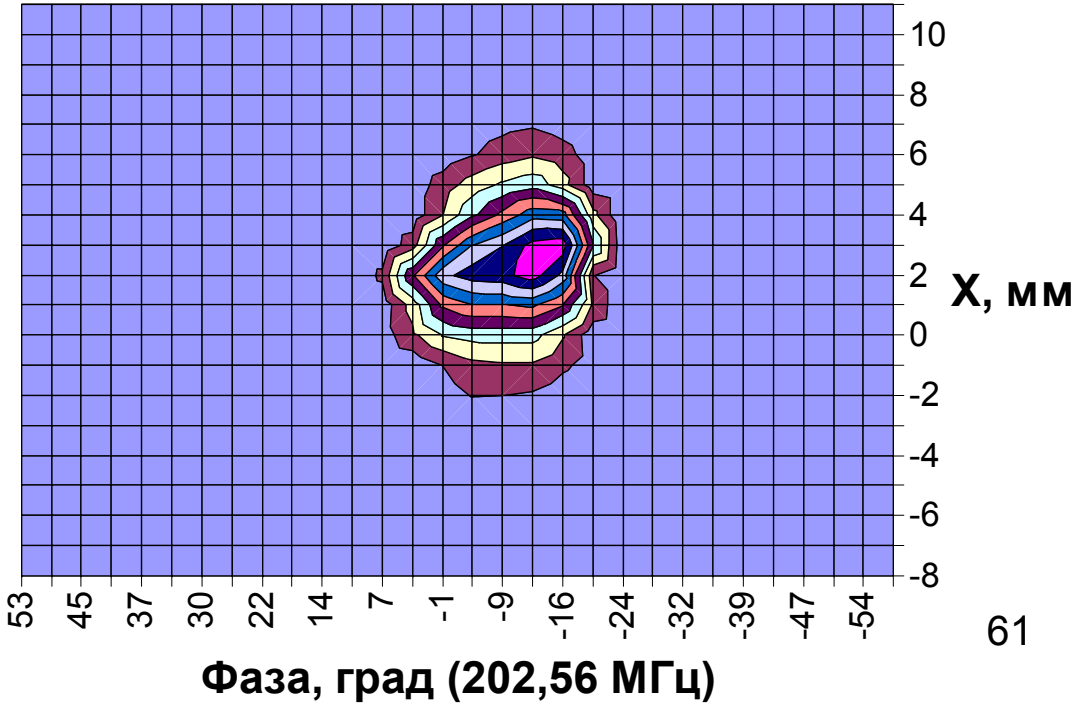

Behavior of 3-D distribution projection on longitudinal vertical and horizontal planes within the beam pulse

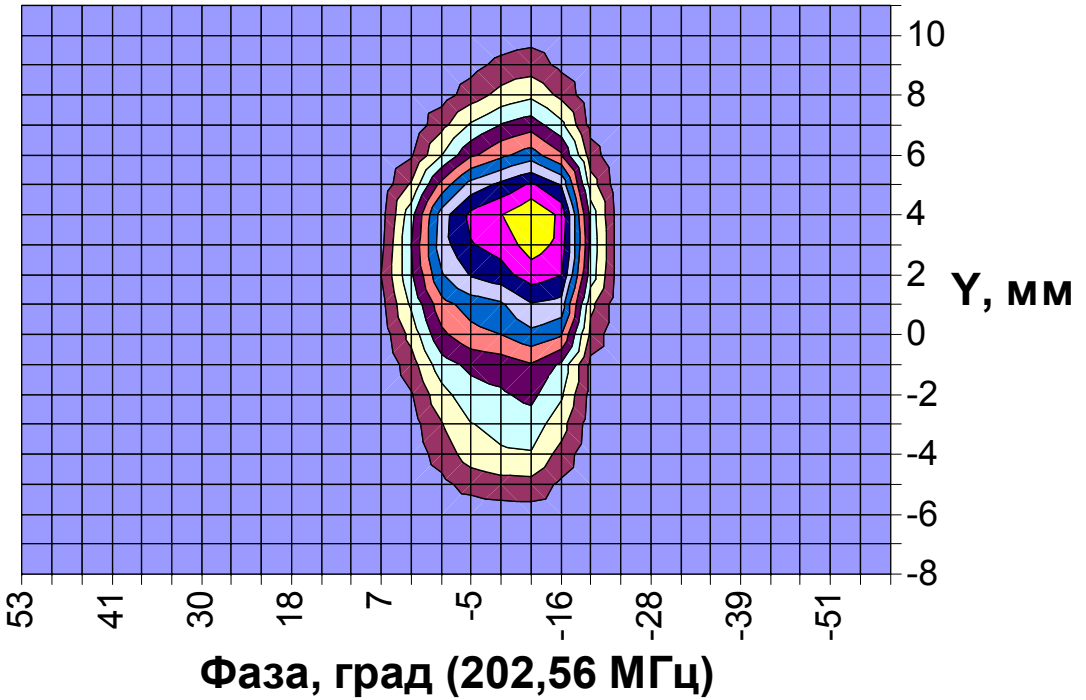

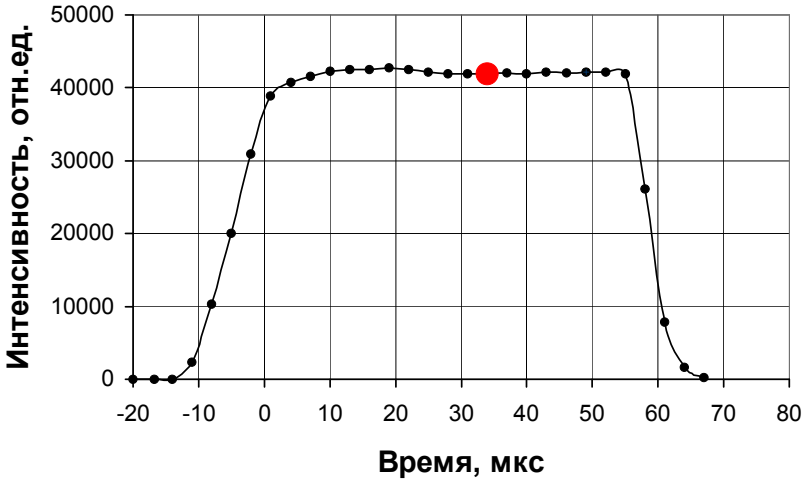

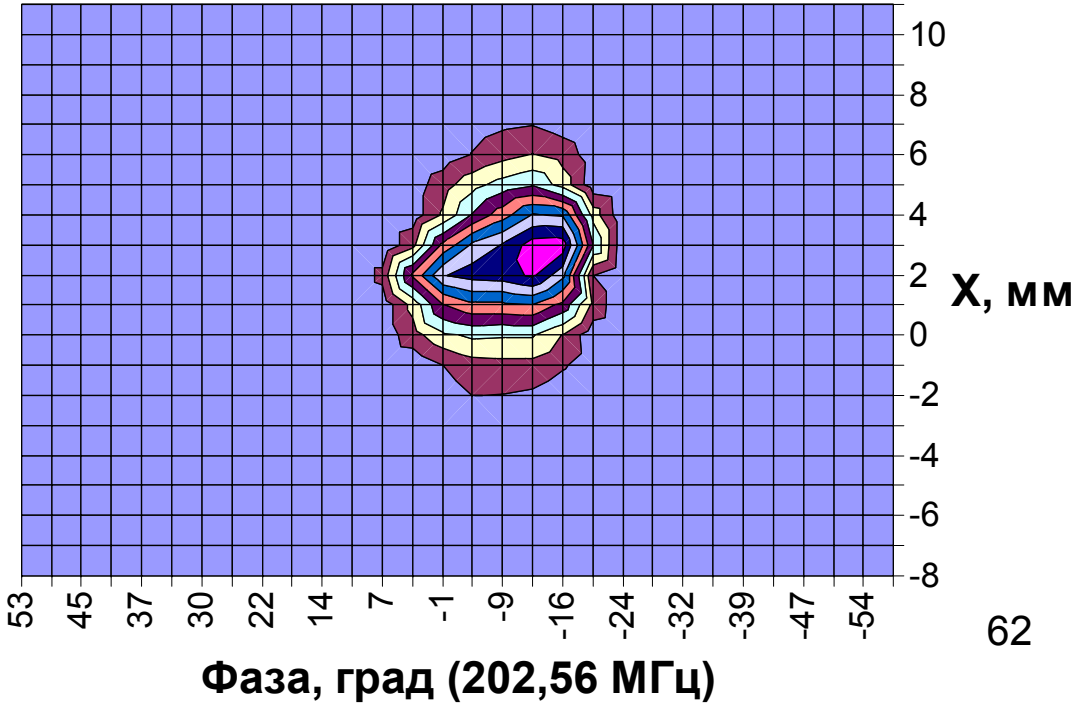

Behavior of 3-D distribution projection on longitudinal vertical and horizontal planes within the beam pulse

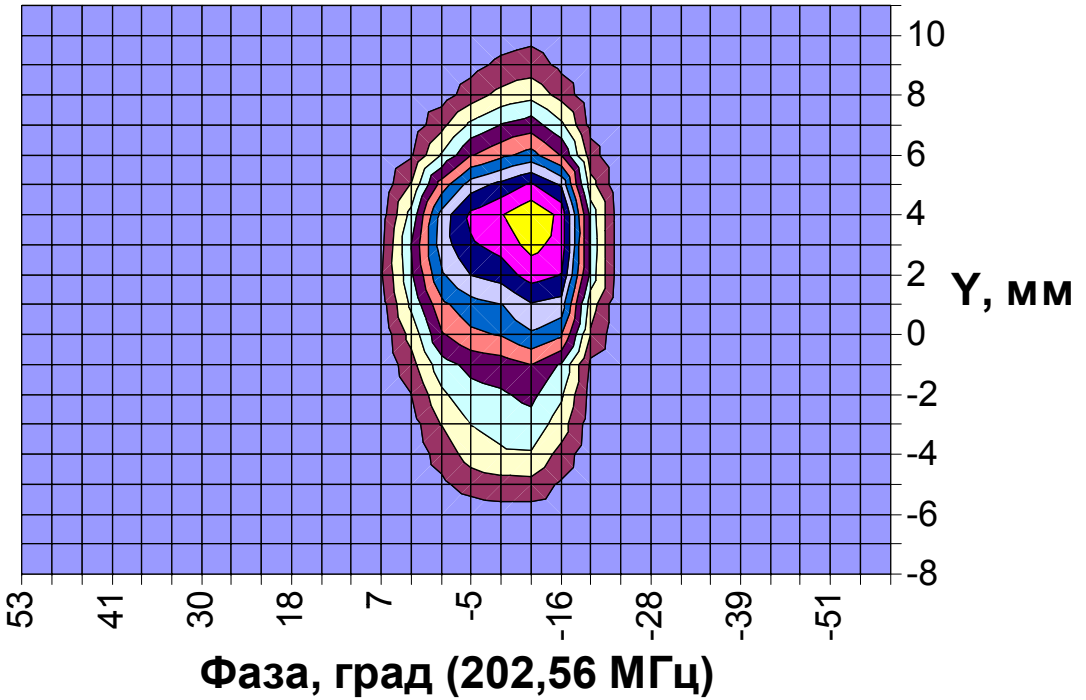

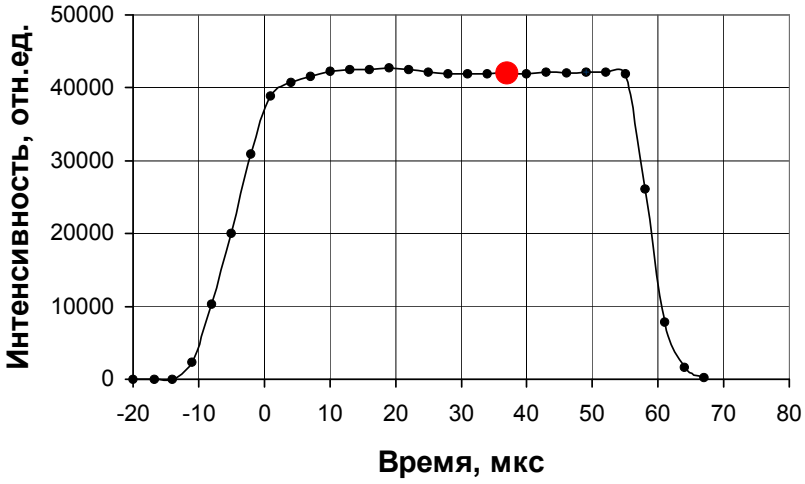

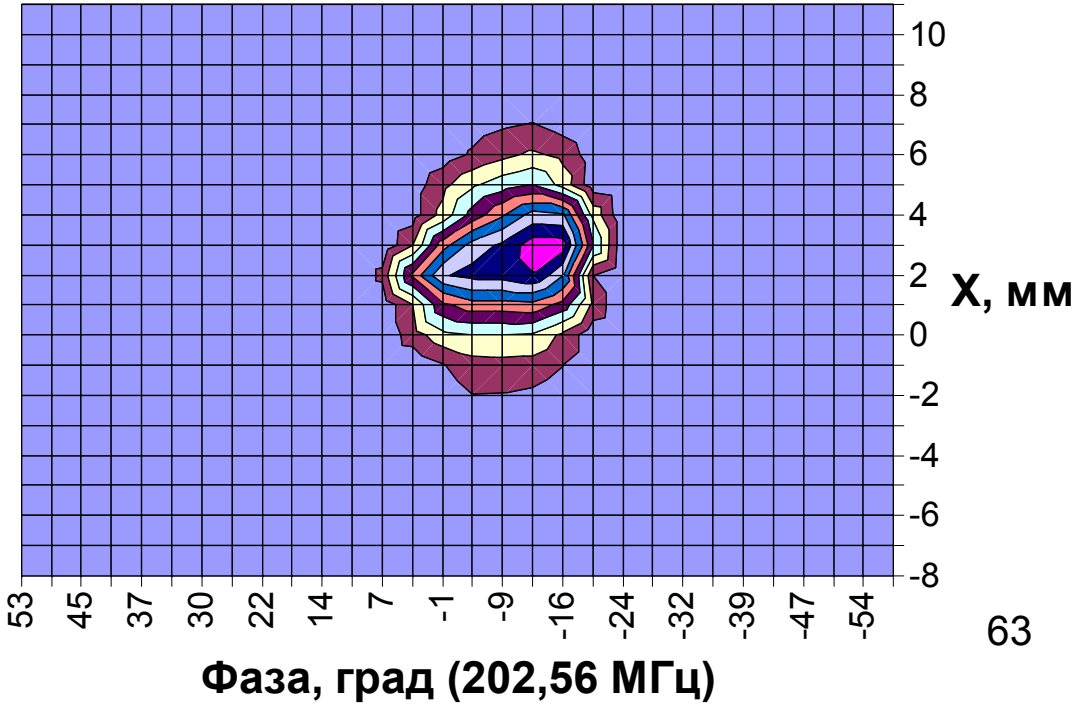

Behavior of 3-D distribution projection on longitudinal vertical and horizontal planes within the beam pulse

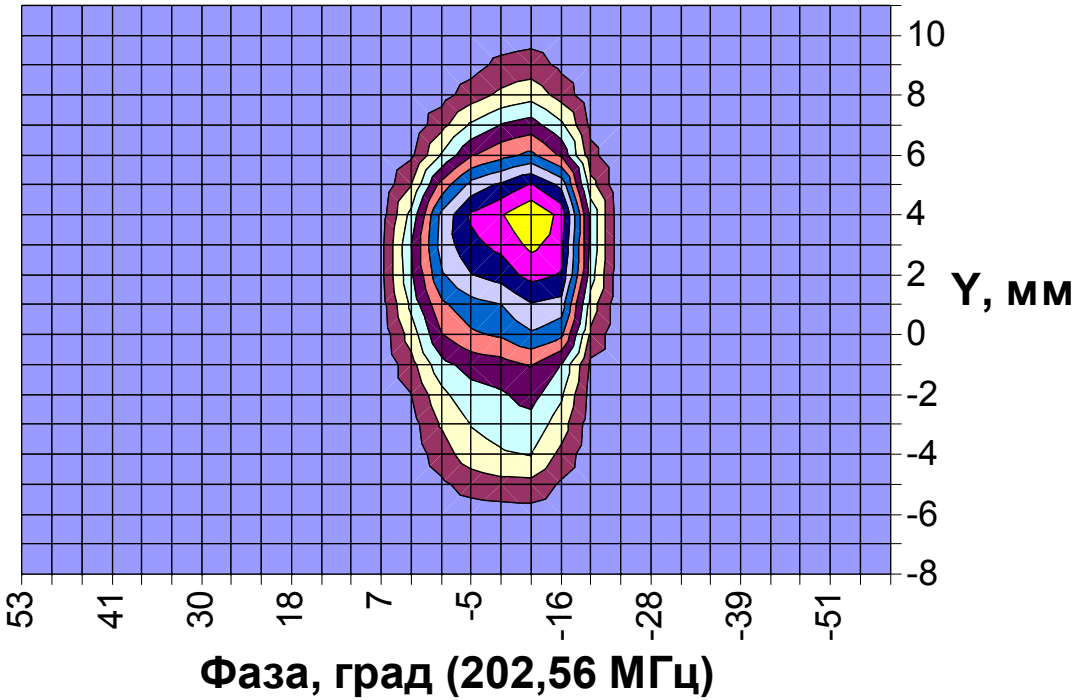

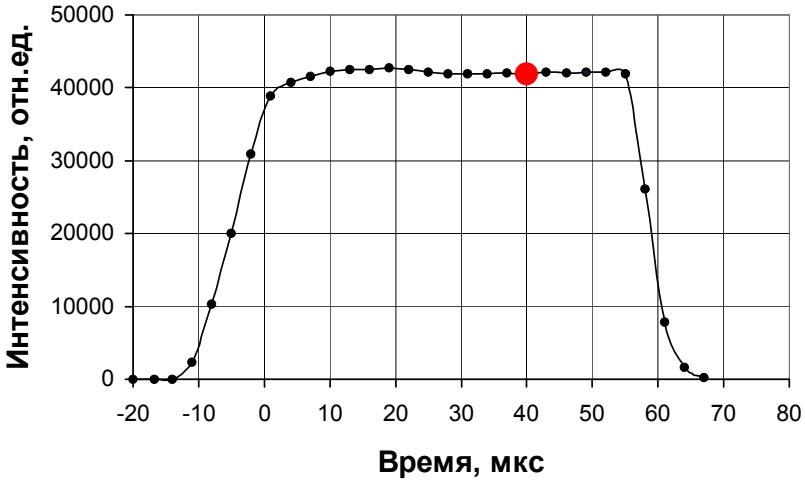

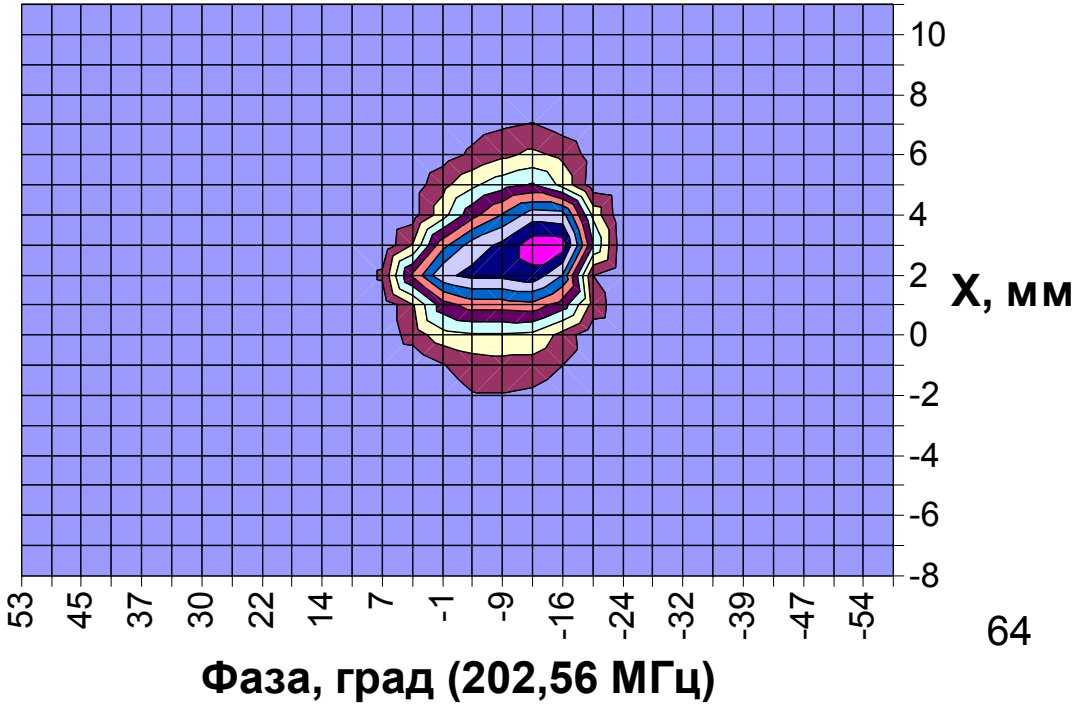

Behavior of 3-D distribution projection on longitudinal vertical and horizontal planes within the beam pulse

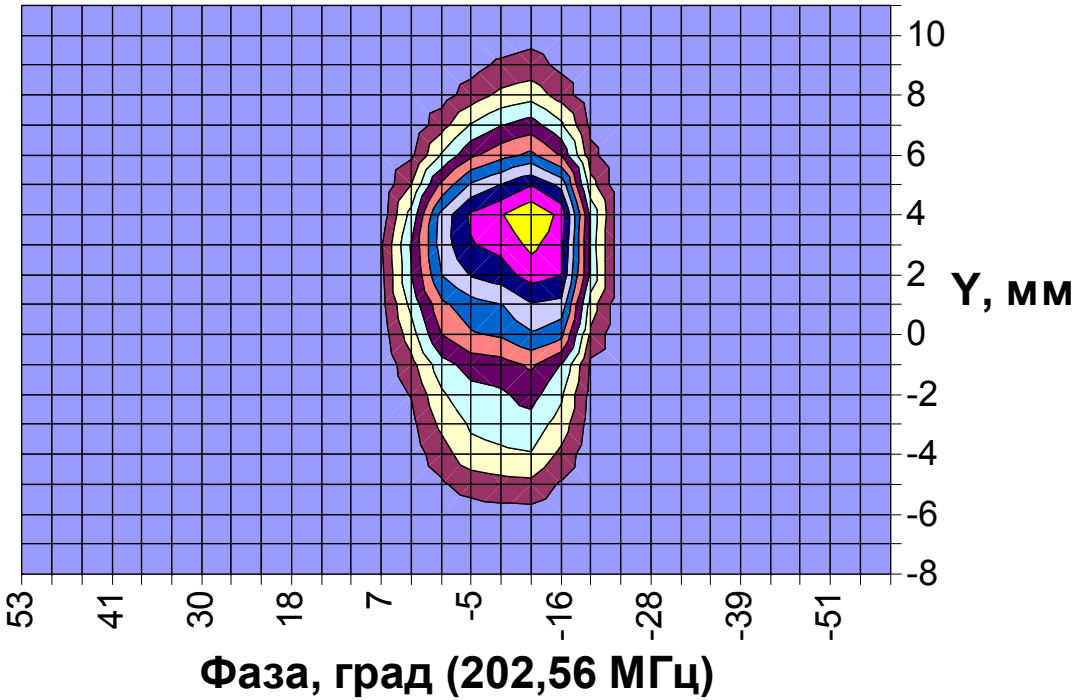

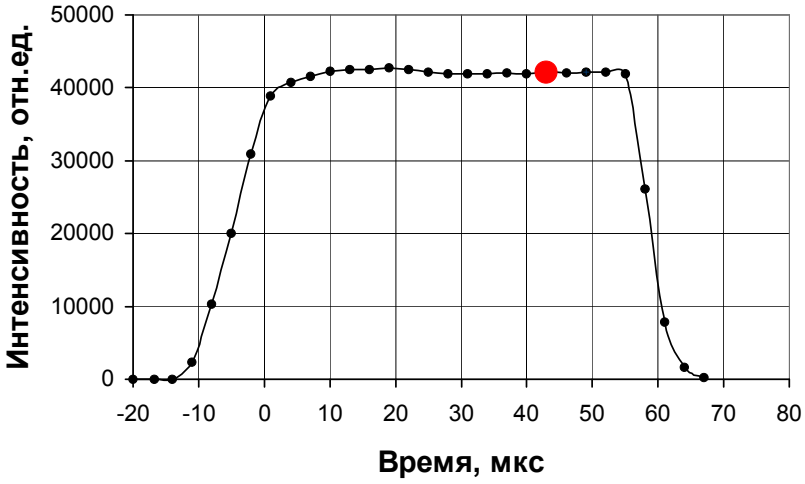

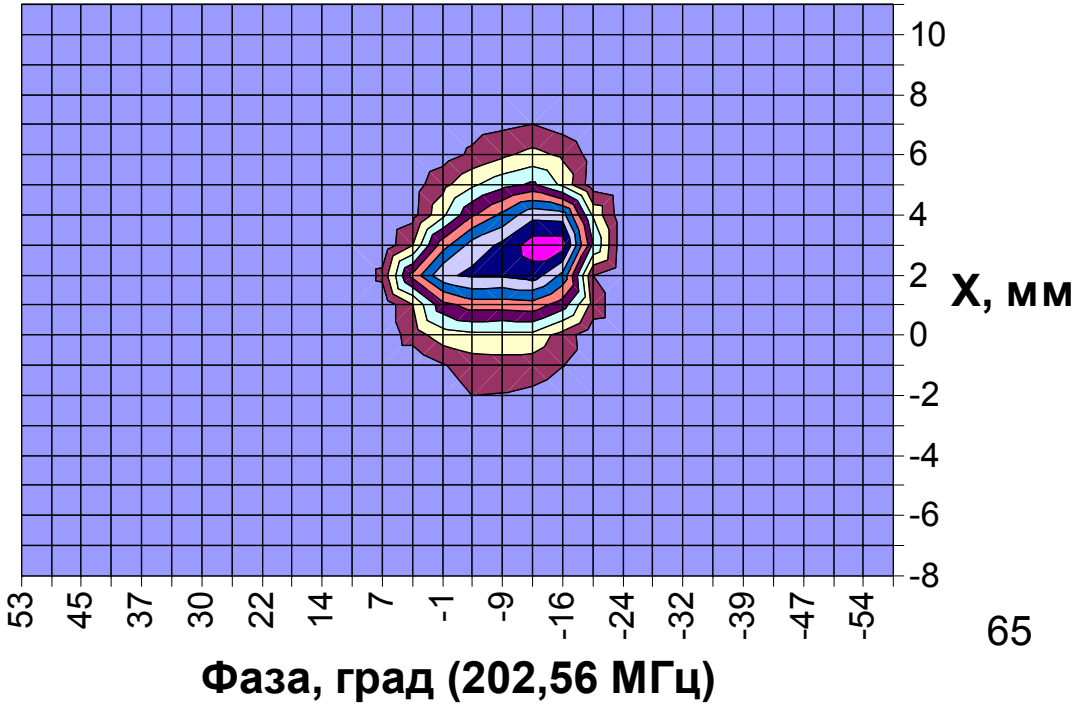

Behavior of 3-D distribution projection on longitudinal vertical and horizontal planes within the beam pulse

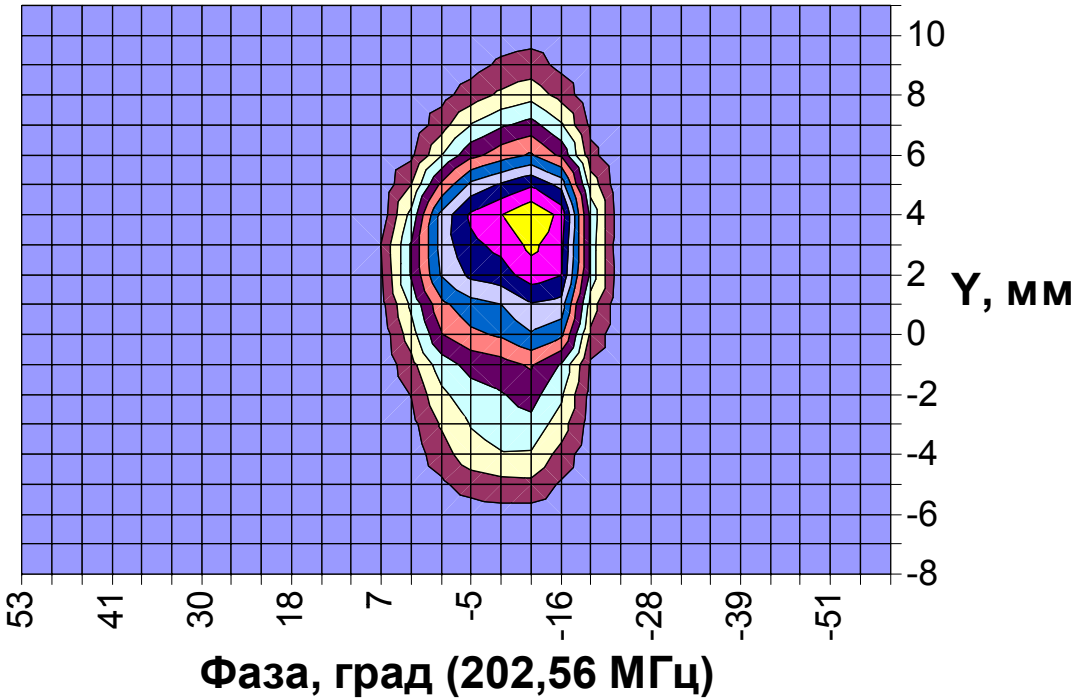

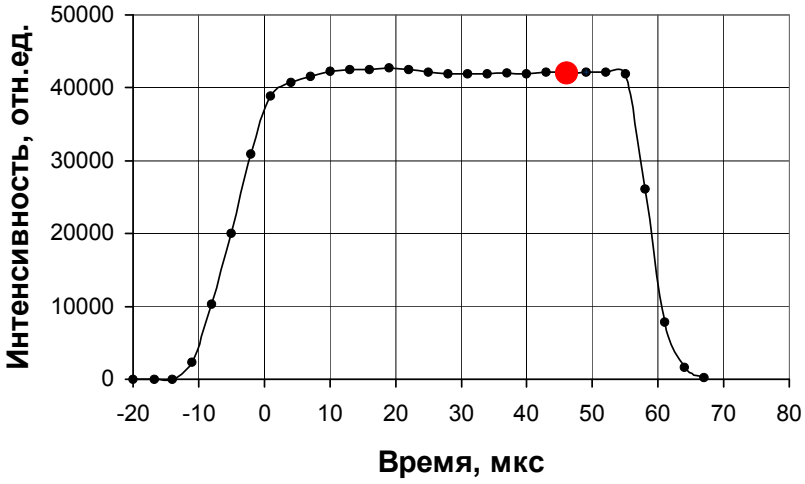

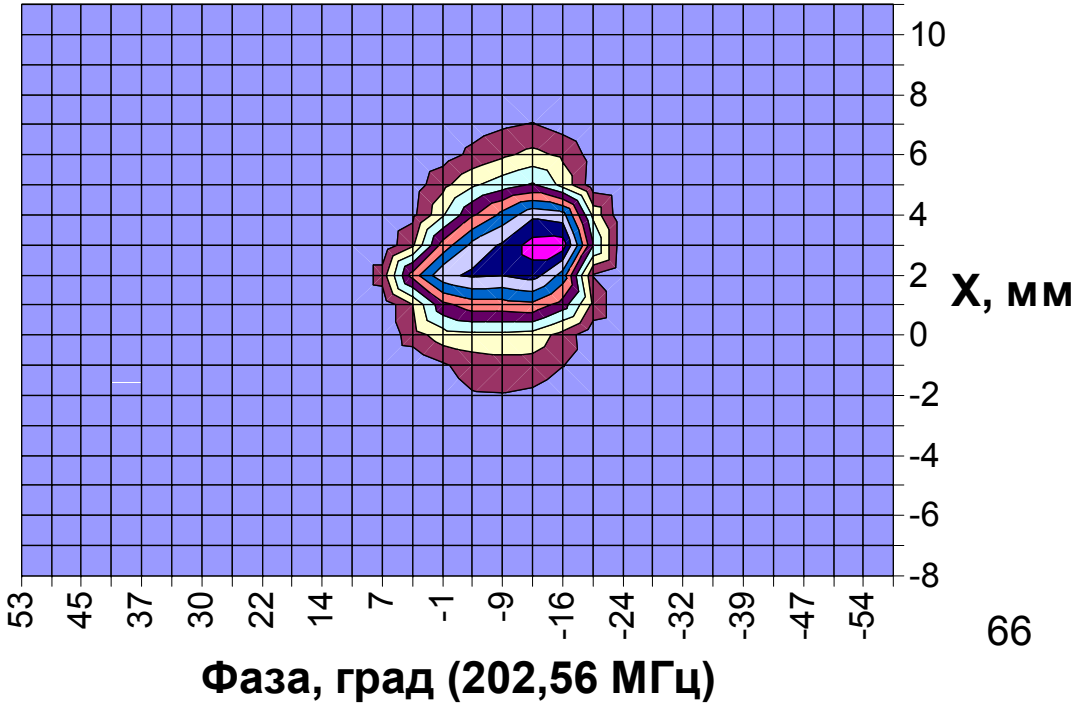

Behavior of 3-D distribution projection on longitudinal vertical and horizontal planes within the beam pulse

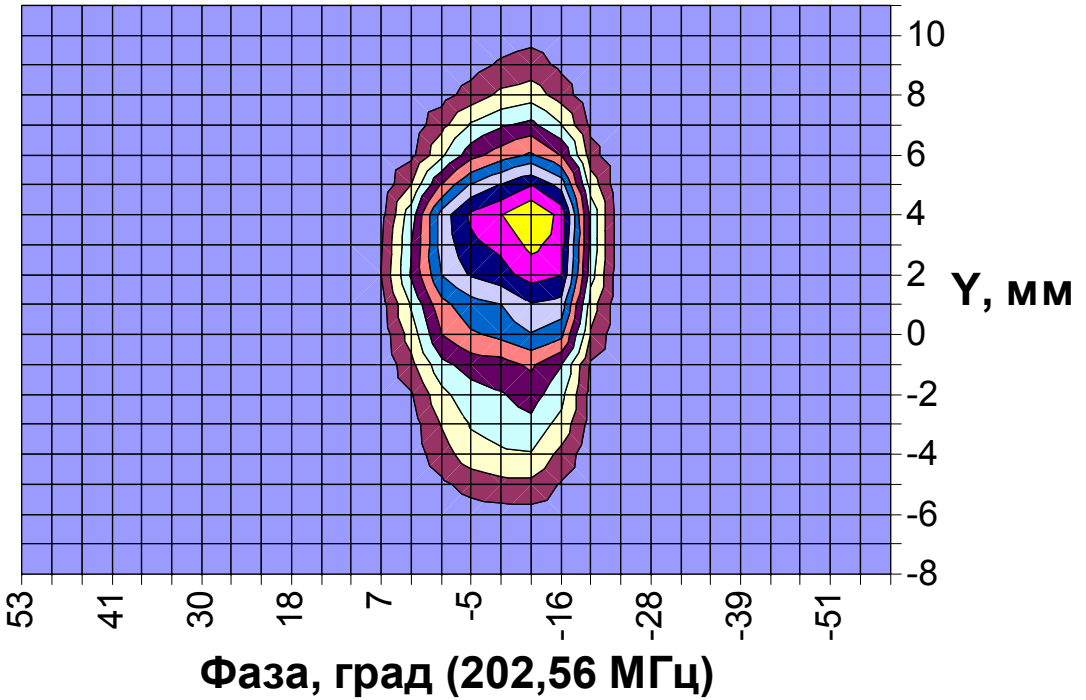

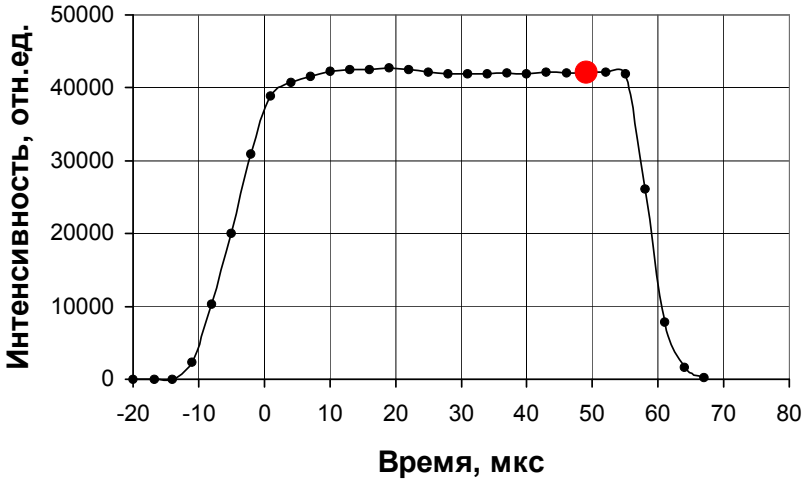

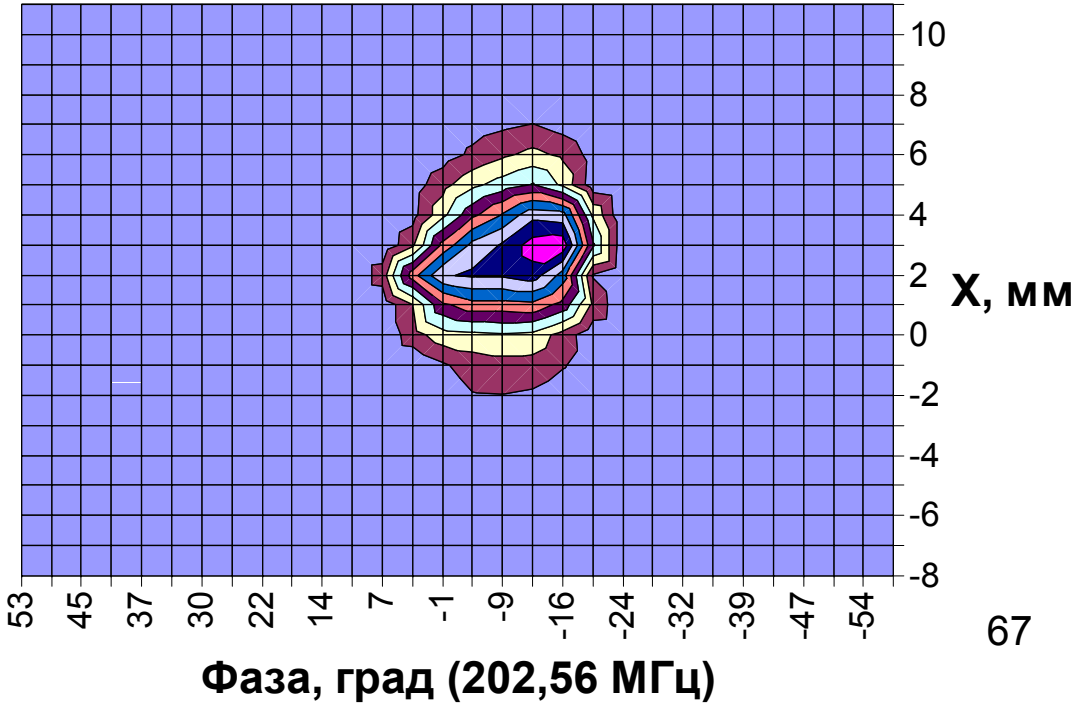

Behavior of 3-D distribution projection on longitudinal vertical and horizontal planes within the beam pulse

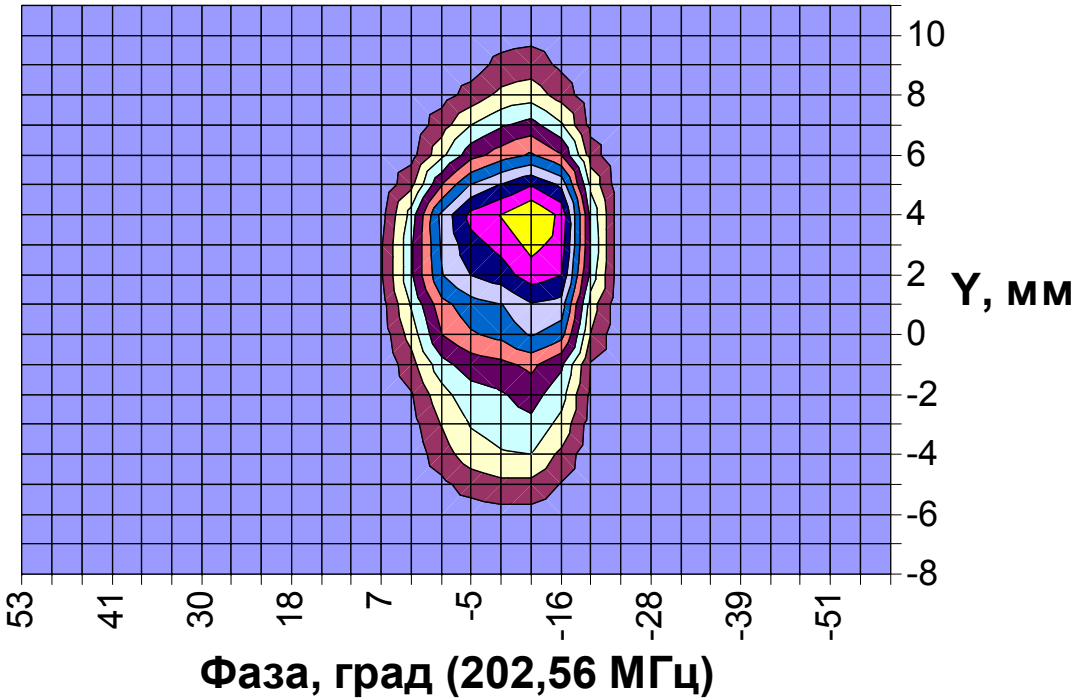

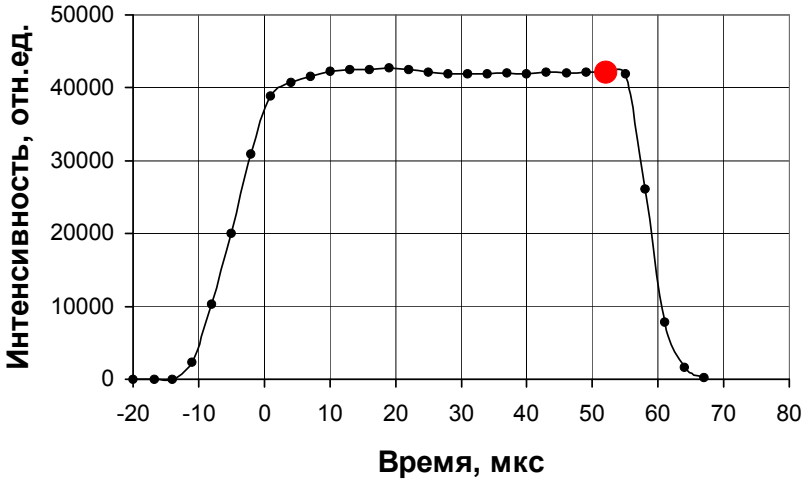

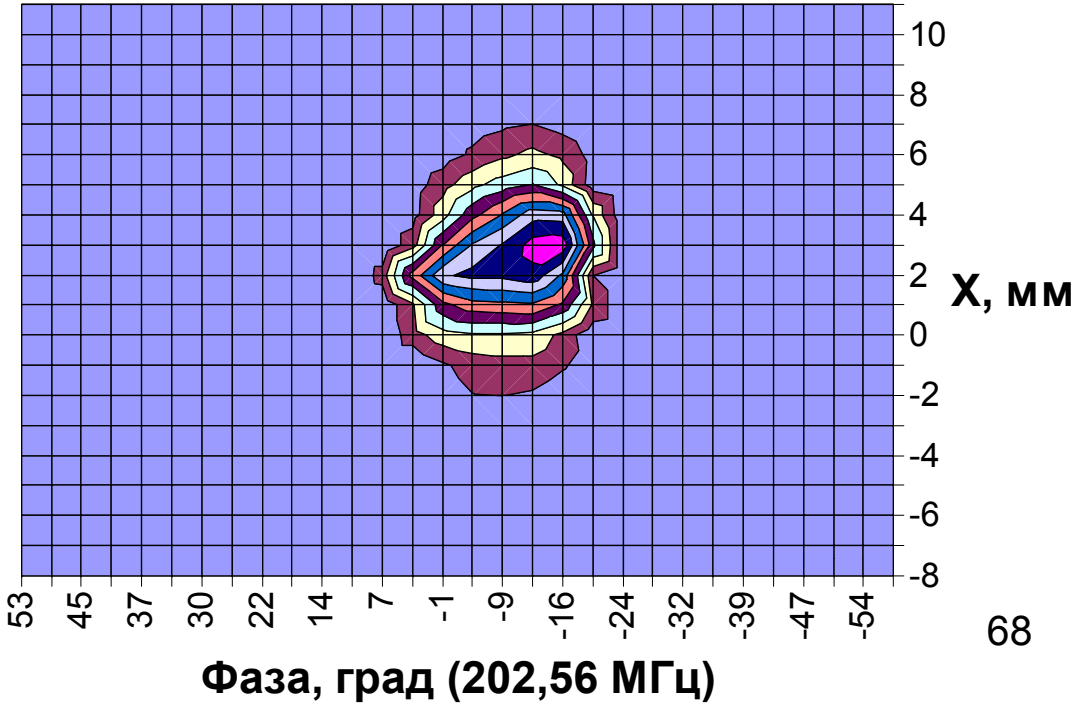

Behavior of 3-D distribution projection on longitudinal vertical and horizontal planes within the beam pulse

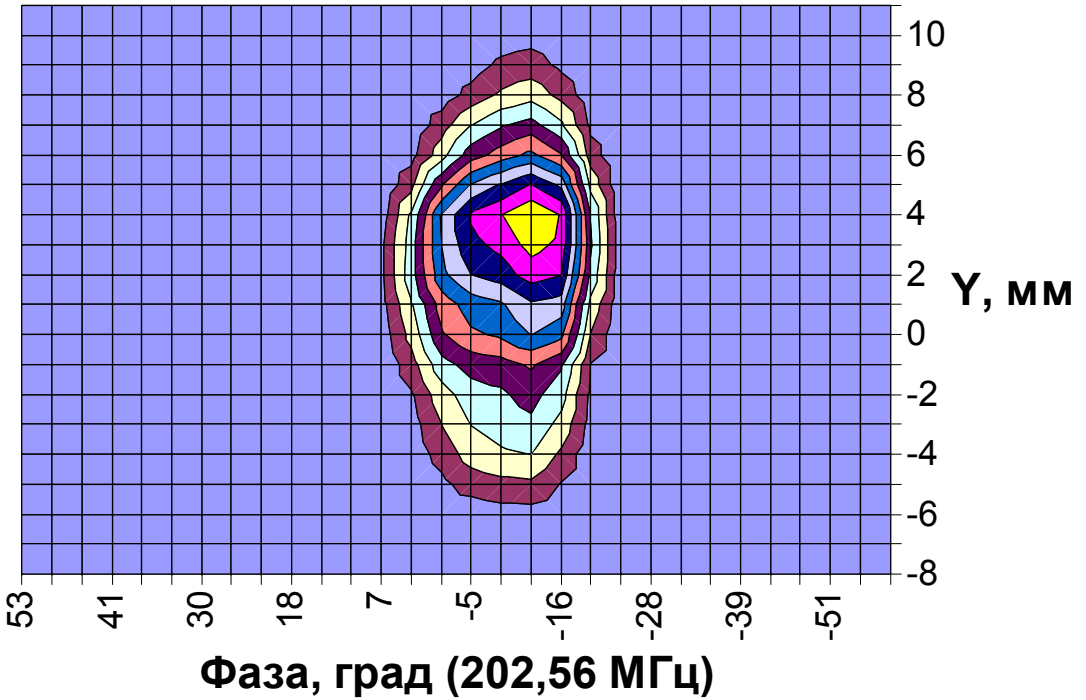

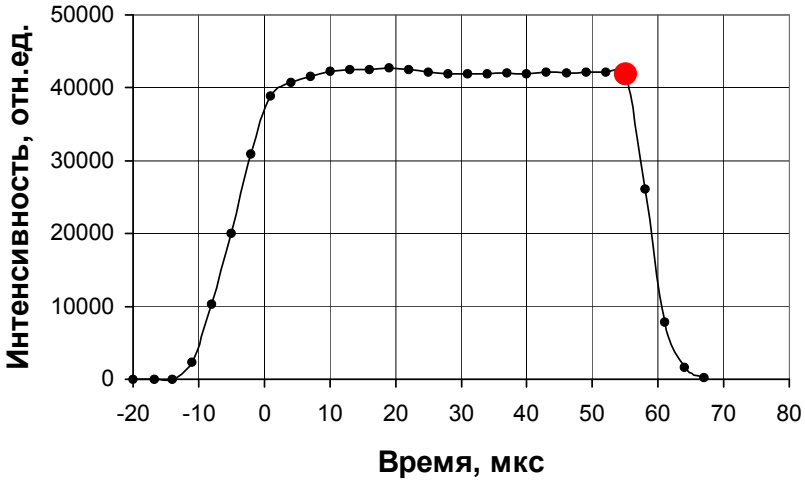

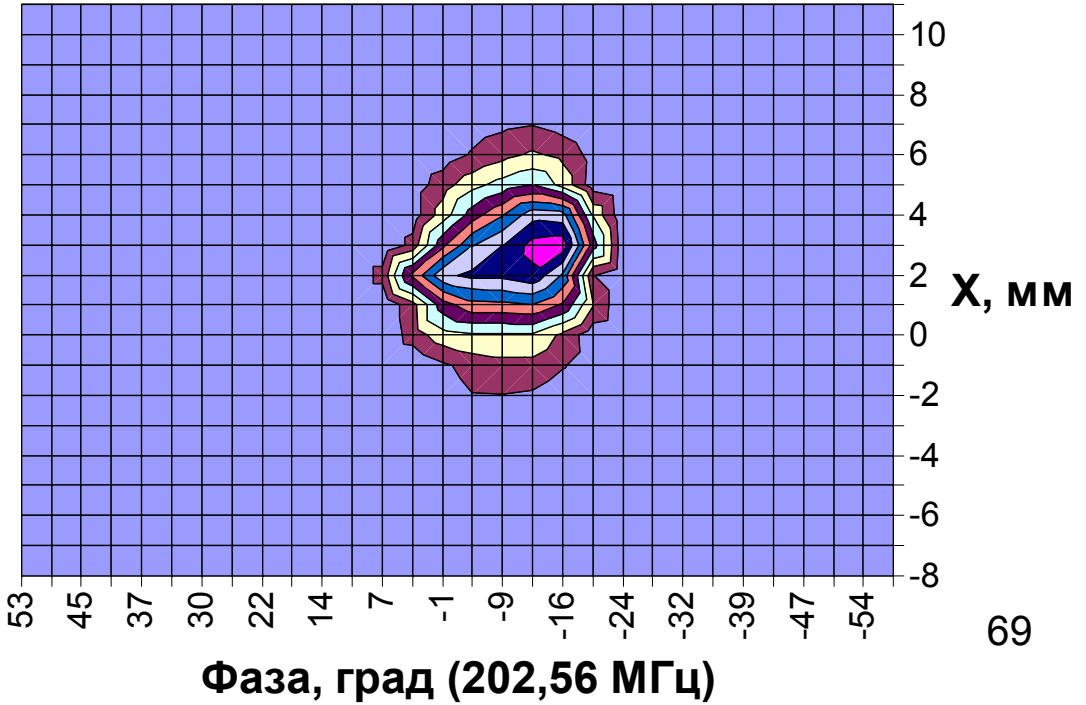

Behavior of 3-D distribution projection on longitudinal vertical and horizontal planes within the beam pulse

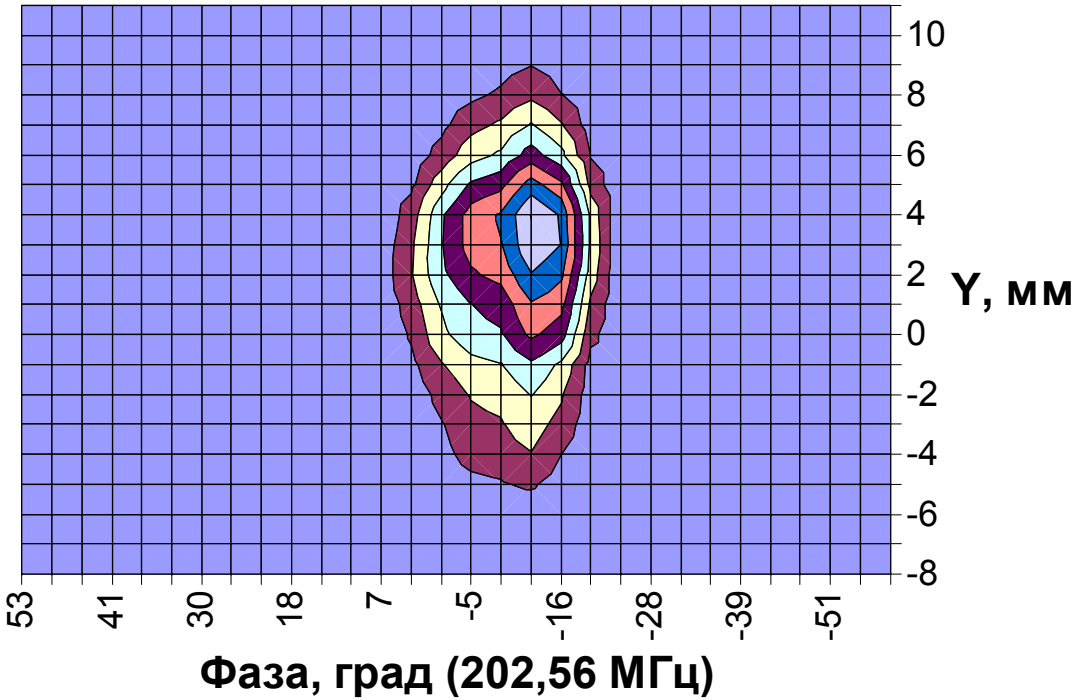

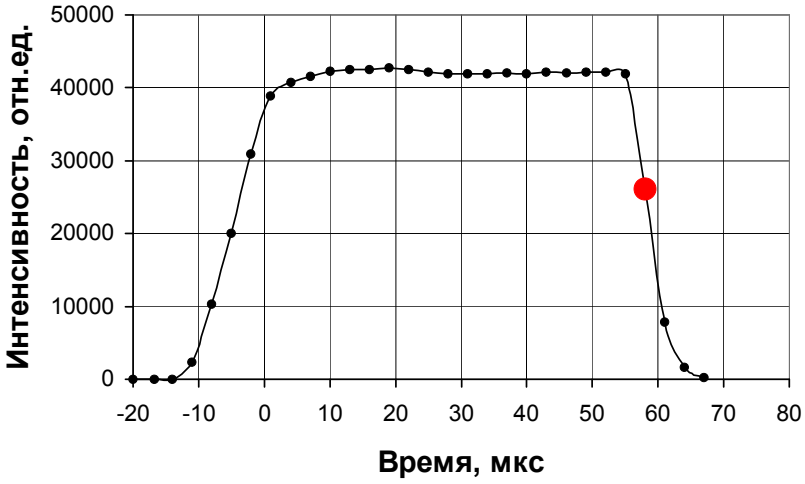

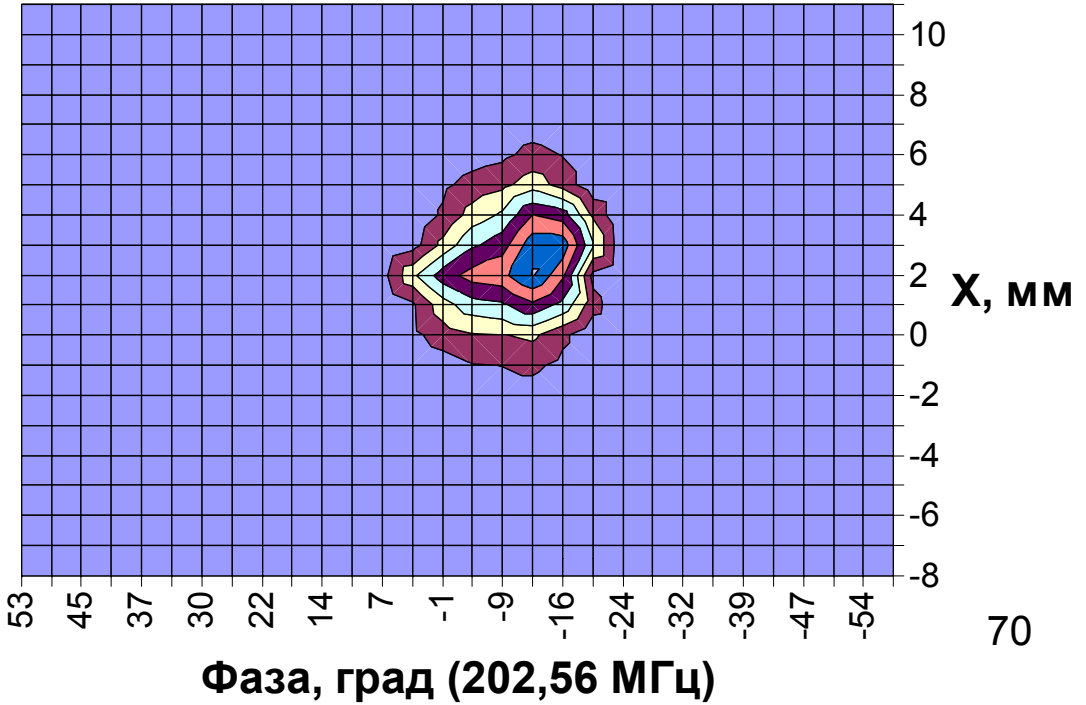

Behavior of 3-D distribution projection on longitudinal vertical and horizontal planes within the beam pulse

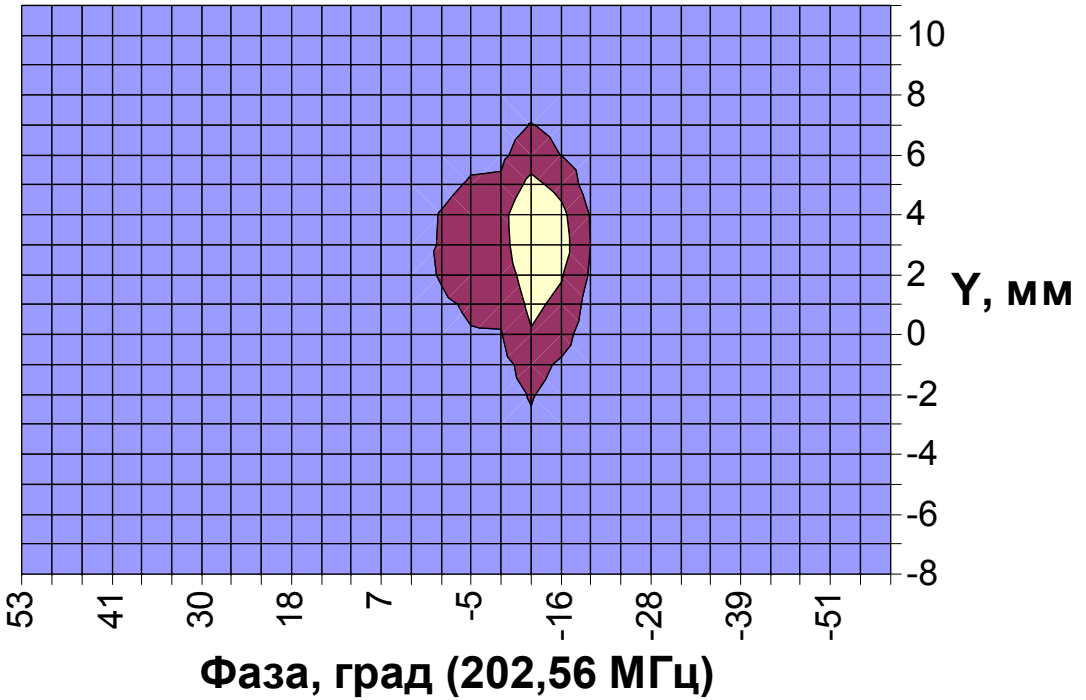

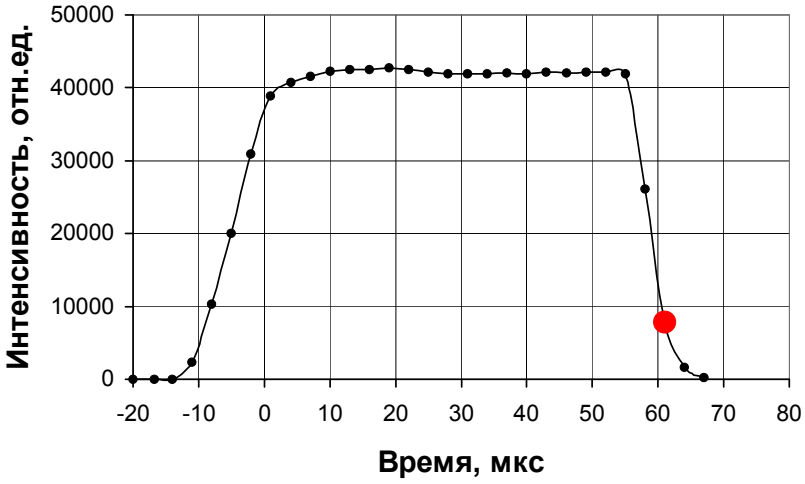

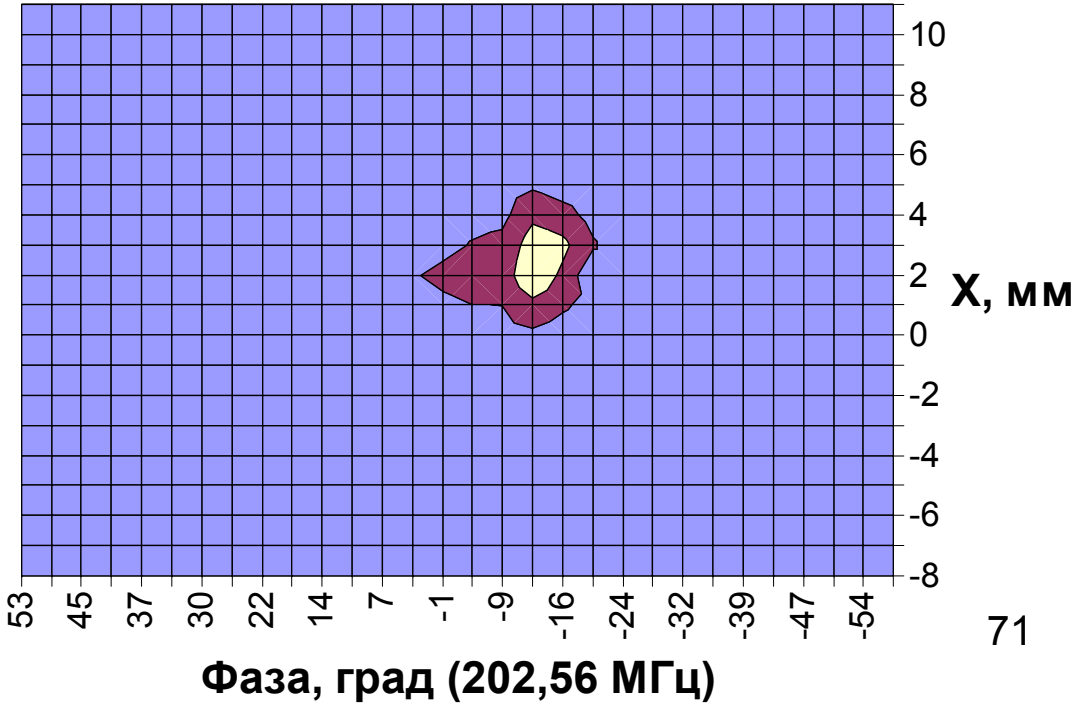

Behavior of 3-D distribution projection on longitudinal vertical and horizontal planes within the beam pulse

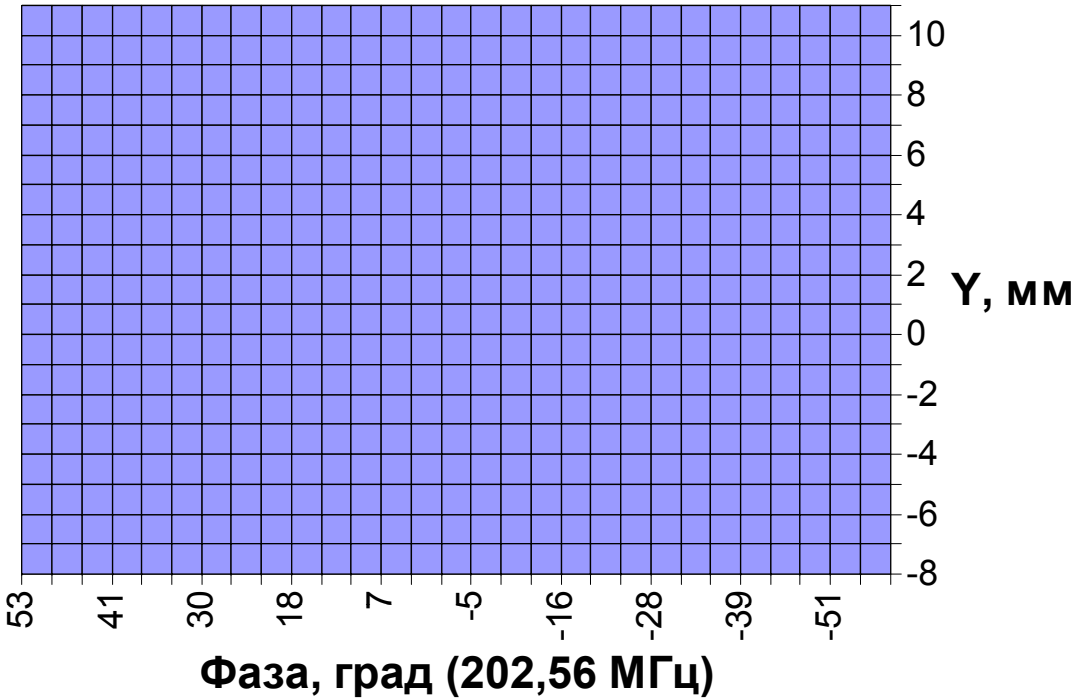

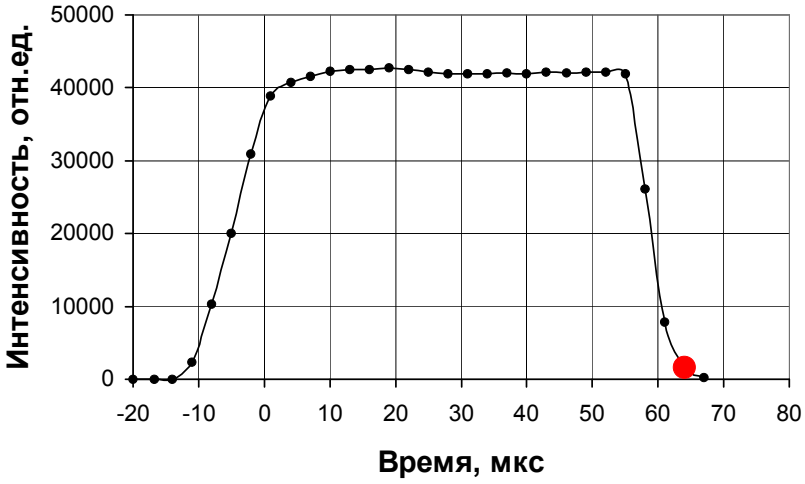

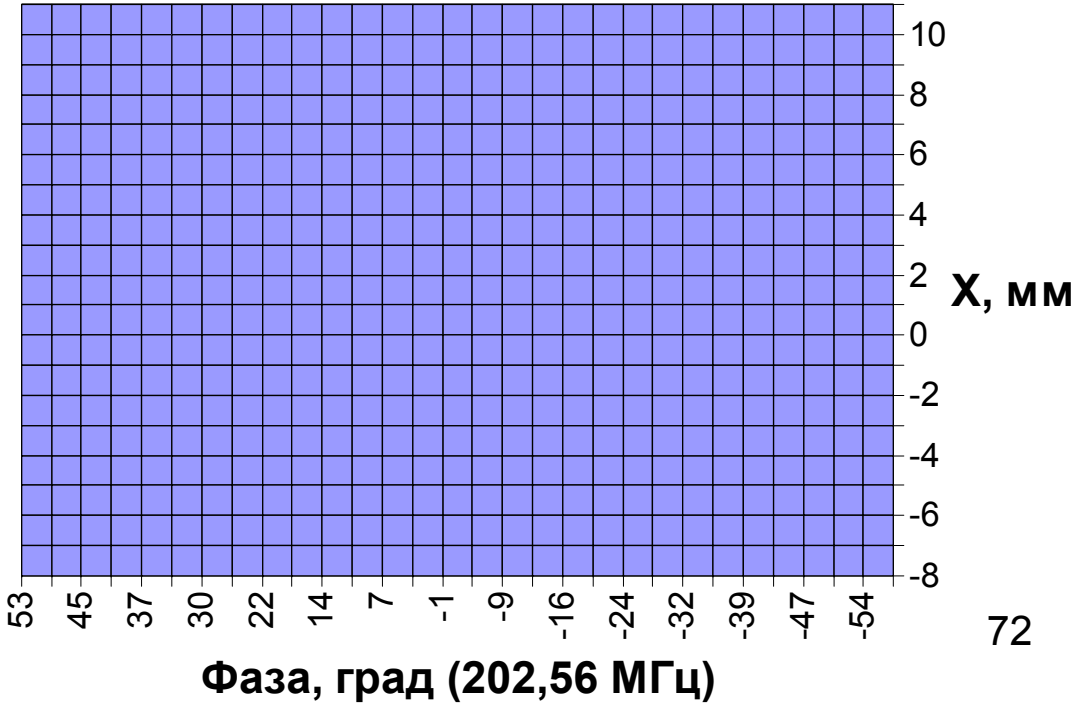

Behavior of 3-D distribution projection on longitudinal vertical and horizontal planes within the beam pulse

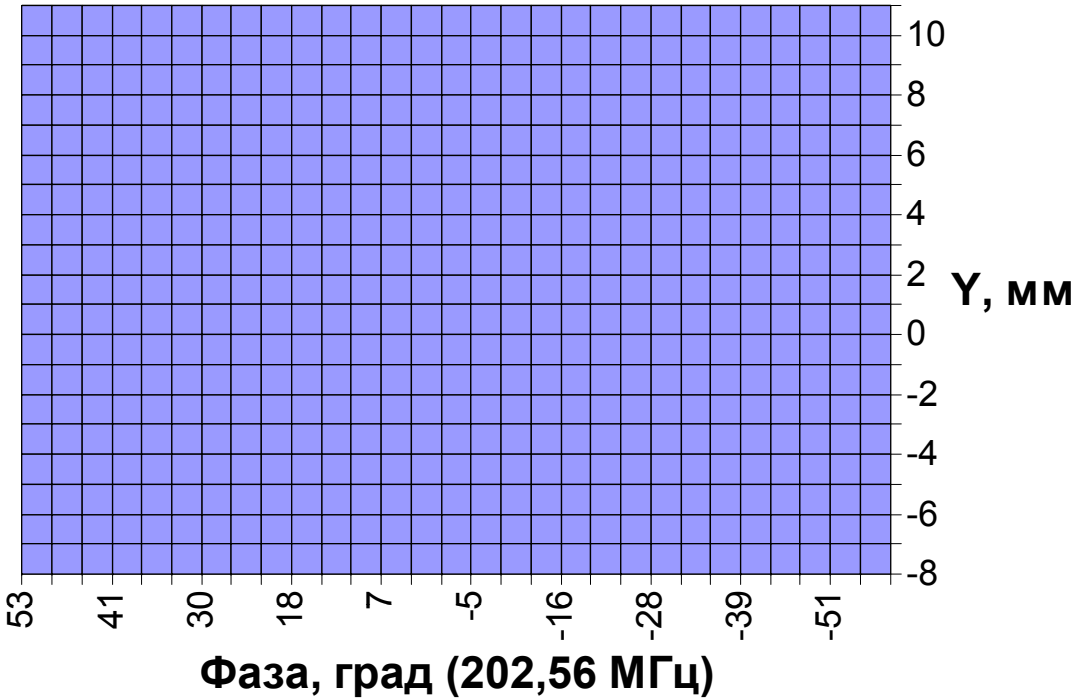

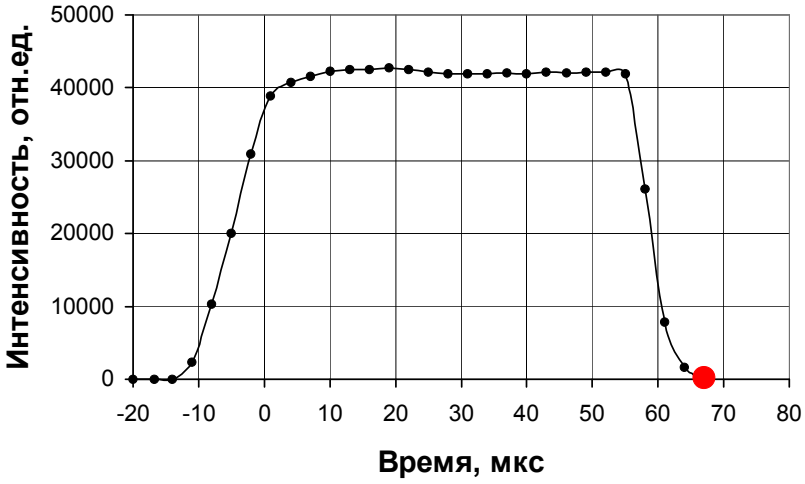

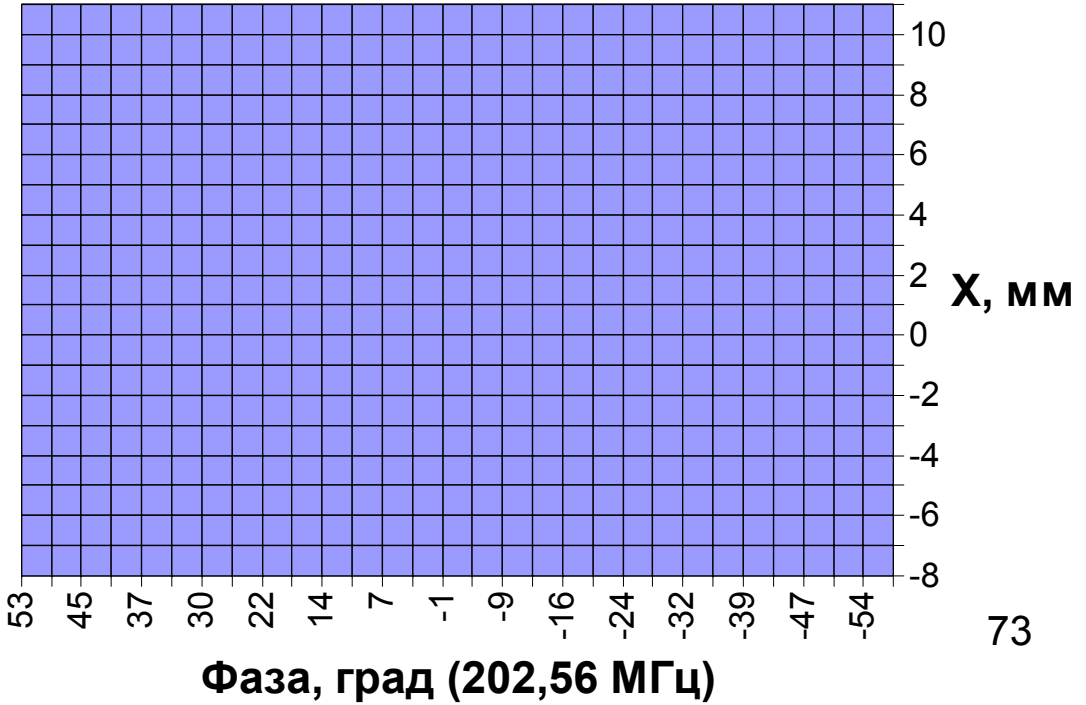

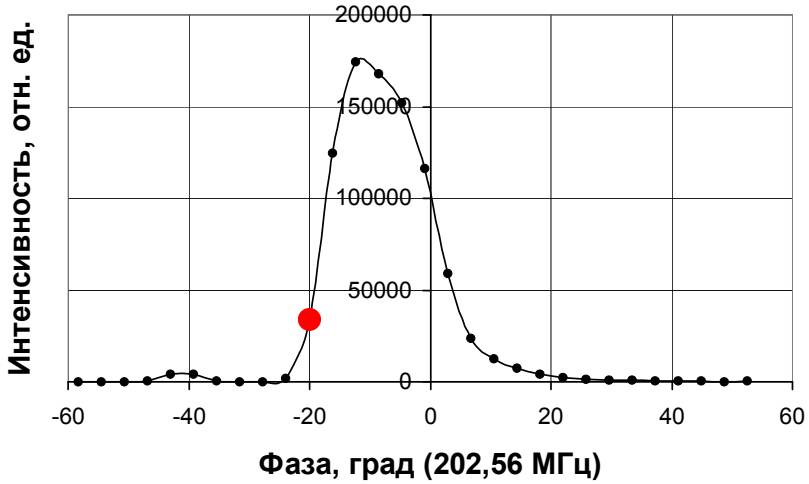

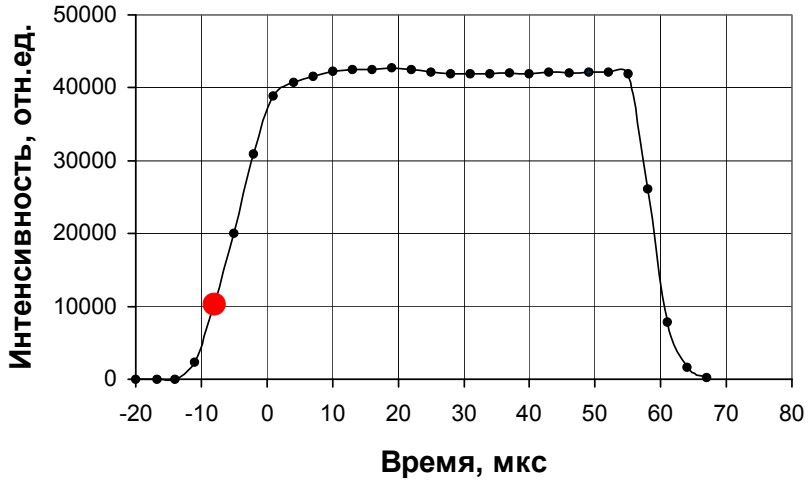

Transverse cross section of a bunch in different phases and at different moments of time within the beam pulse

Bunch #1

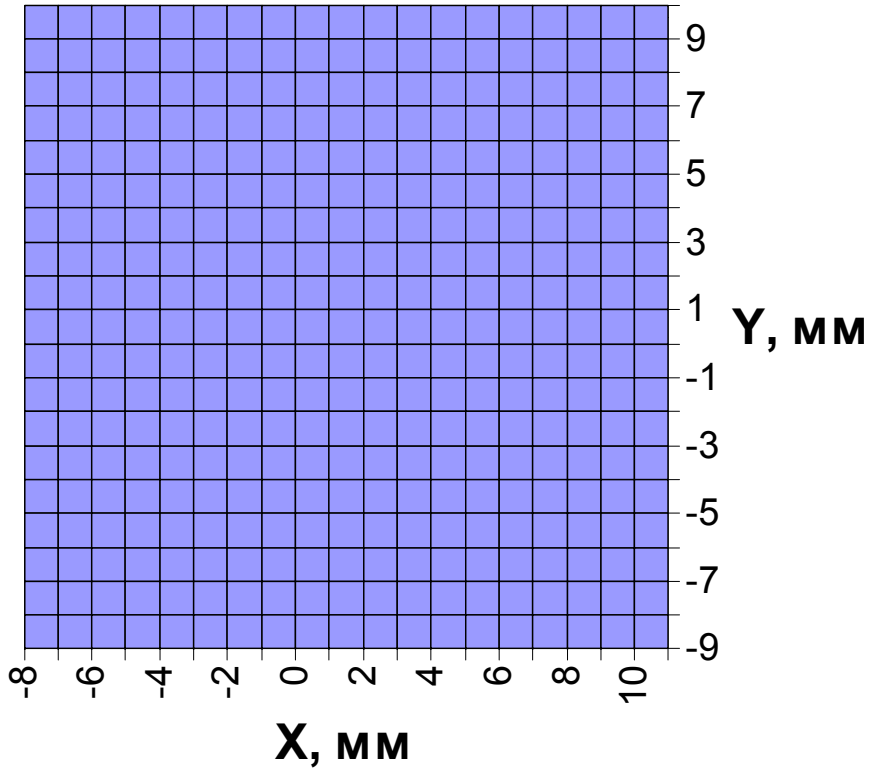

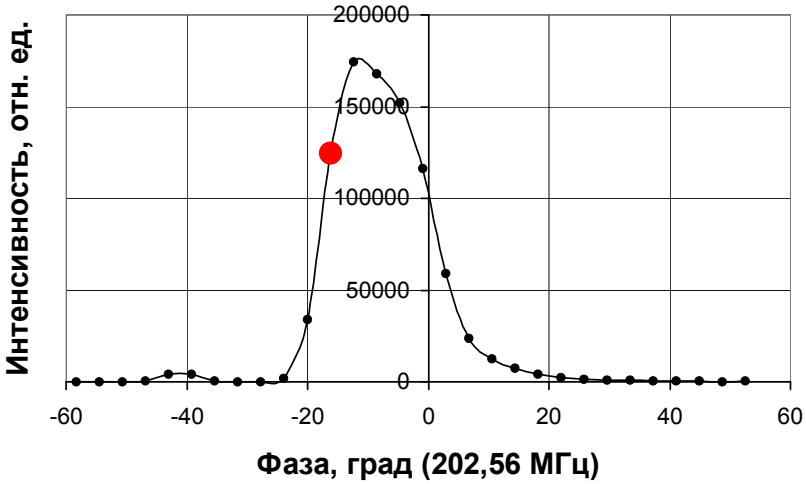

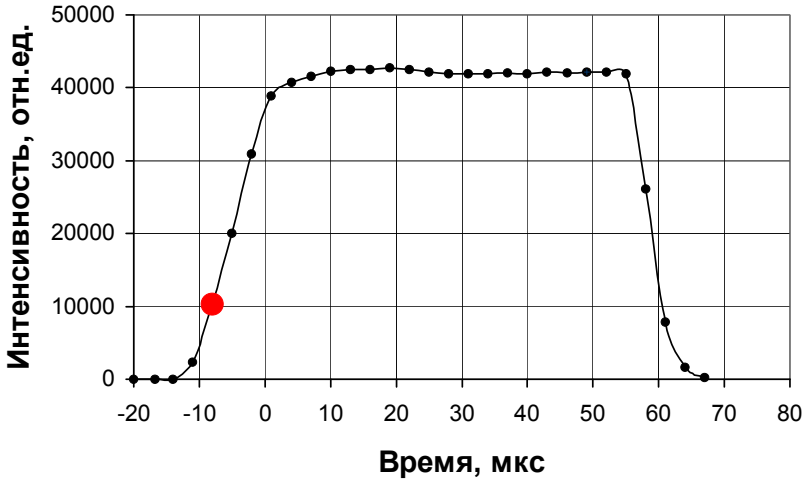

Transverse cross section of a bunch in different phases and at different moments of time within the beam pulse

Bunch #1

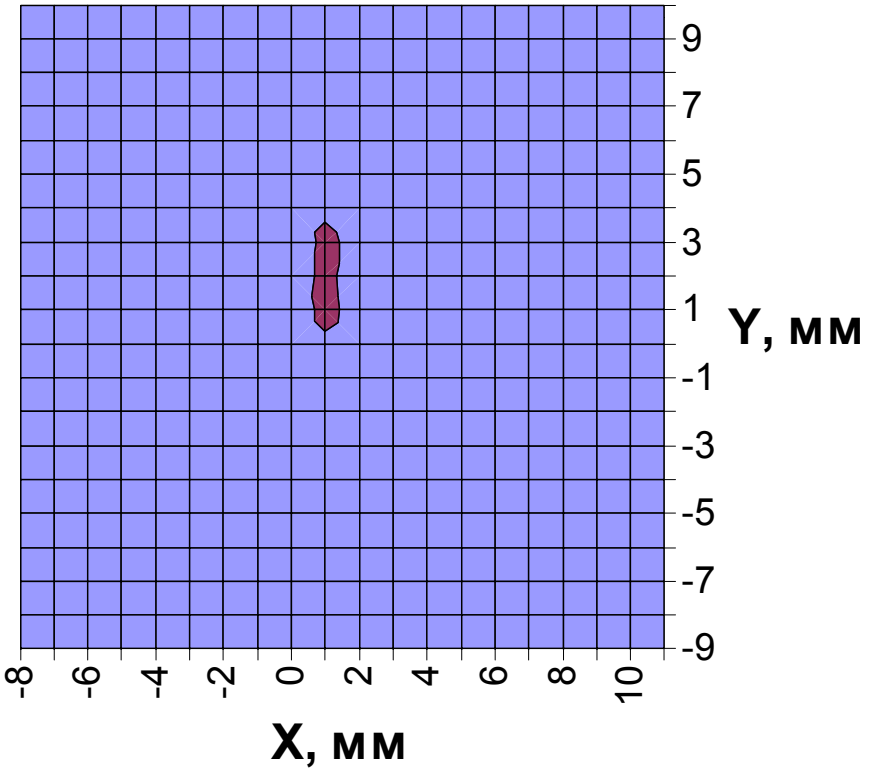

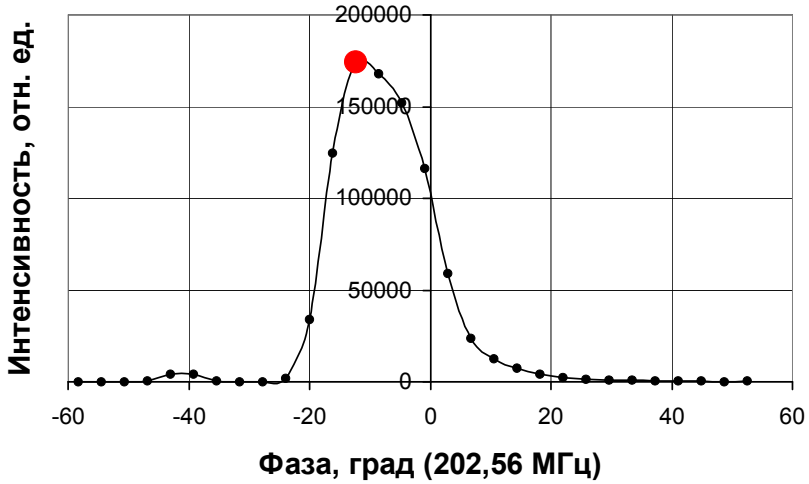

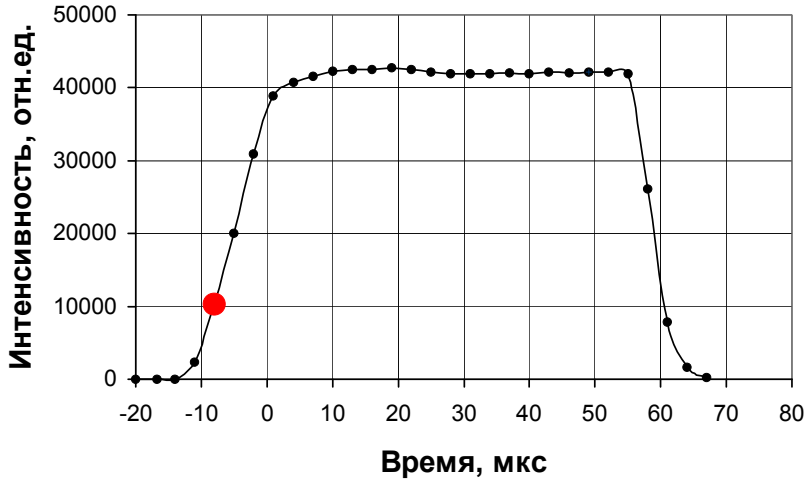

Transverse cross section of a bunch in different phases and at different moments of time within the beam pulse

Bunch #1

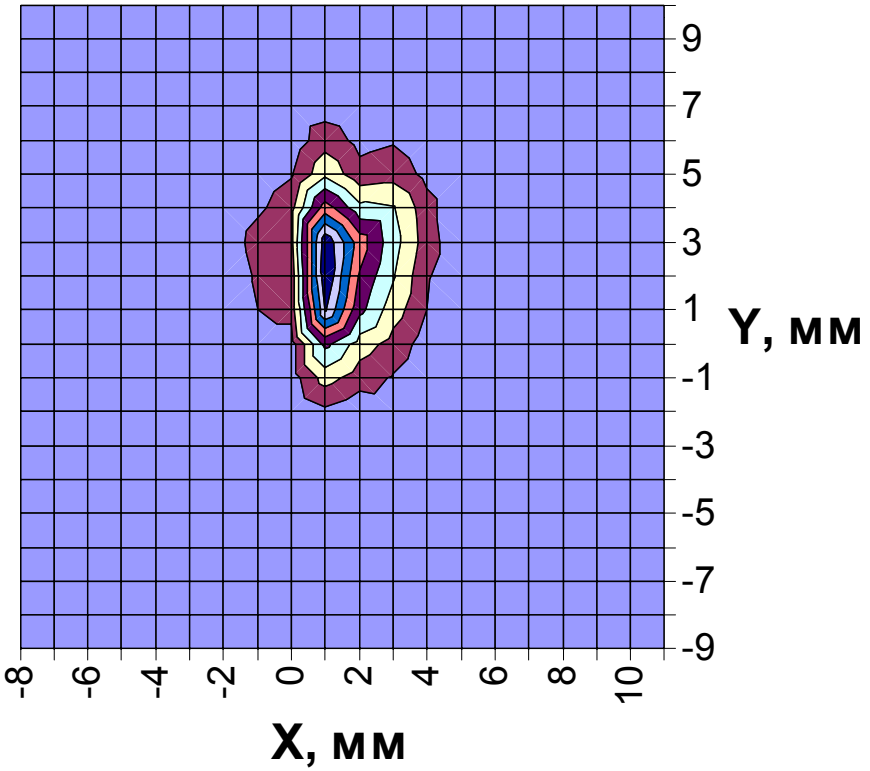

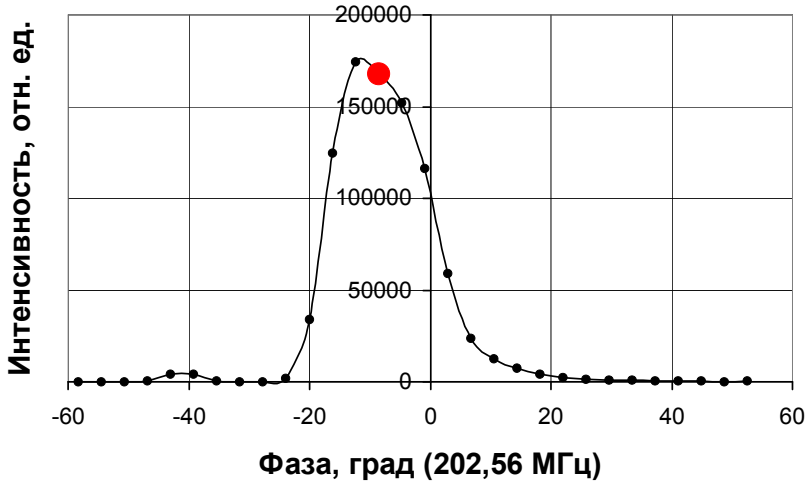

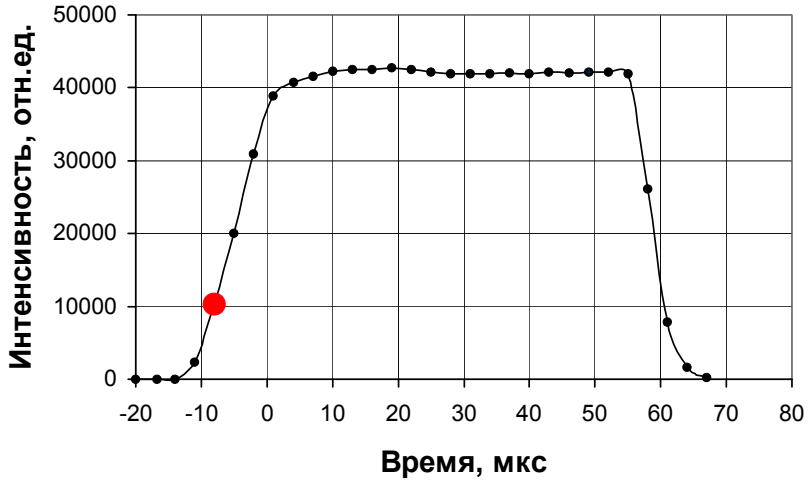

Transverse cross section of a bunch in different phases and at different moments of time within the beam pulse

Bunch #1

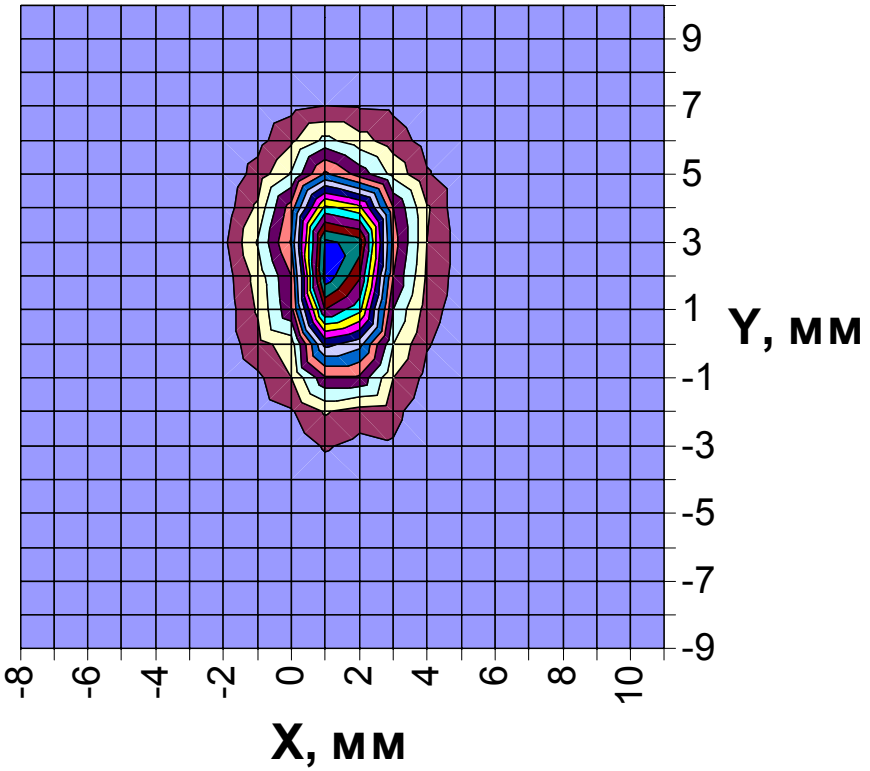

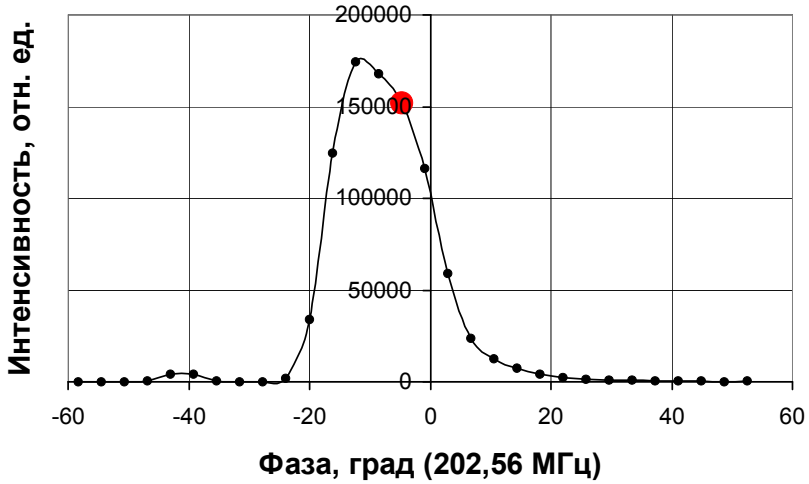

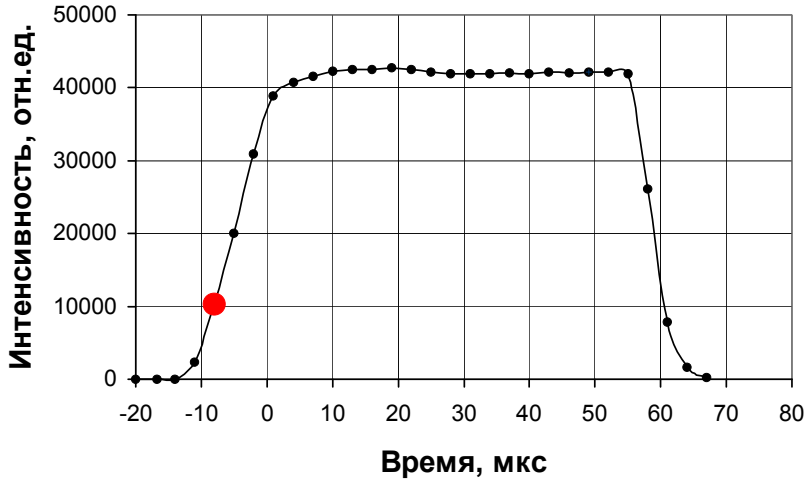

Transverse cross section of a bunch in different phases and at different moments of time within the beam pulse

Bunch #1

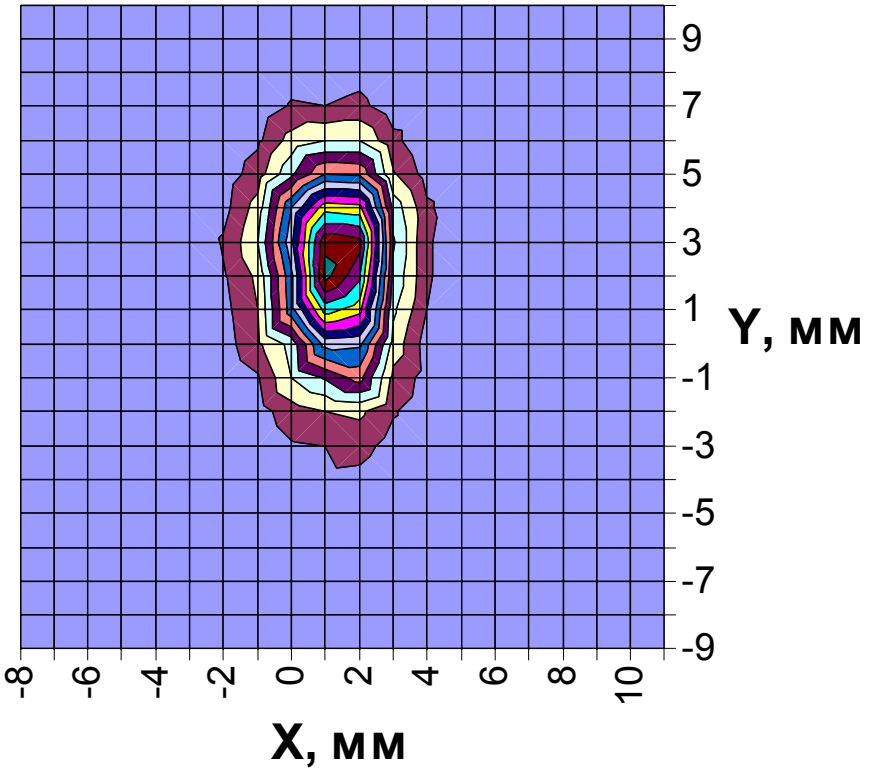

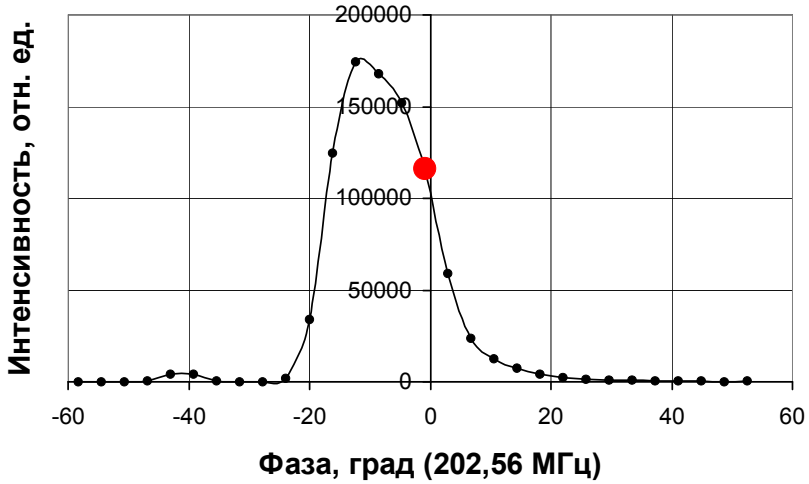

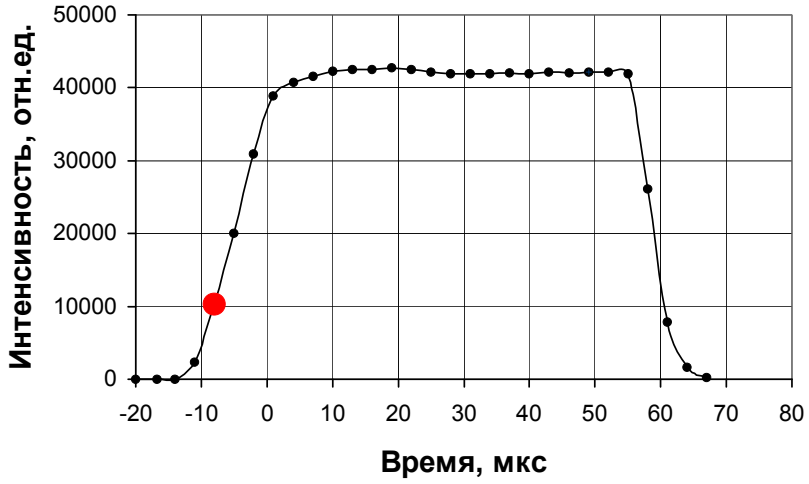

Transverse cross section of a bunch in different phases and at different moments of time within the beam pulse

Bunch #1

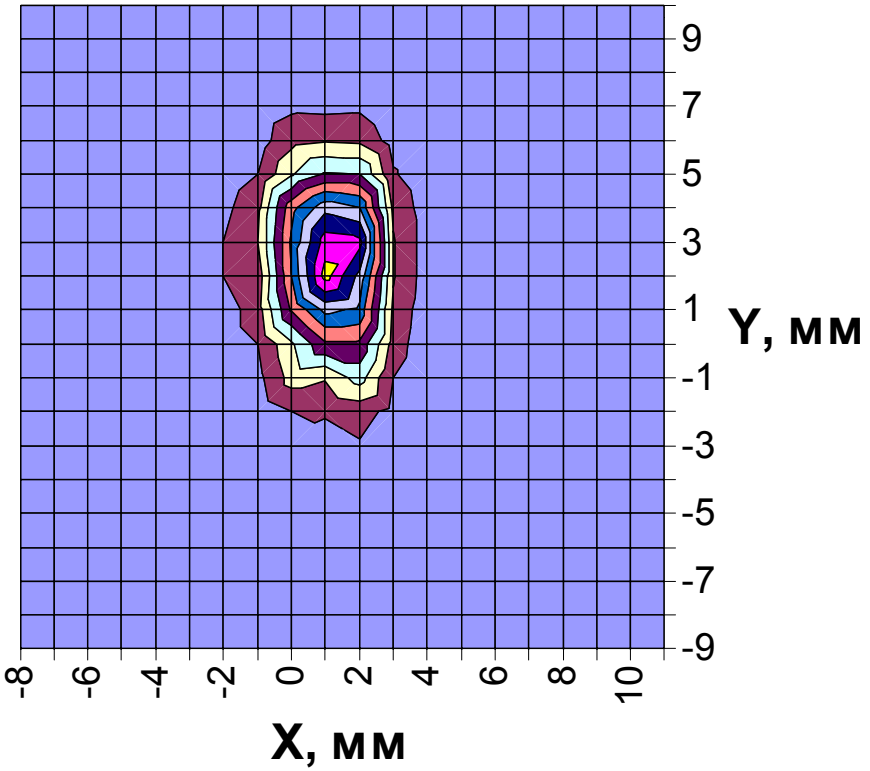

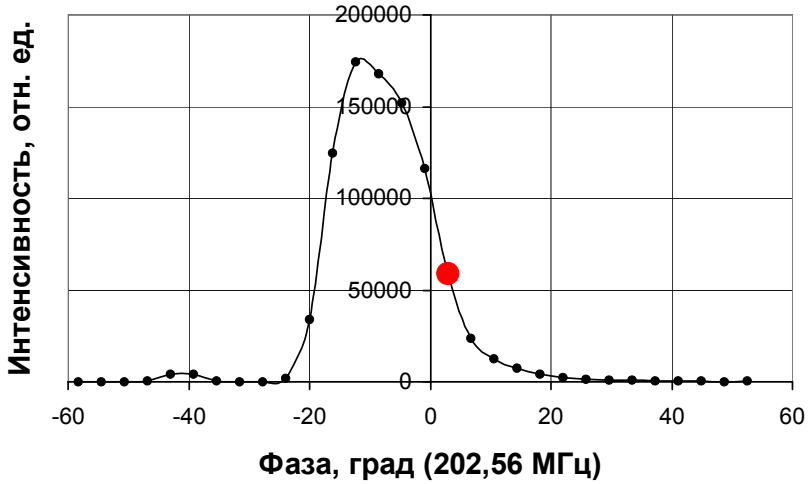

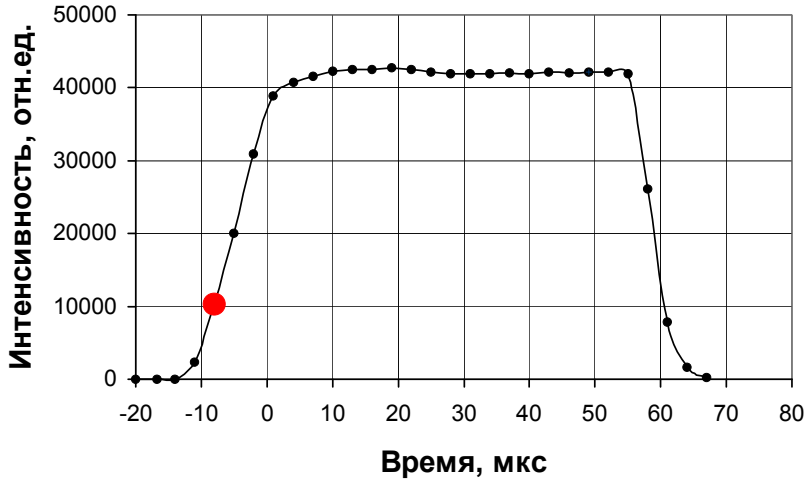

Transverse cross section of a bunch in different phases and at different moments of time within the beam pulse

Bunch #1

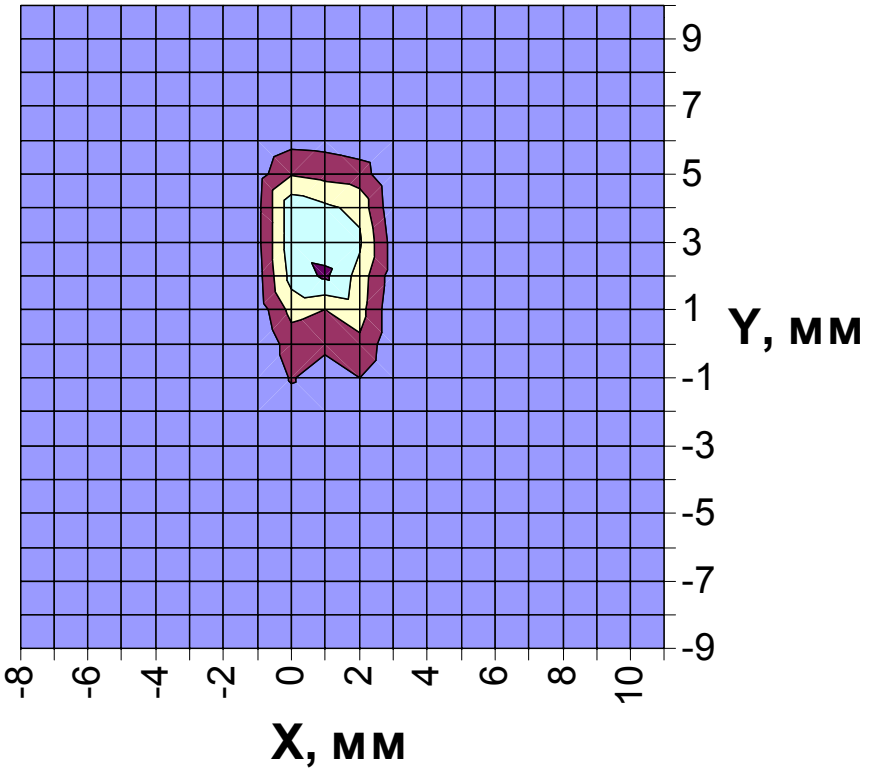

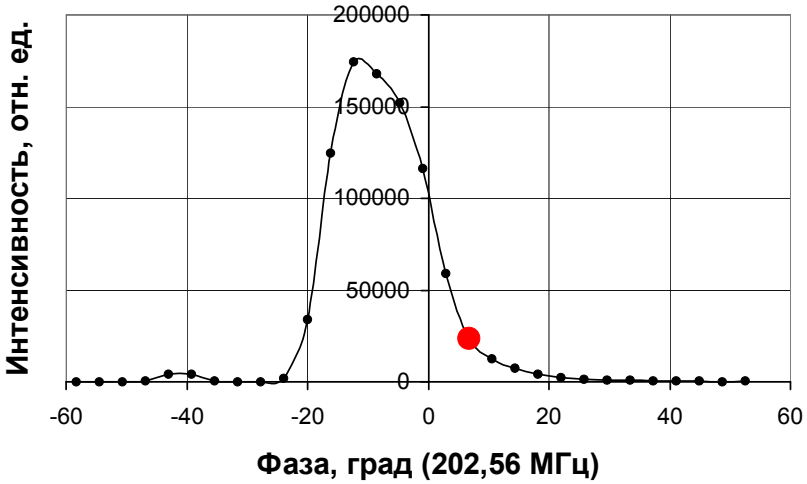

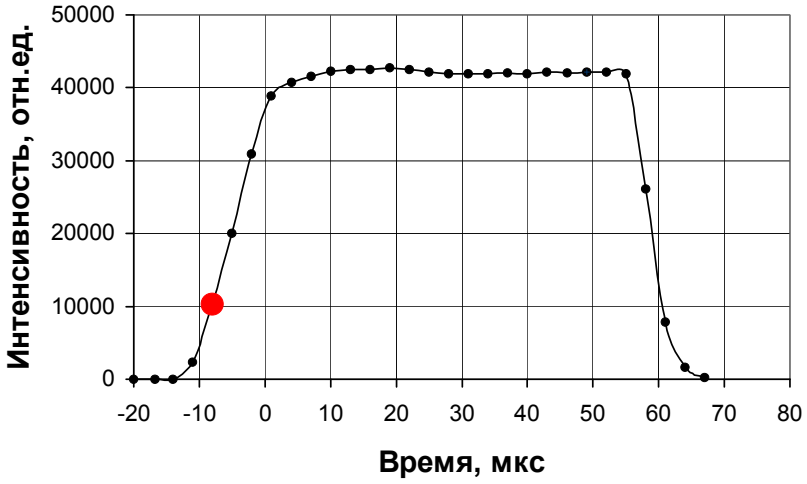

Transverse cross section of a bunch in different phases and at different moments of time within the beam pulse

Bunch #1

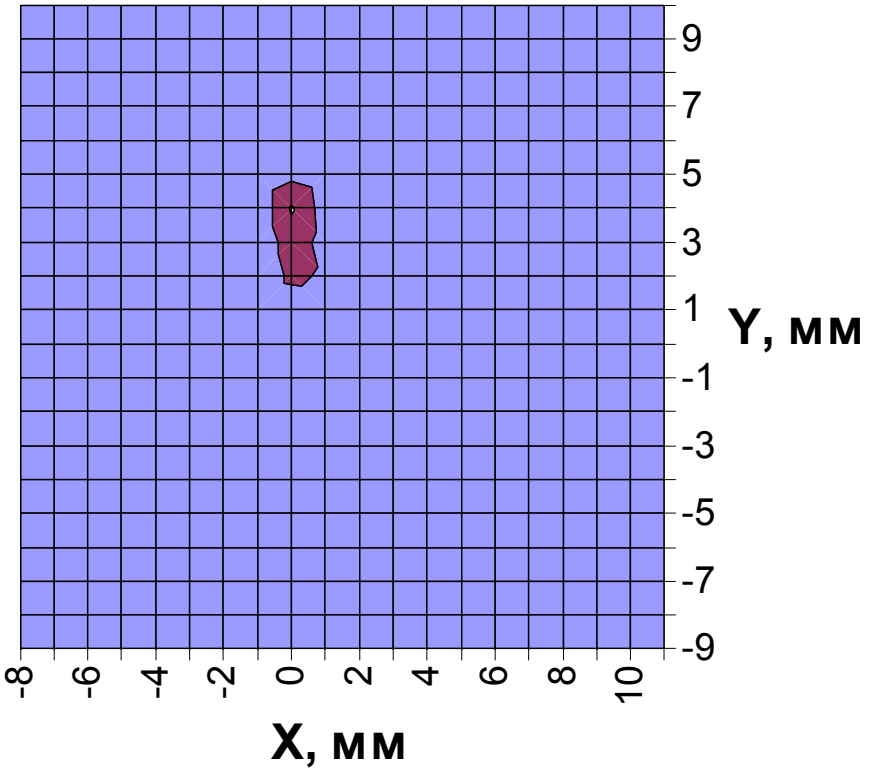

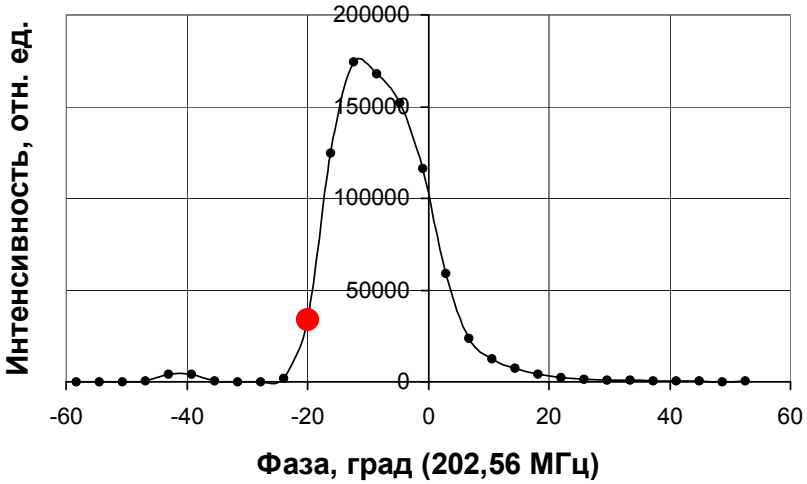

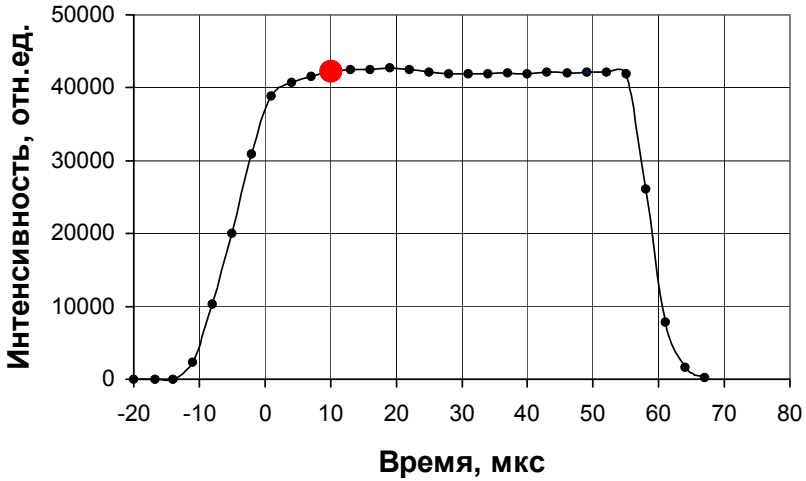

Transverse cross section of a bunch in different phases and at different moments of time within the beam pulse

Bunch #2

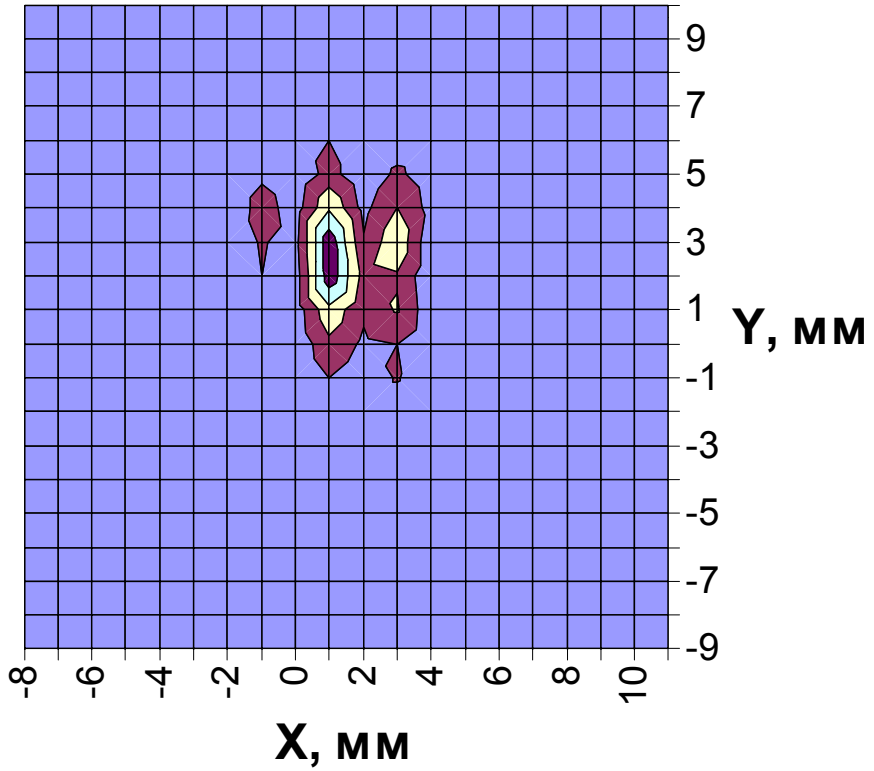

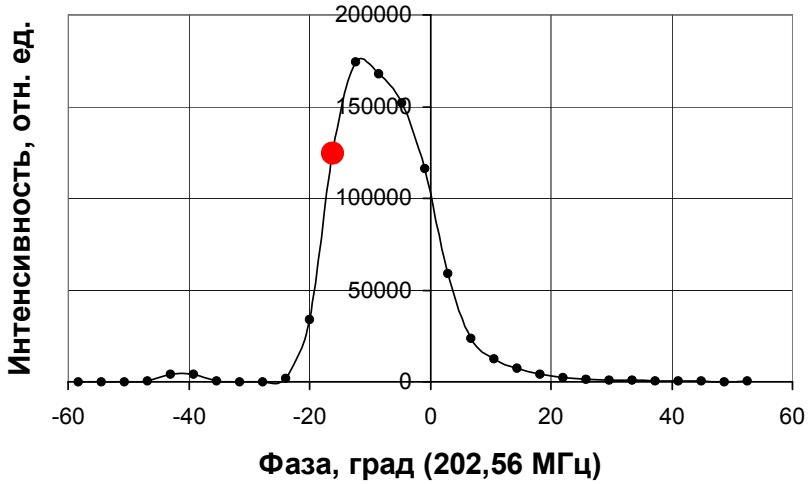

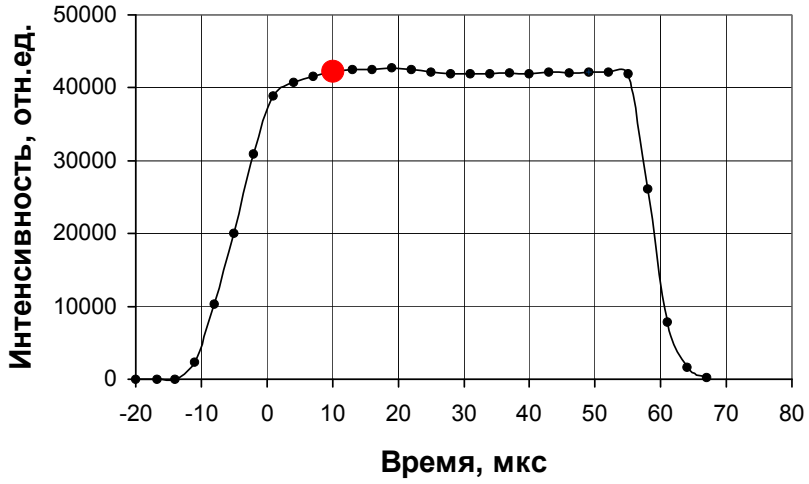

Transverse cross section of a bunch in different phases and at different moments of time within the beam pulse

Bunch #2

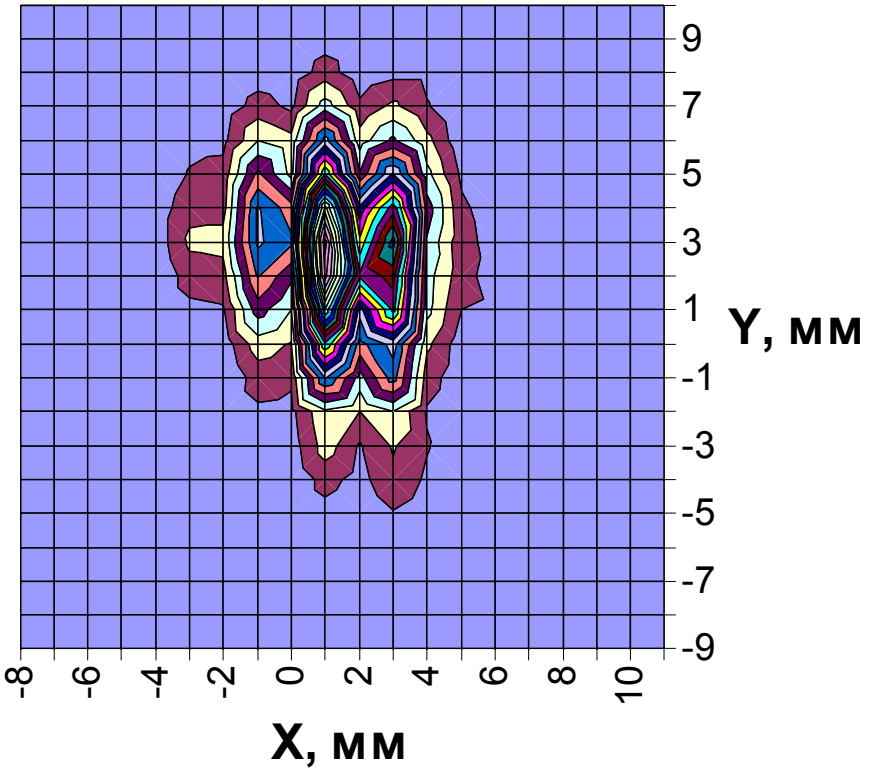

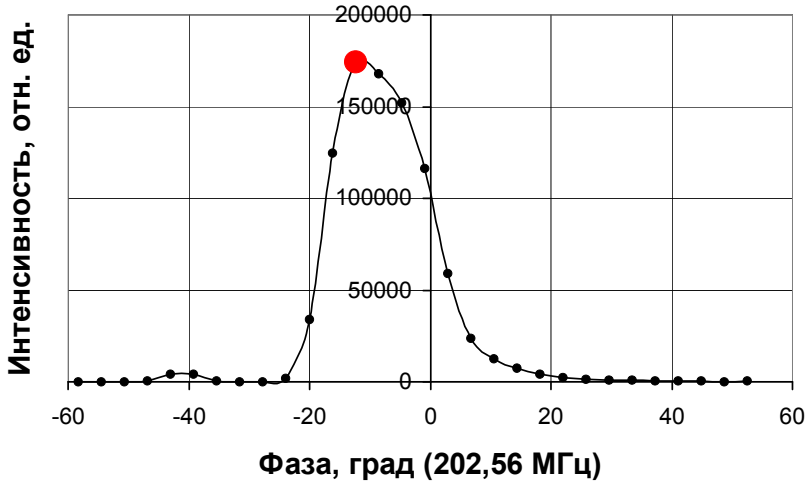

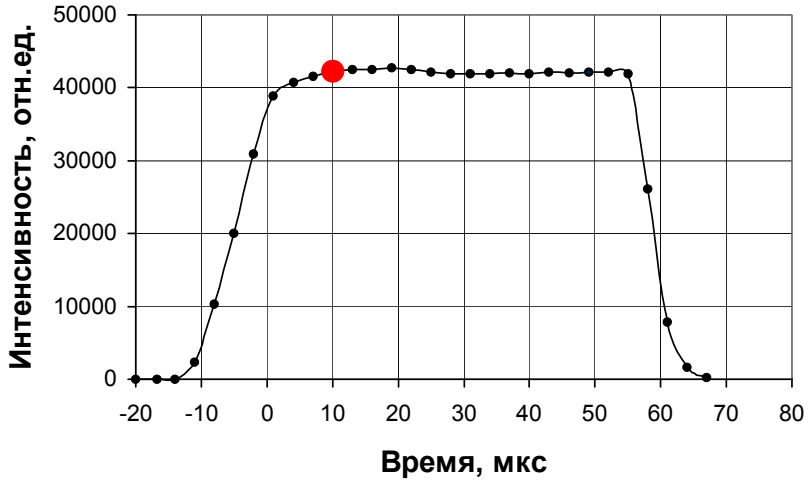

Transverse cross section of a bunch in different phases and at different moments of time within the beam pulse

Bunch #2

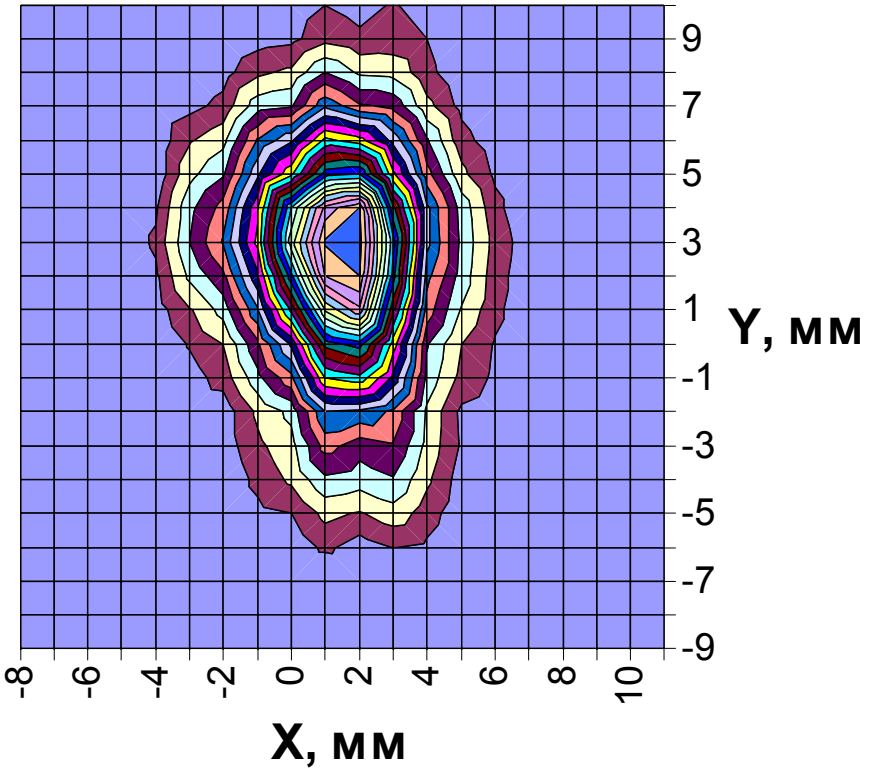

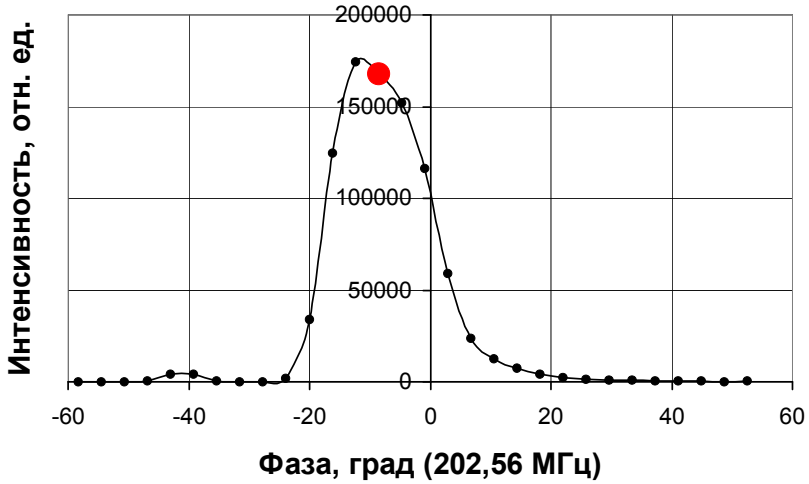

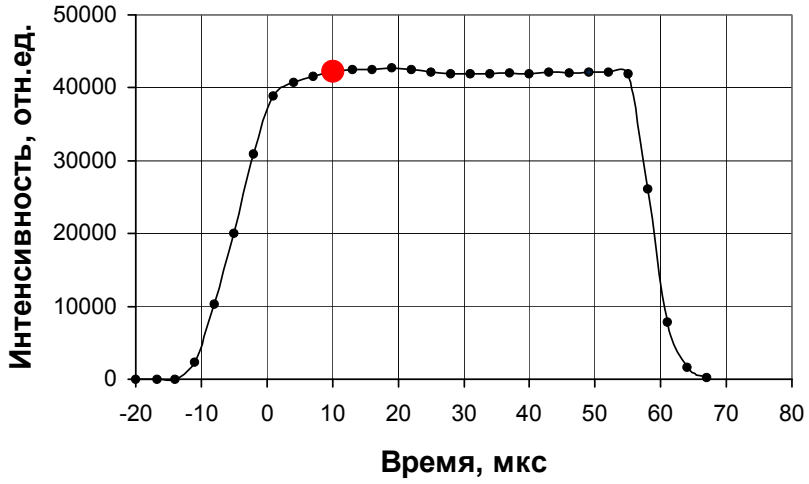

Transverse cross section of a bunch in different phases and at different moments of time within the beam pulse

Bunch #2

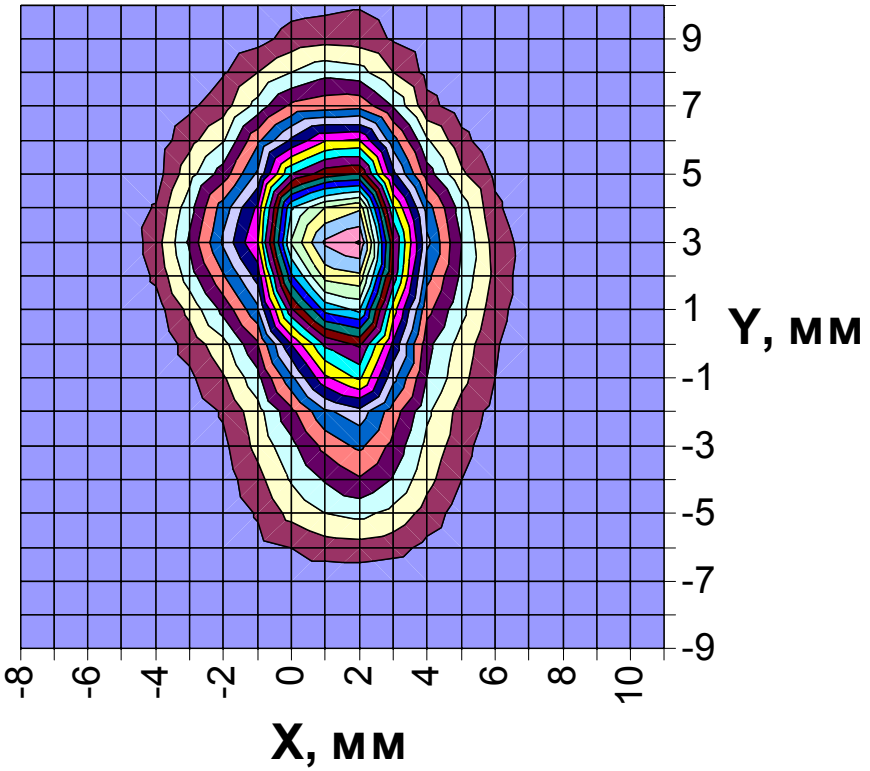

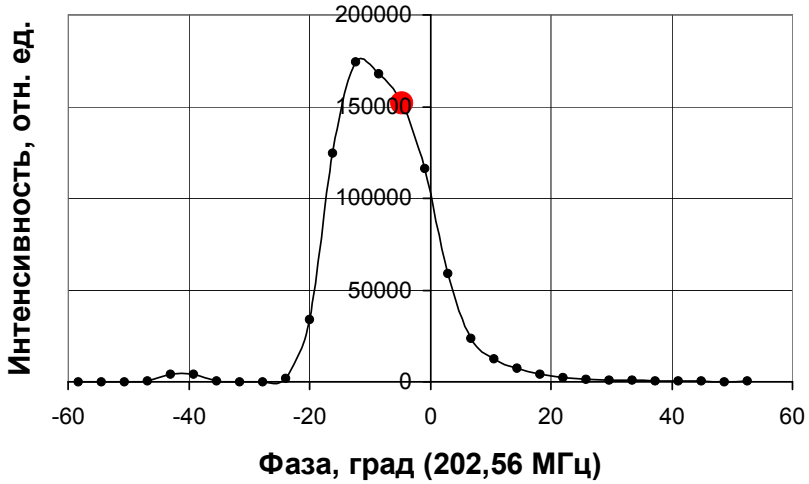

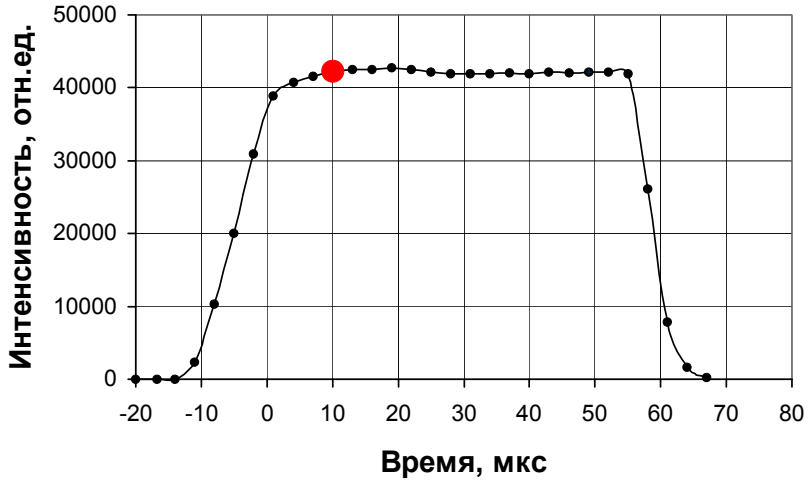

Transverse cross section of a bunch in different phases and at different moments of time within the beam pulse

Bunch #2

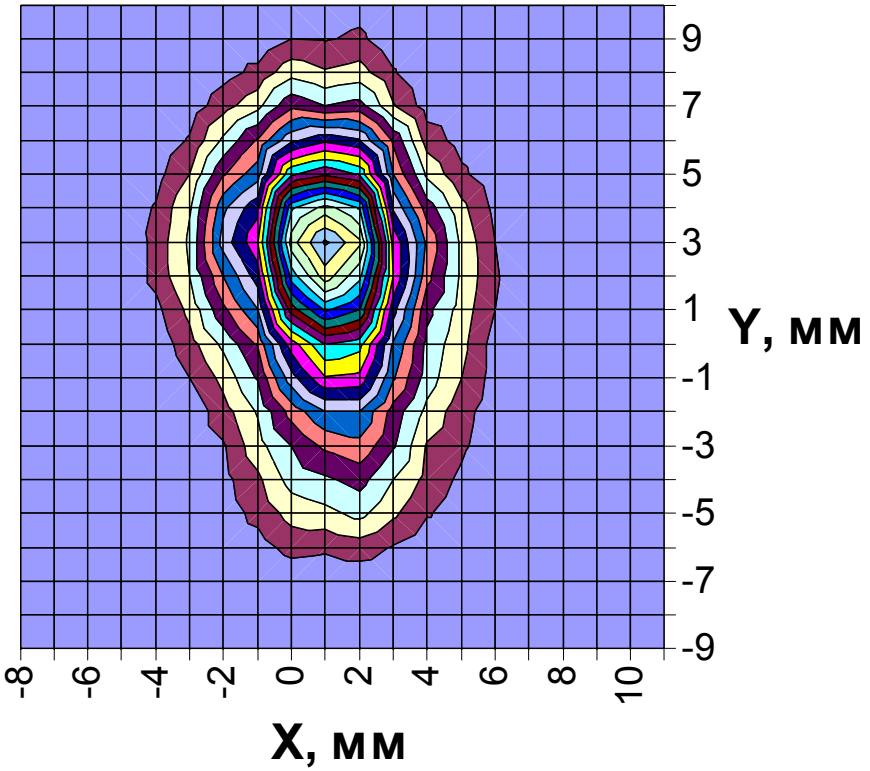

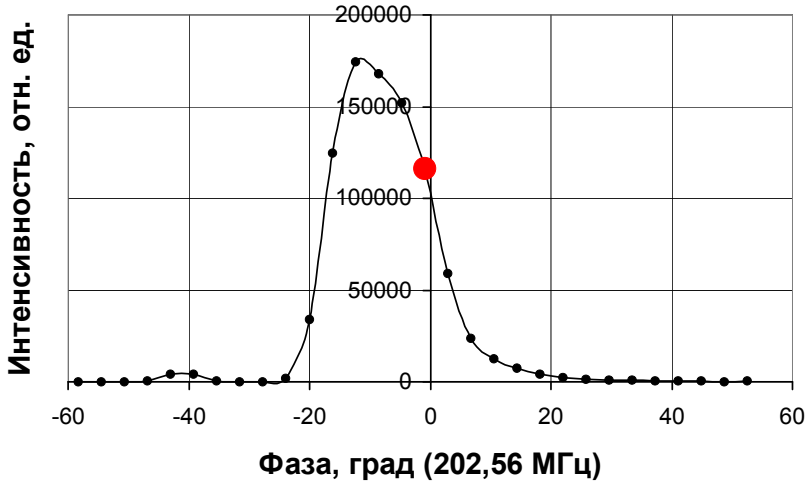

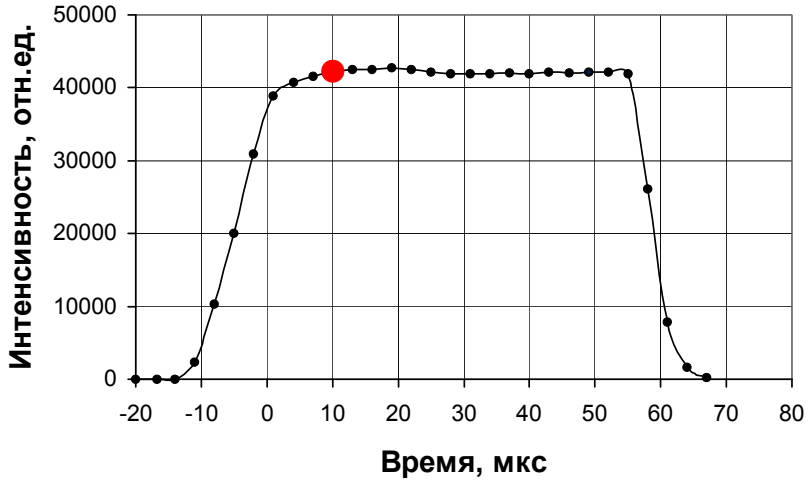

Transverse cross section of a bunch in different phases and at different moments of time within the beam pulse

Bunch #2

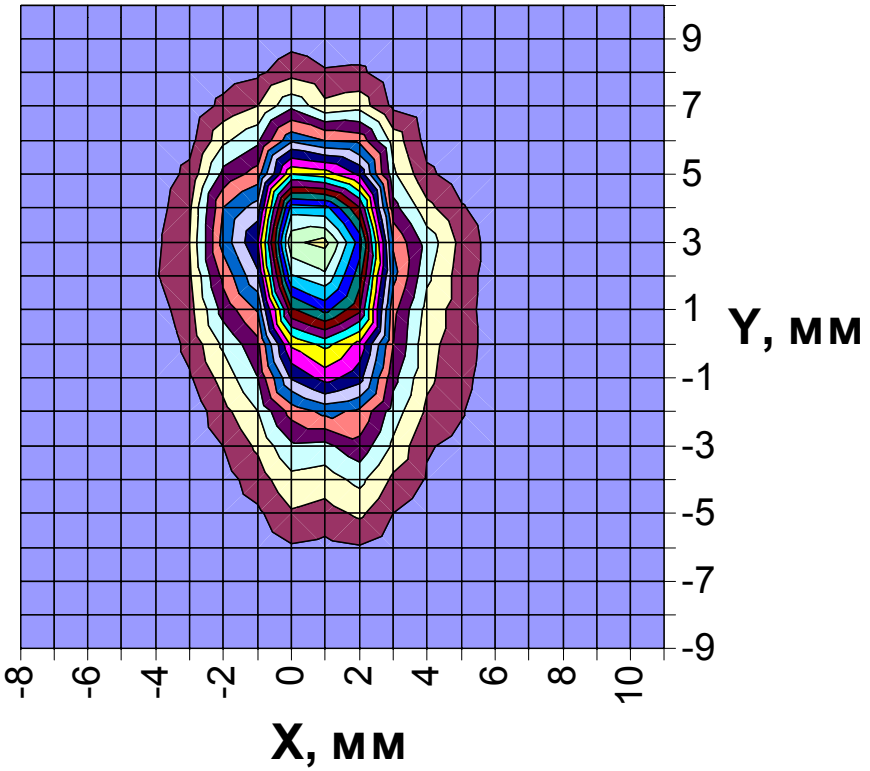

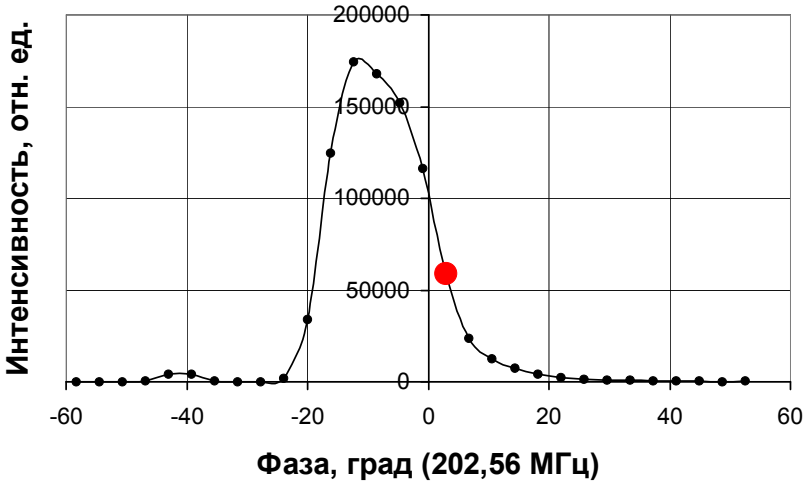

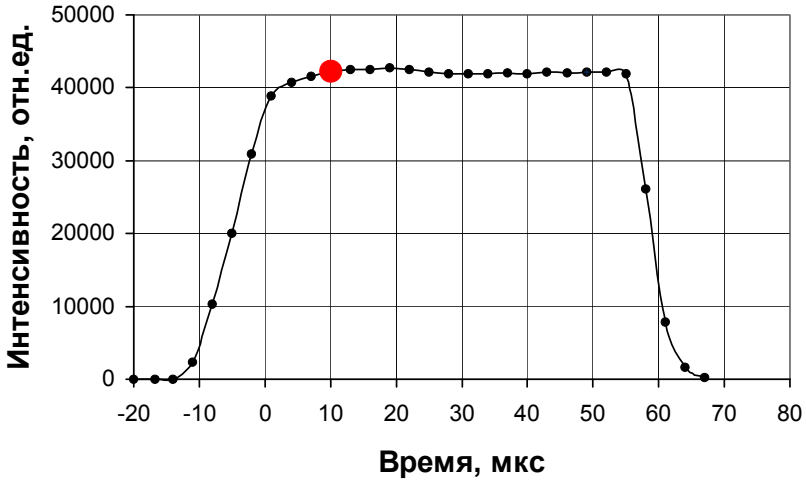

Transverse cross section of a bunch in different phases and at different moments of time within the beam pulse

Bunch #2

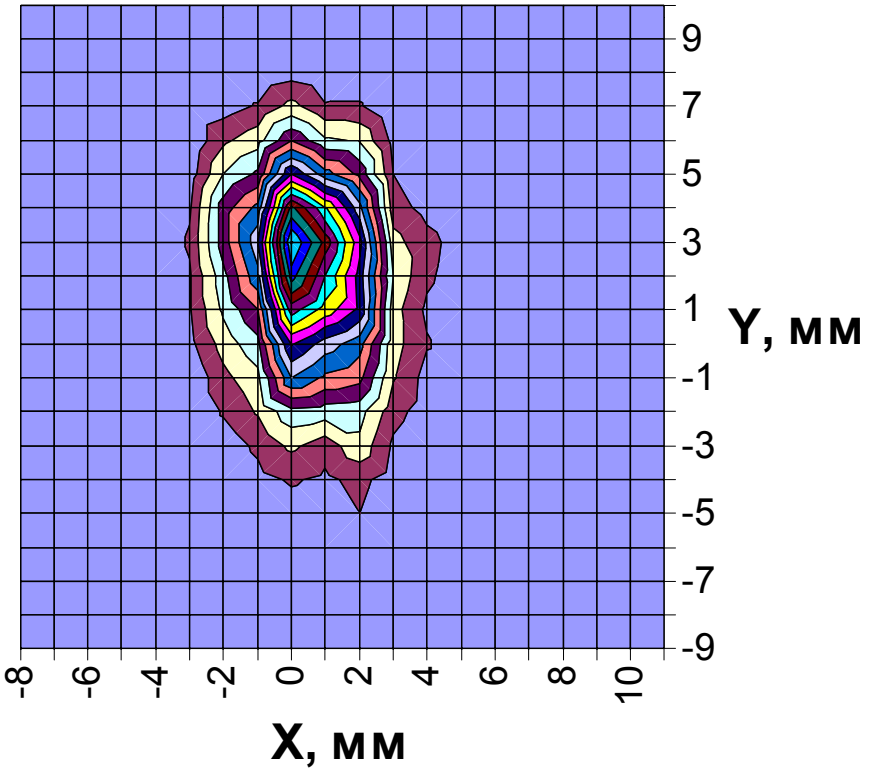

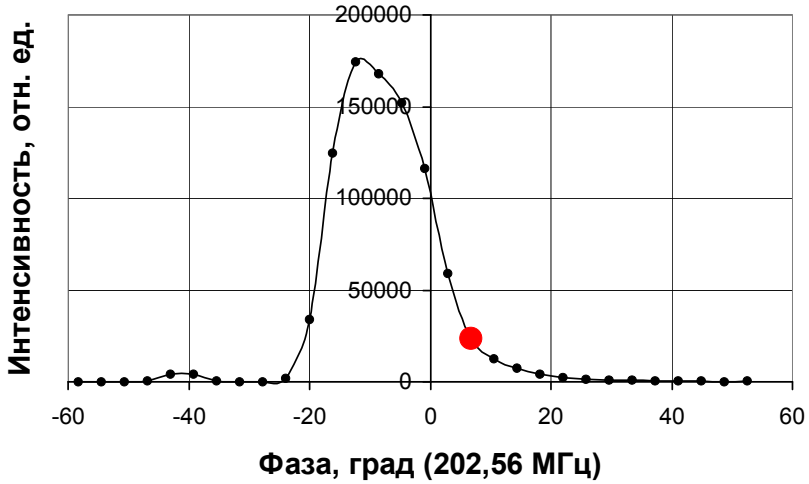

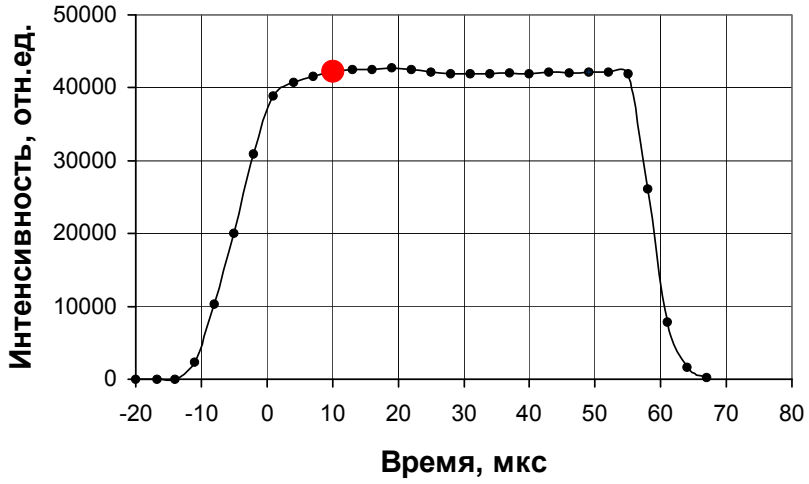

Transverse cross section of a bunch in different phases and at different moments of time within the beam pulse

Bunch #2

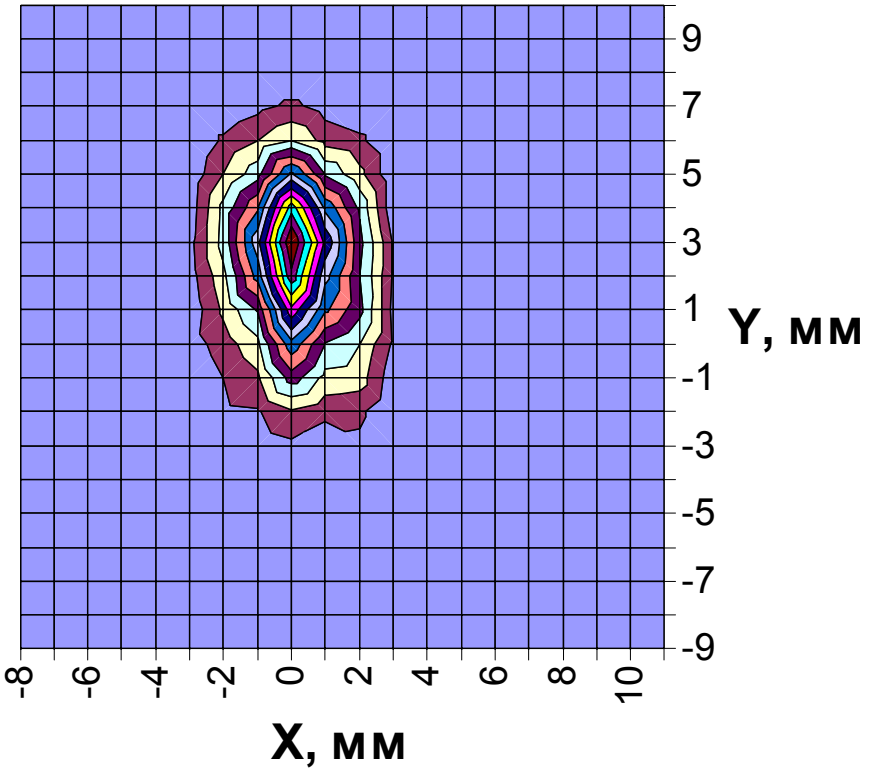

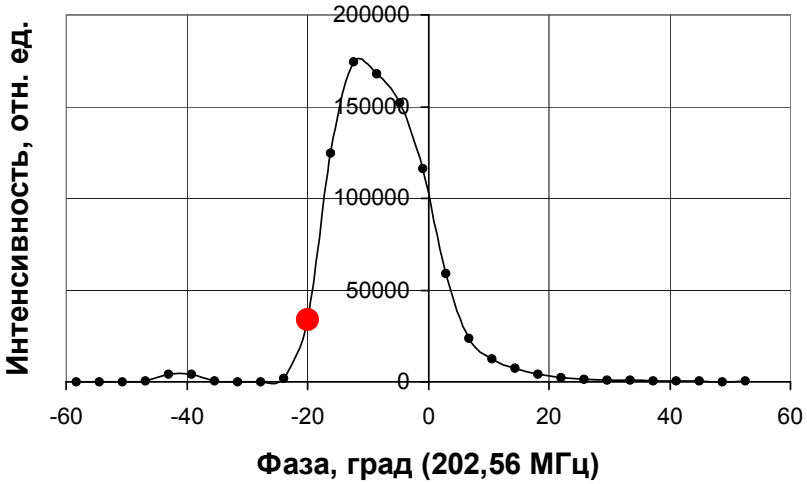

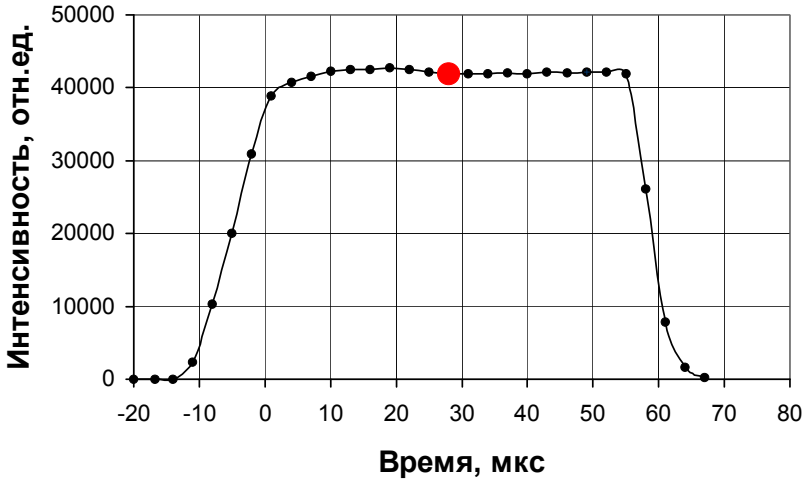

Transverse cross section of a bunch in different phases and at different moments of time within the beam pulse

Bunch #3

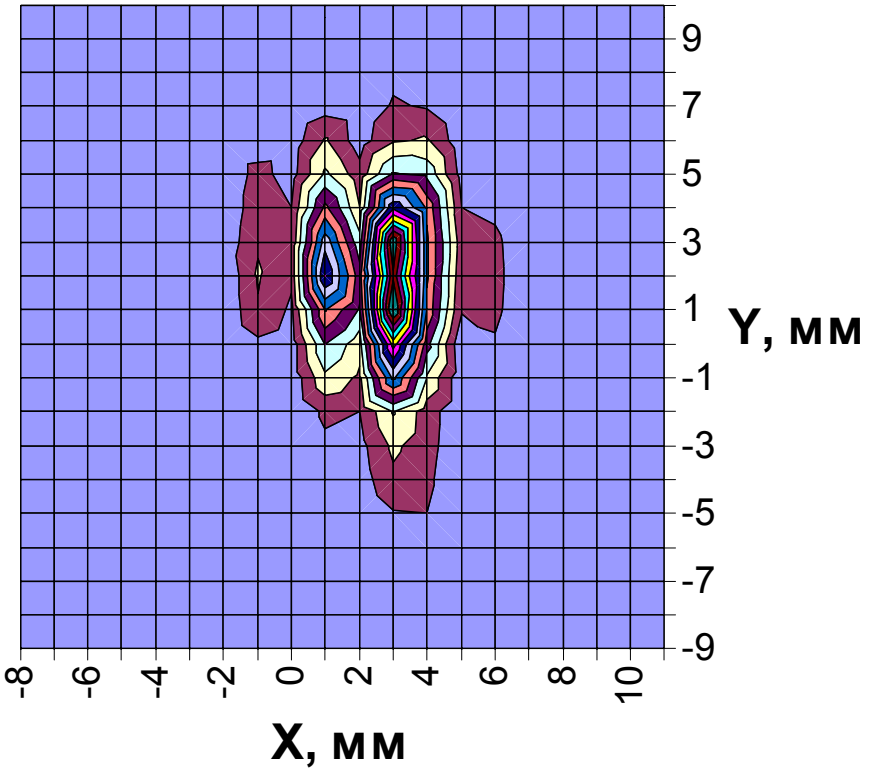

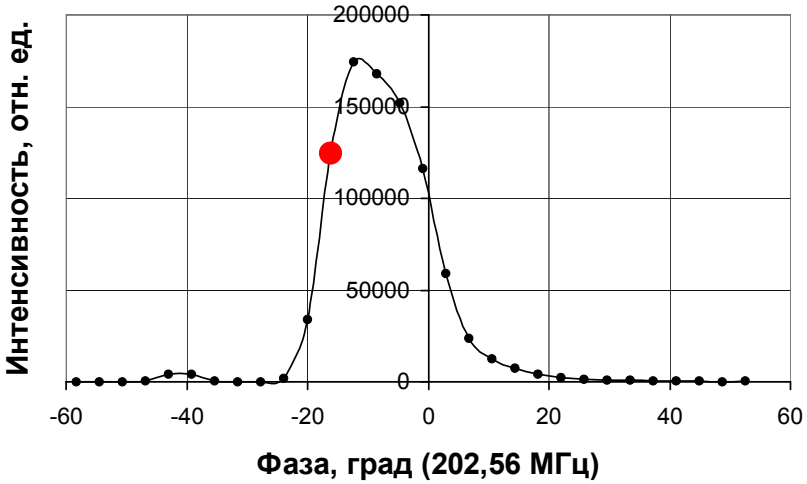

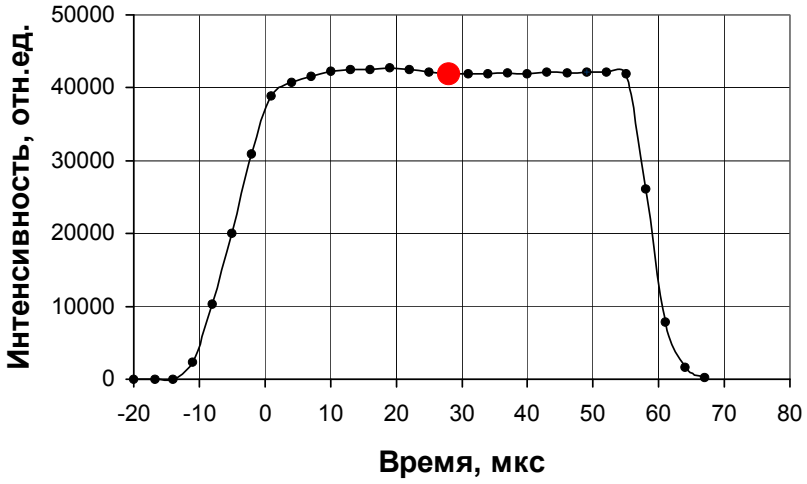

Transverse cross section of a bunch in different phases and at different moments of time within the beam pulse

Bunch #3

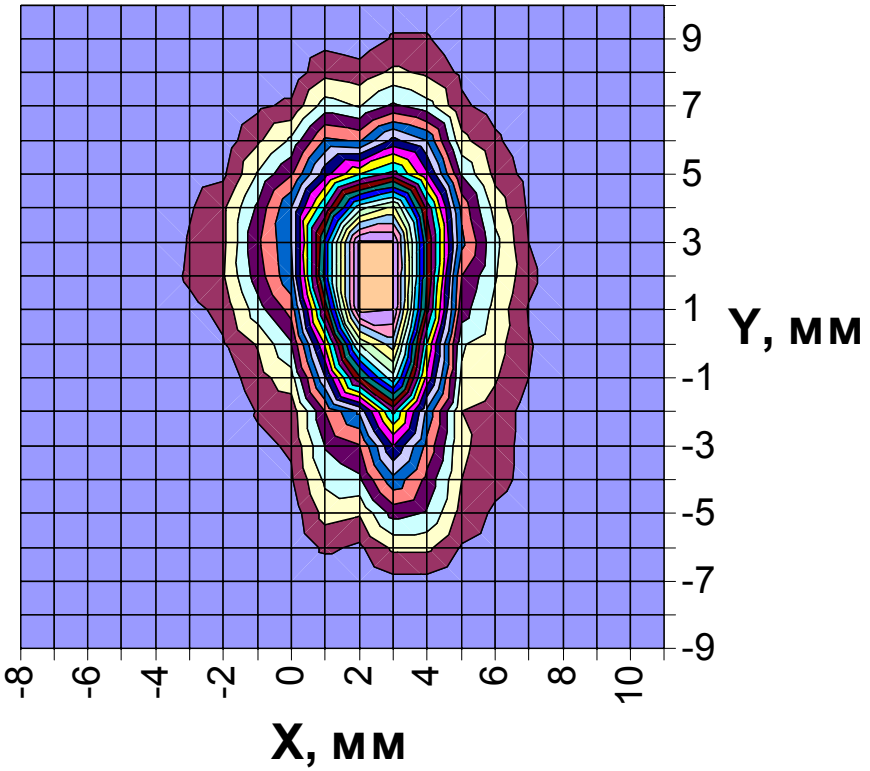

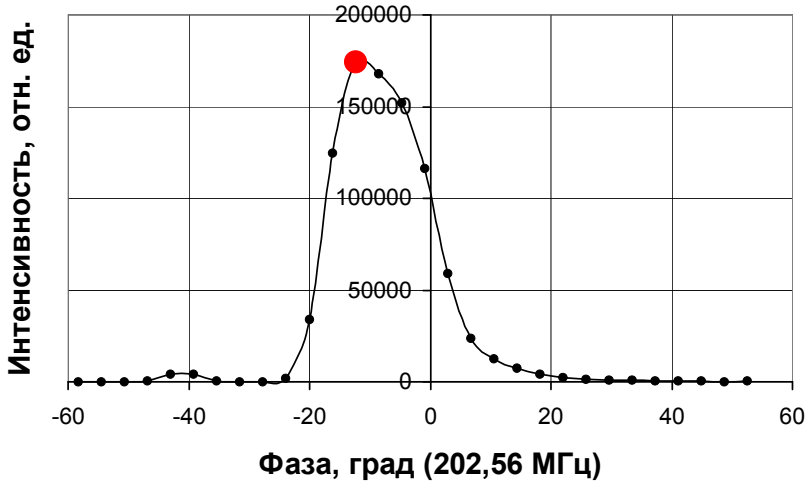

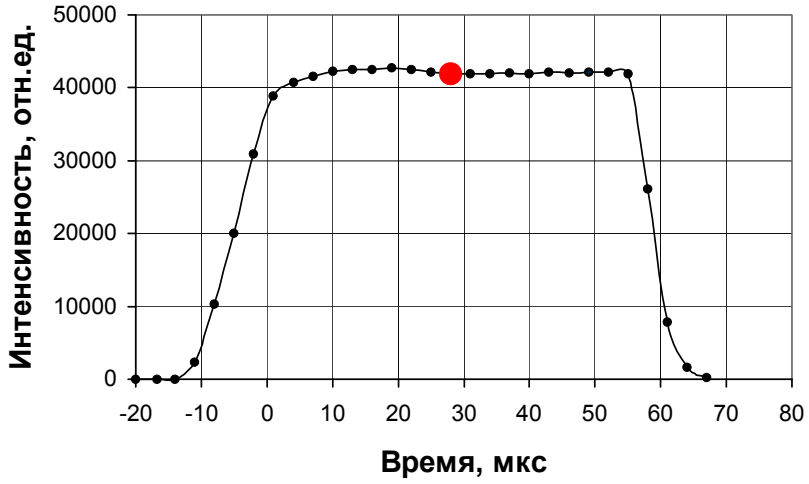

Transverse cross section of a bunch in different phases and at different moments of time within the beam pulse

Bunch #3

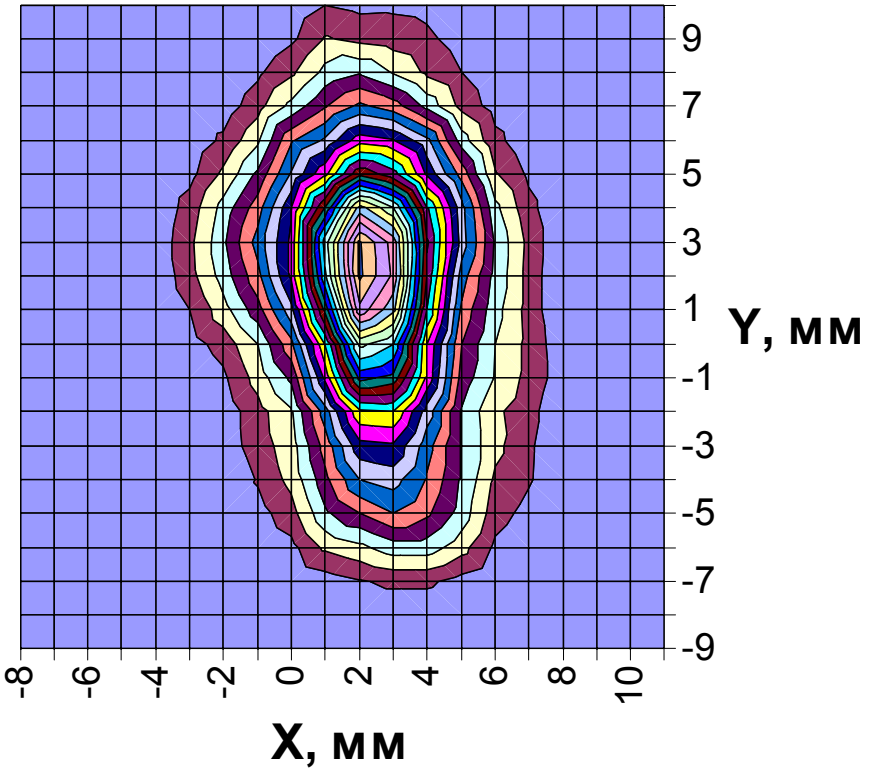

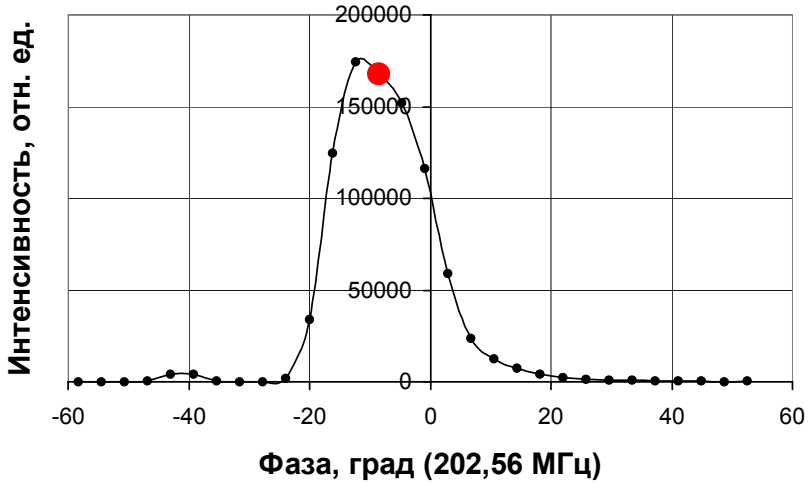

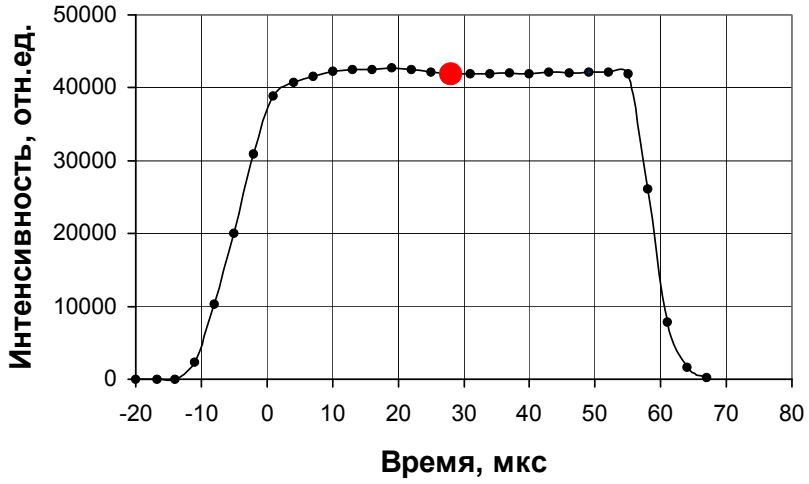

Transverse cross section of a bunch in different phases and at different moments of time within the beam pulse

Bunch #3

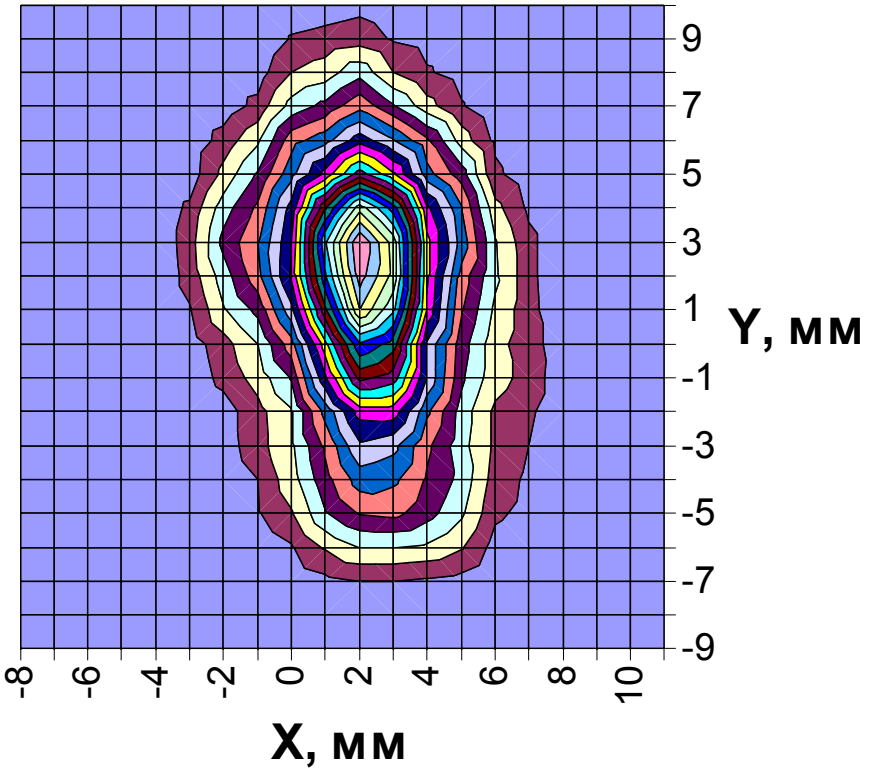

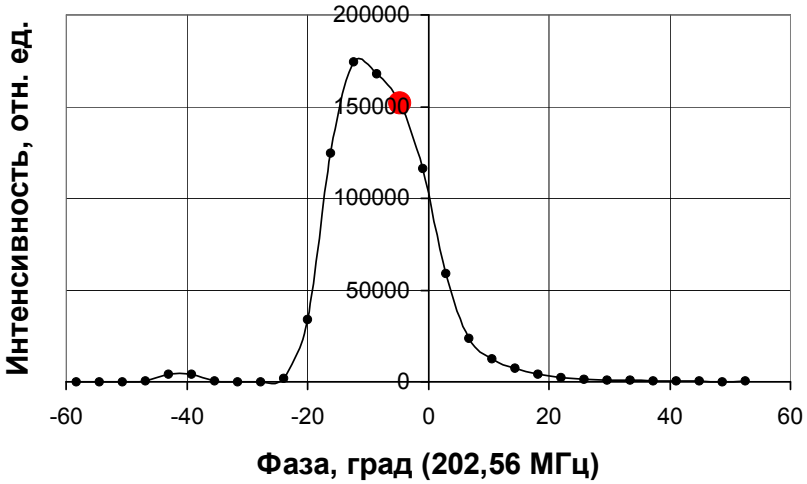

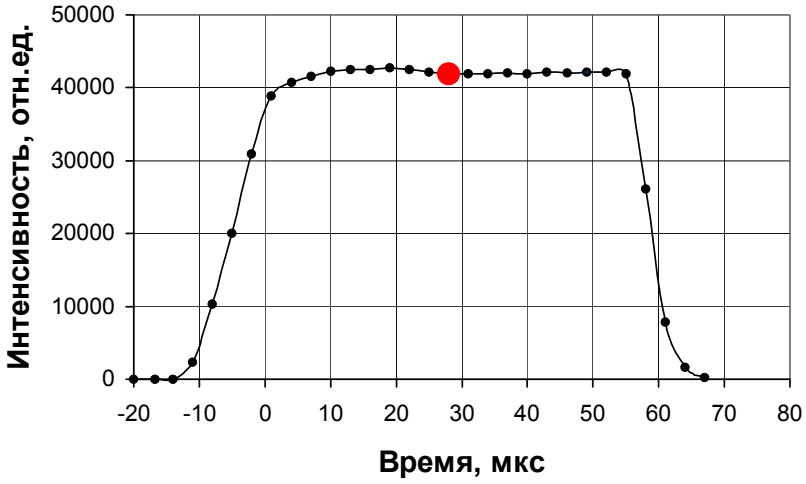

Transverse cross section of a bunch in different phases and at different moments of time within the beam pulse

Bunch #3

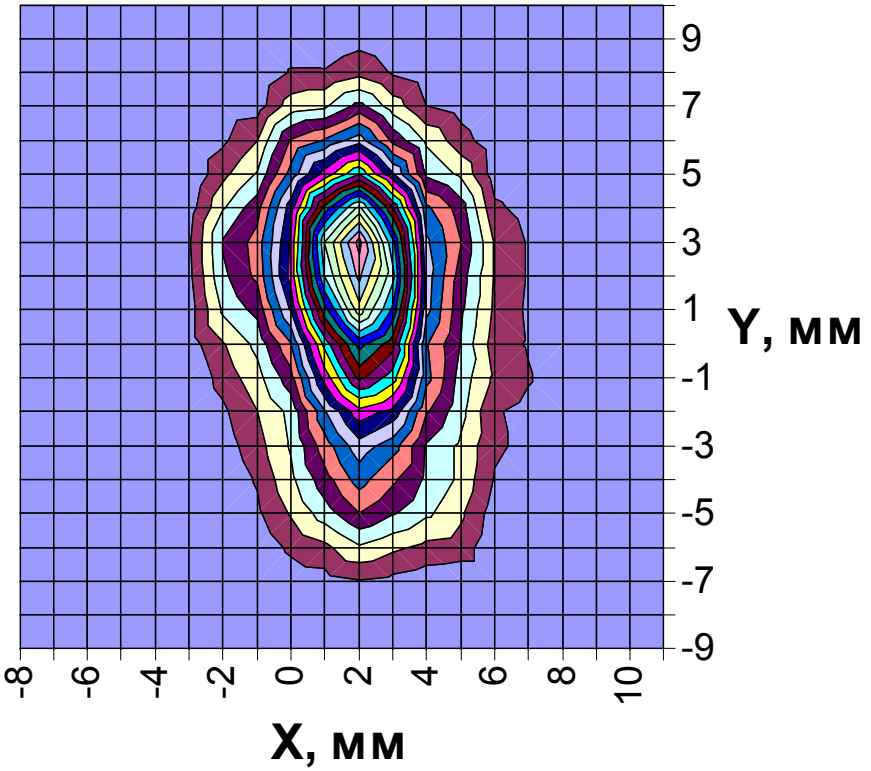

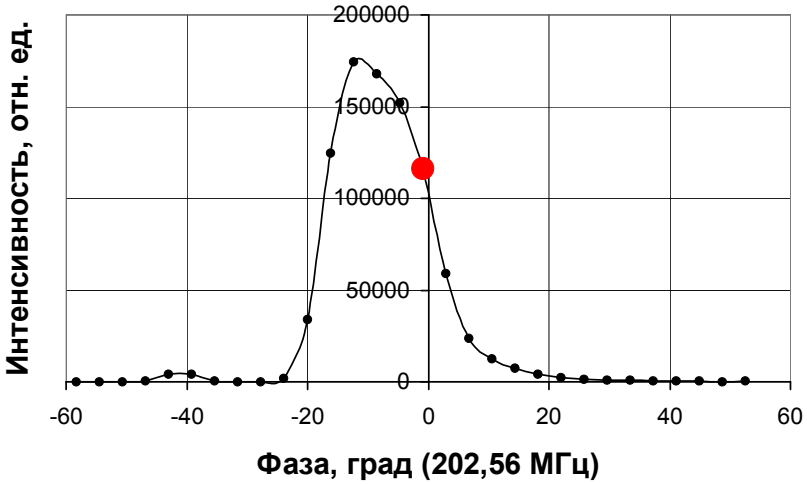

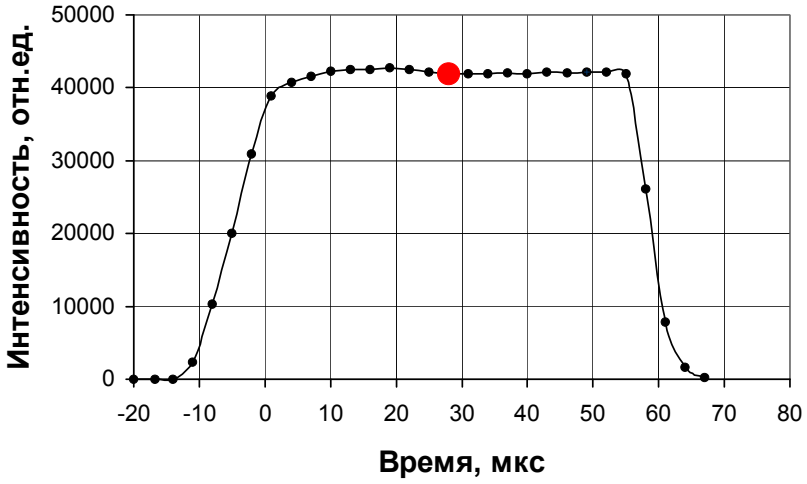

Transverse cross section of a bunch in different phases and at different moments of time within the beam pulse

Bunch #3

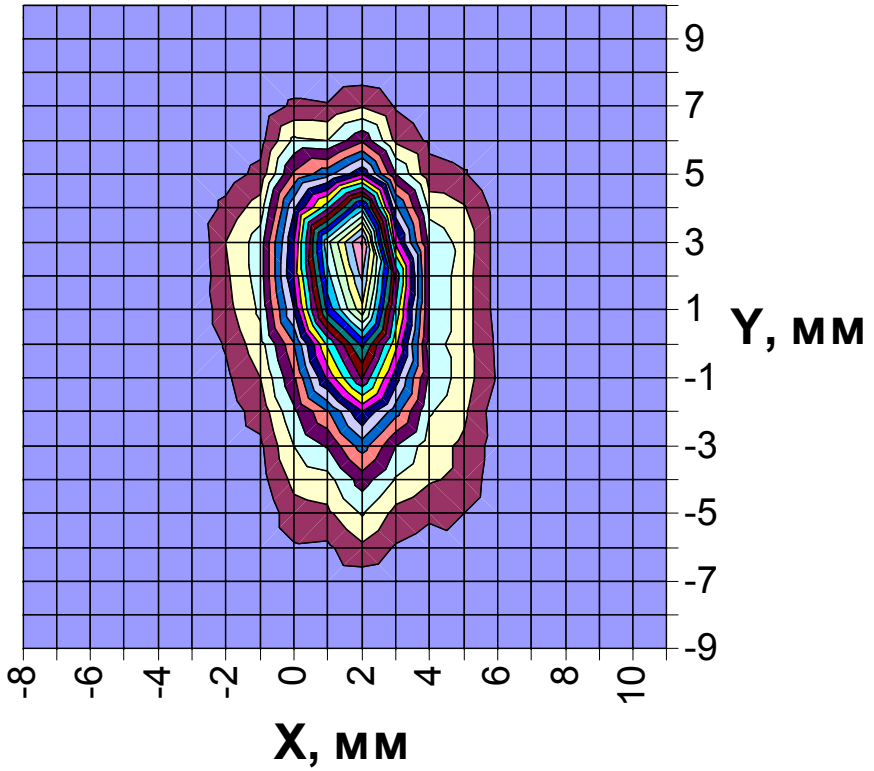

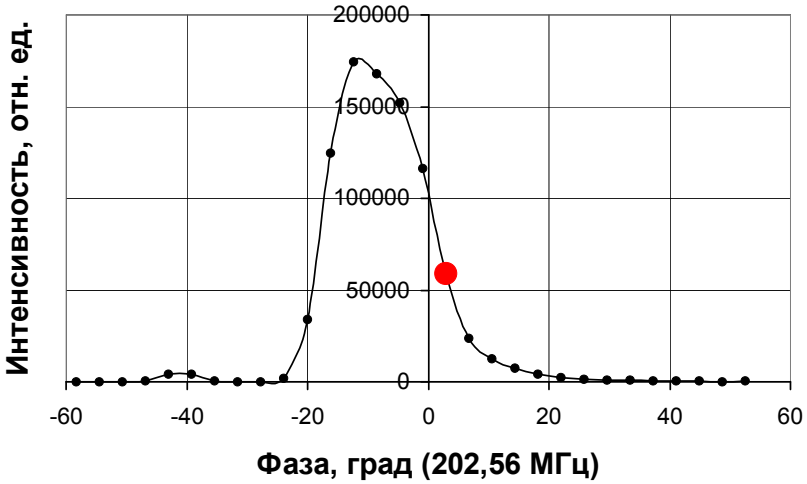

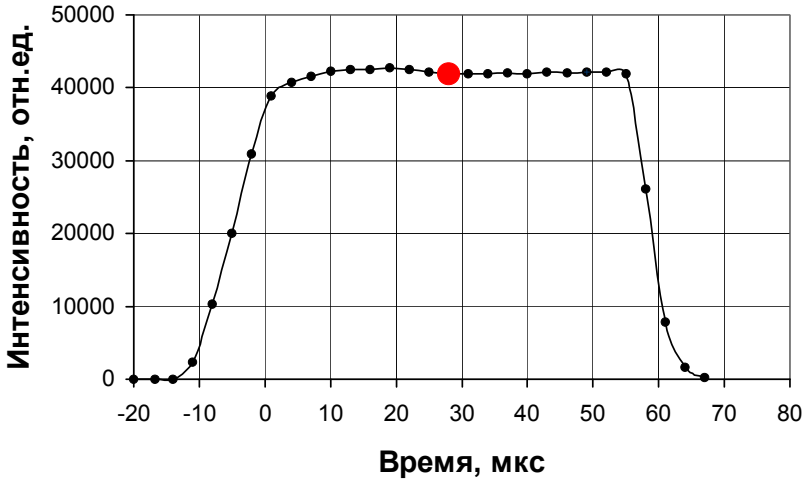

Transverse cross section of a bunch in different phases and at different moments of time within the beam pulse

Bunch #3

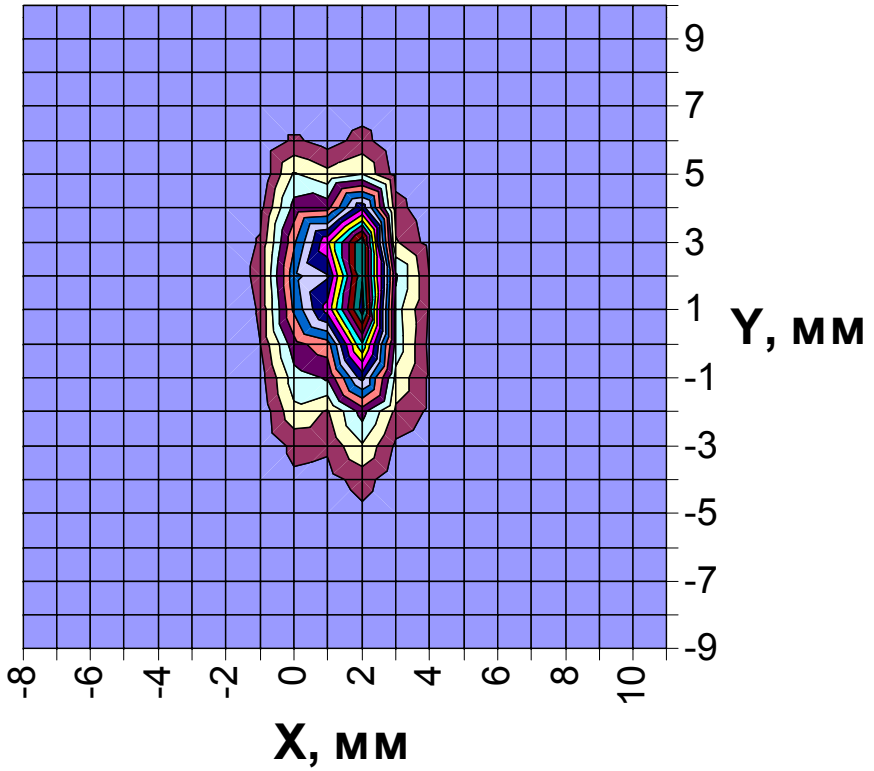

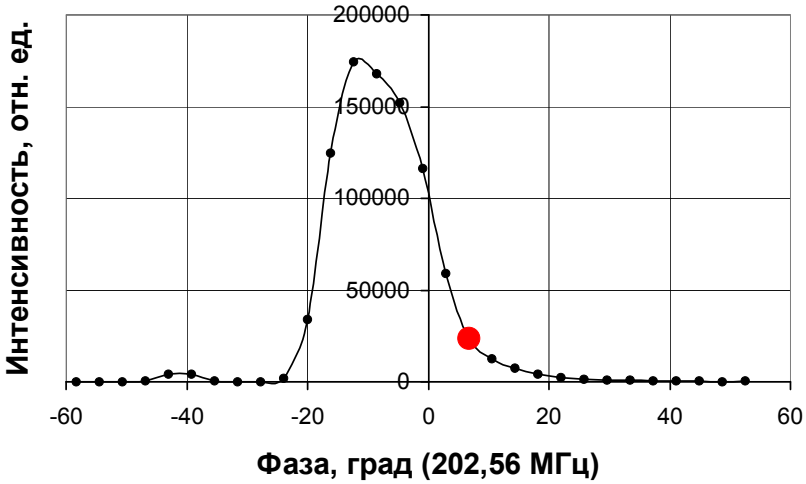

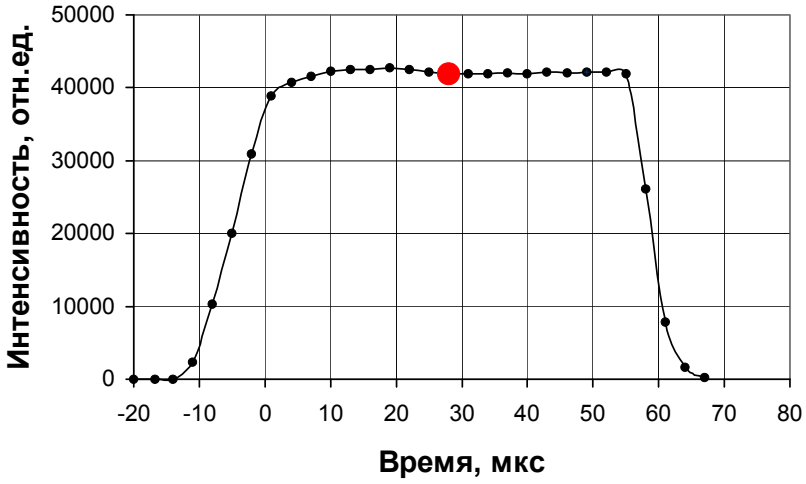

Transverse cross section of a bunch in different phases and at different moments of time within the beam pulse

Bunch #3

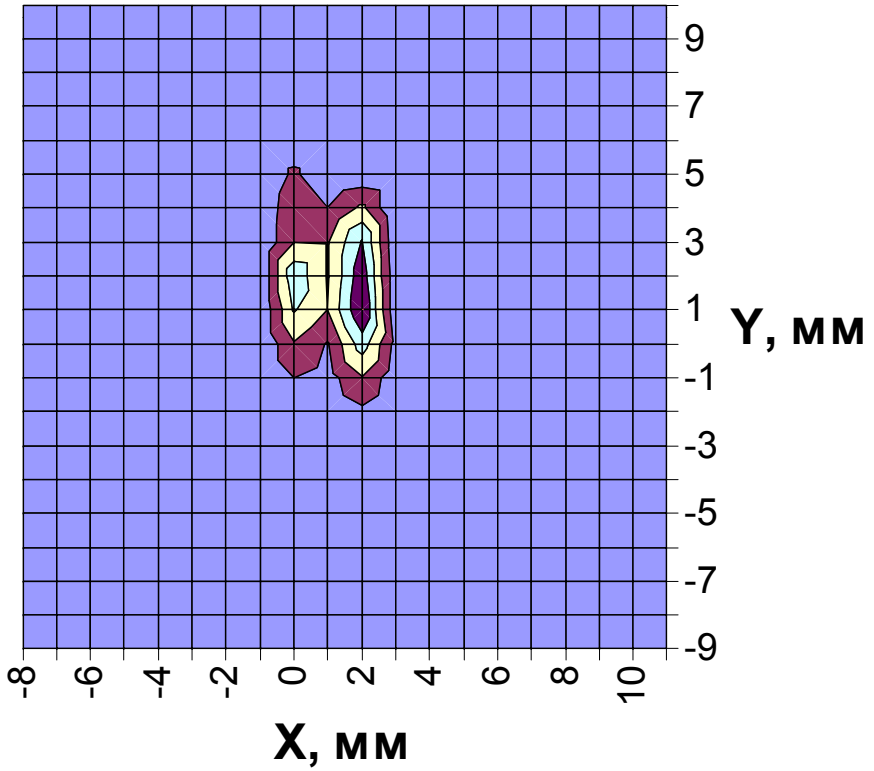

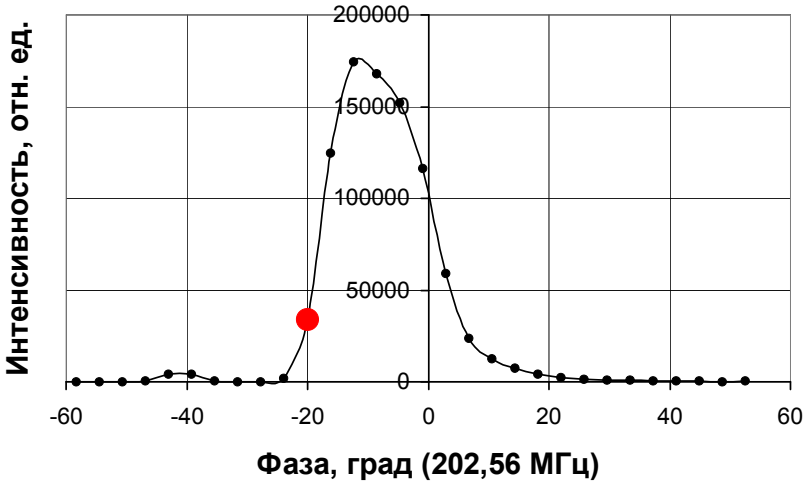

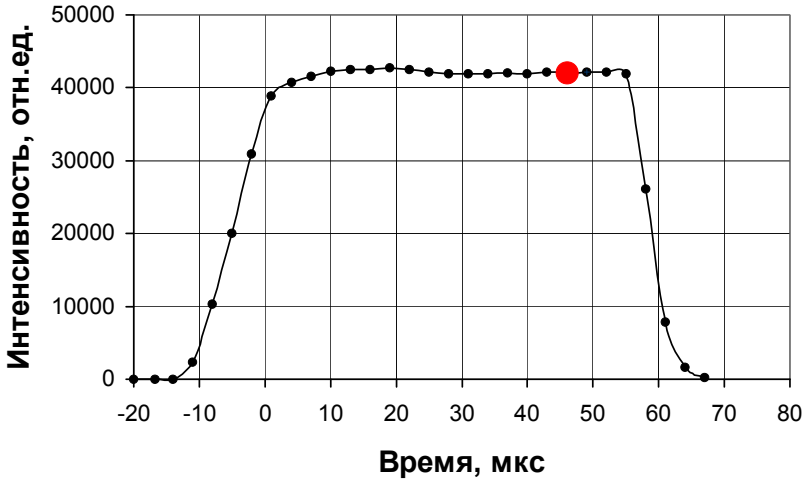

Transverse cross section of a bunch in different phases and at different moments of time within the beam pulse

Bunch #4

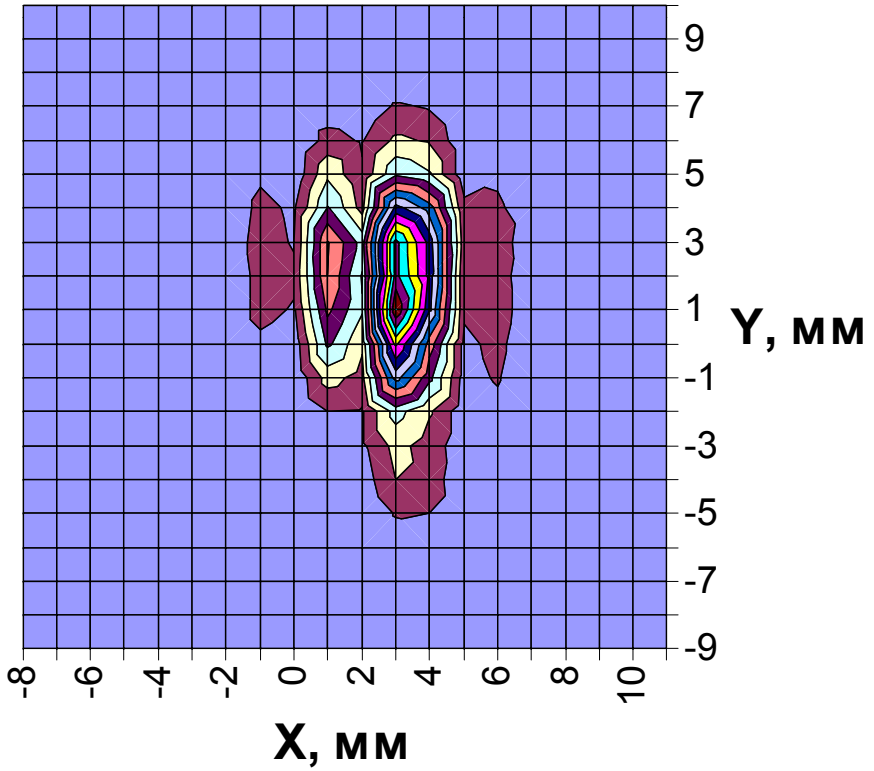

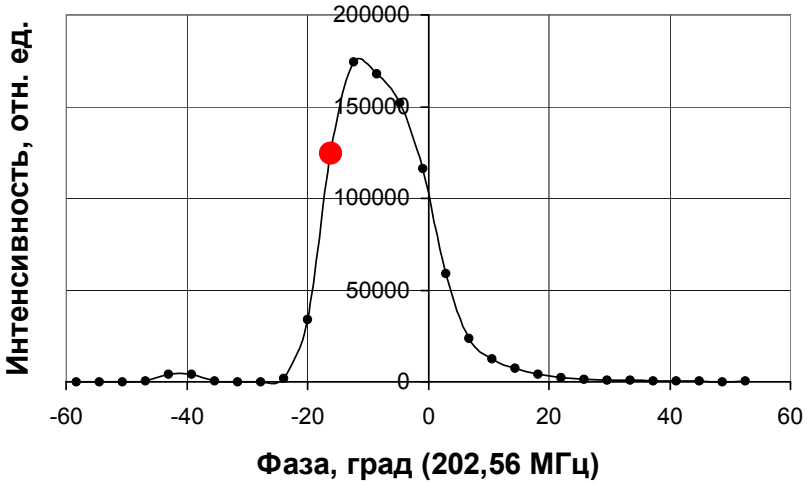

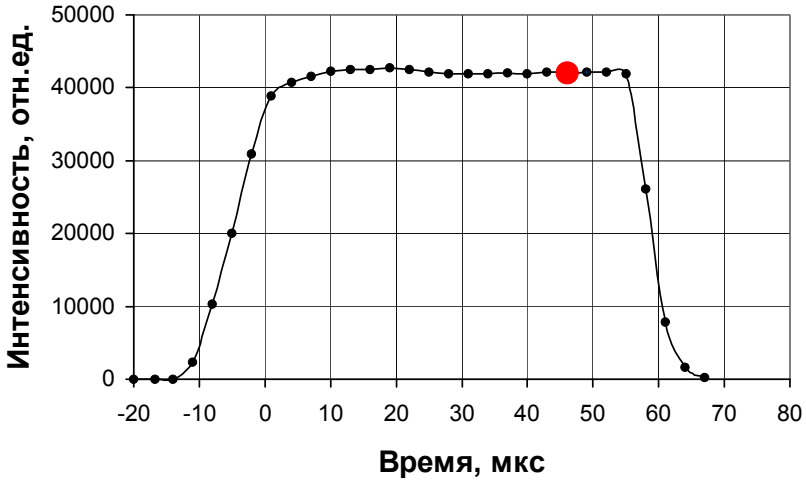

Transverse cross section of a bunch in different phases and at different moments of time within the beam pulse

Bunch #4

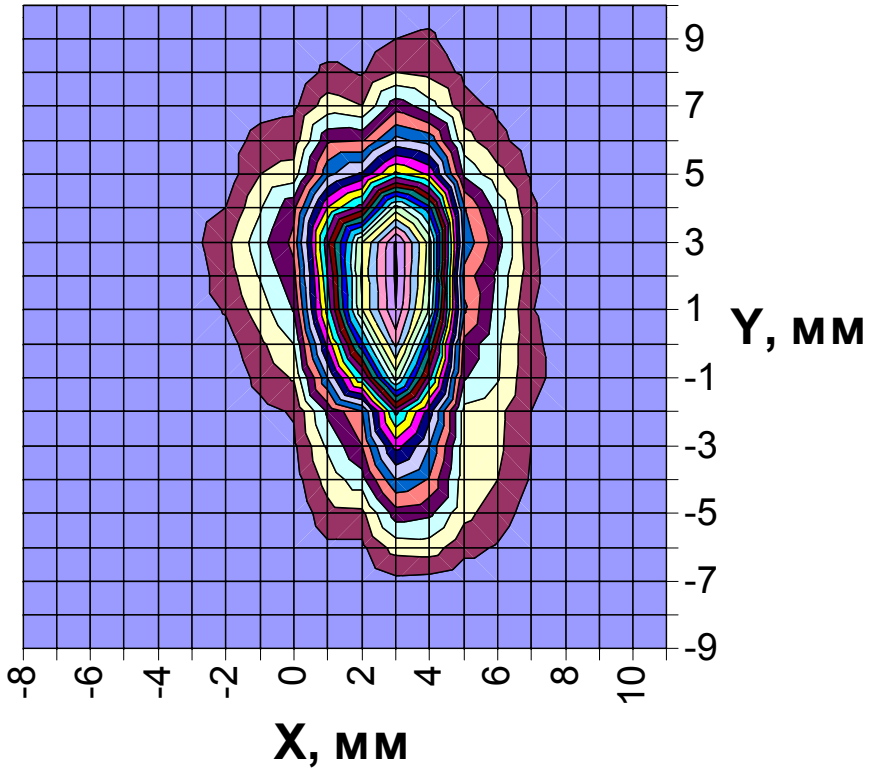

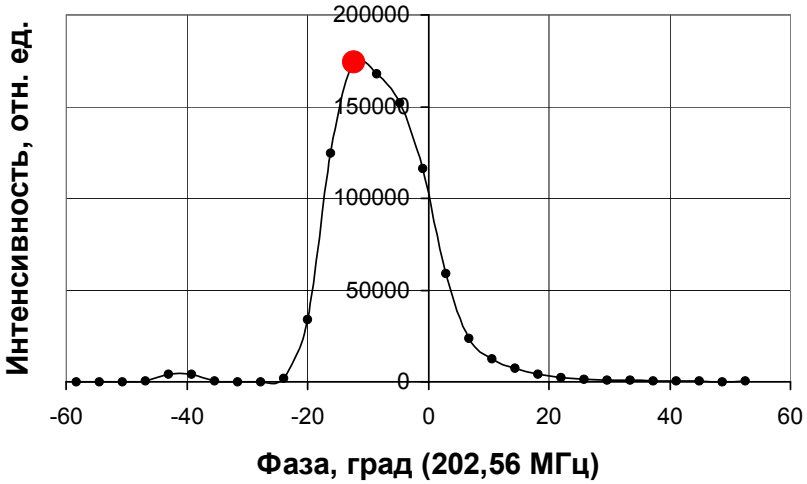

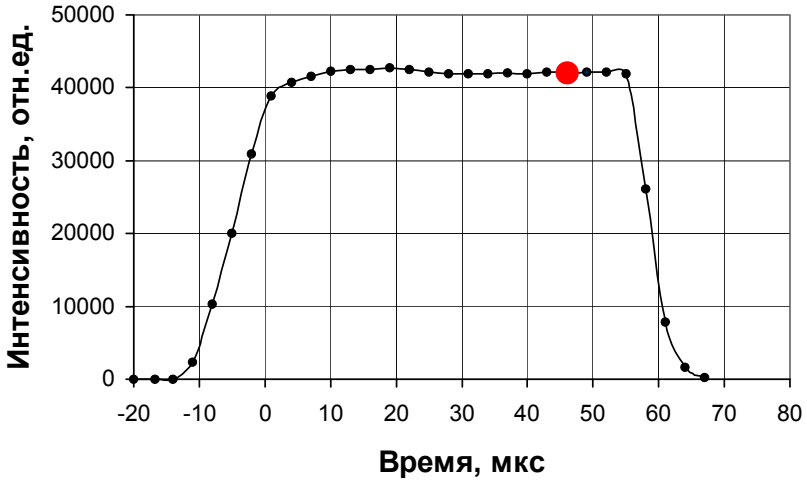

Transverse cross section of a bunch in different phases and at different moments of time within the beam pulse

Bunch #4

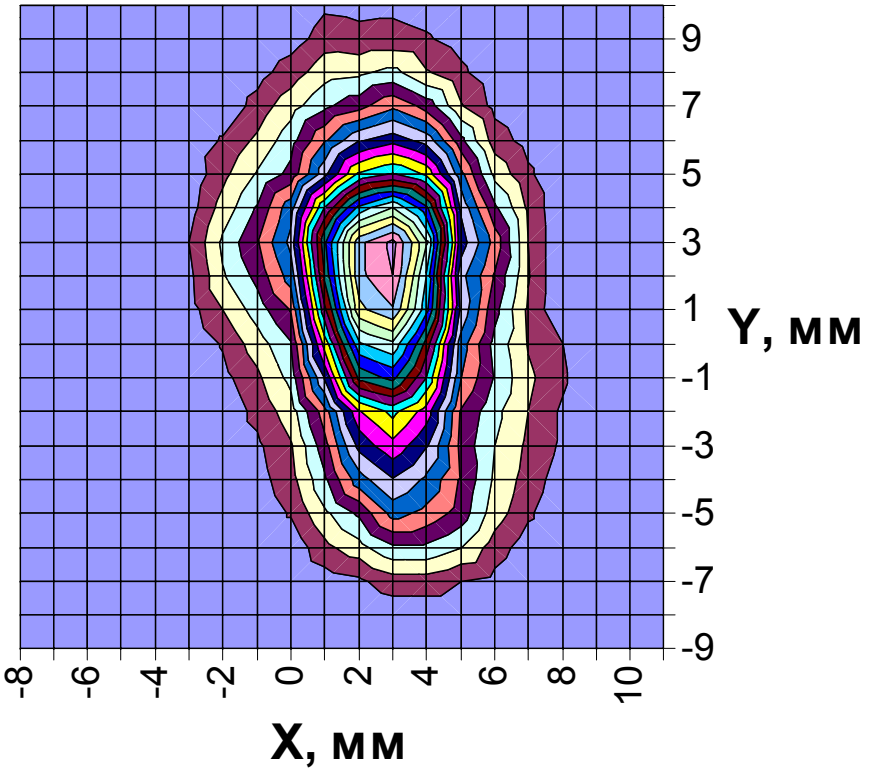

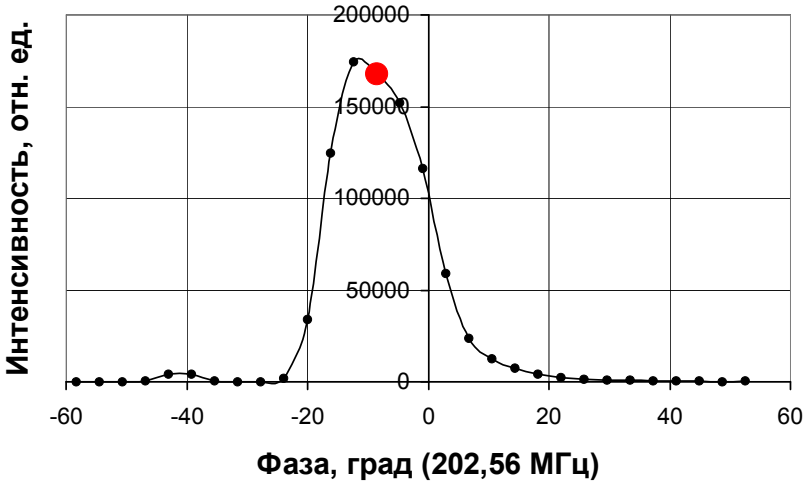

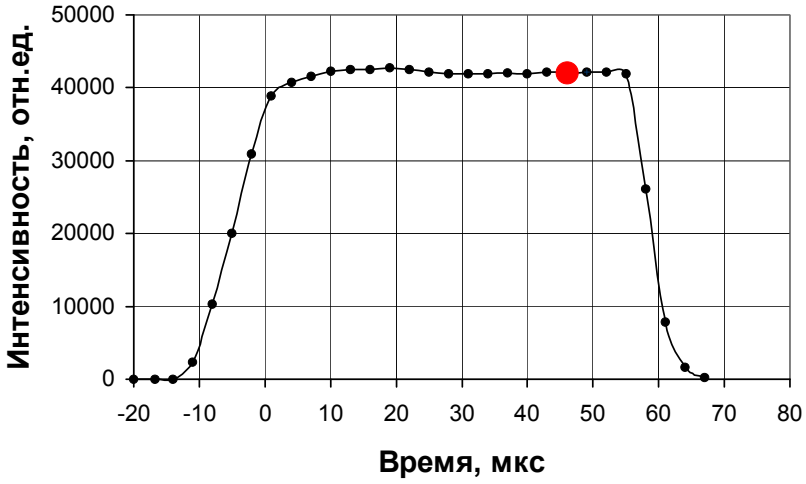

Transverse cross section of a bunch in different phases and at different moments of time within the beam pulse

Bunch #4

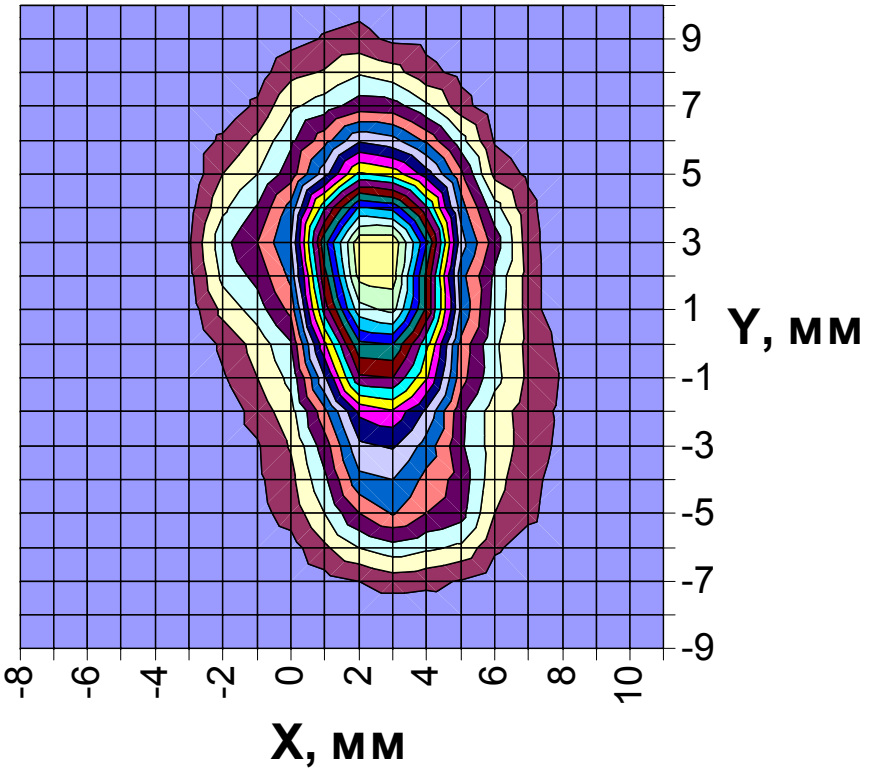

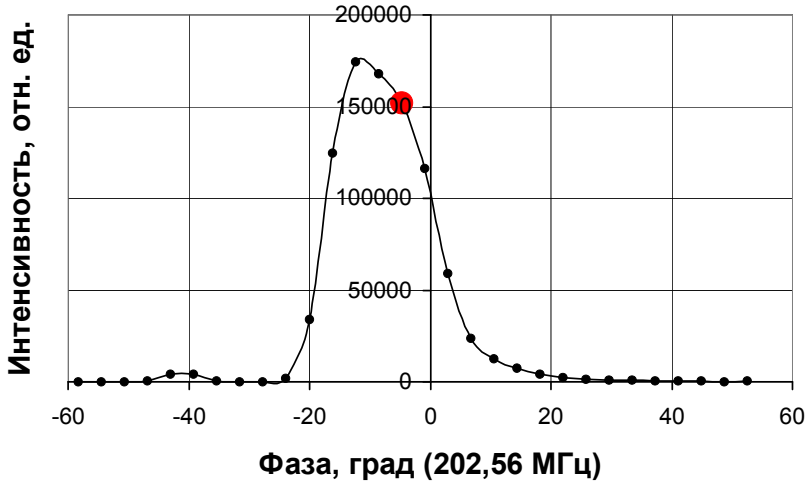

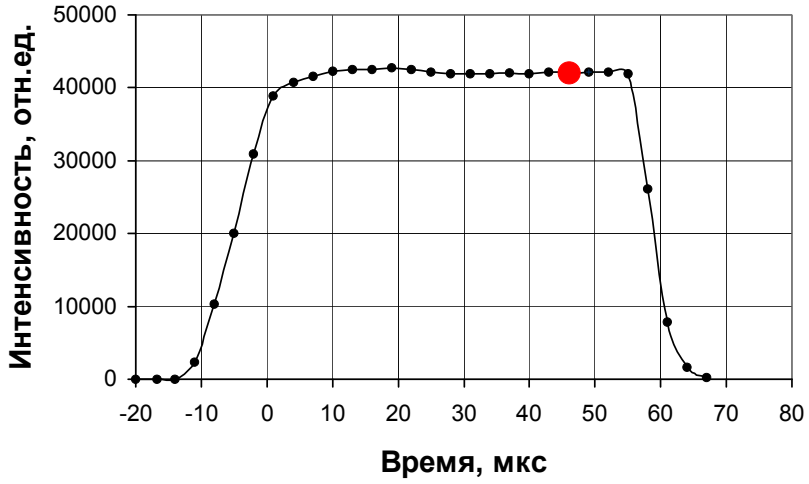

Transverse cross section of a bunch in different phases and at different moments of time within the beam pulse

Bunch #4

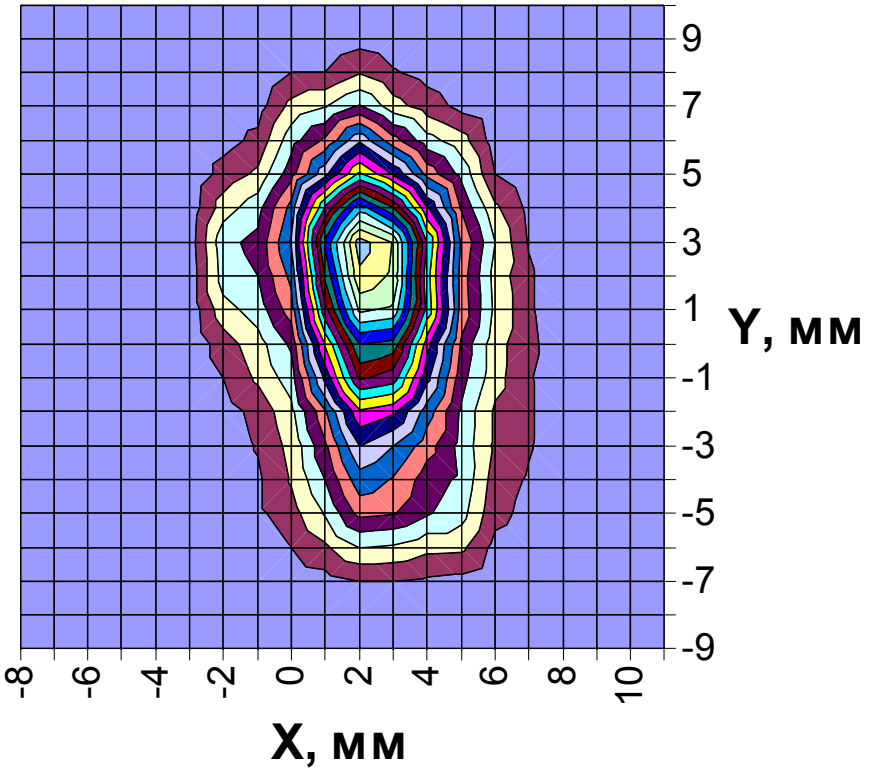

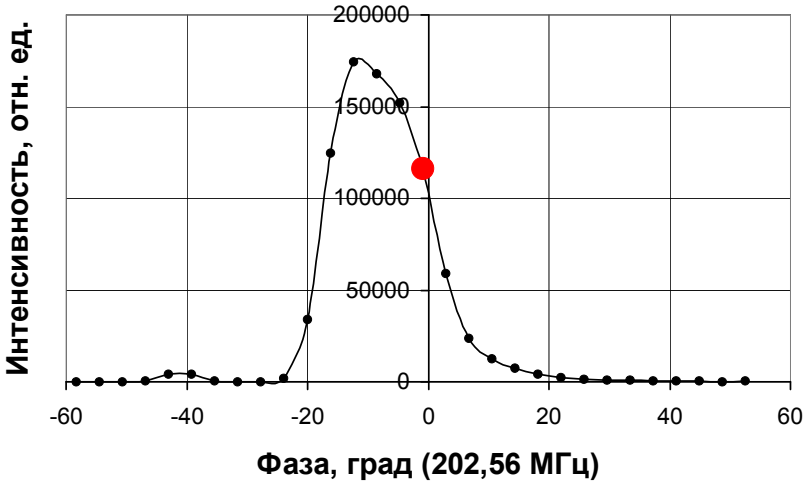

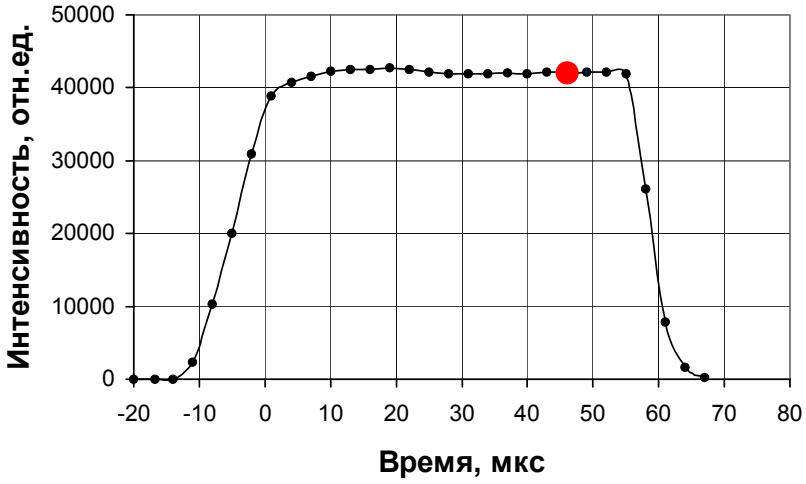

Transverse cross section of a bunch in different phases and at different moments of time within the beam pulse

Bunch #4

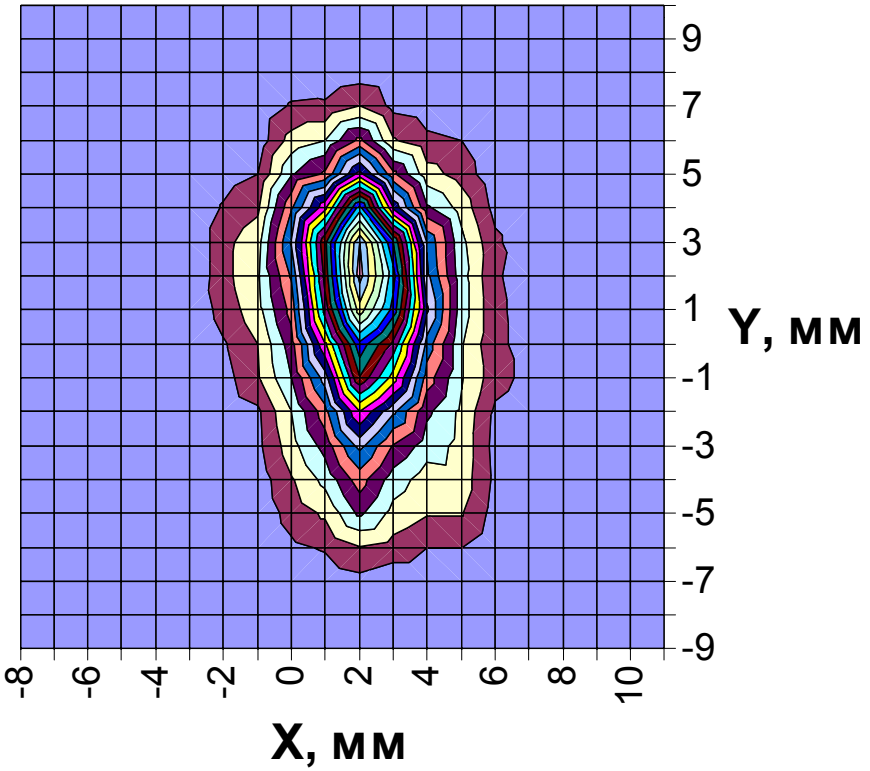

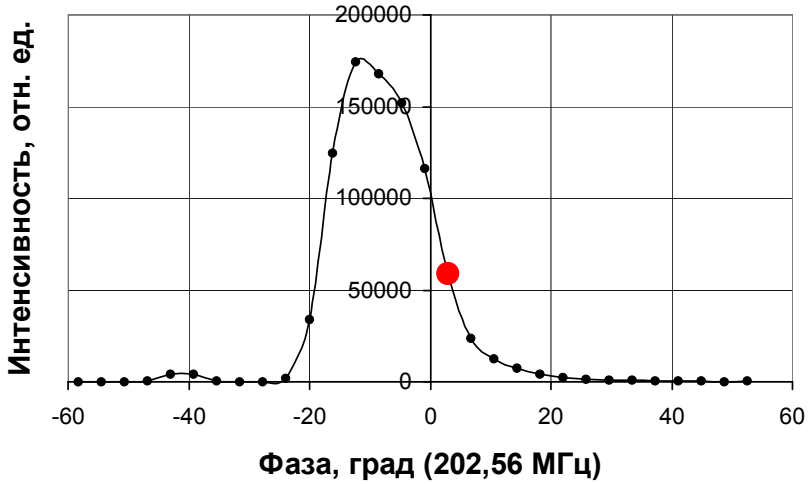

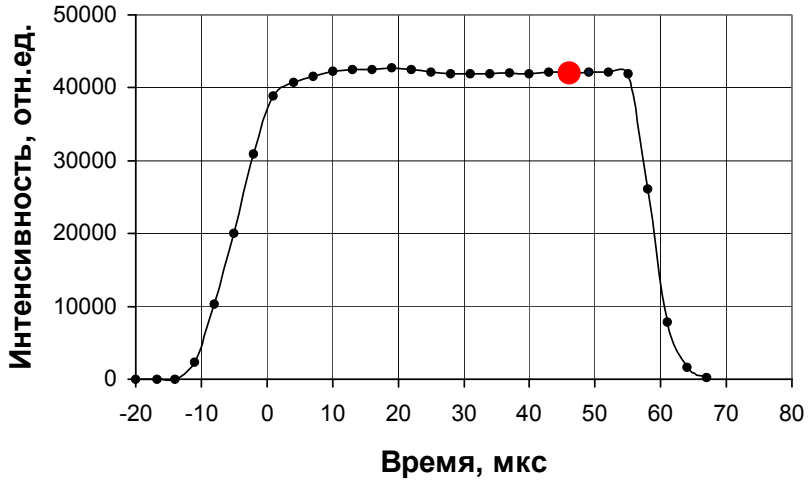

Transverse cross section of a bunch in different phases and at different moments of time within the beam pulse

Bunch #4

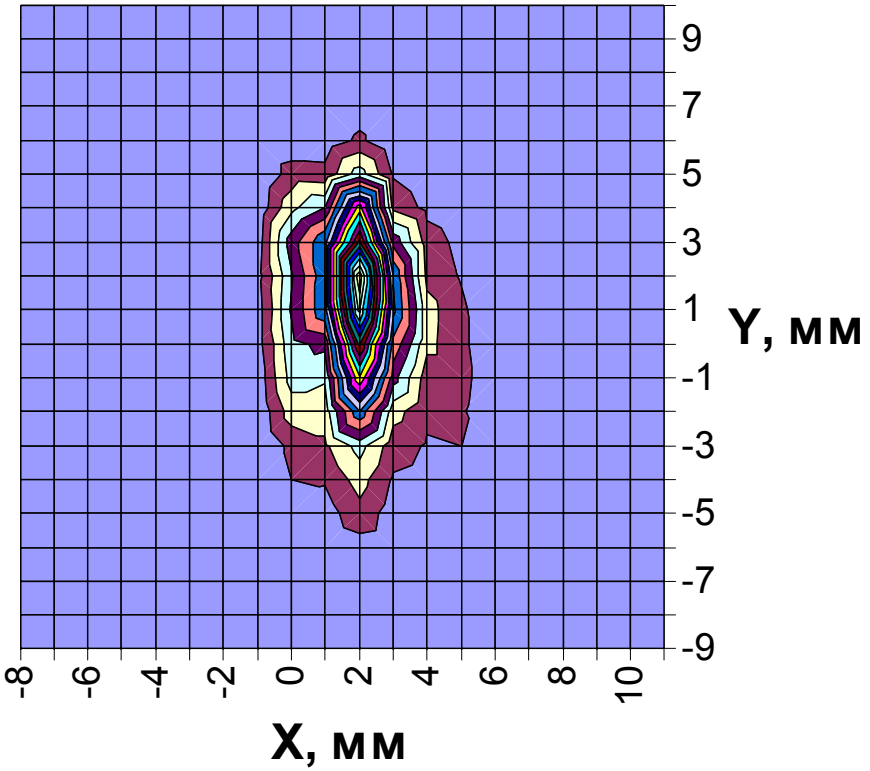

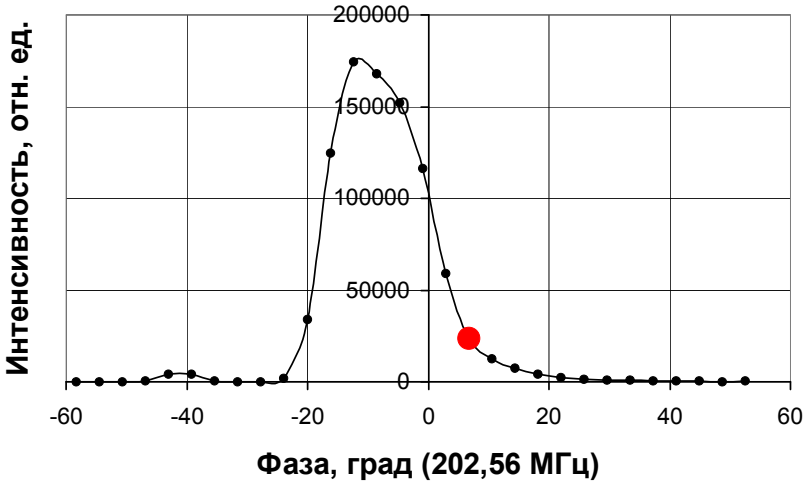

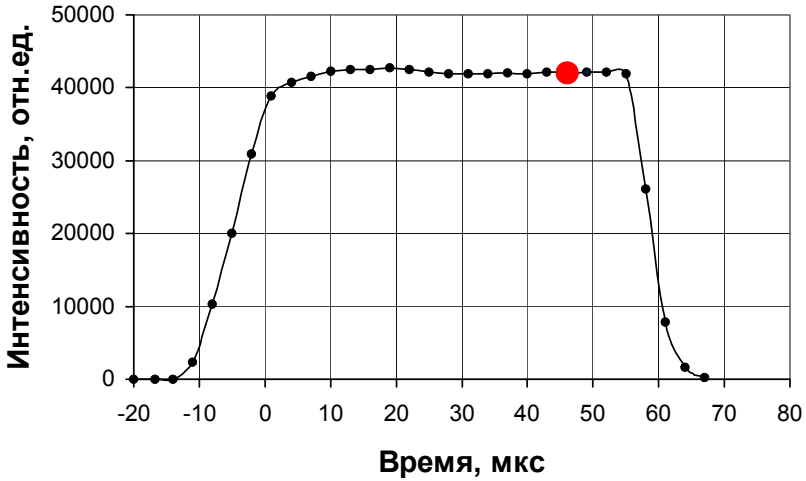

Transverse cross section of a bunch in different phases and at different moments of time within the beam pulse

Bunch #4

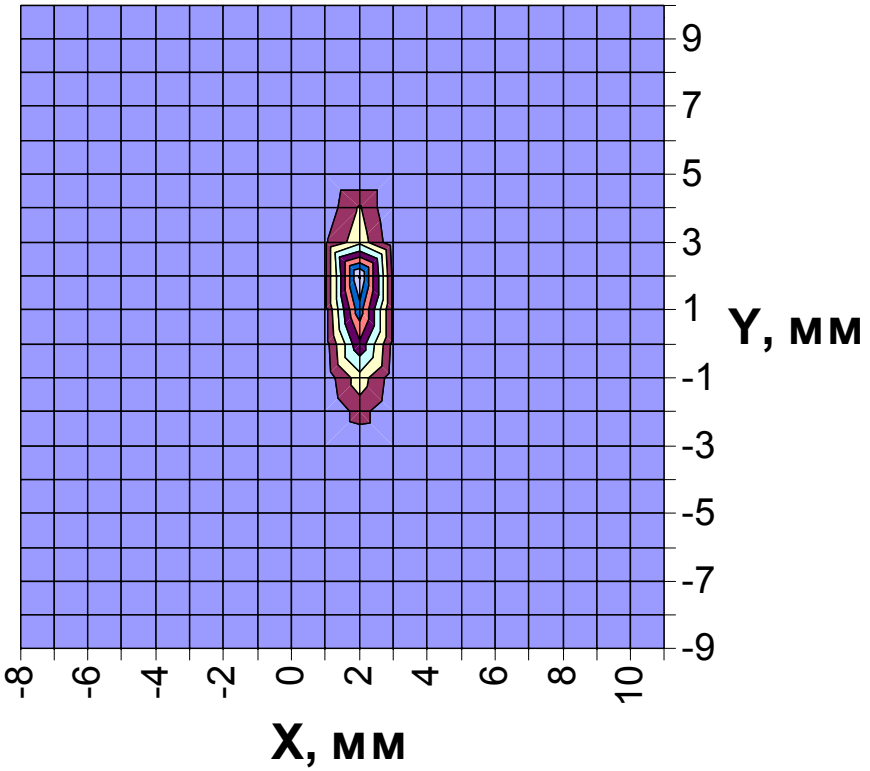

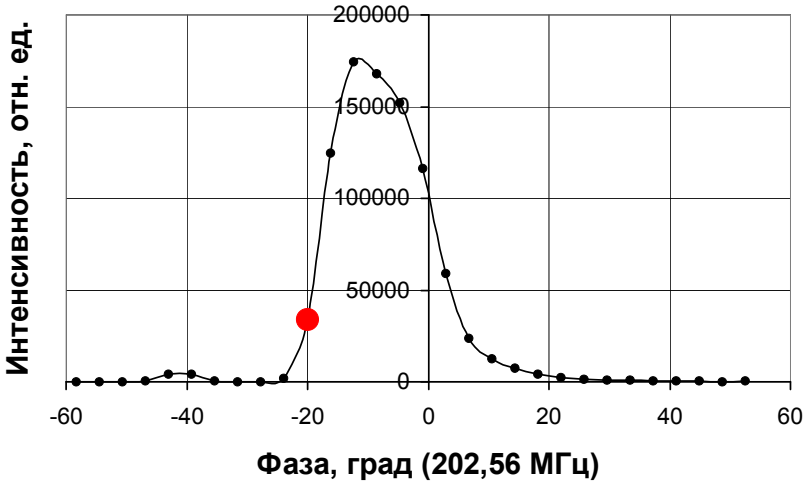

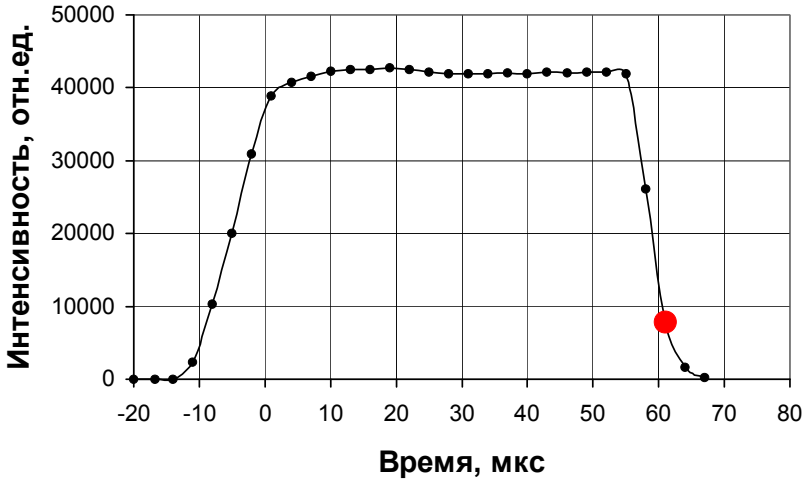

Transverse cross section of a bunch in different phases and at different moments of time within the beam pulse

Bunch #5

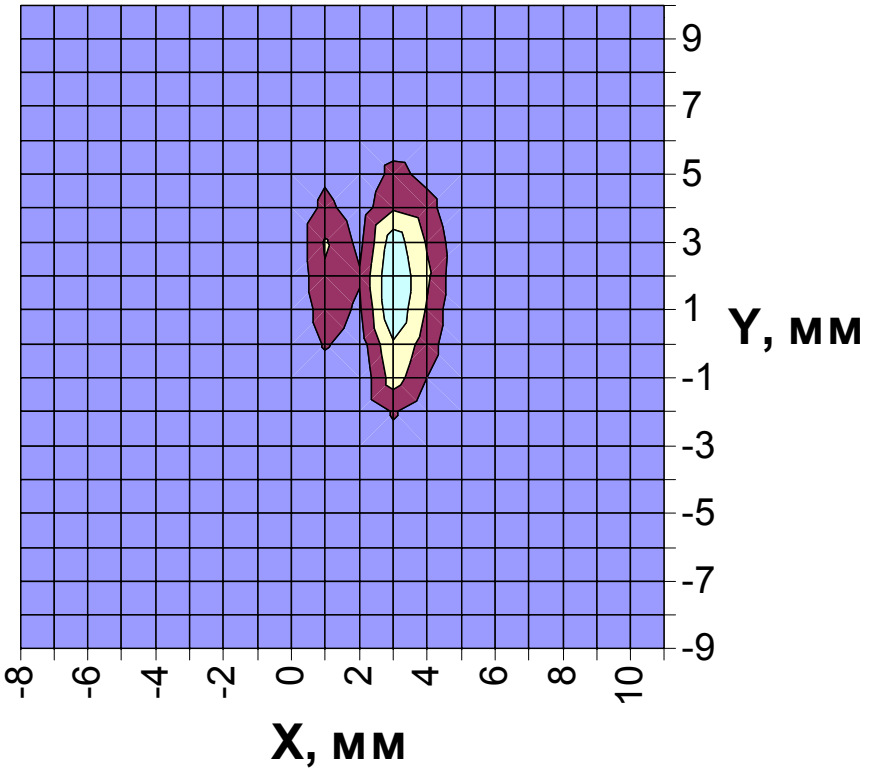

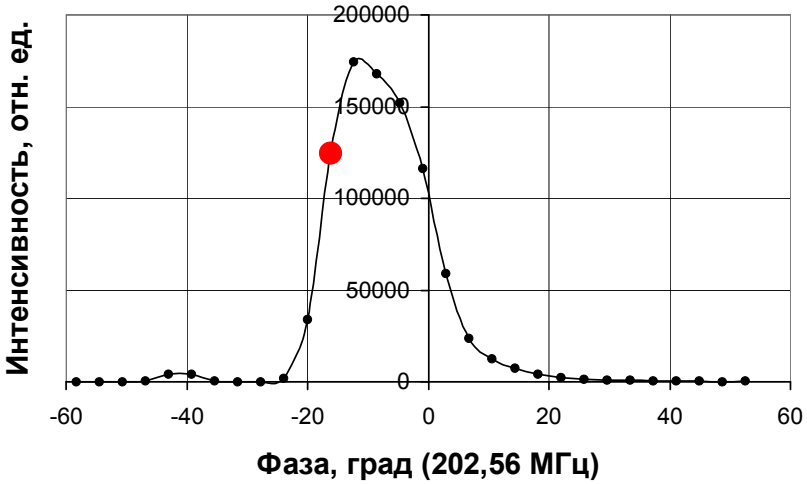

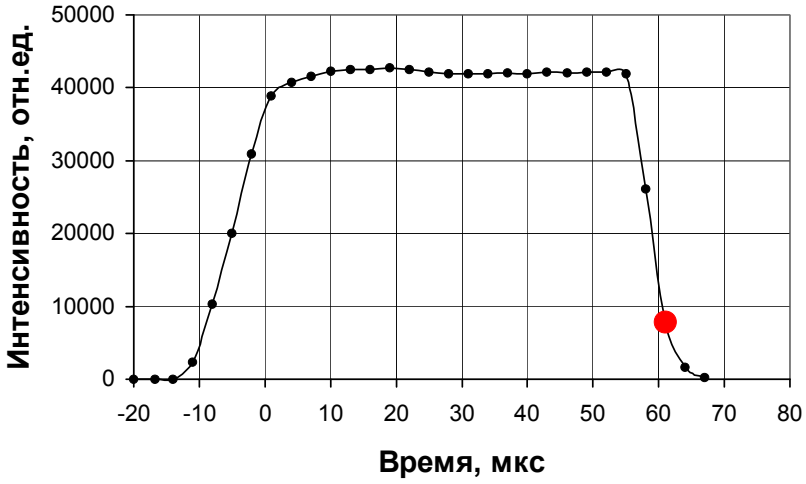

Transverse cross section of a bunch in different phases and at different moments of time within the beam pulse

Bunch #5

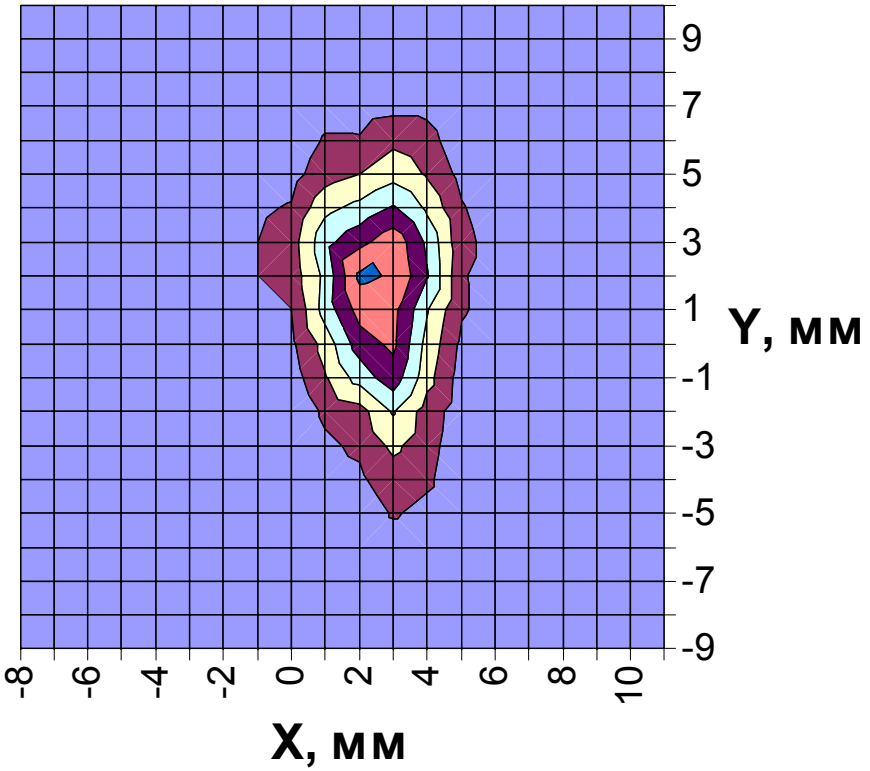

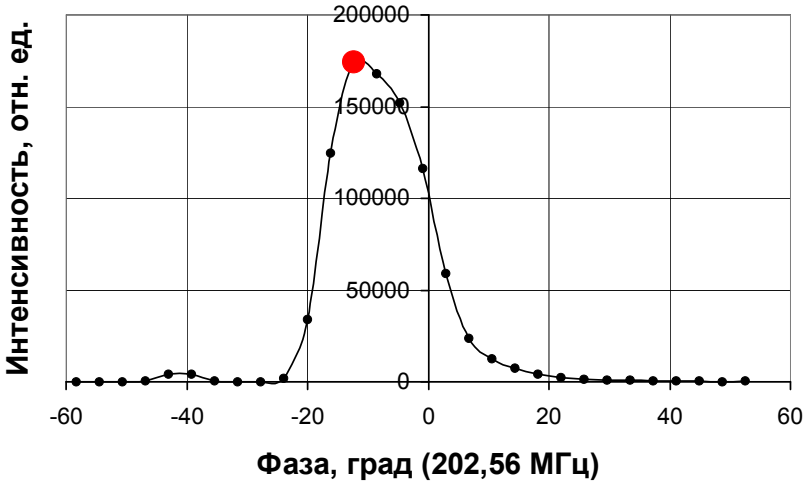

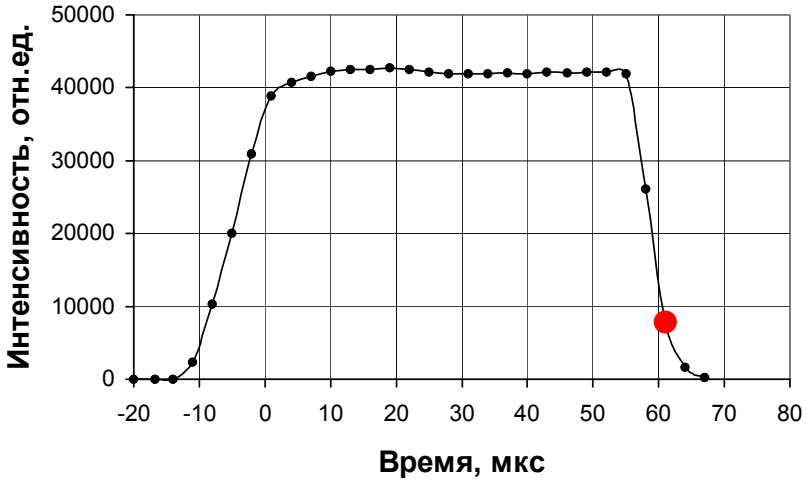

Transverse cross section of a bunch in different phases and at different moments of time within the beam pulse

Bunch #5

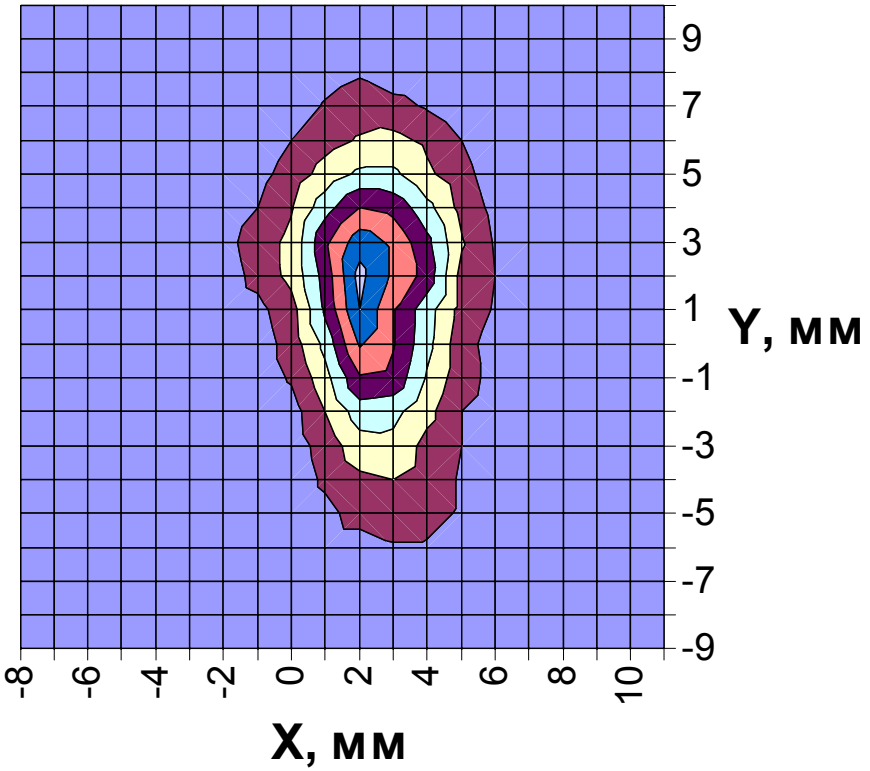

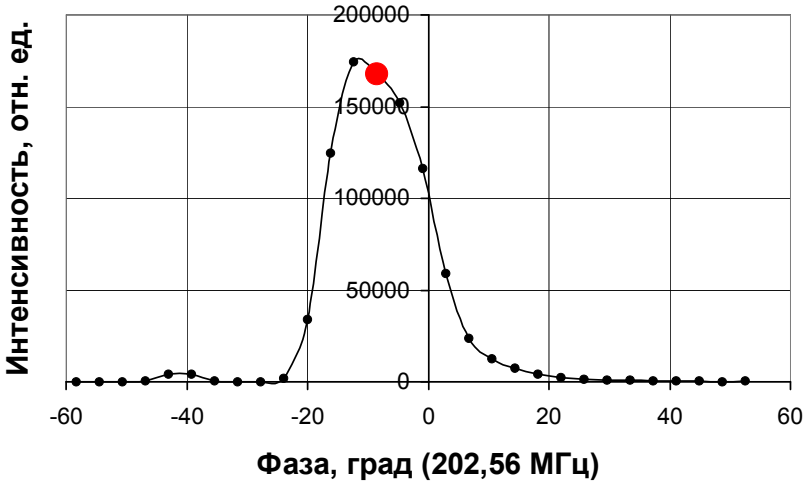

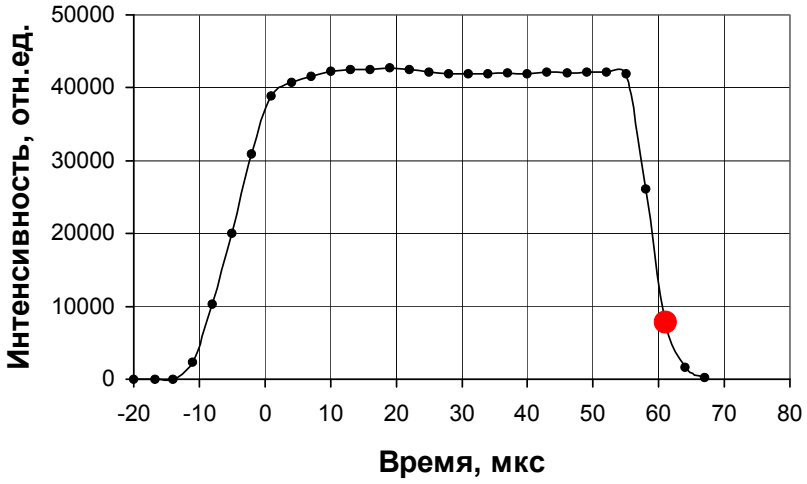

Transverse cross section of a bunch in different phases and at different moments of time within the beam pulse

Bunch #5

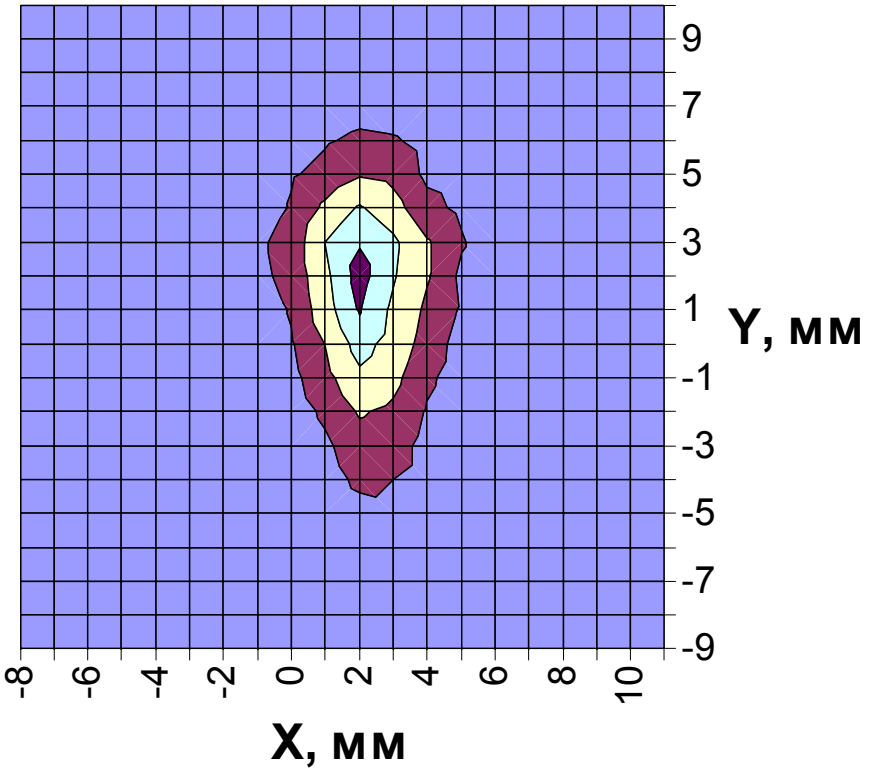

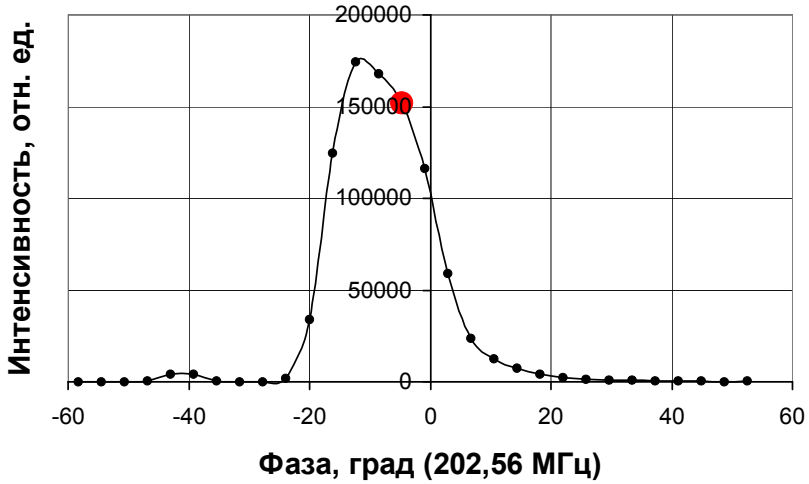

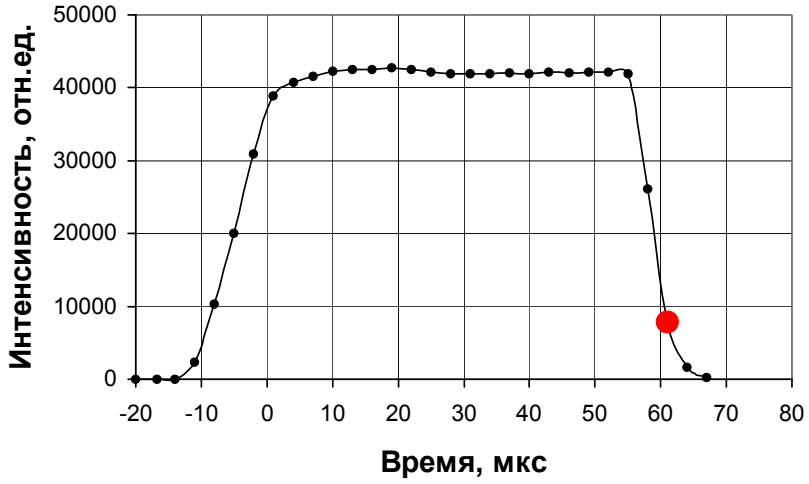

Transverse cross section of a bunch in different phases and at different moments of time within the beam pulse

Bunch #5

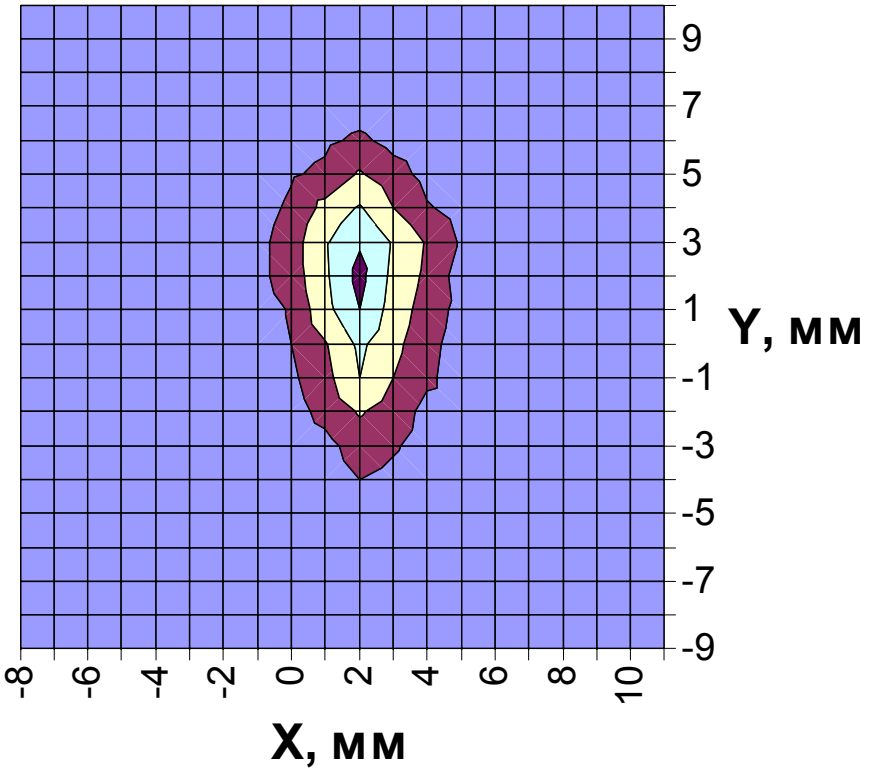

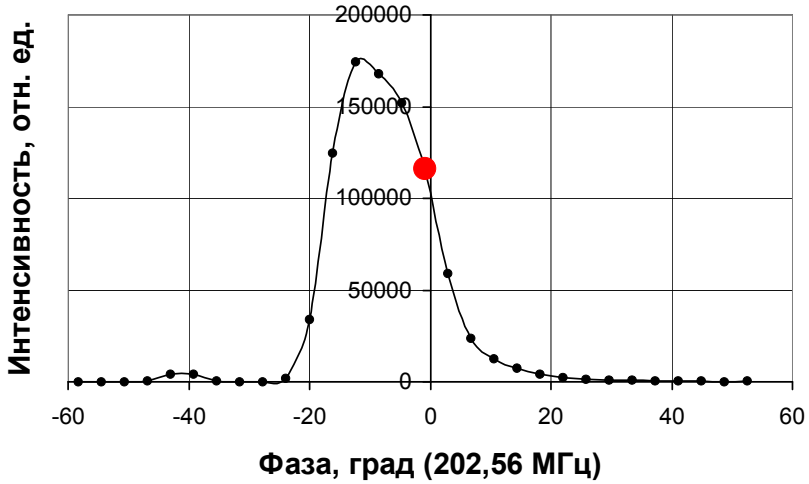

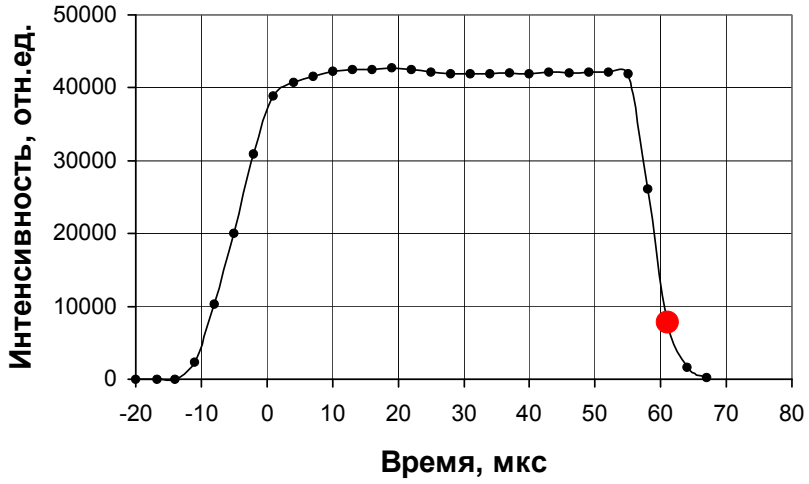

Transverse cross section of a bunch in different phases and at different moments of time within the beam pulse

Bunch #5

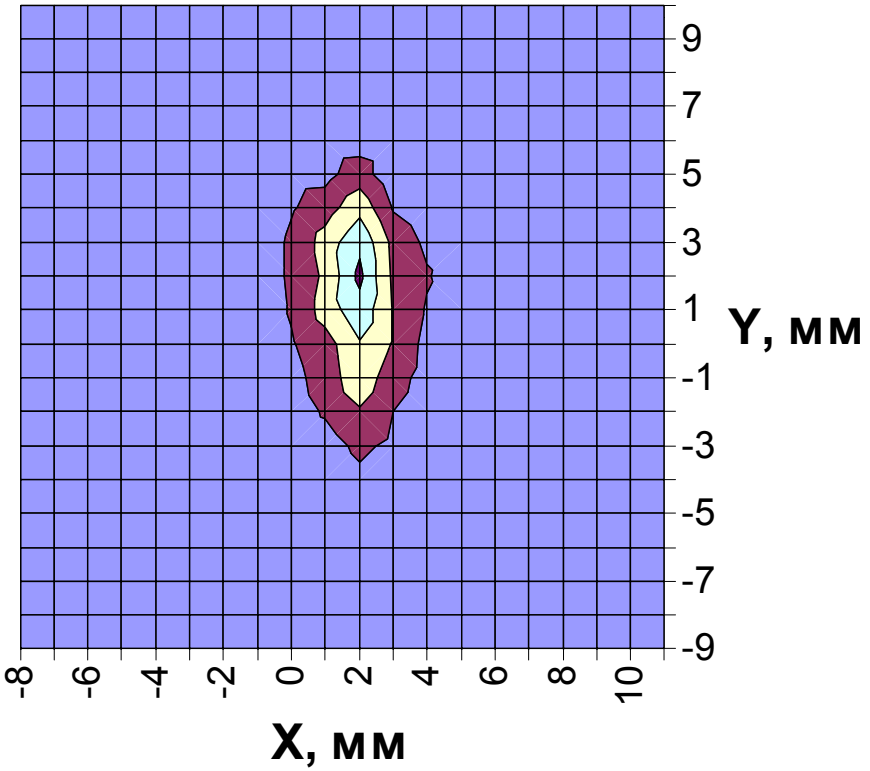

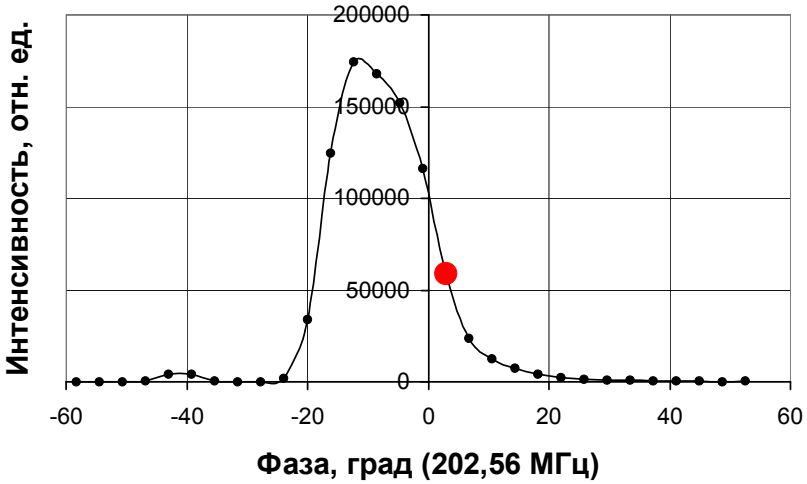

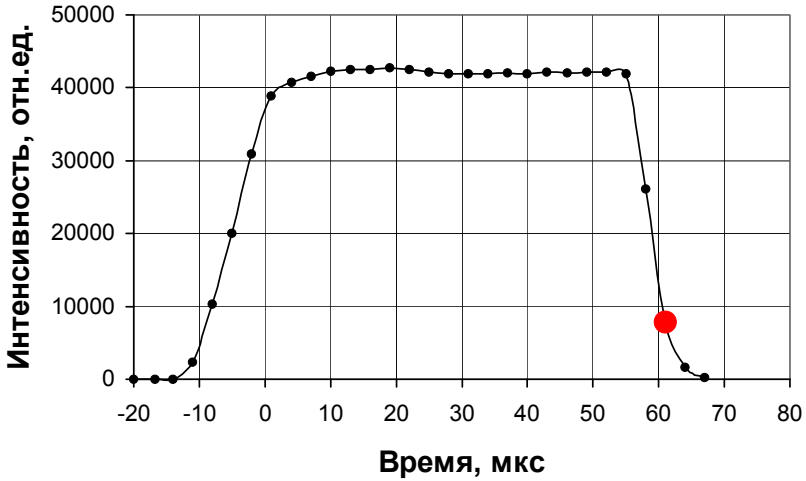

Transverse cross section of a bunch in different phases and at different moments of time within the beam pulse

Bunch #5

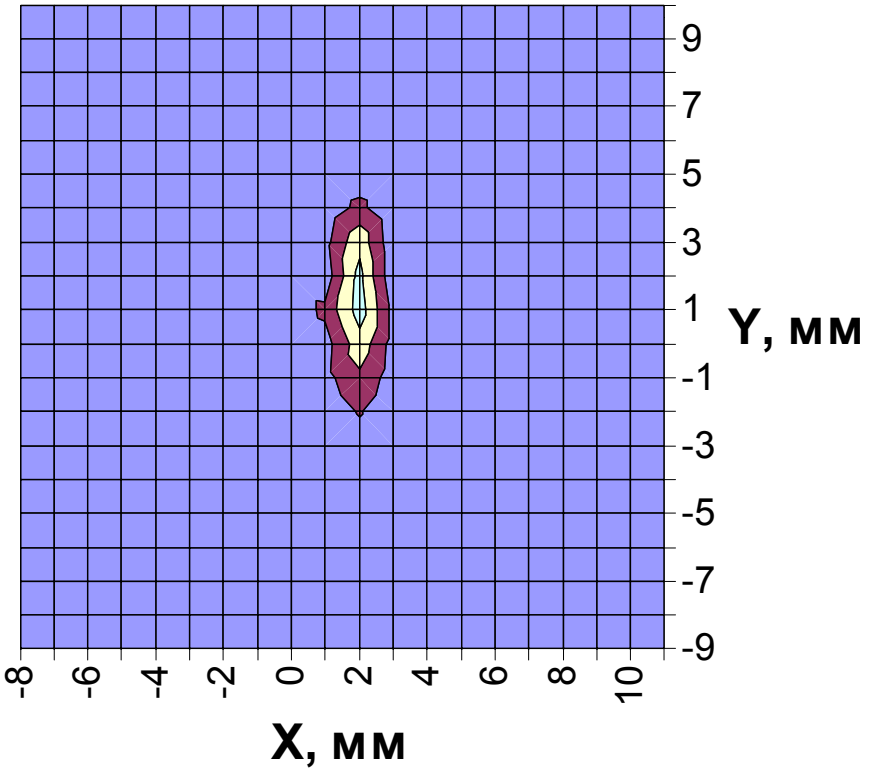

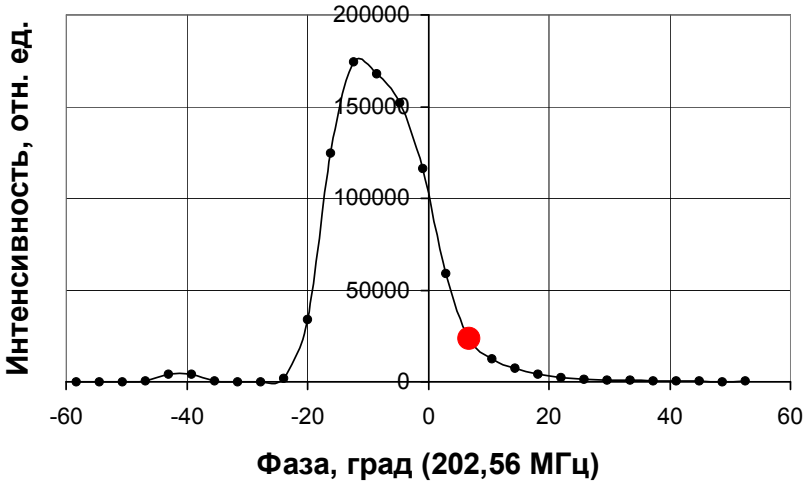

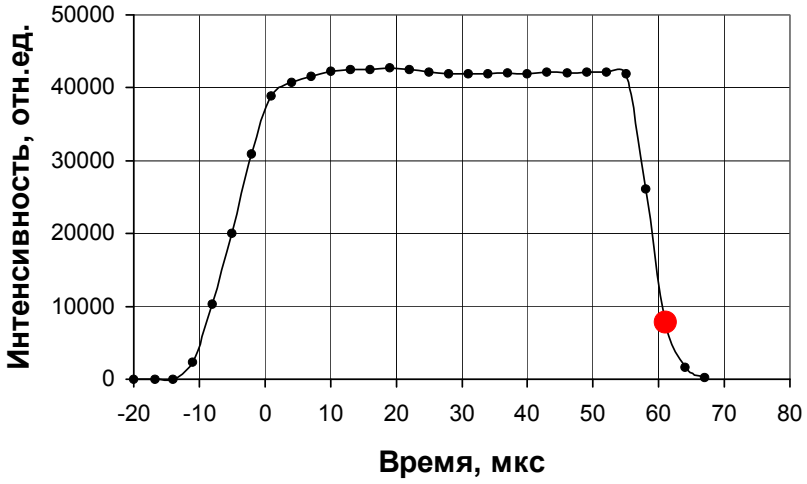

Transverse cross section of a bunch in different phases and at different moments of time within the beam pulse

Bunch #5

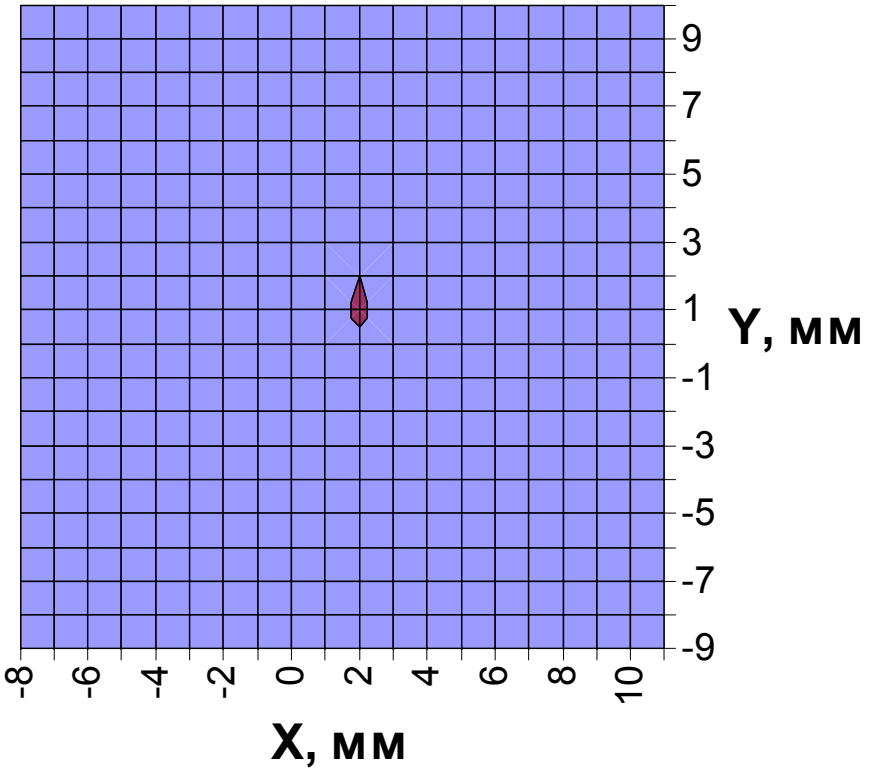

Manifestation of target heating effect (SSC-RFQ. Current 19 mA)

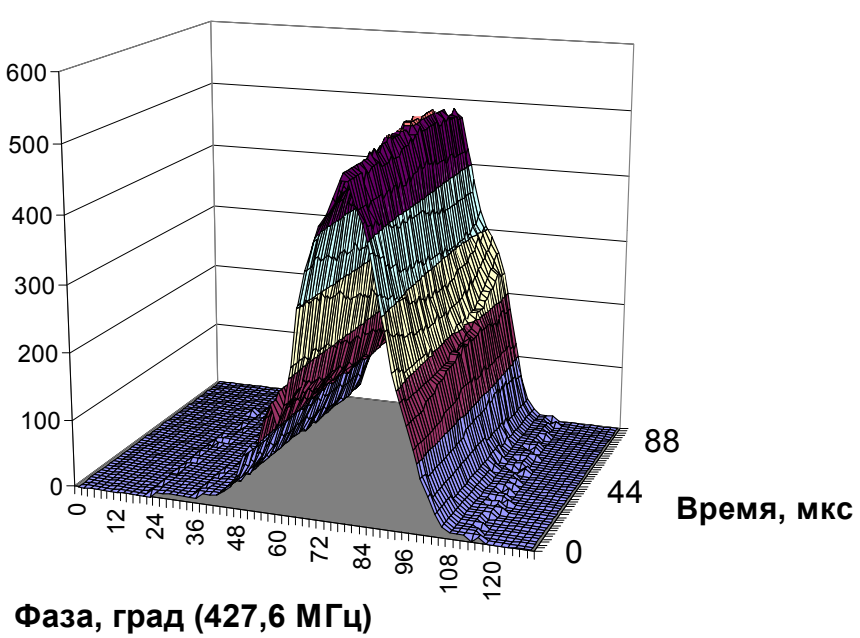

1Hz

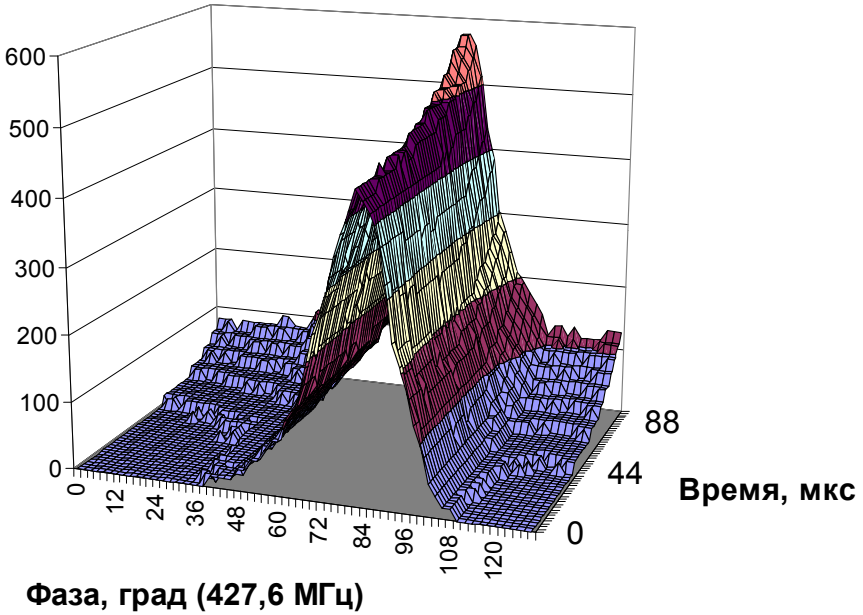

10 Hz

Some examples of measurements in SNS Linac

Typical evolution of bunch shape along the beam pulse.

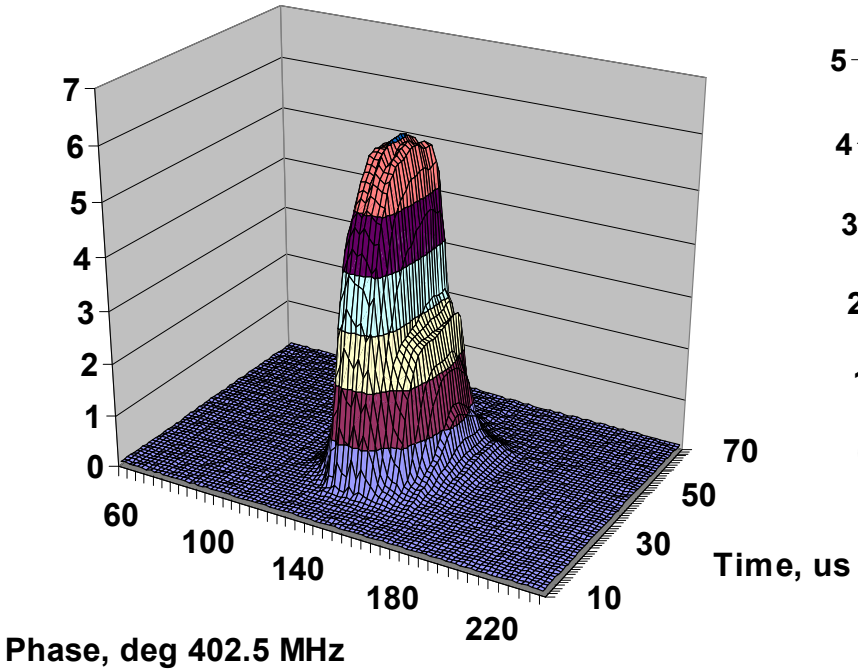

Manifestation of Low Level RF instabilities in Bunch Shape

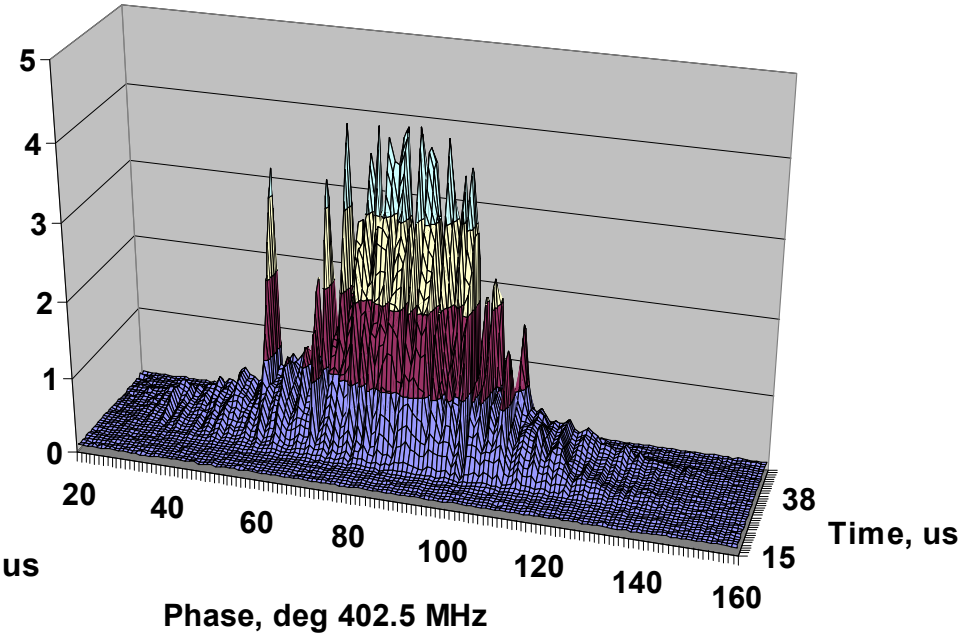

Longitudinal Halo Measurements

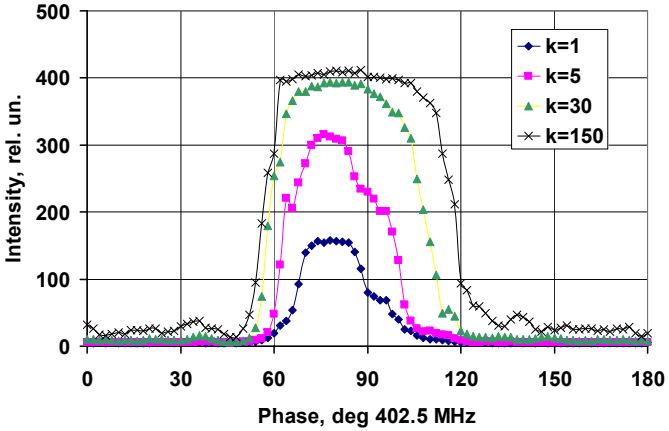

Result of Bunch Shape Measurement for different electron multiplier gains.

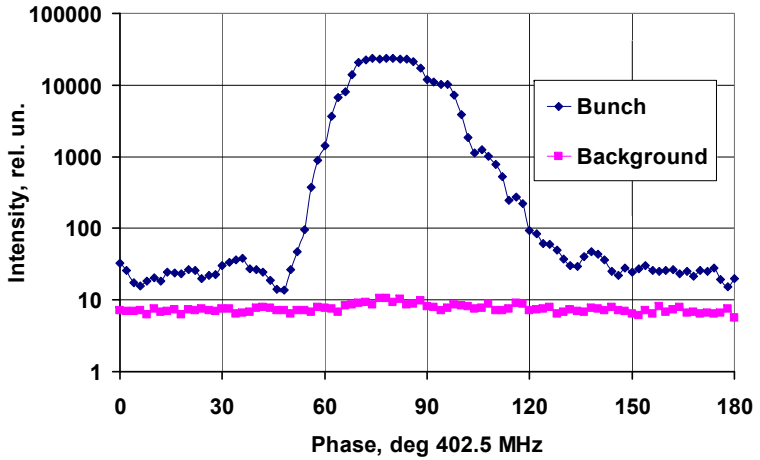

Presentation of bunch shape in a wide intensity range.

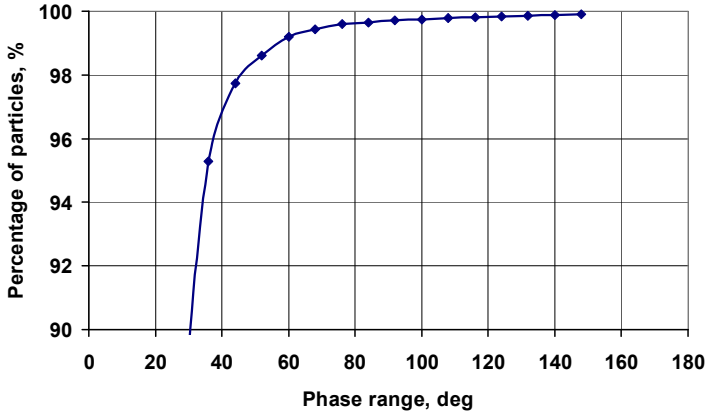

Particle portion as function of phase range.

Longitudinal Emittance Measurements

Calibration of Accelerating Field Amplitude

(by comparing experimental and theoretical changes of bunch phase positions vs accelerating field phase shift)

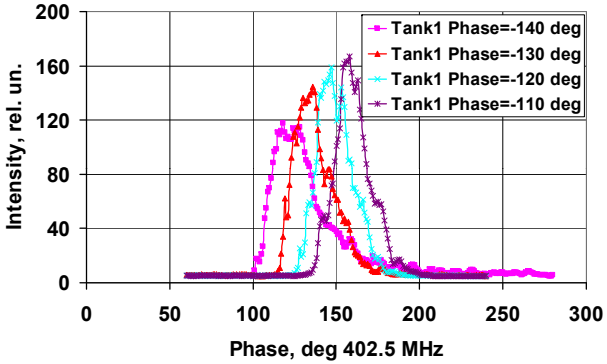

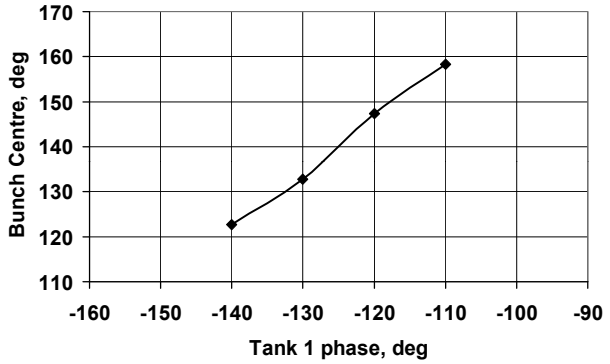

Bunch phase position Φ for different Tank 1 phases.

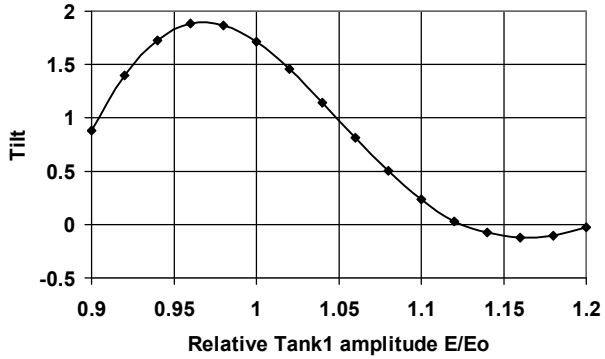

Theoretical dependence of dΦ/dφ on field amplitude.

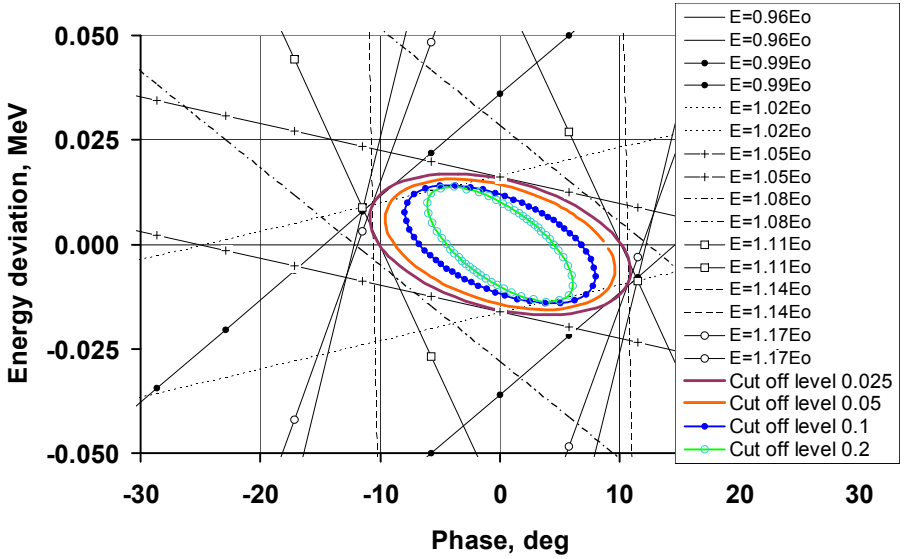

Phase ellipses at the entrance of Tank 1 for different cut off levels (The tangents are shown for 0.025 cut off level).

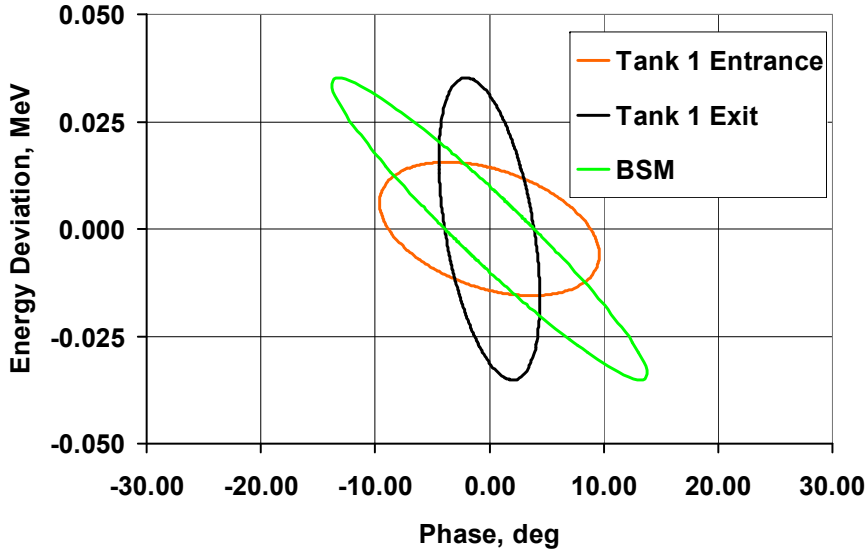

Phase ellipses at the entrance of Tank1, the exit of Tank 1 and at the BSM position for cut off level 0.05

Longitudinal emittance value (the design parameter 0.131 MeV·deg)

Cut off level	0.025	0.05	0.1	0.2
Emittance, MeV·deg	0.171	0.138	0.095	0.062

Example of bunch shape behavior within the beam pulse(15 mA beam current)

BSM107

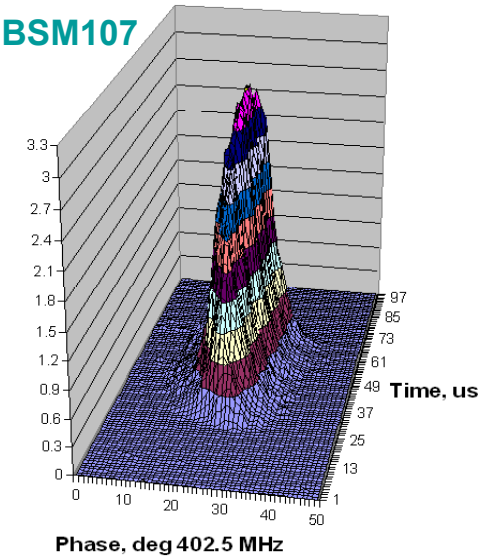

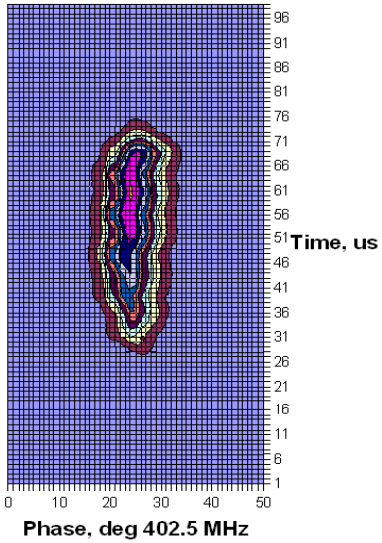

BSM109

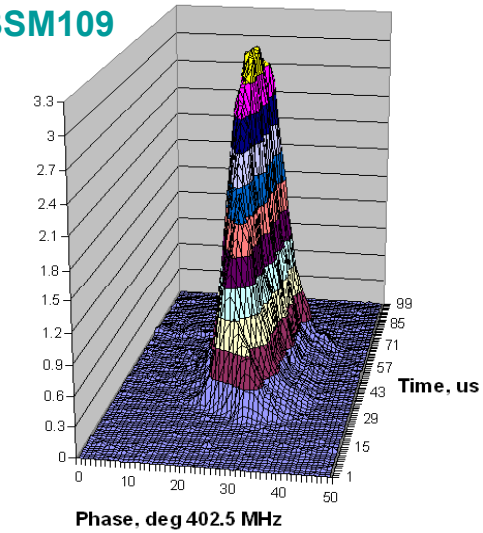

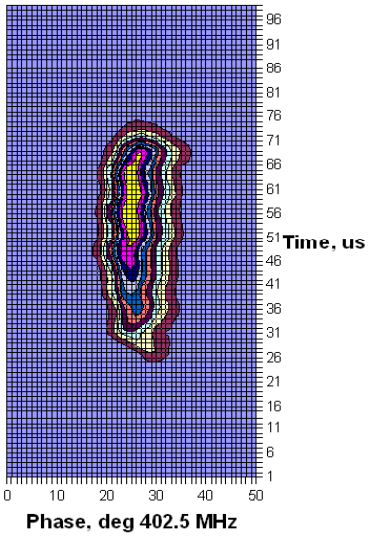

BSM111

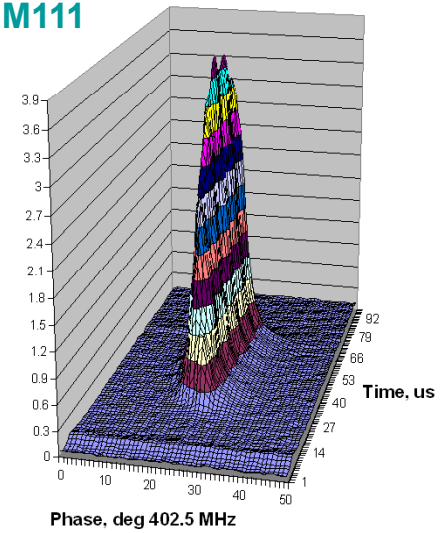

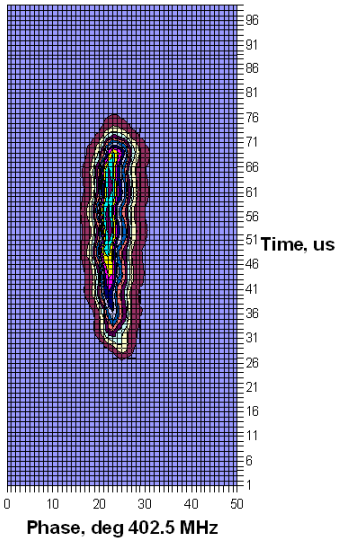

86.8 МэВ

107.1 МэВ

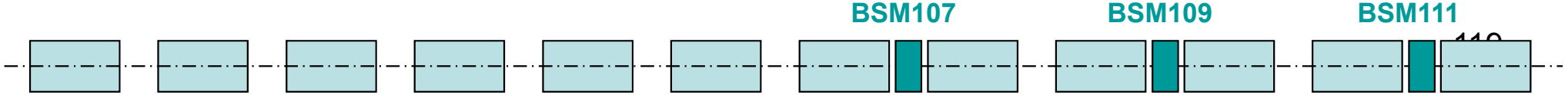

Behavior of bunch shape within the beam pulse at 30 mA beam current

(poor beam loading compensation)

BSM107

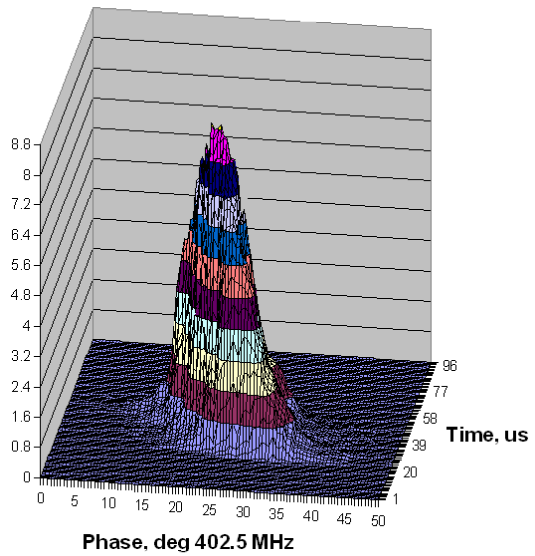

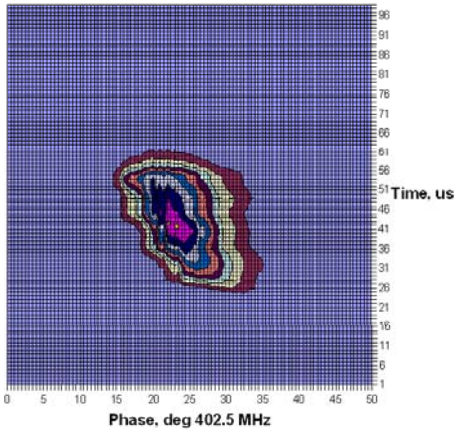

BSM109

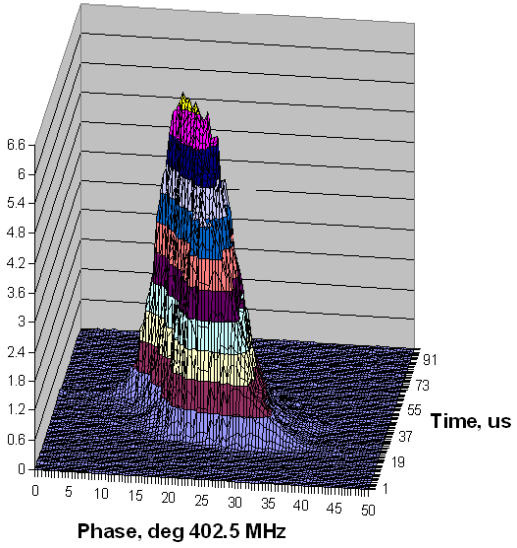

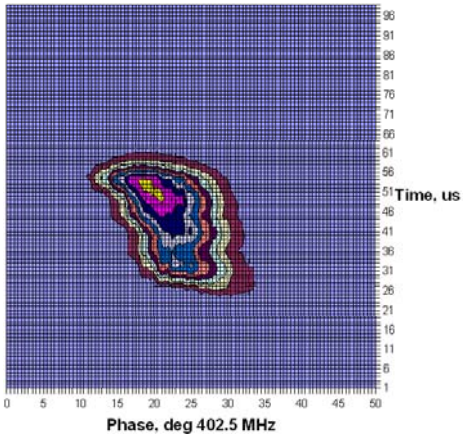

BSM111

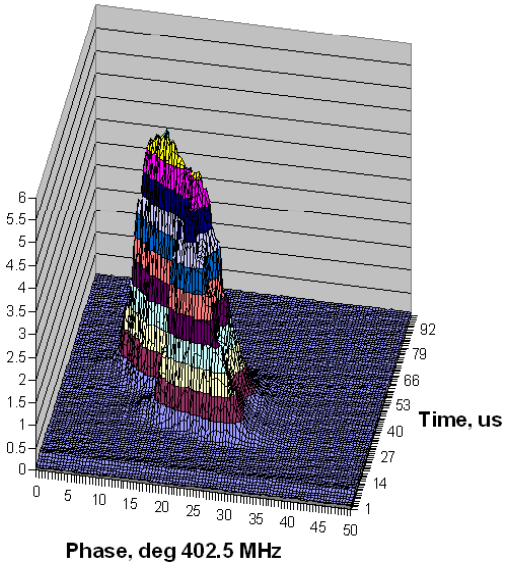

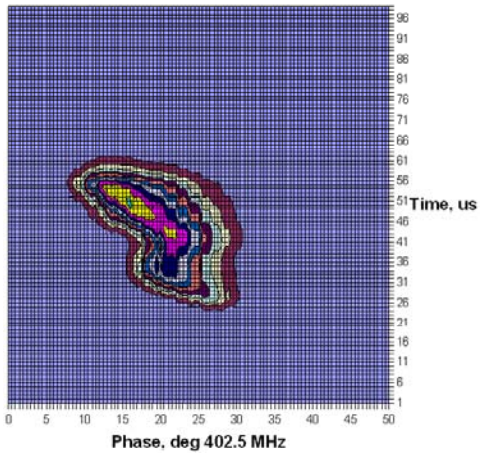

86.8 МэВ

107.1 МэВ

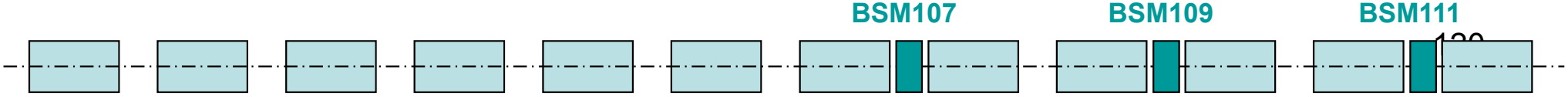

Longitudinal Emittance at the Entrance of CCL #1

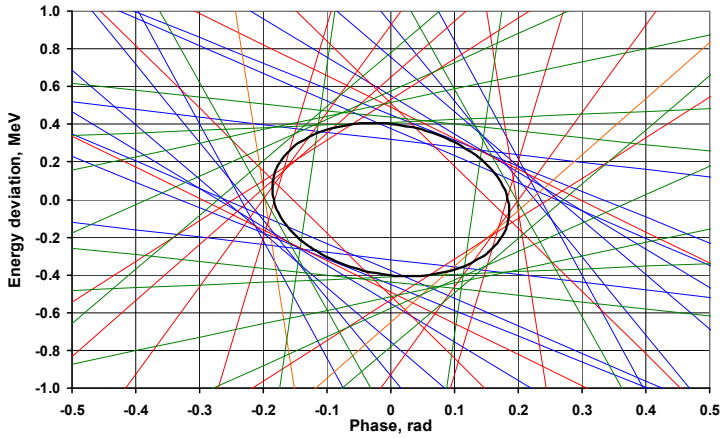

Bunch boundaries transformed to the entrance of CCL#1 and an equivalent phase ellipse.

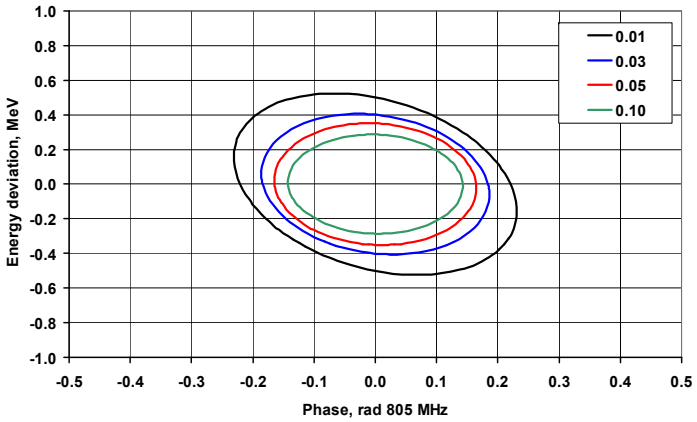

Longitudinal phase ellipses restored from the bunch length measurements of the distribution at different cut-off levels

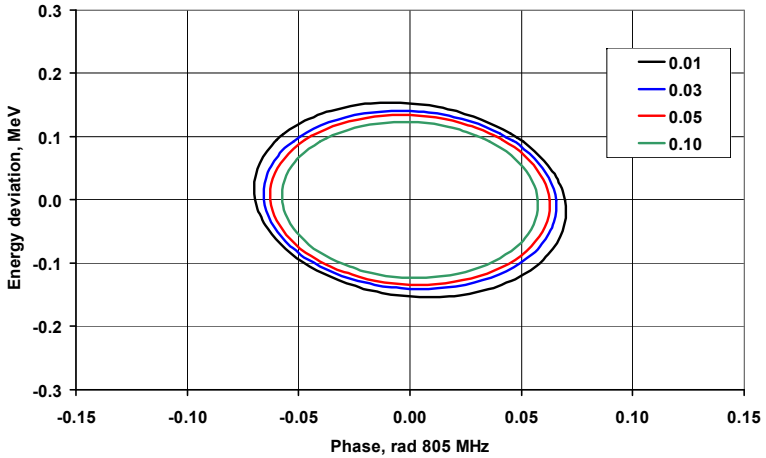

Longitudinal phase ellipses restored from the rms bunch length measurements at different cut-off levels

Cutoff Level	Base				RMS			
	α	β MeV^{-1}	γ MeV	ε MeV	α	β MeV^{-1}	γ MeV	ε MeV
0.01	0.3067	0.4605	2.3760	0.1158	0.1204	0.4595	2.2080	0.0107
0.03	0.1534	0.4636	2.2080	0.0745	0.0697	0.4672	2.1510	0.0092
0.05	0.0654	0.4689	2.1420	0.0578	0.0613	0.4686	2.1420	0.0084
0.10	0.0429	0.4984	2.0100	0.0408	0.0516	0.4661	2.1510	0.0071

Longitudinal Halo and Tail measurements

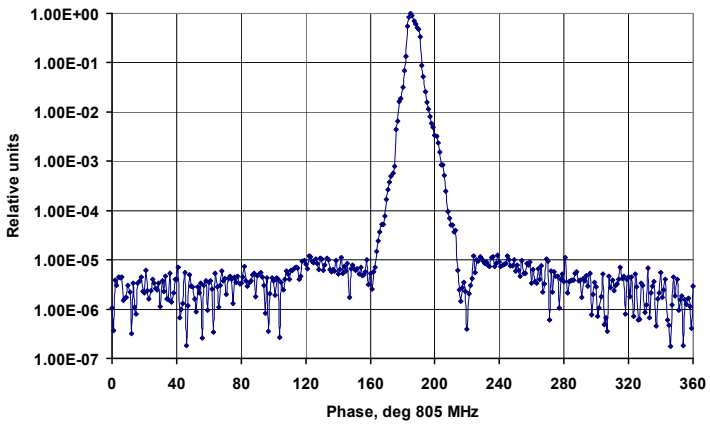

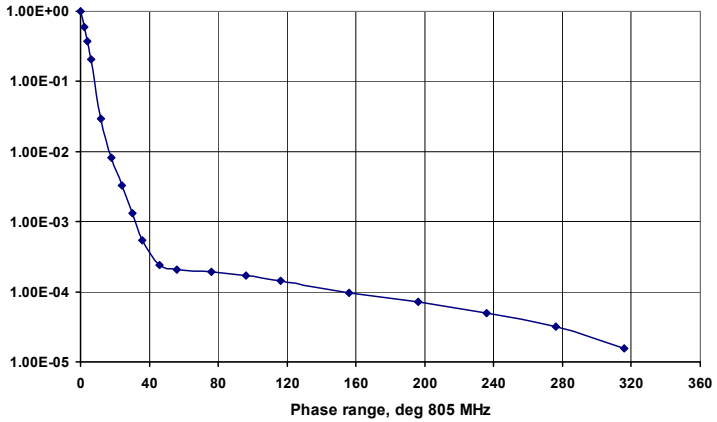

Fraction of particles outside a given phase range

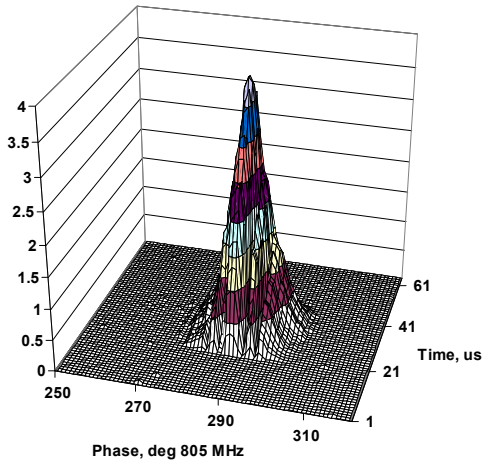

Result of measurement with a nominal SEM gain

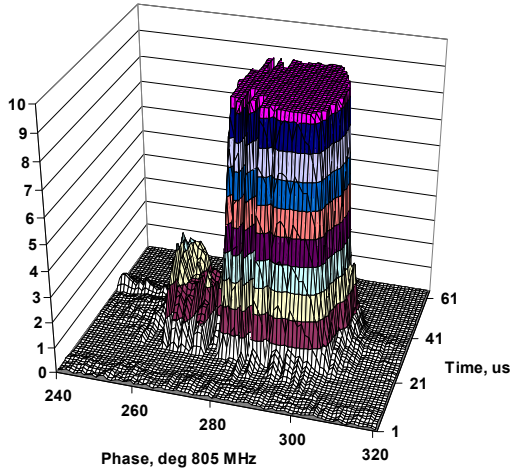

Result of measurement with a SEM gain 160 bigger than the nominal value

Summary

Bunch shape monitors with RF scanning of low energy secondary electrons ***are*** **used for longitudinal parameters measurements of beams of different particles (protons, H-minus ions, heavy ions) within the energy range from several MeV to 1 GeV. The accuracy of measurements is about 1° at several hundred MHz.**